ANALYSIS OF PAMS DATA IN CALIFORNIA VOLUME I: THE USE OF PAMS RADAR PROFILER AND RASS DATA TO UNDERSTAND THE METEOROLOGICAL PROCESSES THAT INFLUENCE AIR QUALITY IN SELECTED REGIONS OF CALIFORNIA

FINAL REPORT
STI-998391-1888-FR

By:
Clinton P. MacDonald
Lyle R. Chinkin
Timothy S. Dye
Craig B. Anderson
Sonoma Technology, Inc.
Petaluma, CA

Prepared for:
U.S. Environmental Protection Agency
Research Triangle Park, NC

May 1999

[BLANK PAGE]

ANALYSIS OF PAMS DATA IN CALIFORNIA VOLUME I: THE USE OF PAMS RADAR PROFILER AND RASS DATA TO UNDERSTAND THE METEOROLOGICAL PROCESSES THAT INFLUENCE AIR QUALITY IN SELECTED REGIONS OF CALIFORNIA

FINAL REPORT
STI-998391-1888-FR

By:
Clinton P. MacDonald
Lyle R. Chinkin
Timothy S. Dye
Craig B. Anderson
Sonoma Technology, Inc.
1360 Redwood Way, Suite C
Petaluma, CA 94954-1169

Prepared for:
Mark Schmidt
U.S. Environmental Protection Agency
OAQPS/EMAD MD-14
Research Triangle Park, NC 27711

May 27, 1999

[BLANK PAGE]

PREFACE

In accordance with the 1990 Clean Air Act Amendments, the U.S. Environmental Protection Agency (EPA) initiated the Photochemical Assessment Monitoring Stations (PAMS) program for serious, severe, and extreme ozone nonattainment areas. The PAMS networks monitor for volatile organic compounds (VOCs), ozone, oxides of nitrogen (NO_x), and meteorological parameters. The PAMS networks were designed to provide data for the assessment of population exposure, ozone formation, and evaluation of ozone control strategies. The EPA Office of Air Quality Planning and Standards has sought to provide the EPA regional offices and the states with the necessary analytical tools, training, and guidance to collect and use the PAMS data. To this end, the EPA, California Air Resources Board (ARB), the Sacramento Metropolitan Air Quality Management District, San Joaquin Valley Unified Air Pollution Control District, and Ventura County Air Pollution Control District staff sponsored research into the analysis of PAMS air quality and meteorological data collected at the Districts' PAMS sites in Sacramento, Fresno, and Ventura counties and the ARB's long-term trend sites located in Los Angeles and San Diego. Requested tasks encompass upper-air meteorological data processing and analyses, emission inventory evaluation, and trends analyses. Results of the data analyses for these three topic areas are presented in three volumes:

Analysis of PAMS Data in California Volume I: The use of PAMS radar profiler and RASS data to understand the meteorological processes that influence air quality in selected regions of California. MacDonald C.P., Chinkin L.R., Dye T.S., Anderson C.B. (1999) Report prepared for the U.S. Environmental Protection Agency, Research Triangle Park, NC by Sonoma Technology, Inc., Petaluma, CA, STI-998391-1888-FR, May.

Analysis of PAMS Data in California Volume II: The use of PAMS data to evaluate regional emission inventories in California. Haste-Funk T.L., Chinkin L.R. (1999) Report prepared for the U.S. Environmental Protection Agency, Research Triangle Park, NC by Sonoma Technology, Inc., Petaluma, CA, STI-998392-1884-FR, May.

Analysis of PAMS Data in California Volume III: Trends analyses of California PAMS and long-term trend air quality data (1987-1997). Wittig A.E., Main H.H., Roberts P.T., Hurwitt S.H. (1999) Report prepared for the U.S. Environmental Protection Agency, Research Triangle Park, NC by Sonoma Technology, Inc., Petaluma, CA, STI-998393-1885-FR, May.

ACKNOWLEDGMENTS

The authors of this report would like to thank Mark Schmidt for coordinating this work effort for the EPA, and the Sacramento Metropolitan Air Quality Management District, San Joaquin Valley Unified Air Pollution Control District, and Ventura County Air Pollution Control District, and Don Hammond of the ARB. We would also like to thank Jana Schwartz, Martina Shultz, and Sandy Smethurst of STI for preparation of the text and figures published in the report.

[BLANK PAGE]

TABLE OF CONTENTS

Section **Page**

PREFACE iii
ACKNOWLEDGMENTS v
LIST OF FIGURES ix
LIST OF TABLES xi

1. INTRODUCTION 1-1

2. BACKGROUND 2-1
   2.1 THE PLANETARY BOUNDARY LAYER 2-1

3. METHODS FOR CHARACTERIZING METEOROLOGICAL PROCESSES WITHIN THE PBL 3-1
   3.1 ESTIMATING DAYTIME MIXING DEPTH AND OTHER LAYERS WITHIN THE PBL 3-1
   3.2 CHARACTERIZING TRANSPORT, VENTILATION, AND RECIRCULATION WITHIN AND ABOVE THE PBL 3-3

4. CASE STUDIES 4-1
   4.1 METEOROLOGICAL PROCESSES THAT INFLUENCE OZONE CONCENTRATIONS IN SACRAMENTO, VENTURA, AND THE SAN JOAQUIN VALLEY 4-1
   4.2 PROFILER LOCATIONS 4-3
   4.3 OZONE EPISODES 4-4
      4.3.1 Sacramento July 16-18, 1998 Episode 4-4
      4.3.2 Sacramento August 2-6, 1998 Episode 4-6
      4.3.3 San Joaquin Valley August 8-10, 1998 Episode 4-7
      4.3.4 San Joaquin Valley August 26-September 3, 1998 Episode 4-8
      4.3.5 Ventura County August 5-8, 1997 Episode 4-9
      4.3.6 Ventura County July 15-20, 1998 Episode 4-11

5. REFERENCES ..... 5 -1

APPENDIX A: NESTED GRID MODEL WEATHER CHARTS A-1

APPENDIX B: RADAR PROFILER WIND PLOTS B-1

APPENDIX C: TRANSPORT STATISTICS C-1

LIST OF FIGURES

Figure **Page**

2-1. Schematic showing the diurnal changes in boundary layer structure 2-3

3-1. Time/height cross section of vertical velocity and radar profiler C_n^2 data at Franklin Field on July 17, 1998 3-5

3-2. Time/height cross section of vertical velocity and radar profiler C_n^2 data at Simi Valley on July 18, 1998 3-6

3-3. RASS virtual temperature profile at LAX on June 20, 1996 at 1200 PST 3-7

3-4. RASS virtual temperature data at Simi Valley on August 6, 1997 showing cool air associated with the sea breeze below about 500 m 3-8

3-5. RASS virtual temperature profile at LAX on December 7, 1996 at 2100 PST..... 3-9

3-6. Twelve hour overnight transport statistics at Visalia from August 8, 1998 at 1600 PST to August 9, 1998 at 0400 PST 3-10

3-7. Twelve hour daytime transport statistics at Visalia from August 9, 1998 at 0400 PST to August 9, 1998 at 1600 PST 3-11

4-1. Time/height cross section of radar profiler a) vertical velocity and b) C_n^2 data at Franklin Field on July 16, 1998 4-13

4-2. Time/height cross section of radar profiler a) vertical velocity and b) C_n^2 data at Franklin Field on July 17, 1998 4-14

4-3. RASS virtual temperature data at Franklin Field on July 17, 1998 showing a subsidence inversion at about 500 m 4-15

4-4. RASS virtual temperature data at Franklin Field on July 16, 1998 showing a subsidence inversion at about 800 m 4-16

4-5. Radar profiler wind data at Franklin Field on July 16, 1998 showing well organized northerly to northwesterly winds below about 1500 m.....4-17

4-6. Radar profiler wind data at Franklin Field on July 17, 1998 showing more disorganized flow below about 1000 m compared to July 16, 1998.....4-18

4-7. Twelve hour daytime transport statistics at Franklin Field from July 17, 1998 at 0400 PST to July 17 at 1600 PST 4-19

[BLANK PAGE]

LIST OF FIGURES (Continued)

Figure **Page**

4-8. Radar profiler wind data and estimated boundary layers (black lines) at Franklin Field on July 17, 1998 4-20

4-9. Time/height cross section of radar profiler a) vertical velocity and b) C_n^2 data at Franklin Field on August 3, 1998 4-21

4-10. Radar profiler wind data at Franklin Field on August 3, 1998 showing well organized northerly to northwesterly winds below about 1500 m 4-22

4-11. Radar profiler wind data at Franklin Field on August 5, 1998 showing the west to southwest delta breeze 4-23

4-12. Time/height cross section of radar profiler a) vertical velocity and b) C_n^2 data at Visalia on August 9, 1998 4-24

4-13. RASS virtual temperature data at Visalia on August 9, 1998 showing a subsidence inversion at about 700 m 4-25

4-14. Radar profiler wind data at Visalia on August 9, 1998 showing the nocturnal jet and eddy flow 4-26

4-15. Winds at 400 m agl for August 5, 1990 at 0400 PDT 4-27

4-16. Twelve-hour nighttime transport statistics at Visalia from August 8, 1998 at 1600 PST to August 9, 1998 at 0400 PST 4-28

4-17. Twelve-hour daytime transport statistics at Visalia from 0400 to 1600 PST on August 9, 1998 4-29

4-18. Time/height cross section of radar profiler a) radial velocity and b) C_n^2 data at Visalia on August 30, 1998 4-30

4-19. Twelve-hour daytime transport statistics at Visalia from 0400 to 1600 PST on August 30, 1998 4-31

4-20. Time/height cross section of radar profiler a) vertical velocity and b) C_n^2 data at Simi Valley on August 6, 1997 4-32

4-21. Time/height cross section of radar profiler a) vertical velocity and b) C_n^2 data at Simi Valley on August 8, 1997 4-33

[BLANK PAGE]

LIST OF FIGURES (Concluded)

Figure **Page**

4-22. RASS virtual temperature data at Simi Valley on August 8, 1997 showing a strong inversion from 450 m to about 650 m 4-34

4-23. Radar profiler wind data at Simi Valley on August 6, 1997 showing the MBL 4-35

4-24. Time/height cross section of radar profiler a) vertical velocity and b) C_n^2 data at Simi Valley on July 15, 1998..... 4-36

4-25. Twelve-hour overnight transport statistics at Simi Valley from July 16, 1998 at 1600 PST to July 17, 1998 at 0400 PST 4-37

4-26. Radar profiler wind data at Simi Valley on July 17, 1998 4-38

LIST OF TABLES

Table **Page**

4-1. Dates and duration of each ozone episode 4-4

[BLANK PAGE]

1. INTRODUCTION

In accordance with the 1990 Clean Air Act Amendments, the U.S. Environmental Protection Agency (EPA) initiated the Photochemical Assessment Monitoring Stations (PAMS) program for serious, severe, and extreme ozone nonattainment areas. The PAMS networks monitor for volatile organic compounds (VOCs), ozone, oxides of nitrogen (NO_x), and meteorological parameters. The PAMS networks were designed to provide data for the assessment of population exposure, ozone formation, and evaluation of ozone control strategies. The EPA, California Air Resources Board (ARB), and the Sacramento Metropolitan Air Quality Management District, San Joaquin Valley Unified Air Pollution Control District, and Ventura County Air Pollution Control District sponsored and requested analytical guidance on the meteorological portion of the Photochemical Assessment Monitoring Stations. This report supplies the requested guidance.

In particular, this report explores the use of PAMS radar wind profiler and Radio Acoustic Sounding Systems (RASS) data to understand the meteorological processes that influence surface ozone concentrations in three California air districts (e.g., Ventura County, Sacramento County, and the San Joaquin Valley). The radar wind profiler measures horizontal and vertical winds and return signal strength up to 4000 m with a resolution of between 60 and 100 m. RASS uses sound combined with radar to measure virtual temperature profiles to about 1500 m with a resolution of 60 m. These instruments allow continuous (hourly or sub hourly) monitoring of aloft winds and temperatures and lower atmospheric structure; these atmospheric features have a strong influence on local air pollution.

The techniques using the radar wind profiler and RASS data are illustrated for two ozone episodes in each of the previously mentioned regions. An ozone episode is defined as the day leading up to a high concentration event (often referred to as the build-up day), the days with high ozone concentrations, and the day following the high ozone concentration day(s) (referred to as the clean-out day).

Section 2 of this report presents general background information on meteorological processes that influence ozone. Section 3 illustrates techniques for using radar wind profiler and RASS data to characterize and understand the meteorological processes that influence local ozone concentrations. Section 4 explores the application of these techniques to two episodes for each region. Section 5 lists references for this report. Appendix A contains Nested Grid Model analysis charts, Appendix B contains radar profiler wind plots, and Appendix C contains transport statistics.

[BLANK PAGE]

2. BACKGROUND

Ground level ozone continues to be a primary concern for most large urban areas in the United States (National Research Council, 1992). In light of this concern, much effort has been made to understand the meteorological phenomena that influence the formation of ozone. Typically, high ozone concentrations occur within or downwind of major urban areas. Nitrogen oxides (NO_x) and volatile organic compounds (VOCs) combine in the presence of sunlight and are transported downwind. During this transport time, a number of conditions (including local emissions, pollutant carryover from the day prior, variations in sunlight, horizontal dispersion of pollution by wind, and the vertical dilution of pollution in the mixed layer), influence the local ozone concentration.

Periods of high ozone concentrations are associated with slow moving high-pressure systems that produce widespread sinking air (i.e., subsidence), clear skies, and warm surface temperatures. This subsidence causes the air to warm adiabatically, and may induce or increase the strength of an inversion that traps ozone and ozone precursors and hinders the vertical dispersion of pollutants within the planetary boundary layer (PBL) (Neiburger et al., 1971).

The PBL is the lowest portion of the atmosphere that is influenced by thermal and frictional forces from the Earth's surface. These forces cause significant diurnal changes in the depth of the PBL from hundreds of meters at night to several kilometers during the day. Diagnosing the evolution and structure of the PBL is important for understanding the dispersion and transport of pollutants such as ozone and ozone precursors. This report demonstrates techniques that can be used to diagnose important characteristics of the PBL using radar profiler data and virtual temperature profiles measured by RASS during two episodes each in the Sacramento, Ventura, and San Joaquin Valley air districts.

2.1 THE PLANETARY BOUNDARY LAYER

The major components of the PBL are the nocturnal boundary layer (NBL), convective boundary layer (CBL), and the residual layer (RL) as shown in **Figure 2-1**. The NBL forms at night when air near the surface cools. In response to this cooling, stable conditions reduce vertical mixing in the NBL, thus confining surface-based pollutants to the lowest several hundred meters and acting as a barrier to aloft pollutant concentrations. Starting shortly after sunrise, the CBL grows as the ground warms and thermals mix air vertically. At sunset, these thermals decay and the stable conditions of the NBL return. Aloft at night, a RL remains and initially possesses characteristics of the recently decayed CBL. This general diurnal cycle is modified near the shoreline, where the vertical extent of mixing is often reduced when the cooler, stable air over water moves onshore (Angevine et al., 1996).

The surface-based mixed layer is the portion of the PBL above the surface through which vigorous vertical mixing of heat, moisture, momentum, and pollutants occurs (Holtzworth, 1972). During the daytime, the mixing depth is defined as the altitude of a stable

layer or the altitude of an inversion capping a well-mixed convective boundary layer. At night, identification of the top of the mixed layer is more complicated because oftentimes several stratified layers exist with vertical mixing confined to the lowest several hundred meters in the NBL. In addition, mixing processes at night occur on a longer time scale and mechanical mixing dominates convective mixing (Beyrich and Weill, 1993).

The typical diurnal cycle of ozone is closely linked to the diurnal cycle of the PBL. At night, ozone concentrations within the nocturnal boundary layer remain low due to deposition and to titration of ozone by nitric oxide at urban sites. Above the NBL in the residual layer, ozone concentrations mix upwards during the previous day can remain through the night (Clark, 1997). As the sun warms the ground in the morning, the NBL transitions to the CBL. Any ozone precursors that accumulate in the NBL over night mix upwards. Likewise, aloft ozone and ozone precursors are entrained into the growing CBL. This transition also occurs during a time of increasing ozone precursor emissions and plays an important role in the vertical dispersion of pollutants (Uno et al., 1992). As the CBL grows, ozone and ozone precursors are vertically dispersed and aloft air is entrained into the mixed layer, enhancing or slowing ozone formation. On days when aloft ozone concentrations are low, entrainment of aloft air dilutes surface ozone concentrations. On the other hand, when the aloft ozone concentrations are high, entrainment may increase surface ozone concentrations.

Historically, mixing depths and PBL winds have been estimated and observed from hourly surface temperature observations, twice daily National Weather Service rawinsonde data (Holzworth, 1972), and observational models that use rawinsonde data (Berman et al., 1997). As discussed in Baxter (1991) there are several techniques for estimating mixing depth using data from a variety of upper-air instruments. By using rawinsonde data, the daytime mixed layer can be identified as the height of an inversion that caps a layer where the temperature lapse rate is close to the adiabatic lapse rate. Reflectivity signals from radar wind profilers can detect density gradients associated with the inversion at the top of the mixed layer. Although somewhat intermittent in time and space, mixing depths estimated from the aircraft profiles of pollutant concentrations, turbulence, and temperatures can be used to fill in gaps between the rawinsonde and radar wind profiler sites during field studies.

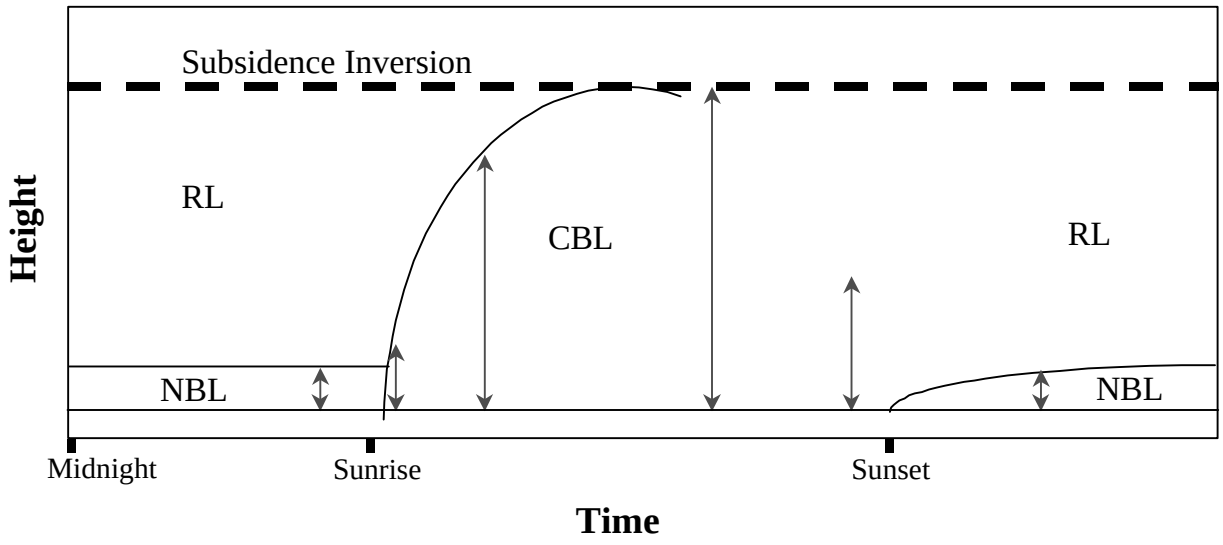

Figure 2-1. Schematic showing the diurnal changes in boundary layer structure. The regions of the boundary layer are the residual layer (RL), nocturnal boundary layer (NBL), and the convective boundary layer (CBL). The arrows refer to vertical mixing.

[BLANK PAGE]

3. METHODS FOR CHARACTERIZING METEOROLOGICAL PROCESSES WITHIN THE PBL

With the development and widespread deployment of 915-MHz radar wind profilers and RASS, the ability to study the planetary boundary layer has greatly improved (White et al., 1991). Many regional air quality studies have used networks of radar profilers to improve our understanding of atmospheric processes that influence pollutant concentration (Neff, 1994; Roberts et al., 1993; Dye et al., 1995; MacDonald et al., 1998; Blumenthal et al., 1998). This section discusses how radar profiler and RASS data can be used to characterize important processes in the PBL.

3.1 ESTIMATING DAYTIME MIXING DEPTH AND OTHER LAYERS WITHIN THE PBL

Radar Profilers

The radar profiler reflectivity data can be used to estimate the height of the surface-based mixed layer, the marine boundary layer, the convective boundary layer, the residual layer, and the subsidence inversion. The radar profiler reflectivity data can be characterized by the refractive index structure parameter (C_n^2). The refractive index parameter is a measure of the variations in the refractive index of the atmosphere. Turbulence produces variations in atmospheric temperature, humidity, and pressure, which in turn cause variations in the radar refractive index. In the planetary boundary layer, humidity fluctuations contribute most to the variations in the radar refractive index. The greatest humidity variations tend to occur at the top of the aforementioned boundary layers. For example, Wyngaard and LeMone (1980) showed that C_n^2 peaked at the inversion located at the top of the convective boundary layer due to warm dry aloft air entraining into cooler and moister air below the inversion. Although the C_n^2 data is the primary parameter used to estimate the mixing depth, vertical velocity data collected by the profiler is useful as a secondary check of the estimated mixing depth. Typically, strong vertical motions occur within the CBL, and thus the vertical motion field can be used depict the depth of the CBL.

Simply viewing time-height cross-sectional plots of C_n^2 can be an effective method of estimating the mixing depth. **Figure 3-1** shows a time/height C_n^2 at Franklin Field, Bruceville, California in the Sacramento District. The blues and greens in the cross section show weak signal returns and the orange and red show strong returns. At times, the peak C_n^2 may not always define the surface-based mixed layer and may depict some other aloft layer such as a subsidence inversion. It is therefore important to view the C_n^2 plots in conjunction with other data, to be sure that the peak C_n^2 is properly characterizing the surface-based mixing depth.

Measurements of vertical velocity serve as a good complimentary source of information to the C_n^2 data. The vertical velocity data plotted as a time/height cross-section coupled with the C_n^2 can help define layers of mixing and accurately characterize the different layers within

the PBL. For example, the C_n^2 and vertical velocity data at Simi Valley in the Ventura District often shows the existence of two layers (**Figure 3-2**). The vertical velocity data depict a lower surface-based mixing layer to about 400 m (shown in Figure 3-2 as the area of alternating blue and red colors indicating updrafts and downdrafts). The top of this layer also shows moderate C_n^2 data. A second layer with peak C_n^2 is shown at about 1000 m. The lower layer capped at 400 m is the marine boundary layer in which surface mixing is confined and the layer at 1000 m likely depicts a subsidence inversion.

Other automated methods for estimating mixing depth include computing a median hourly profile of C_n^2 for each altitude and selecting the peak median profile for each hour as the estimated mixing depth. This method is described in detail by Dye et al. (1995). Automated methods can do a good job of estimating the surface-based mixing depth, though close review of the results is often required.

RASS Virtual Temperature Data

Generally C_n^2 measured by boundary layer profilers will not resolve low-level inversions associated with the top of the NBL when such inversions are less than about 200 to 300 m agl. Consequently, virtual temperature data (T_v) collected by RASS, coupled with surface T_v measurements, are used to provide estimates of the depth of the NBL. The virtual temperature of an air parcel is the temperature that dry air would have if its pressure and density were equal to those of a parcel of moist air. When several different layers exist within the PBL, the peak C_n^2 data does not always depict the layer of interest or the lowest layer. For example, the C_n^2 data may not resolve a marine boundary layer that undercuts a convective boundary layer or the shallow NBL. However, RASS virtual temperature data can be used to distinguish the marine boundary layer.

During the daytime, when the surface virtual temperature is greater than the aloft virtual temperature, the Holtzworth algorithm can be used to estimate the depth of the surface-based mixed layer. With this algorithm, the depth of the mixed layer is defined as the altitude at which an ascending air parcel is cooled adiabatically and becomes cooler than the ambient air. This approach ignores the effects of saturation of the air parcel and the subsequent diabatic cooling rate. Ignoring the latent heat is acceptable for ozone pollution research because ozone episodes in California generally occur under cloud free weather conditions.

Figure 3-3 shows a daytime RASS virtual temperature profile at the Los Angeles International Airport (LAX) on June 20, 1996 at 1200 PST. This plot illustrates the method used to determine mixing depth during the daytime (MacDonald et al., 1999). Because the surface virtual temperature (22.2°C) is greater than the aloft virtual temperature (16.7°C) at 120 m agl (167 m msl), the Holtzworth algorithm is employed. The surface air parcel is theoretically ascended adiabatically, cooling at a rate of 9.8°C/1000 m until it is cooler than the surrounding temperature, which occurs at 620 m agl (767 m msl). At this altitude the parcel has cooled to 15.1°C and the surrounding environmental temperature is 16.5°C. The

parcel is no longer buoyant and will not mix with air above 720 m agl; thus, the mixing depth is estimated at 720 m msl.

In areas near cool coastal waters, cool marine air that moves inland can undercut the convective boundary layer. This undercutting of the CBL causes the surface air to be cooler than the aloft air and the Holtzwoth algorithm does not accurately define the depth of the marine boundary layer. Under these circumstances the top of the marine boundary layer is often observed where there is a large increase in temperature with height. For example, **Figure 3-4** shows a cool RASS temperature sounding below 500 m, with a sharp increase in temperature at 500 m. The cool surface temperatures in this example are associated with the afternoon sea breeze that blew into Simi Valley on August 6, 1997.

At night, when the surface temperature is lower than the aloft temperature, the Holtzworth method does not apply. Under these conditions, a stable nocturnal boundary layer exists near the surface. Within the NBL, the greatest static stability is near the ground, with the stability decreasing to near neutral with increasing elevation. When these conditions are observed, the mixing depth is estimated at the top of the NBL where there is an inflection point in the virtual temperature profile. At this transition point, the virtual temperature profile changes from very stable to near neutral.

Figure 3-5 shows a nighttime virtual temperature profile at LAX on December 7, 1996 at 2100 PST as diagnosed from RASS and surface temperature. This plot illustrates the method used to determine mixing depth during the nighttime (MacDonald, 1998). Because the surface virtual temperature (14.4^{o}C) is less than the aloft virtual temperature at the second range gate (15.2^{o}C) at 180 m agl (227 m msl), the Holtzworth algorithm is not employed. Instead, an algorithm that finds the lowest point at which the atmospheric stability significantly changes from strongly stable to a less stable condition is used. This point occurs at an inflection point in the virtual temperature profile. As shown in Figure 3-5, the lowest inflection point (i.e., where the temperature profile changes from stable to neutral) in virtual temperature occurs at 420 m agl (467 m msl). This altitude is therefore estimated to be the top of the NBL and is the estimated mixing depth. Within the NBL the atmosphere is strongly stable. Above the NBL from 660 m agl up to about 900 m agl is the residual layer (the old daytime mixed layer) in which the air becomes less stable compared to the air within the NBL. The top of the residual layer is at about 900 m agl; here again the stability of the atmosphere changes, becoming near neutral above 900 m agl.

3.2 CHARACTERIZING TRANSPORT, VENTILATION, AND RECIRCULATION WITHIN AND ABOVE THE PBL

The transport of ozone and ozone precursors at the surface and aloft horizontally is a critical component of ozone formation potential. For example, Roberts et al. (1997) showed that despite reduced vertical mixing, the export and dilution of ozone and ozone precursors by surface winds results in significantly lower ozone concentrations than on days with calm winds and little export (or re-circulating flow) in El Paso, Texas. Blumenthal et al. (1997) showed that aloft transport and import of ozone into aloft layers can contribute significantly to local surface ozone concentrations in the northeastern United States. The nocturnal jet (a layer of

high wind speeds that forms at night at about 2200 EST when the NBL forms and de-couples the aloft layers from surface frictional forces and the air accelerates has the potential to transport pollution over significant distances. Ray et al. (1997) showed that aloft pollutants could be transported up to 300 km during the overnight hours in the northeastern United States. The transported pollutants could then contribute to local pollution when mixed to the surface during the day.

To investigate transport, ventilation, and re-circulation over all hours of the day and at all levels within the mixed layer, a procedure developed by Allwine and Whiteman (1994) can be used. The quantities computed using this procedure represent the scalar wind run S (km), the resultant (vector) transport distance L (km), the resultant (vector-averaged) wind direction Θ (degrees from true north adjusted to the proper quadrant), and the recirculation factor, R. Note that the vector transport distance is not a trajectory, but a wind run. It quantifies the transport assuming that the wind observed by the profiler is spatially consistent through the maximum transport distance. The recirculation factor is the ratio of the resultant transport distance to the scalar transport distance (wind run). When R is equal to 1, straight-line, steady transport has occurred during the integration period. When R is equal to zero, no net transport has occurred during the integration period. Values of R close to 1, combined with transport distances of a few hundred kilometers, would typically characterize good ventilation conditions. Conversely, low values of R represent periods of stagnation or recirculation. Stagnation would be indicated by short scalar wind runs (i.e., low wind speeds); recirculation would be characterized by low values of the vector transport distance (e.g., L less than 50 km) compared to the scalar wind run. For example, if R were 0.25 and the vector-averaged wind run were 50 km, the scalar wind run would be 200 km. This would be characteristic of recirculation conditions; air must have recirculated in the area of interest.

To illustrate the use of transport statistics, these quantities were computed for the San Joaquin Valley Visalia radar profiler data set at each measurement height, using available wind observations on August 8-9, 1998. The integration time, T, was specified as 12 hours and the transport statistics were computed from August 8 at 1600 PST to August 9 at 0400 PST and from August 9 at 0400 PST to August 9 at 1600 PST. These time periods were selected to capture nighttime and daytime flow patterns, respectively. At least six wind observations were needed at a sampling height to compute a valid set of transport statistics. A cursory examination of the observations shows that the overnight flow from August 8 at 1600 PST to August 9 at 0400 PST below about 500 m was dominated by a northwest nocturnal jet. Overnight transport distances below 400 m were about 350 km **(Figure 3-6).** Note that transport distances are based on the assumption that the wind measured by the profiler is spatially representative to the distance of maximum transport; in this case 350 km. Transport in this layer was from the northwest and there was no evidence of recirculation within this layer as indicated by the high recirculation factors. Above 500 m, the transport distances slowly decreased and turned more from the west. At about 1200 m the overnight transport was about 90 km from the west. Again, the recirculation factor was near one (i.e., flow through). During the daytime, the transport distances were much shorter below 500 m compared to the overnight transport. Daytime transport distances below 500 m were about 30 to 50 km from the west and northwest **(Figure 3-7)**. Recirculation factors in this layer were around 0.6 to 0.3 indicating moderate recirculation during the day on August 9.

a.

b.

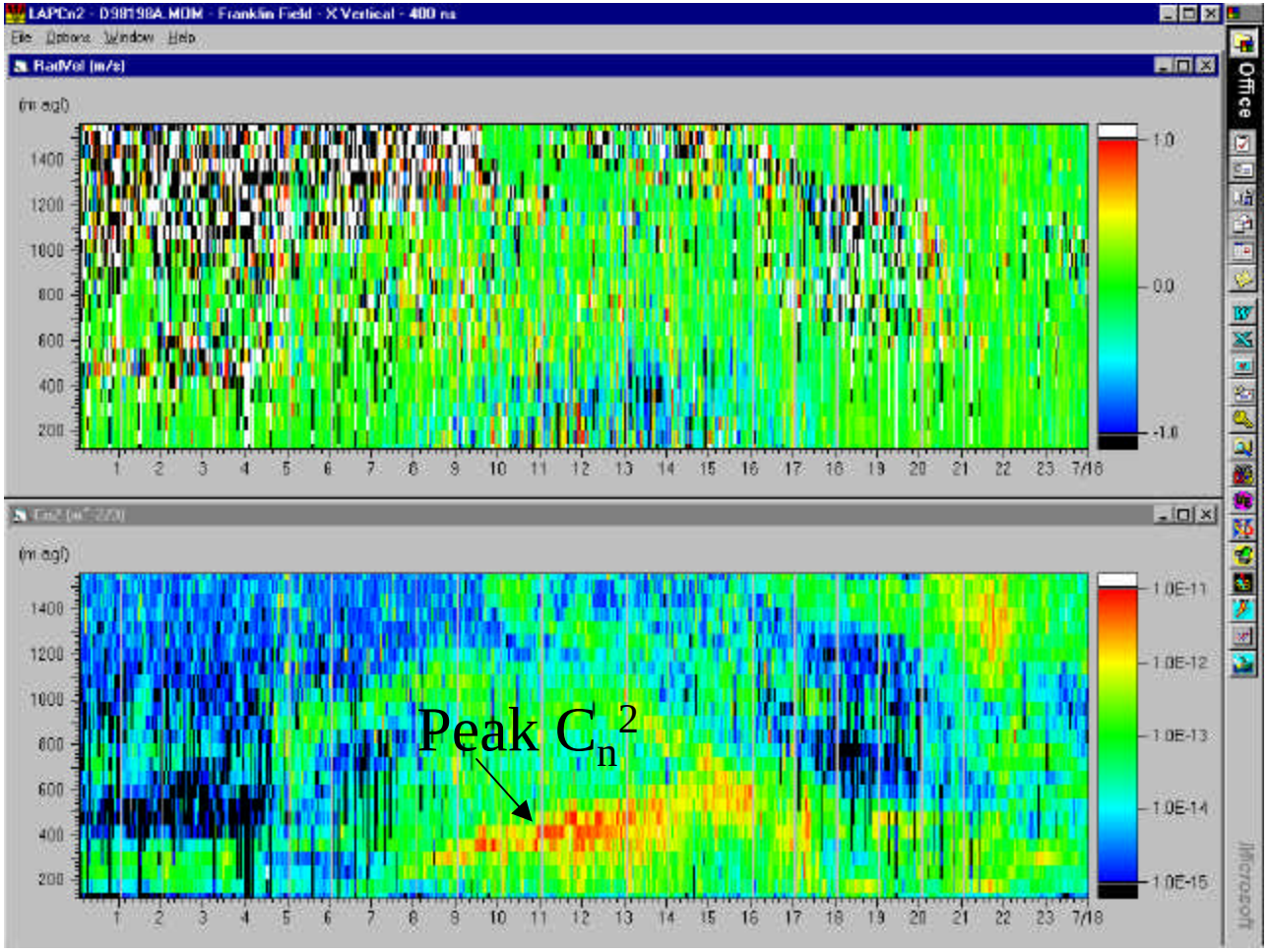

Time (PST)

Figure 3-1. Time/height cross section of radar profiler a) vertical velocity and b) C_n^2 data at Franklin Field on July 17, 1998. The peak C_n^2, shown as red and orange, identifies the top of the convective boundary layer.

a.

b.

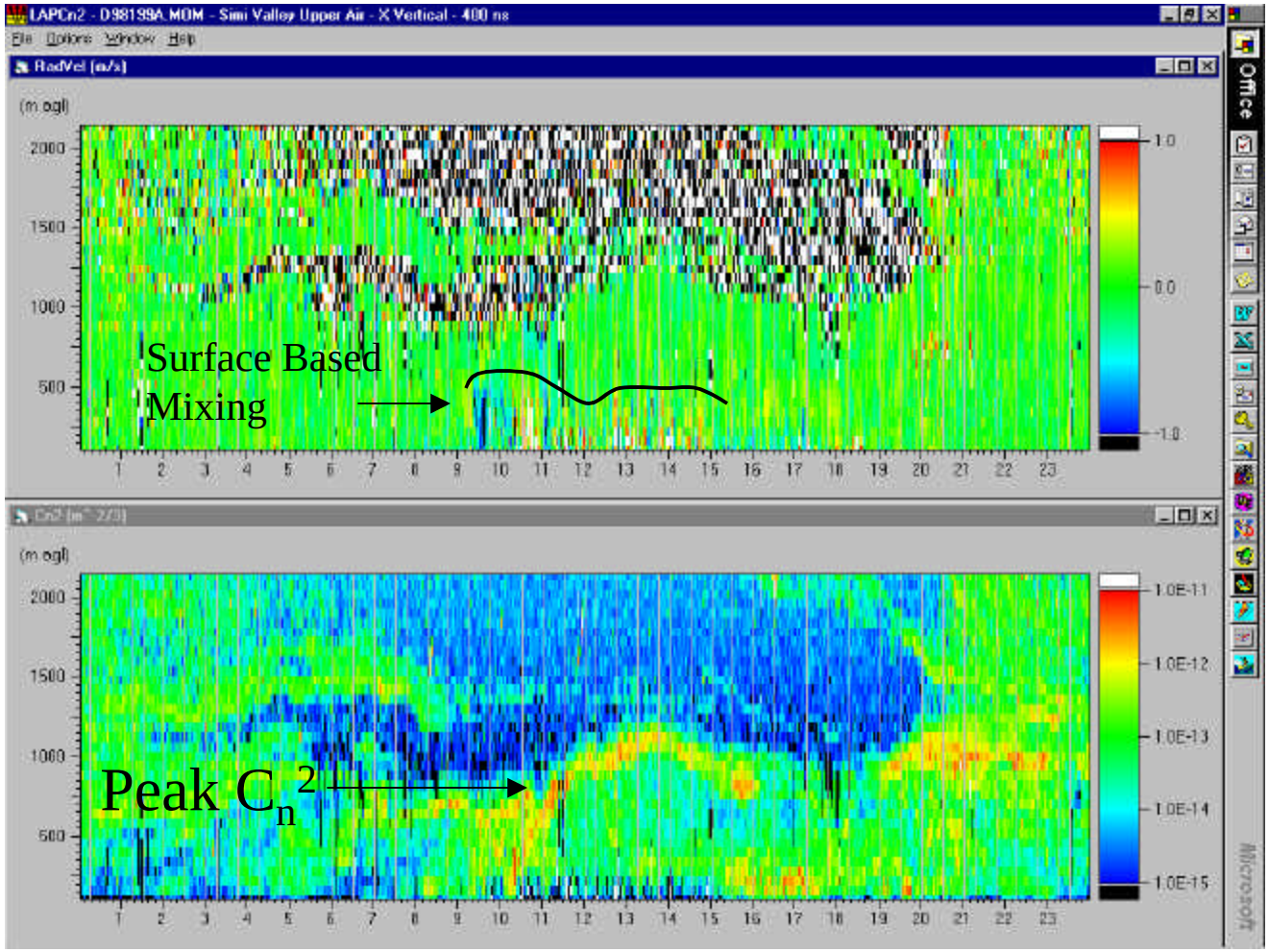

Time (PST)

Figure 3-2. Time/height cross section of radar profiler a) vertical velocity and b) C_n^2 data at Simi Valley on July 18, 1998. The vertical velocity data identifies the surface-based mixing depth at about 400 m. The peak C_n^2, shown as red and orange, identifies the existence of a secondary layer at about 1000 m.

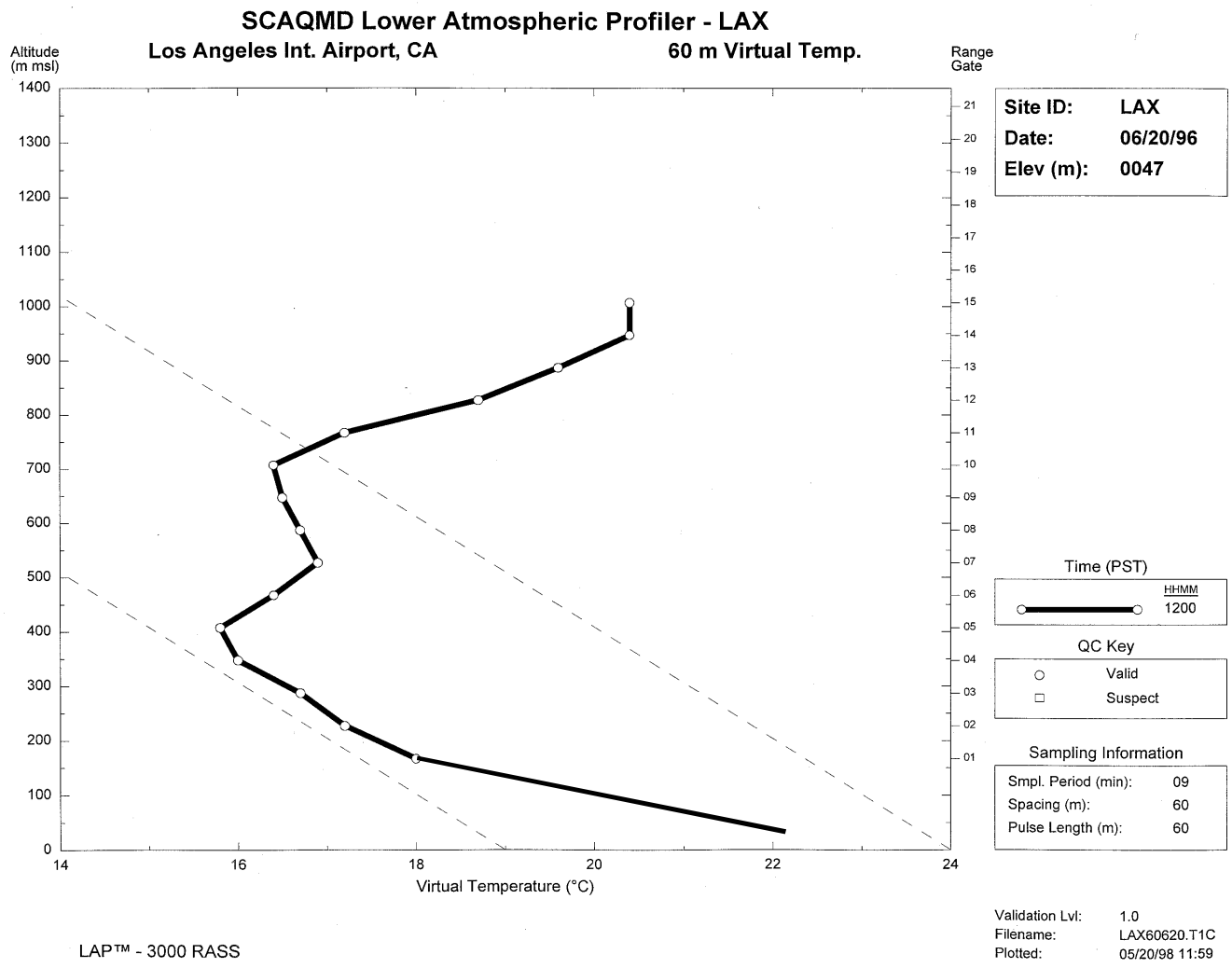

Figure 3-3. RASS virtual temperature profile at LAX on June 20, 1996 at 1200 PST.

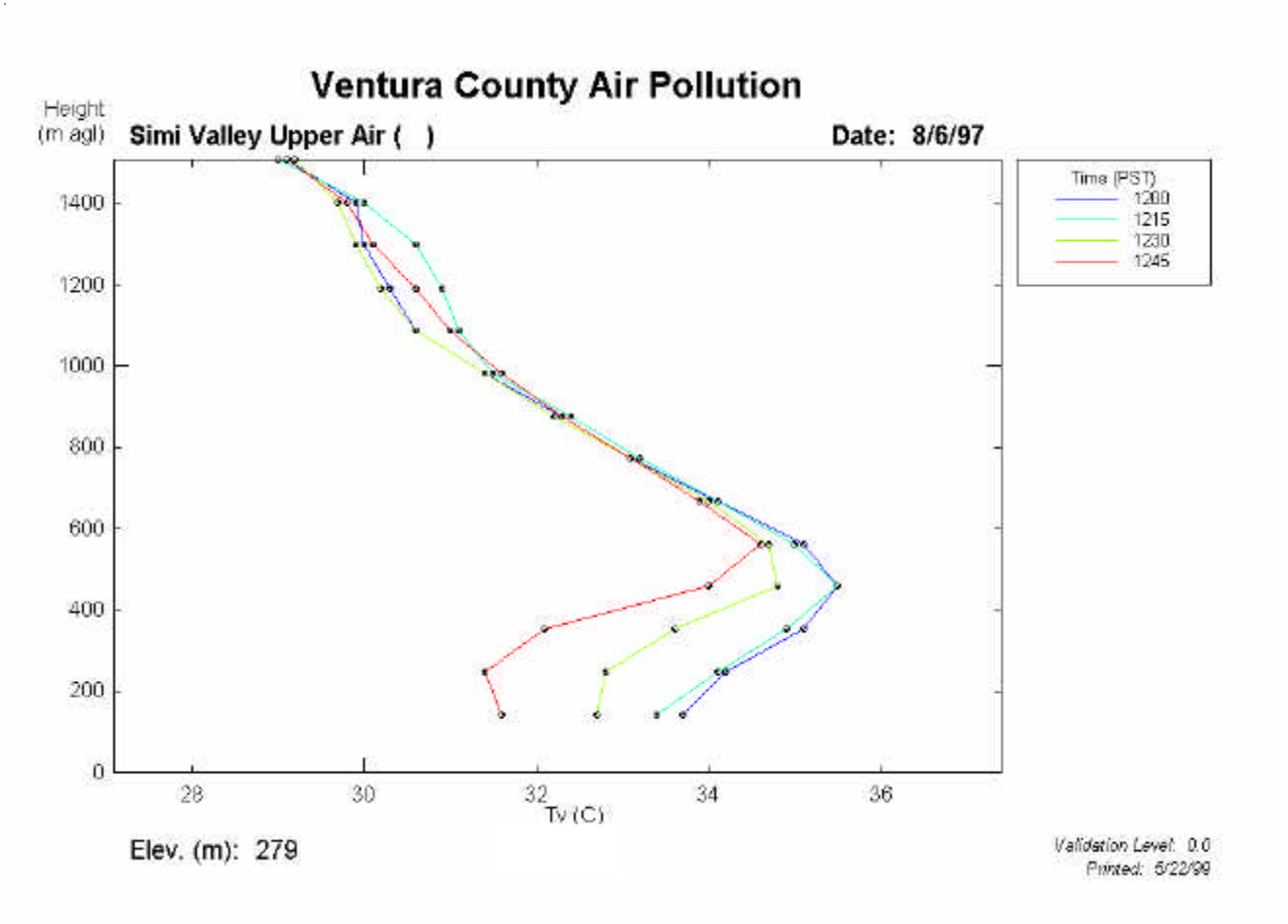

Figure 3-4. RASS virtual temperature data at Simi Valley on August 6, 1997 showing cool air associated with the sea breeze below about 500 m.

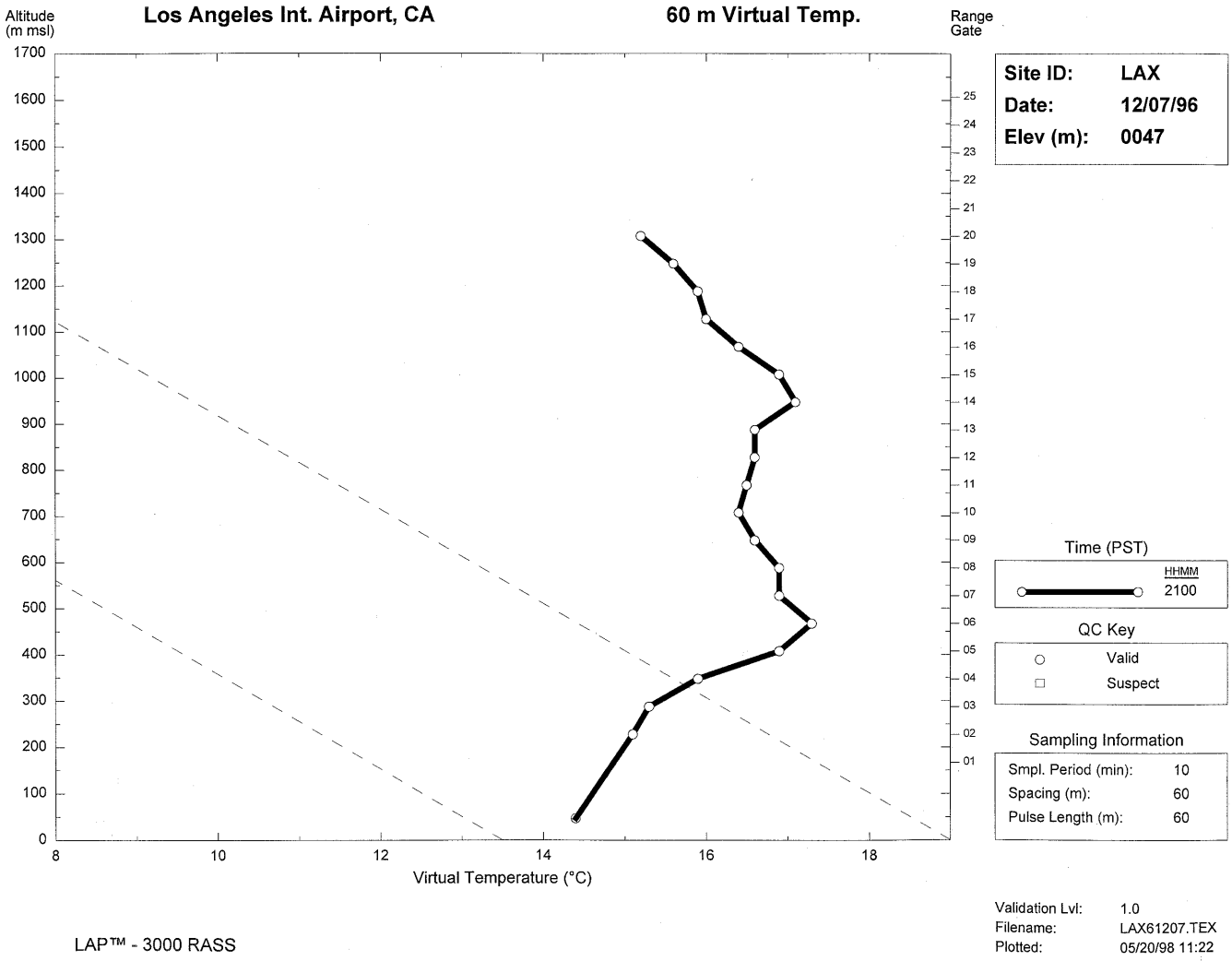

Figure 3-5. RASS virtual temperature profile at LAX on December 7, 1996 at 2100 PST.

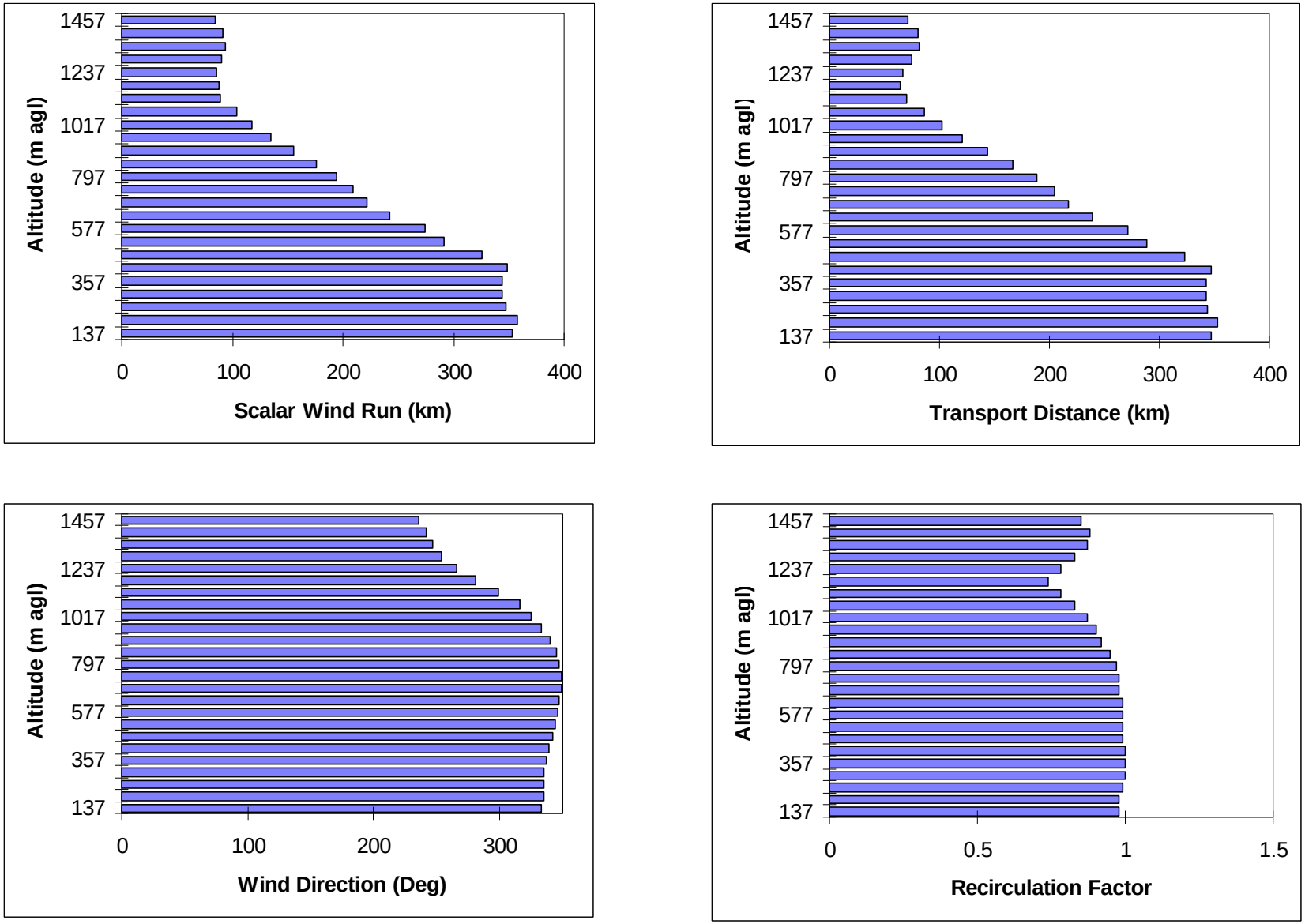

Figure 3-6. Twelve-hour overnight transport statistics at Visalia from August 8, 1998, at 1600 PST to August 9, 1998, at 0400 PST.

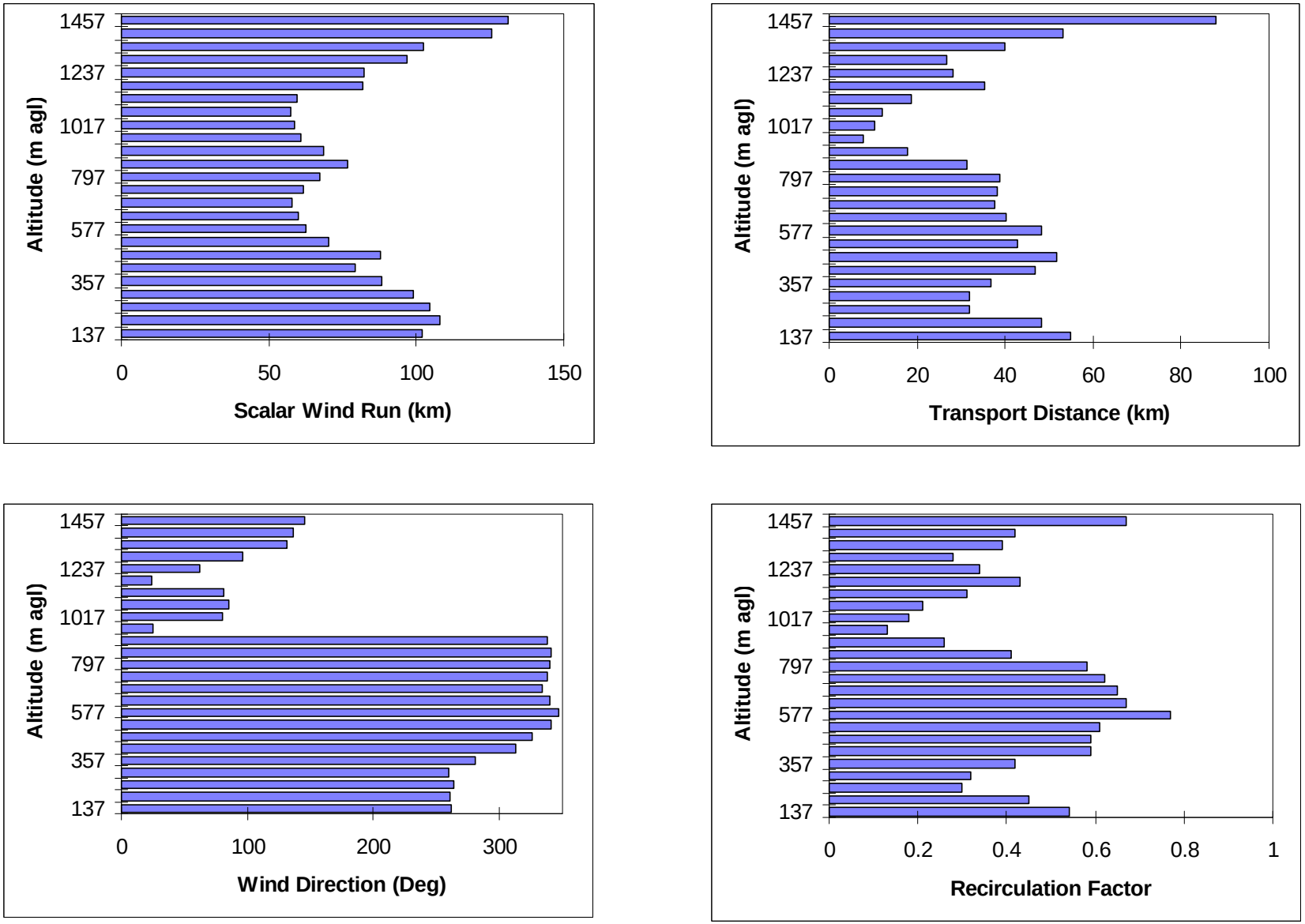

Figure 3-7. Twelve-hour daytime transport statistics at Visalia from August 9, 1998, at 0400 PST to August 9, 1998, at 1600 PST.

[BLANK PAGE]

4. CASE STUDIES

In this section we provide a brief description of the synoptic meteorological patterns associated with each of the ozone episodes and important meteorological features as observed and calculated from the profiler and RASS data. In general, the synoptic weather influences the winds, temperature, mixing structure, and evolution within the PBL. These meteorological features in turn influence the ozone concentrations. The radar profiler data and RASS data characterize these important meteorological phenomena.

This section contains example figures, and extensive sets of figures for each episode are contained in the appendices. Appendix A contains Nested Grid Model analysis charts; Appendix B contains radar profiler wind data; and Appendix C contains transport statistics.

4.1 METEOROLOGICAL PROCESSES THAT INFLUENCE OZONE CONCENTRATIONS IN SACRAMENTO, VENTURA, AND THE SAN JOAQUIN VALLEY

A number of studies have been conducted to improve our understanding of the relationship between meteorological conditions and ozone formation in the three study areas. In particular, Blumenthal et al., 1986 addressed the relationship between meteorology and air quality in Ventura County; Blumenthal et al., 1997 conducted a three-dimensional distribution and transport analysis for the San Joaquin Valley; and MacDonald et al., 1997 and MacDonald, 1998 examined the relationship between meteorology and air quality in Sacramento County.

Before describing the meteorology during each episode in this study, we first present a conceptual model of the fundamental physical processes that control air pollution in the three study areas. In general, the mixing level depth (MLD) is controlled by local surface heating and cooling, and by regional-scale vertical motion. The higher the temperature aloft compared to the temperature below, the stronger the inversion and the greater the stability of the atmosphere. Given equal amounts of surface heating, if the upper levels are cool and the air unstable, the MLD may grow to significantly greater heights and at a faster rate than when the aloft temperatures are higher and the air stable (Dye et al., 1995). Near coastal areas of California the vertical extent of the mixing is often reduced when cooler air over the Pacific Ocean flows onshore undercutting the convective mixed layer. This undercutting by cool marine air often produces two inversions: the upper inversion, which caps the convective boundary layer, and the lower inversion, which caps the marine layer.

The stability of the free atmosphere, which helps control the depth of the mixed layer, is primarily controlled by the regional vertical motion and associated temperatures aloft. Under conditions of upstream ridging aloft, negative vorticity advection tends to drive regional subsidence, which warms and stabilizes the atmosphere. The growth of the mixed layer is suppressed, resulting in low mixing depths (Dye et al., 1995). Under conditions of upstream troughing aloft, associated positive vorticity advection tends to produce regional rising motion,

which cools and destabilizes the atmosphere. The growth of the mixed layer is enhanced, resulting in deeper mixing depths. However, upstream troughing may also increase marine penetration, which would result in lower than expected mixing depths near coastal areas because of the cool stable marine air undercutting the daytime convective boundary layer.

Typically, the combination of the subtropical high located in the eastern Pacific Ocean and a thermal trough in the Sacramento and San Joaquin Valleys create an almost continuous onshore marine flow. The marine air typically flows through the Golden Gate, through the Carquinez Strait, and into the San Joaquin Valley. If the marine layer is deep enough, it may spill over the coastal hills, greatly increasing the volume of marine air intrusion. As discussed in Carroll and Baskett (1979), upstream ridging and negative vorticity advection over California and Nevada causes a synoptic offshore pressure gradient that counteracts the typical onshore flow. A moderate synoptic offshore gradient may cause stagnation, eliminating the onshore flow.

In Ventura County, high ozone concentrations can occur at the beginning of extended periods of warm temperatures aloft (Blumenthal et al., 1986). This represents the early stages of a high pressure development when offshore winds tend to reach their peak and mixing depths are relatively low. As the high pressure center moves eastward, the mixing layer tends to deepen and the sea breeze is re-established, with the inland areas usually receiving higher concentrations than the coastal sections.

Blumenthal et al., 1997 showed that air flows that transport ozone and its precursors within the Sacramento and San Joaquin Valleys can be divided into three regimes. These regimes include “synoptically driven” flows above about 1000 m agl, “locally driven aloft” flows from 200 m to 1000 m agl, and “surface” flows from the surface to about 200 m agl. Synoptic pressure gradients tend to drive the flows at higher altitudes. These flows tend to have little diurnal variation. Between 200 and 1000 m, the flows are strongly influenced by local driving forces, including thermal pressure gradients, frictional effects, channeling by terrain, and confinement by inversions. At night, this layer is typically decoupled from the surface by the nocturnal radiation inversion. Jet and eddy flows can form in this layer and can be confined between the nocturnal radiation inversion and the subsidence inversion.

Surface flows are also locally driven and are coupled to the aloft flows during the day. At night, the surface flow is often stagnant or can be affected by drainage and eddy flows, while flows a few hundred meters higher can be quite strong. Surface emissions in the night and morning hours are emitted into the surface flows and are decoupled from the aloft flow regimes, allowing fresh emissions to accumulate near the surface. As surface heating deepens the mixing layer during the day, the surface flow and the locally driven aloft flows are coupled, and the same-day surface emissions are mixed with reactants carried over aloft from the prior day in the elevated flows.

If mixing is deep enough, all three flow regimes can be merged by late afternoon. Ozone concentrations in the Sacramento and San Joaquin Valleys may be controlled by either the surface or aloft flows. In rural areas outside the influence of local urban plumes, ozone

aloft can be mixed to the surface in midmorning, causing rapid increases in ozone concentration. In urban plumes, ozone can form from local surface emissions. When the surface-based emissions or ozone mix with the air above, they are diluted somewhat by the air aloft. If the upper layers contain high levels of ozone, the surface ozone is not diluted as much as if the aloft air were clean. Thus, ozone downwind of cities can include contributions from both local precursors and from ozone transported aloft. In the afternoon, when peak ozone concentrations often occur, air from the three flow regimes can merge, and ozone and/or precursors transported from different places can mix. Only detailed understanding of the aloft flows for a continuous 24-hr period can determine which flow regime (and the source area) is dominant in a particular ozone episode. Section 4.3 demonstrates how radar profiler and RASS data are used to define the flows aloft.

4.2 PROFILER LOCATIONS

In any analysis of source and receptor relationships, it is important to assess the relative proximity of the data points used in the analysis. Ideally, air quality and surface and aloft meteorology are measured in very close vertical and horizontal proximity. In this study, the radar profilers and RASS systems and air quality monitors were not always co-located or even in close proximity (e.g., the peak ozone levels were not always observed near the profiler site).

Ventura County

Both the Simi Valley profiler and the RASS system in Ventura County are located where the peak Ventura County ozone is usually observed.

San Joaquin Valley

The San Joaquin Valley profiler and RASS systems are centrally located in Visalia, approximately 40 km south of Fresno and 60 km north of Bakersfield. However, Visalia is not the location of peak ozone in the Valley. Peak ozone concentrations are typically measured at Fresno and Bakersfield. Local meteorology within the PBL can be different over such distances; therefore, conclusions about how the meteorology within the PBL (as diagnosed with data from the Visalia profiler and RASS) influences peak San Joaquin Valley ozone concentrations should be viewed with this in mind. Note that Visalia ozone concentrations were unavailable for this illustrative analysis.

Sacramento County

The Sacramento County profiler and RASS systems are located at Franklin Field near Bruceville, approximately 20 km south of downtown Sacramento. Peak ozone concentrations in Sacramento County generally occur to the north and east of the site; although high ozone at Bruceville can occur under north wind conditions. Local meteorology within the PBL can be

different over such distances; therefore, conclusions about how the meteorology within the PBL (as diagnosed with data from the Franklin Field radar profiler and RASS) influences peak Sacramento ozone concentrations should be viewed with this in mind.

4.3 OZONE EPISODES

Table 4-1 lists the dates and duration of each ozone episode discussed in this section. As seen in the table, two episodes for each district have been selected, with duration ranging from 3 days to 9 days per episode. Episodes were selected from 1997 and 1998 (based in part upon the availability of radar profiler and RASS data). Also note that some of the selected episodes in one area correspond to high ozone periods in another area (i.e., the Sacramento and Ventura districts both experienced an ozone episode during July 16-18, 1998; the Ventura episode started one day earlier and persisted 2 days longer). For each of the episodes, we first present an overview of the synoptic meteorology and peak ozone pattern. This is followed by a discussion of mixing depth, transport, ventilation, and recirculation within and above the PBL computed from radar profiler and RASS data.

Table 4-1. Dates and duration of each ozone episode.

Study Region	Episode Period	Episode Duration
Sacramento County	July 16-18, 1998 August 2-6, 1988	3 days 5 days
San Joaquin Valley Air District	August 8-10, 1998 August 26-September 3, 1998	3 days 9 days
Ventura County	August 5-8, 1997 July 15-20, 1998	4 days 6 days

4.3.1 Sacramento July 16-18, 1998 Episode

The meteorology of the July 16-18, 1998 episode was typical of episodes in Sacramento County. High pressure moved over the area from the south, with increasing subsidence and slight offshore flow throughout the episode. Peak ozone levels rose from 66 parts per billion (ppb) on July 15 to 112 ppb on July 16, peaking at 152 ppb on July 17, and then decreasing to 104 ppb on July 18. On July 17, the peak of the episode, the high pressure center located east of California reached its strongest point. A decline in the strength of the high pressure center and concurrent subsidence (and likely temperatures aloft) coincided with the decrease in ozone on the subsequent days. Note that this episode coincided with an episode in Ventura County except that the Ventura County episode started one day earlier and persisted two days longer. As discussed in Section 4.3.6, the high pressure center built up from the south leading to favorable conditions for ozone formation in southern California a few days ahead of northern California and as the high pressure receded, conditions favorable for ozone formation in southern California persisted a few days longer.

The important meterological features as observed and calculated from the profiler and RASS data are as follows.

Mixing Depth

The daytime C_n^2, vertical velocity, and RASS virtual temperature data indicate that the daytime mixing (i.e., the convective boundary layer) was highest on the first day (July 16) of this three-day episode, peaking at about 1100 m, and lowest on July 17, peaking at only 600 m. **Figures 4-1 and 4-2** show C_n^2 and vertical velocity time/height cross sectional plots on July 16 and July 17, 1998, respectively. The daytime evolution of the CBL is estimated at the peak C_n^2 and is drawn in black. The CBL is also estimated on the vertical velocity profile.

The shallow CBL on July 17 likely confined pollutants near the surface contributing to high pollutant concentrations on this day. RASS virtual temperature data indicate that the restricted mixing on July 17 is caused by a low and strong subsidence inversion at about 500 m (**Figure 4-3**); while on July 16 the subsidence inversion is observed at about 800 m (**Figure 4-4**). On both of these days, the subsidence inversion is caused by sinking air associated with the high pressure system.

Transport, Ventilation, and Recirculation

The wind profiler data show more organized and consistent winds on July 16 and 18, the two moderate ozone days, compared to the high ozone day of July 17. On July 16 (**Figure 4-5**) and 18 there was generally moderate northwest to west winds during the night and most of the day below about 1500 m. At about 1200 PST the winds in the lowest 500 m came from the west indicating the onset of the delta breeze. On July 17, the winds were light and variable in the layer below 1000 m from about 0600 to 1200 PST (**Figure 4-6**). From about 1200 PST through the rest of the day, westerly delta winds blew within the CBL. The morning stagnation on July 17 probably allowed for the accumulation of pollution within the CBL and the afternoon delta breeze then transported this air downwind about 120 km (as indicated by the July 17 transport statistics, **Figure 4-7**). This pattern of morning stagnation, which allows for a build up of pollution, followed by afternoon transport to the ozone monitors in the eastern Sacramento District, likely contributed to the high ozone concentrations on July 17 observed east of downtown Sacramento.

There was no evidence of recirculation at the Franklin Field profiler; however, it is possible that recirculation did occur east of downtown Sacramento (north of the radar profiler). Typically in eastern Sacramento morning northerly flow gives way to the afternoon delta breeze during ozone episodes.

On the evening of July 17, the delta breeze undercut the daytime CBL, stratifying the PBL into two layers: a nighttime marine boundary layer from the surface to about 300 m and a residual layer that extended from 300 m to about 500 m. This process is depicted in **Figure 4-8**, a time/height section of wind and boundary layers. Note that the depth of the delta breeze during the evening is collaborated with RASS virtual temperature data.

4.3.2 Sacramento August 2-6, 1998 Episode

The meteorology of the August 2-6, 1998 episode was typical of episodes in the Sacramento air district. High pressure moved over the area from the west, with increasing subsidence and slight offshore flow throughout the episode. Peak ozone levels rose from 108 ppb on August 2 to 151 ppb on August 3, remaining high at 148 ppb on August 4, and peaking at 159 ppb on August 5, then decreasing to 119 ppb on August 6. With each successive day of the episode, the high moved slightly eastward and strengthened, reaching a peak on August 5, coinciding with the peak observed ozone day. A decline in the strength of the high pressure center and concurrent subsidence (and likely temperatures aloft) coincided with the decrease in ozone on the subsequent days.

It is not surprising that this August 2 through 6 episode had similar PBL characteristics as the July episode because the synoptic weather patterns were similar during both episodes. The most striking similarities include:

- A daytime CBL confined below 800 m for all days during this 5-day episode, as indicated by the C_n^2 and RASS data. The CBL only reached 500 m on August 3 as shown by the time/height cross section of C_n^2 and vertical velocity data (**Figure 4-9**). In the early morning hours, the CBL grew from about 150 m at 0800 PST to about 500 m at 1130 PST. The CBL remained at about 500 m for the remainder of the day, confined by the strong subsidence inversion. The shallow CBL confines pollution near the surface and could have contributed to the high ozone concentrations on this day.
- There was very little evidence of recirculation at the Franklin Field profiler during this episode; recirculation factors were generally near 1, meaning there was steady persistent flow.

The radar profiler wind data show other interesting features during this episode.

- During the first 3 days of this episode the winds within the lowest 1000 m were generally northwesterly, probably driven by a synoptic north/south pressure gradient. This type of flow pattern is typically observed during the beginning of an episode, as the synoptic high builds into the region. The wind profiler on August 3 (**Figure 4-10**) shows an example of this flow pattern.
- During the final 2 days of the episode the winds in the lower PBL turned west to southwest. The wind profiler data on August 5 (**Figure 4-11**) shows an example of this flow pattern. The west to southwest wind direction indicates a return of the delta breeze. This type of flow is typically observed at the end of an ozone episode as the north-south synoptic gradient associated with the high pressure system weakens, and local mesoscale flows can again dominate the local flows. Notice that the depth of the delta breeze on August 5 is confined to a shallow layer from 0000 PST to 1300 PST. Thus, it is not likely that this delta breeze transported much cool marine air into Sacramento until later in the afternoon when the depth of the westerly winds increased to about 1000 m. Peak ozone concentrations reached 159 ppb on this day.

4.3.3 San Joaquin Valley August 8-10, 1998 Episode

The meteorology of the August 8-10, 1998 episode can be described as a broad flat ridge of high pressure over central and southern California, concurrent with a weak trough in northern California. The flat ridge was accompanied by negative vorticity advection, resulting in subsidence and increased atmospheric stability. The high pressure ridge grew in strength and the weak trough in northern California dissipated. Peak ozone levels rose from 118 ppb on August 8 to 127 ppb on August 9, then decreased to 115 ppb on August 10. On each successive day of the episode, the high moved slightly eastward and strengthened, reaching its maximum strength on August 9. The peak ozone levels were observed on the day with the maximum negative vorticity advection. A decline in the strength of the high pressure center and negative vorticity advection (and likely temperatures aloft) coincided with the decrease in ozone on the subsequent days.

The important meteorological features as observed and calculated from the profiler and RASS data are presented below. Note that the Visalia profiler did not have a vertical beam, therefore, there is no vertical velocity data with which to estimate the daytime CBL. We recommend changing the sampling configuration to include vertical velocity measurements.

Mixing Depth

The daytime C_n^2 and RASS virtual temperature data indicate CBL was confined below 700 m agl on all three episode days. This shallow CBL confines pollutants near the surface contributing to high pollutant concentrations. **Figure 4-12** shows a C_n^2 time/height cross sectional plot on August 9, 1998. This C_n^2 plot is similar to the C_n^2 plots on the preceding and following episode days. The daytime evolution of the CBL is estimated at the peak C_n^2 and is drawn in black. As the sun warms the ground at dawn, the NBL is undercut by the newly formed CBL. (Note that the depth of the CBL is estimated using RASS temperature data from 0500 to 0800 PST.) As the ground continues to warm, the mixing becomes more vigorous and the CBL grows upward. This CBL would continue to grow if it were not for the temperature inversion that caps it. This temperature inversion is associated with the high pressure over California as shown on the synoptic charts during this episode. The existence of this temperature inversion and the peak height of the CBL are confirmed by the RASS temperature data. RASS virtual temperature data from the afternoon of August 9 (**Figure 4-13**) depicts the temperature inversion at about 700 m agl, the maximum height of the CBL as estimated from the C_n^2 data.

Transport, Ventilation, and Recirculation

The wind profiler data show the development of a northwest nocturnal jet at around 1800 PST on August 8, 1998, in a layer from just above the surface to about 600 m that continues into August 9, 1998 (**Figure 4-14**). At 0400 PST on August 9, a southerly wind developed in the layer once occupied by the northwest nocturnal jet. This jet and eddy circulation pattern was observed on most episode days. The southerly wind then turned west

to northwest at 1200 PST. Past analysis has shown that this southerly wind is part of the eddy flow driven by the topography of the San Joaquin Valley (SJV). As the northwesterly nocturnal jet drives air down to the end of the Valley, the air is dammed by the Tehachapi Mountains. The dammed air is forced to return up the eastern SJV, the path of least resistance. **Figure 4-15** shows observations of this flow pattern during the 1990 SJV study. This eddy can cycle pollutants within the San Joaquin Valley, contributing to the high ozone concentration during this episode.

Transport statistics show that the noctural jet can transport material 250 to 350 km overnight (**Figure 4-16**). The transport statistics were calculated from 1600 PST one day to 0400 PST the following day. The winds observed at the profiler are assumed to be spatially consistent to a distance of 350 km (the calculated transport distance). The true transport distance is probably slightly different. Air, possibly containing ozone and ozone precursors, can travel from as far as San Francisco or Sacramento in 12 hours given this transport distance. Ozone and ozone precursors (if any) in this transported air can contribute to the local surface ozone when mixed to the surface during the day.

From 0400 to 1600 PST, the early morning southerly winds associated with the eddy and afternoon northwesterly winds recirculate the air in the SJV. For example, **Figure 4-17** shows high recirculation (i.e., low recirculation factors) and low vector transport distances on August 9. The recirculation allows for local pollution concentrations to build and therefore the recirculation may be an important phenomenon in producing high ozone concentrations in the San Joaquin Valley.

4.3.4 San Joaquin Valley August 26-September 3, 1998 Episode

The meteorology of the August 26–September 3, 1998 episode is similar to that in the August 8-10, 1998 episode. It can be described as a broad flat ridge of high pressure over central and southern California, concurrent with a weak trough in northern California. The flat ridge was accompanied by negative vorticity advection, resulting in subsidence and increased atmospheric stability. The high pressure ridge grew in strength and the weak trough in northern California dissipated. Peak ozone levels rose from 95 ppb on August 26 to 120 ppb on August 27, reaching a peak of 169 ppb on September 1, then decreasing to 119 ppb on September 3. This was an exceptionally long episode, lasting more than a week. The location and strength of the high pressure center throughout this period varied. However, close examination of the National Weather Service charts and peak ozone concentrations reveal that the variations in ozone concentrations correlate well with the periodic short waves of negative vorticity advection into central California. A decline in the strength of the high pressure center and negative vorticity advection (and likely temperatures aloft) coincided with the decrease in ozone on the subsequent days.

Although the synoptic meteorology of this episode is similar to that of August 8-10, 1998, only some of the days during this extended episode had PBL characteristics similar to those of the August 8-10 episode. Similarities include the following:

- C_n^2 and RASS data indicate that the CBL was confined below 800 m for nearly all days.

- The nocturnal jet typically began around 1900 PST.

- Transport of air by the nocturnal jet from the northwest during the overnight hours was observed.

- Early morning eddy flow followed by afternoon northwesterly winds within the PBL resulted in low transport distances and recirculation of air during the day.

On some days during this long episode the PBL characteristics were different than on other days during this episode and during the August 8-10 episode. These dissimilar characteristics as described by mixing depth, transport, ventilation, and recirculation within and above the PBL include the following:

- The CBL grew to 1000 m on August 30 (**Figure 4-18**) and September 3, about 200 to 400 m higher than on other episode days. The increase in depth of the CBL on August 30 did not result in a decrease in the daytime peak surface ozone concentration as would be expected if the aloft air was clean. This implies that 1) the aloft air that was mixed downward during the day contained sufficiently high ozone or ozone precursor concentrations so that it did not dilute the surface ozone concentrations and/or 2) other factors dominated the production of ozone on this day.

- The nocturnal jet ended earlier in the morning. Consequently the overnight transport distances were about half the distance of the prior episode. The shortest overnight transport occurred on August 31 and September 1.

- Eddy flow began earlier and lasted longer compared to the August 8-10 episode. For example, the profiler wind data on August 30 shows that the southerly wind associated with the eddy began at about midnight and lasted until 1100 PST that morning. This morning eddy flow followed by afternoon northwesterly winds within the PBL resulted in very short transport distances ranging from about 35 km at the surface to near zero at about 500 m (**Figure 4-19**). These low transport distances were not a result of light winds, but rather recirculating air. The scalar wind run on this day ranged from about 120 km at the surface to about 60 km at about 500 m (Figure 4-19). The low vector transport distances divided by the moderate scalar wind run, translates into high recirculation of air in the region on this day (Figure 4-19). This high recirculation could have contributed to the 161 ppb peak ozone concentration observed at Clovis on this day.

4.3.5 Ventura County August 5-8, 1997 Episode

The meteorology of the August 5-8, 1997 episode could be described as a strong ridge of high pressure over southern California, extending well to the north. The ridge was accompanied by negative vorticity advection, resulting in subsidence and increased atmospheric stability. The high pressure ridge grew in strength reaching its peak on the peak ozone day. Peak ozone levels rose from 96 ppb on August 5 to the episode peak of 134 ppb on August 6, then decreased to 116 ppb on August 7. A decline in the strength of the high pressure center and negative vorticity advection coincided with the decrease in ozone on the subsequent days.

The important meterological features as observed and calculated from the profiler and RASS data include the following:

Mixing Depth

On two of the episode days (August 6 and 7) the daytime mixing depth was characterized by convective mixing (this was the CBL) in the morning hours and by the marine intrusion (the marine boundary layer) in the afternoon hours. **Figure 4-20** shows a time/height cross section of C_n^2 data and vertical velocity data on August 6, 1997 and this figure is used to illustrate the daytime mixing characteristics. From dawn to midday the convective boundary layer grows upward until about 1100 PST. During this same time period, the daytime heating, which drives the CBL growth, also creates and onshore pressure gradient between the cool Pacific Ocean and the warm interior valley. This onshore pressure gradient draws marine air inland. This relatively cool marine air undercuts the CBL at about 1100 PST, immediately lowering the mixing depth from about 1000 m to about 400 m. Note that the peak C_n^2 data continued to depict the top of the CBL even after it was undercut by the marine boundary layer.

The growth of the CBL mixes air from 1000 m to the surface on August 6. This means that if the aloft air contains high ozone concentrations, then the air up to 1000 m would contribute to the surface ozone concentration. When the marine boundary layer (MBL) forms at about 1100 PST, the aloft air above the MBL no longer contributes to the surface ozone.

August 8 is a particularly interesting case because the C_n^2 data do not resolve the marine boundary layer or CBL. The C_n^2 data only depict the subsidence inversion, at about 800 m (**Figure 4-21**). On the other hand, the vertical velocity data (Figure 4-21), the profiler winds, and the RASS virtual temperature data (**Figure 4-22**) show the mixed layer at about 600 m. This layer is either the marine boundary layer or CBL or a combination of both. The fact that the mixed layer never grows higher than about 600 m means that air above this layer did not contribute to the high surface ozone concentrations on this day.

Transport, Ventilation, and Recirculation

At the Simi Valley profiler site the onset of the marine boundary layer that is shown in the C_n^2 and RASS data is also observed in the profiler wind data. For example, during the morning of August 6, the air flow in the lowest 300 m is variable within the growing CBL. At about 1100 PST, a marine front is indicated by the onset of westerly flow, undercutting the CBL **(Figure 4-23)**. Throughout the afternoon, the depth of the marine boundary layer grows. At about 1600 PST the westerly winds reach about 500 m.

It was mentioned above that the CBL growth on August 6 mixed aloft air (air up to 1000 m) with the surface air. The profiler data indicate that this aloft air was transported about 200 km from the north over night, assuming that the profiler winds are spatially representative over such a distance. If this air is polluted then aloft transport could play a role in the high surface ozone concentrations observed in Simi Valley on August 6.

The northeasterly and easterly winds to 0800 PST on August 6 followed by westerly winds during the afternoon of August 6 resulted in low recirculation factors. The low recirculation factors mean that the air below 500 m was recirculated in Simi Valley and this could have contributed to the high ozone concentrations observed on this day.

4.3.6 Ventura County July 15-20, 1998 Episode

The meteorology of the July 15-20, 1998 episode was typical of episodes in California. High pressure moved over the area from the south, with increasing subsidence and slight offshore flow throughout the episode. Peak ozone levels rose from 110 ppb on July 15 to 124 ppb on July 16, peaking at 174 ppb on July 17, decreasing to 137 ppb on July 18, 125 ppb on July 19, and 72 ppb on July 20. On July 17 the peak of the episode, the high pressure center located east of California reached its strongest point. A decline in the strength of the high pressure center and concurrent subsidence coincided with the decrease in ozone on the subsequent days. Note that this episode coincided with an episode in Sacramento County except that the Sacramento County episode started one day later and ended two days earlier. However, both regions experienced peak ozone levels on the same day, coinciding with the highest pressure and other favorable conditions for ozone formation.

The Radar profiler and RASS data indicate a few differences in the PBL structure during this episode compared to the August, 1997, episode, including the following:

- From July 15 through July 18 the mixing depth was never deeper than about 600 m. This shallow mixing depth confines pollution near the surface, thereby contributing to the high ozone concentrations during the episode. The shallow mixing depth also means that ozone or ozone precursors in the air above 600 m did not contribute to the local surface ozone. During the August 1997 episode air up to 1000 m mixed with surface air and could have contributed to the surface ozone.

- From July 15 through July 18 the mixing appeared to be defined by the marine boundary layer, rather than by the CBL. For example, **Figure 4-24** shows a time/height cross section of C_n^2 and vertical velocity data on July 15. The peak C_n^2 and vertical velocity data show the mixing depth at about 350 to 400 m throughout the day.
- On July 19 and 20 the CBL defined the mixing depth in the morning hours and the MBL defined the mixing depth in the afternoon hours. This pattern was observed in the August 1997 episode. The increase in the vertical dilution of surface pollution caused by the increase in mixing associated with the CBL may partially explain why peak ozone concentrations were lower on July 19 and 20 compared to the first three days of this episode. This conclusion assumes that the aloft air was relatively clean.

Other interesting characteristics of this episode are the short transport distances and high recirculation. Most notably, the overnight transport from July 16 at 1600 PST to July 17 at 0400 PST was only 25 km within the lowest 800 m (**Figure 4-25**). Note that air only up to about 600 m could contribute to the surface ozone concentration (i.e., the peak mixing height on July 17). Also, the daytime recirculation factors on July 17 were low in the lowest 800 m, meaning that there is evidence of recirculation of air in Simi Valley. The recirculation on this day was caused by early morning southeasterly winds followed by midmorning westerly winds (**Figure 4-26**). The short transport distance coupled with recirculation is likely a major contributor to the high ozone concentrations on July 17.

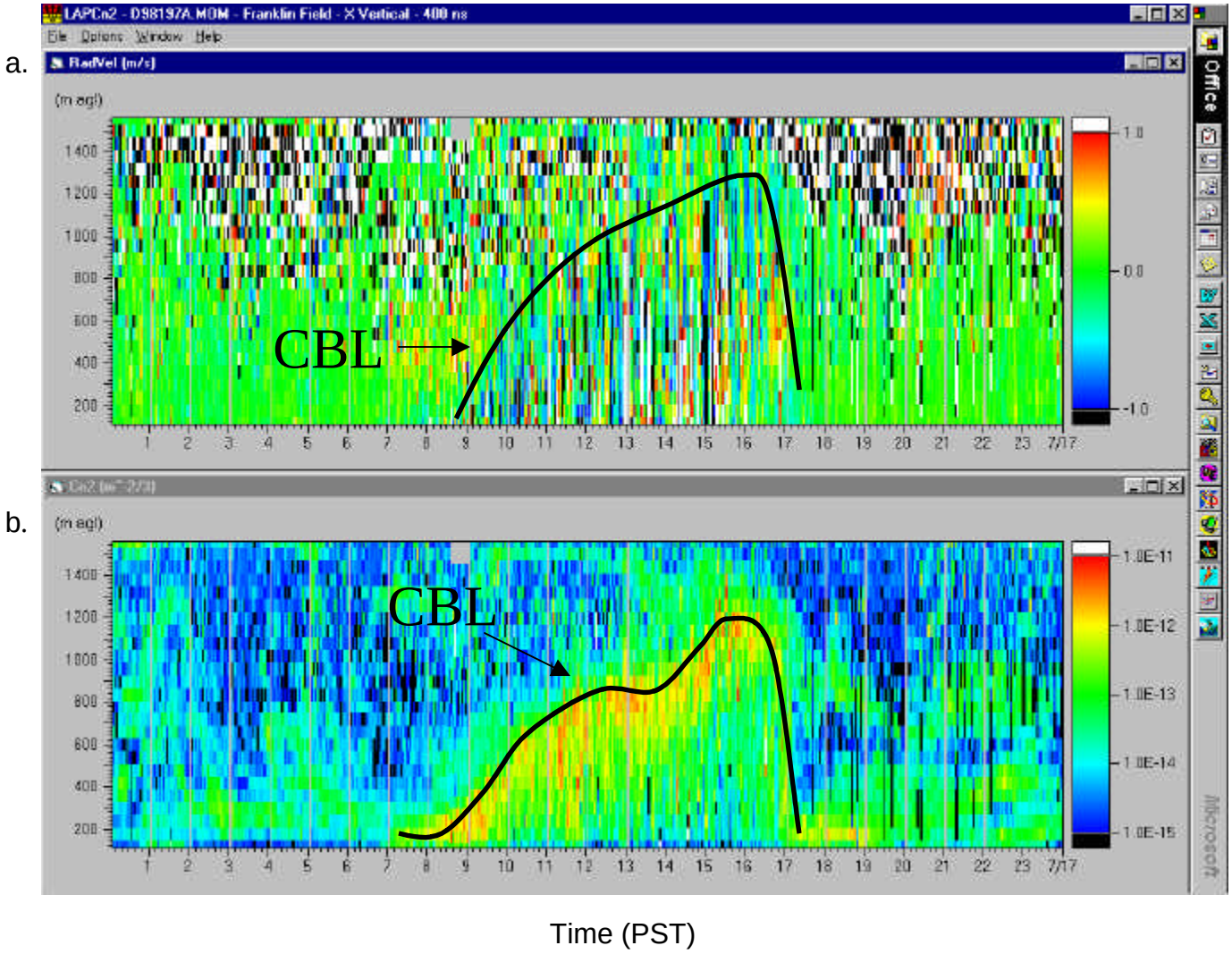

Figure 4-1. Time/height cross section of radar profiler a) vertical velocity and b) C_n^2 data at Franklin Field on July 16, 1998. The top of the CBL is shown as a black line.

a.

b.

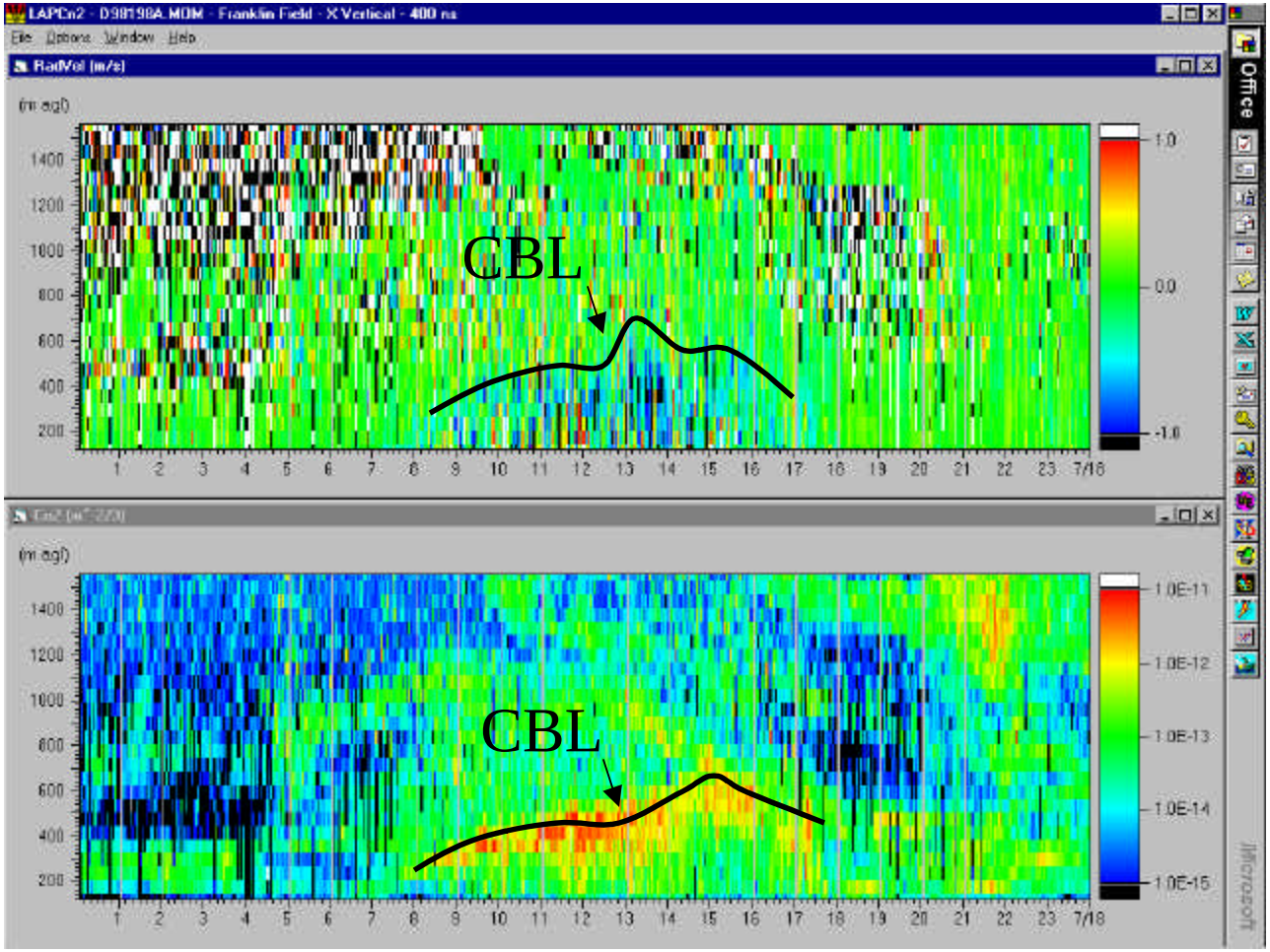

Time (PST)

Figure 4-2. Time/height cross section of radar profiler a) vertical velocity and b) C_n^2 data at Franklin Field on July 17, 1998. The top of the CBL is shown as a black line.

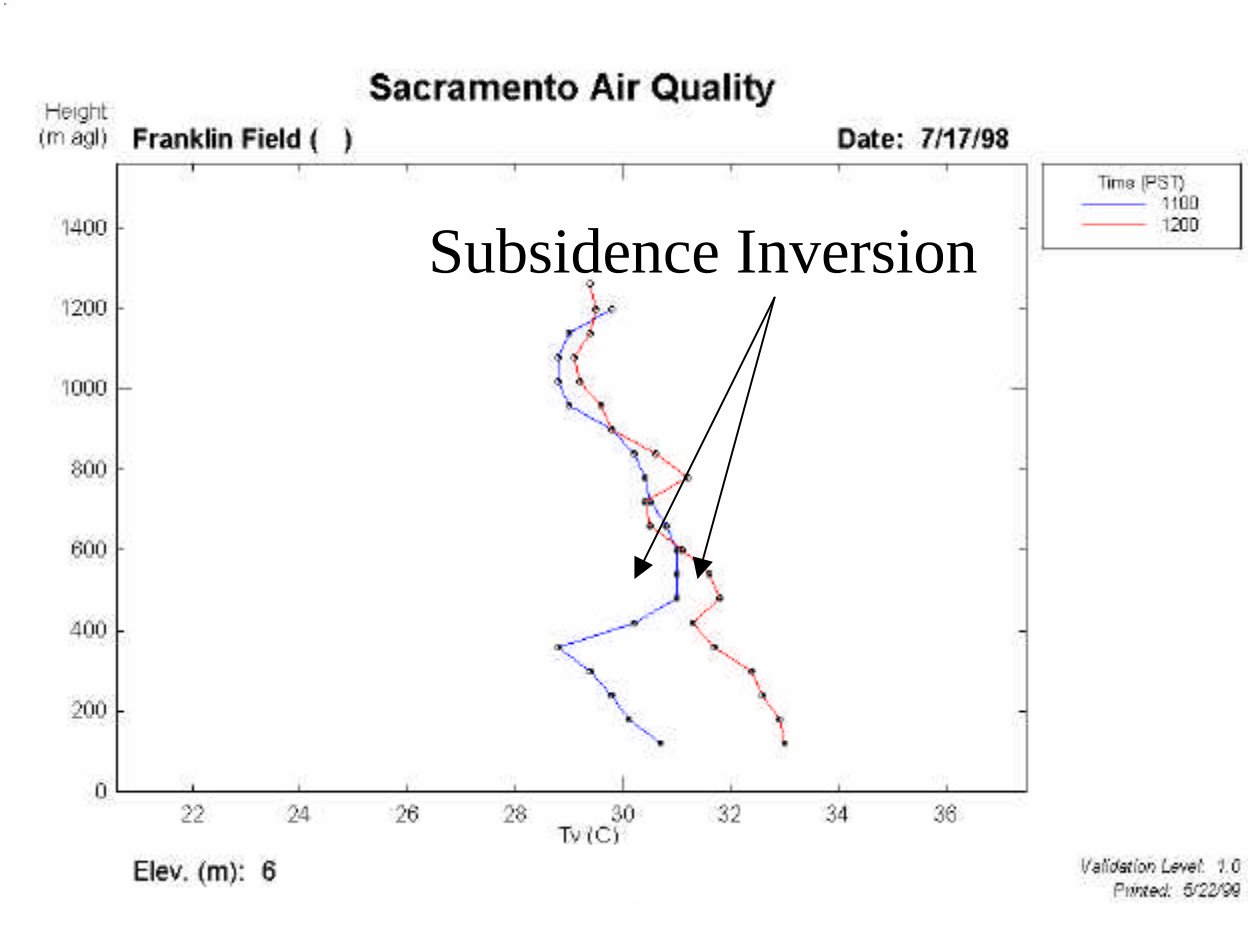

Figure 4-3. RASS virtual temperature data at Franklin Field on July 17, 1998 showing a subsidence inversion at about 500 m.

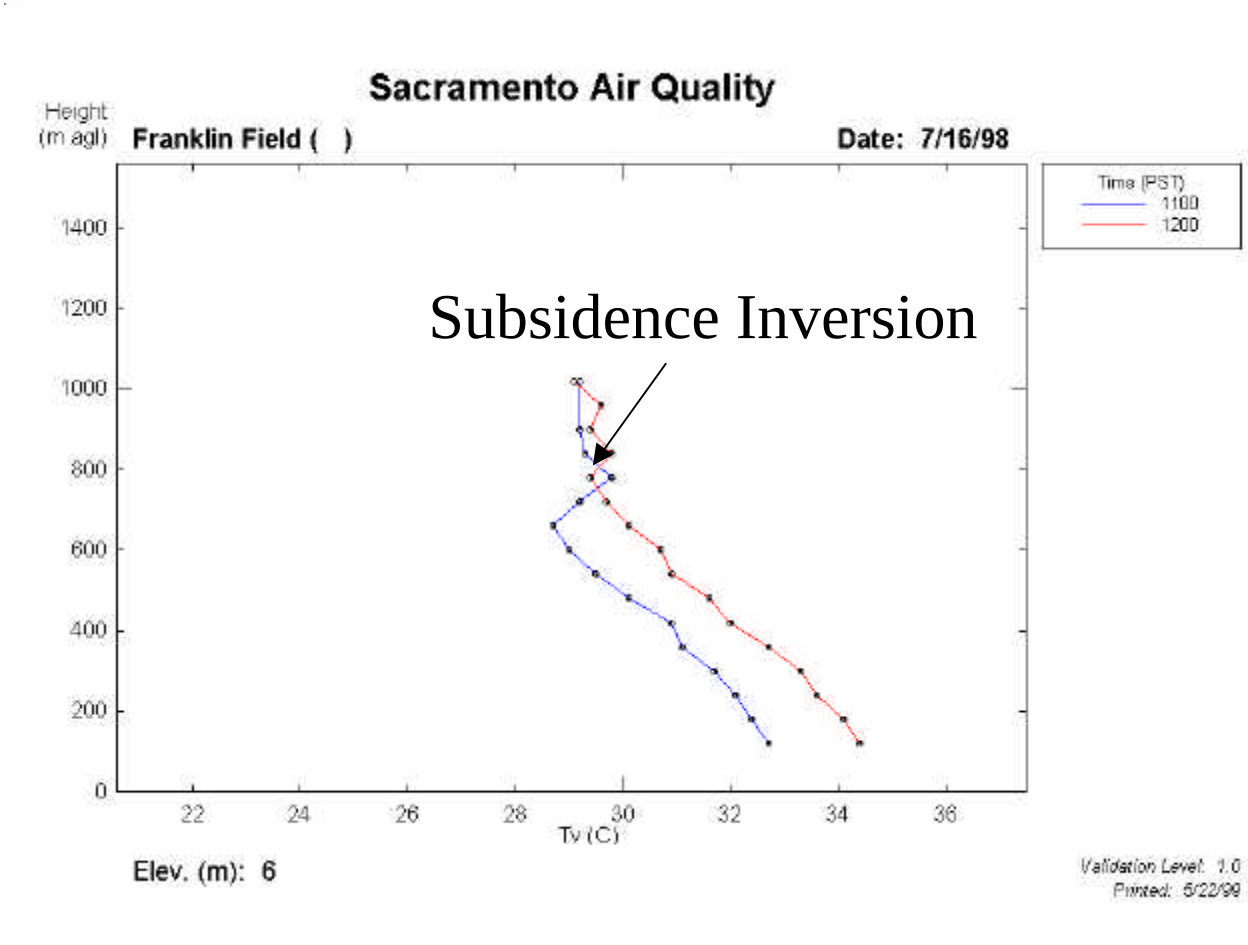

Figure 4-4. RASS virtual temperature data at Franklin Field on July 16, 1998 showing a subsidence inversion at about 800 m.

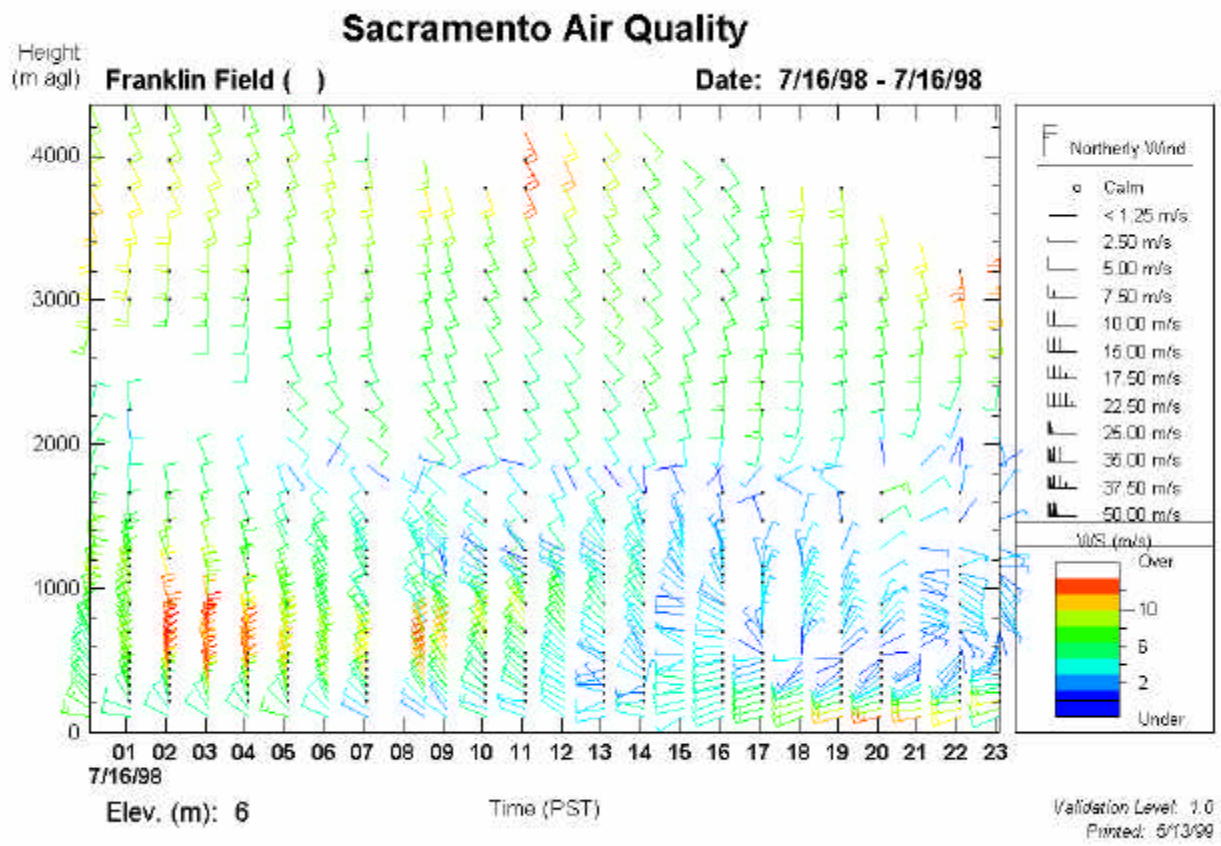

Figure 4-5. Radar profiler wind data at Franklin Field on July 16, 1998 showing well organized northerly to northwesterly winds below about 1500 m. Notice the onset of the delta breeze at about 1300 PST below 500 m.

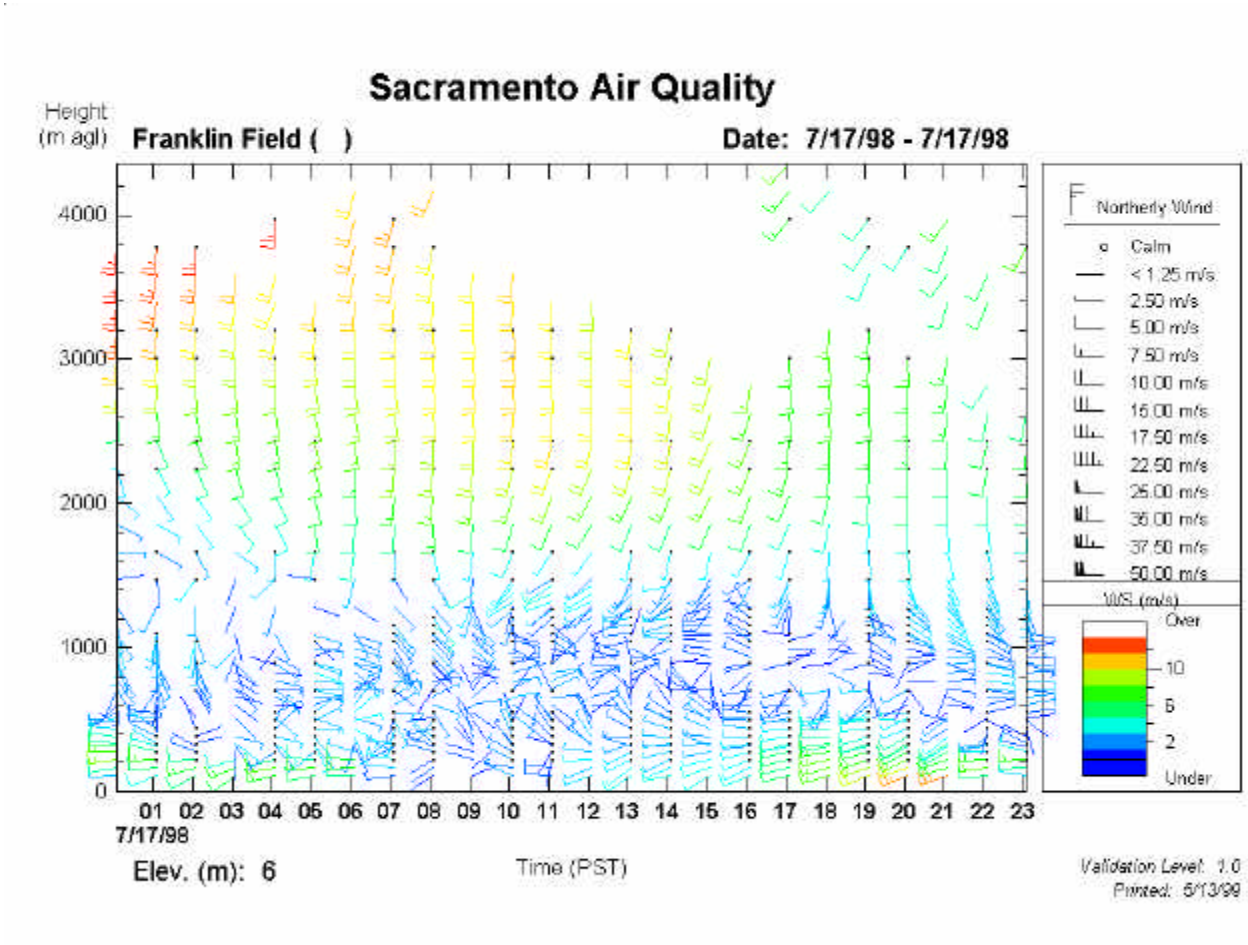

Figure 4-6. Radar profiler wind data at Franklin Field on July 17, 1998 showing more disorganized flow below about 1000 m compared to July 16, 1998. Notice the onset of the delta breeze at about 1200 PST below 500 m.

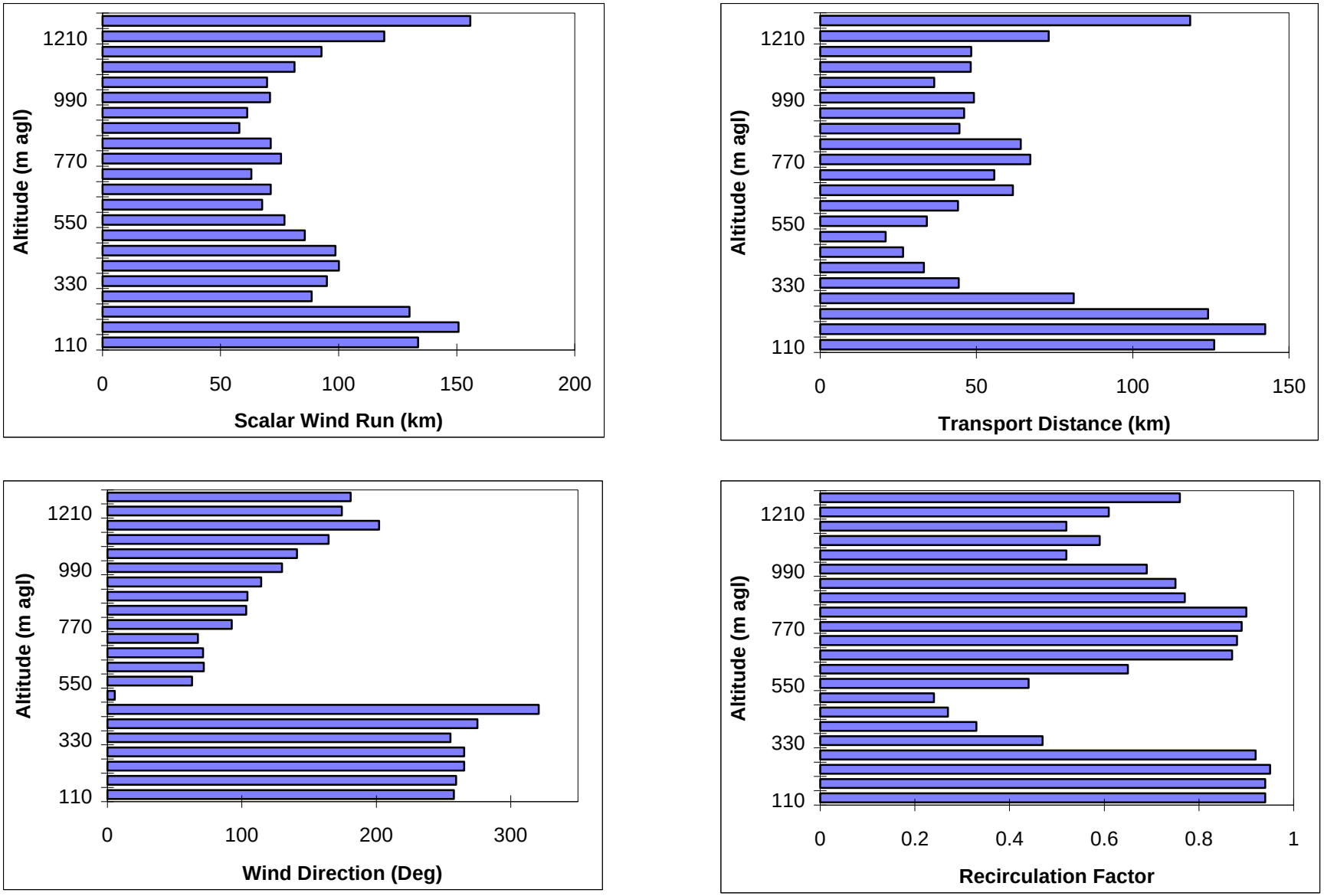

Figure 4-7. Twelve-hour daytime transport statistics at Franklin Field from 0400 to 1600 PST on July 17, 1998.

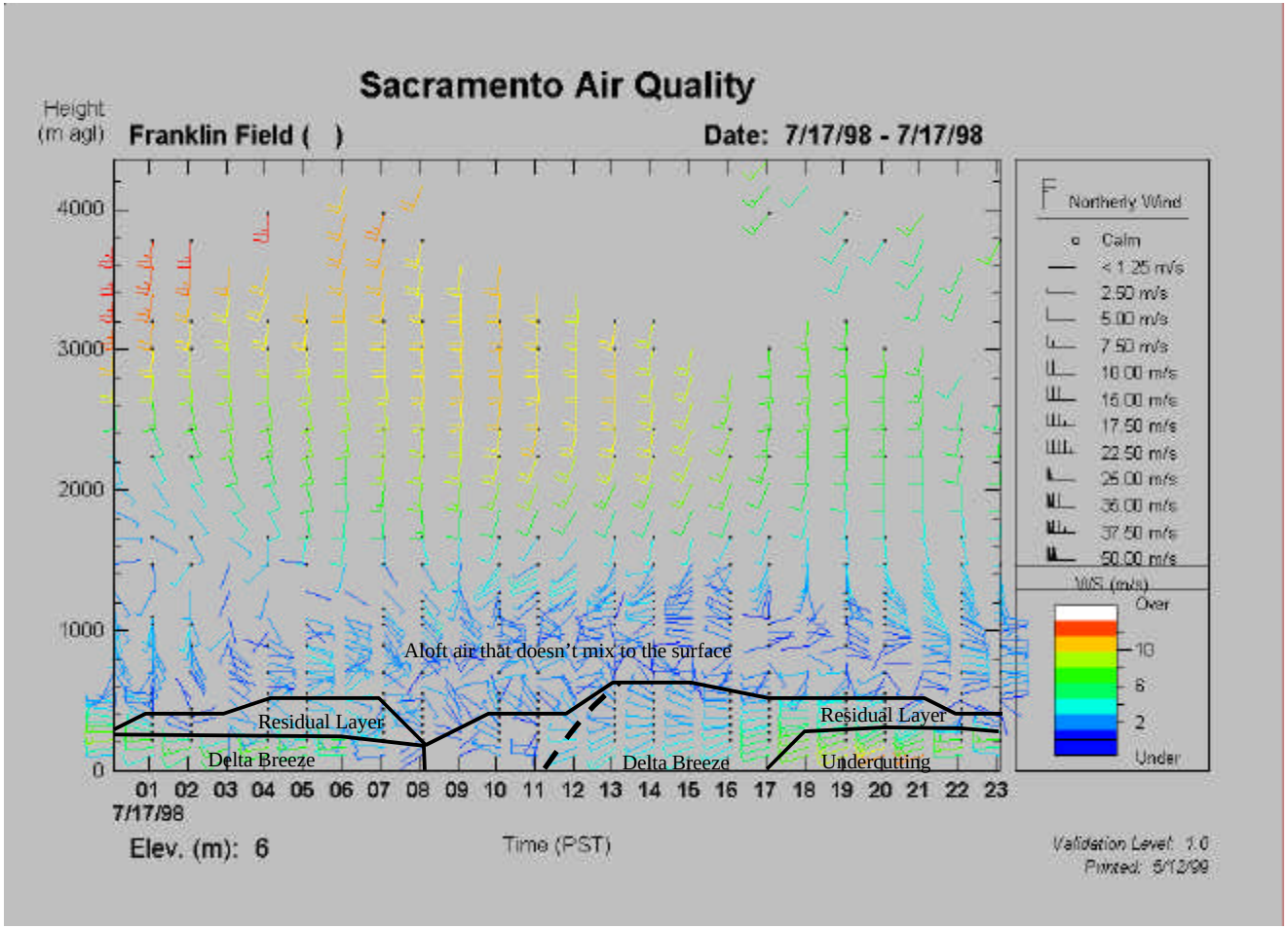

Figure 4-8. Radar profiler wind data and estimated boundary layers (black lines) at Franklin Field on July 17, 1998.

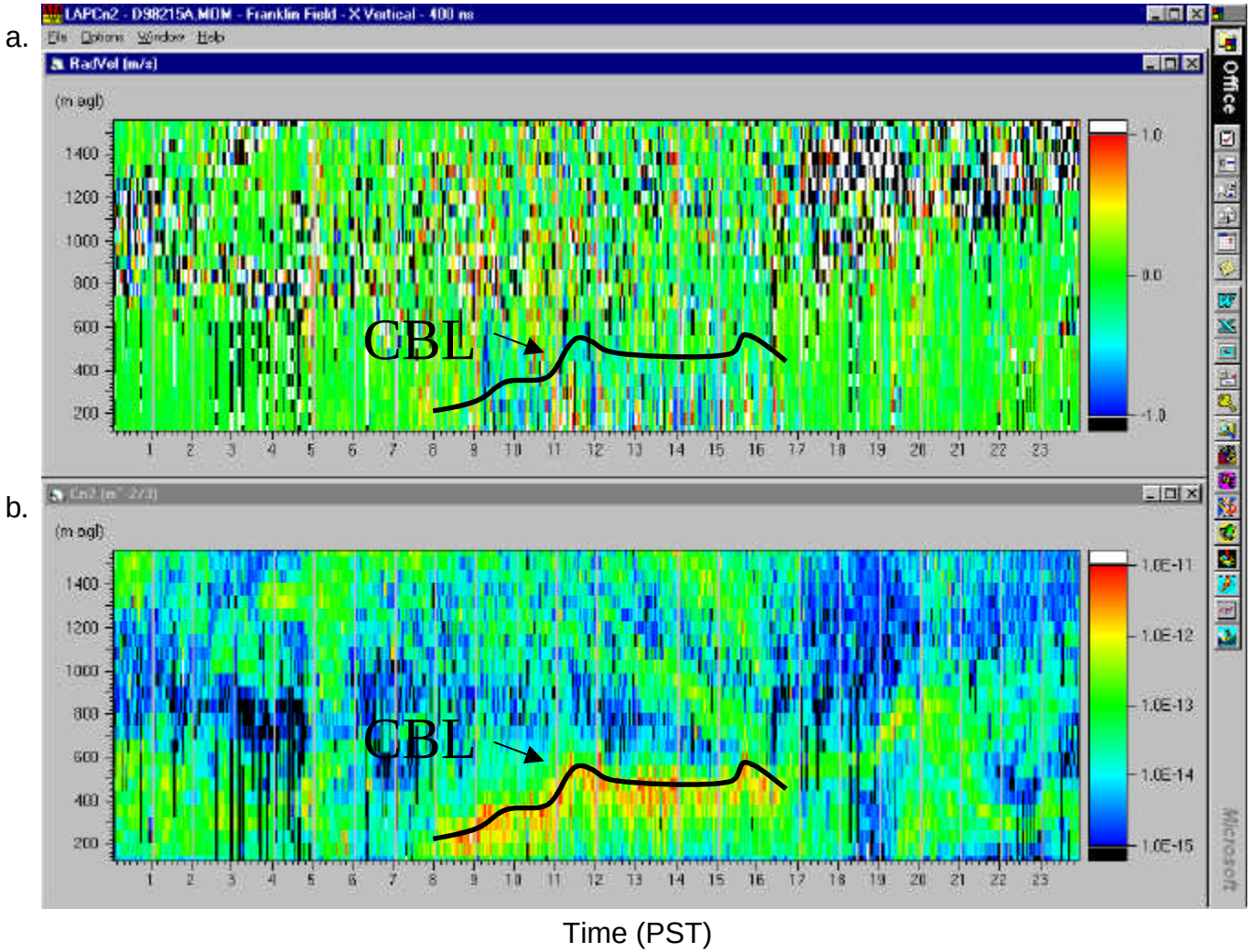

Figure 4-9. Time/height cross section of radar profiler a) vertical velocity and b) C_n^2 data at Franklin Field on August 3, 1998. The top of the CBL is shown as a black line.

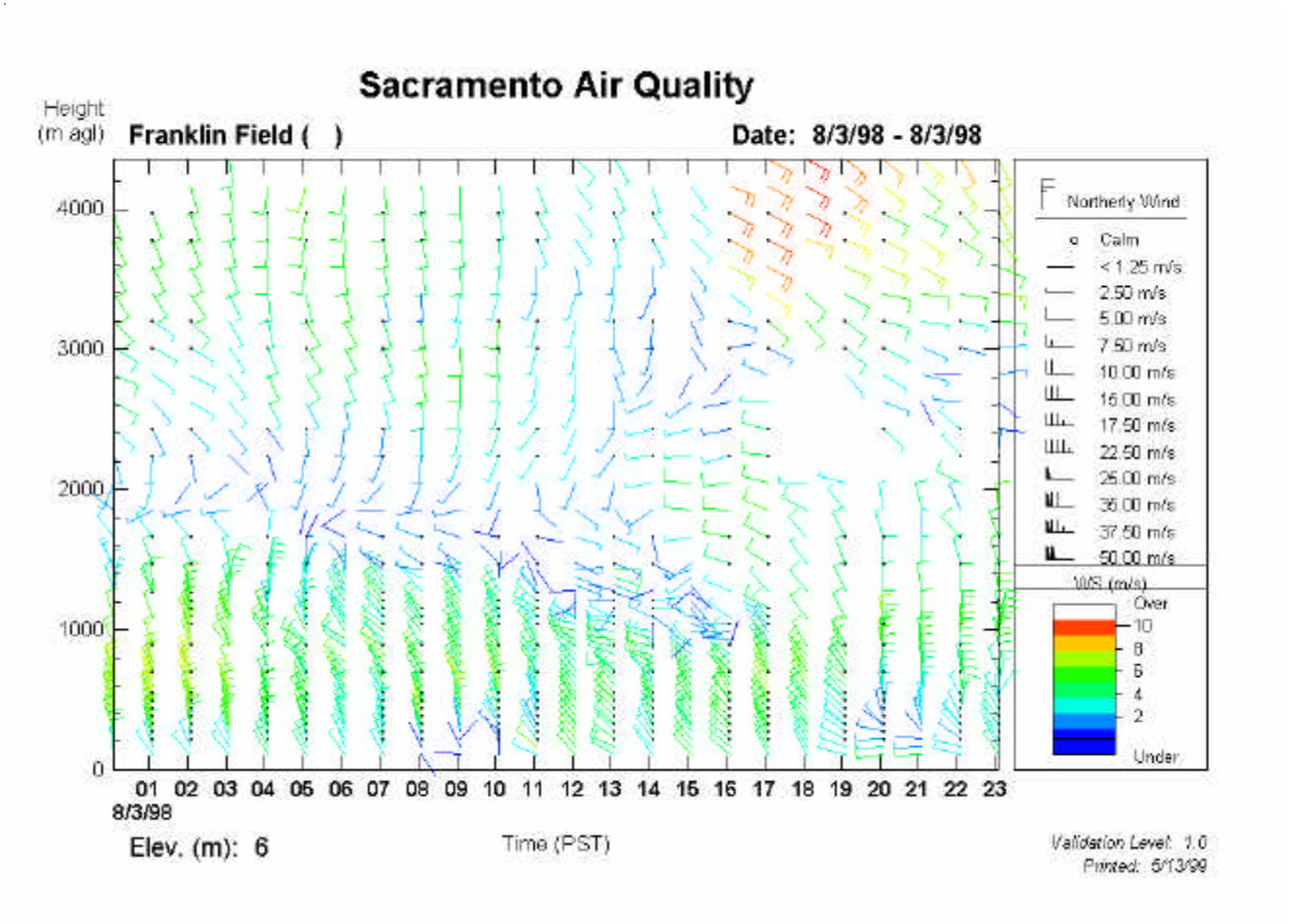

Figure 4-10. Radar profiler wind data at Franklin Field on August 3, 1998 showing well organized northerly to northwesterly winds below about 1500 m. Notice the late onset of the delta breeze at about 1900 PST below 200 m.

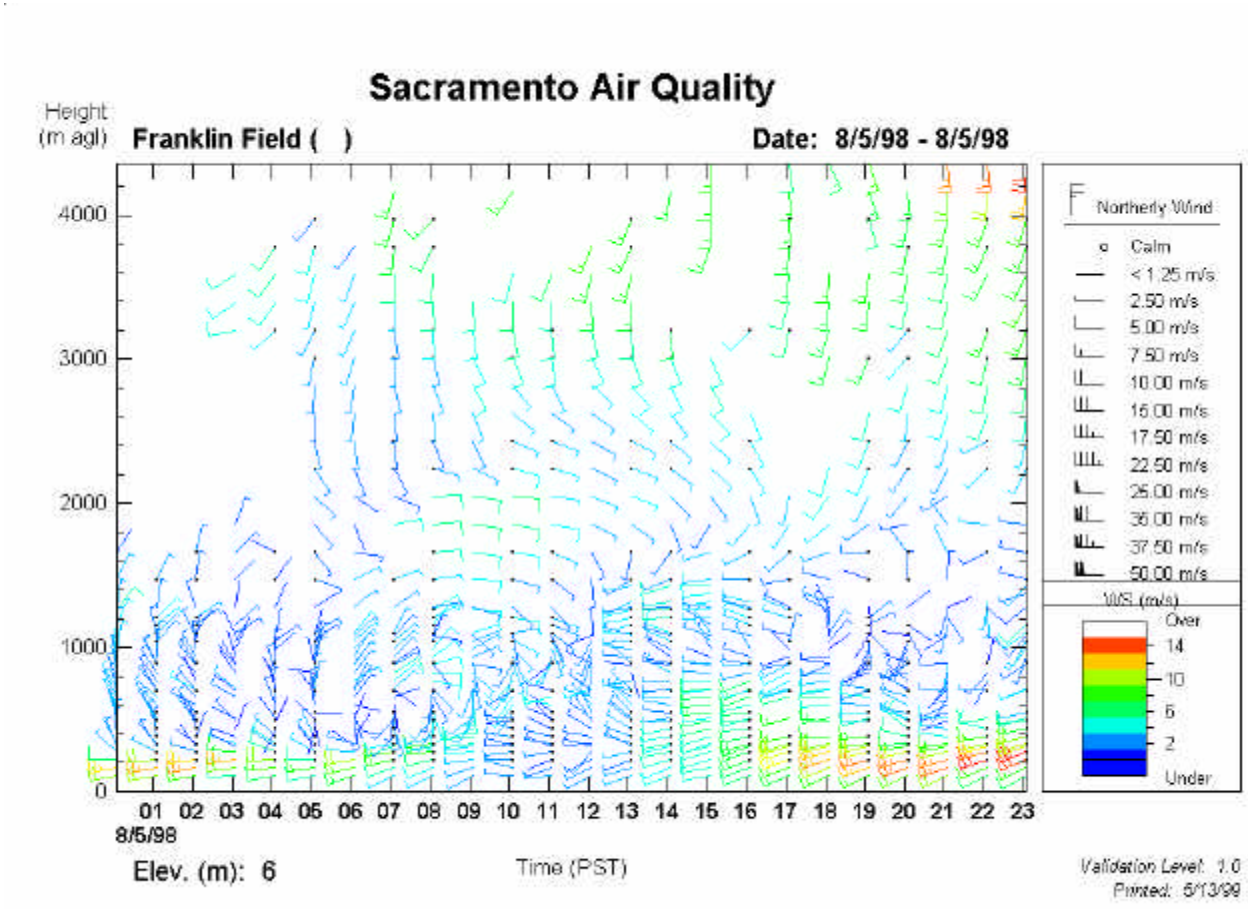

Figure 4-11. Radar profiler wind data at Franklin Field on August 5, 1998 showing the west to southwest delta breeze. Notice that the delta breze is confined to about 200 m from 0000 PST until 1300 PST.

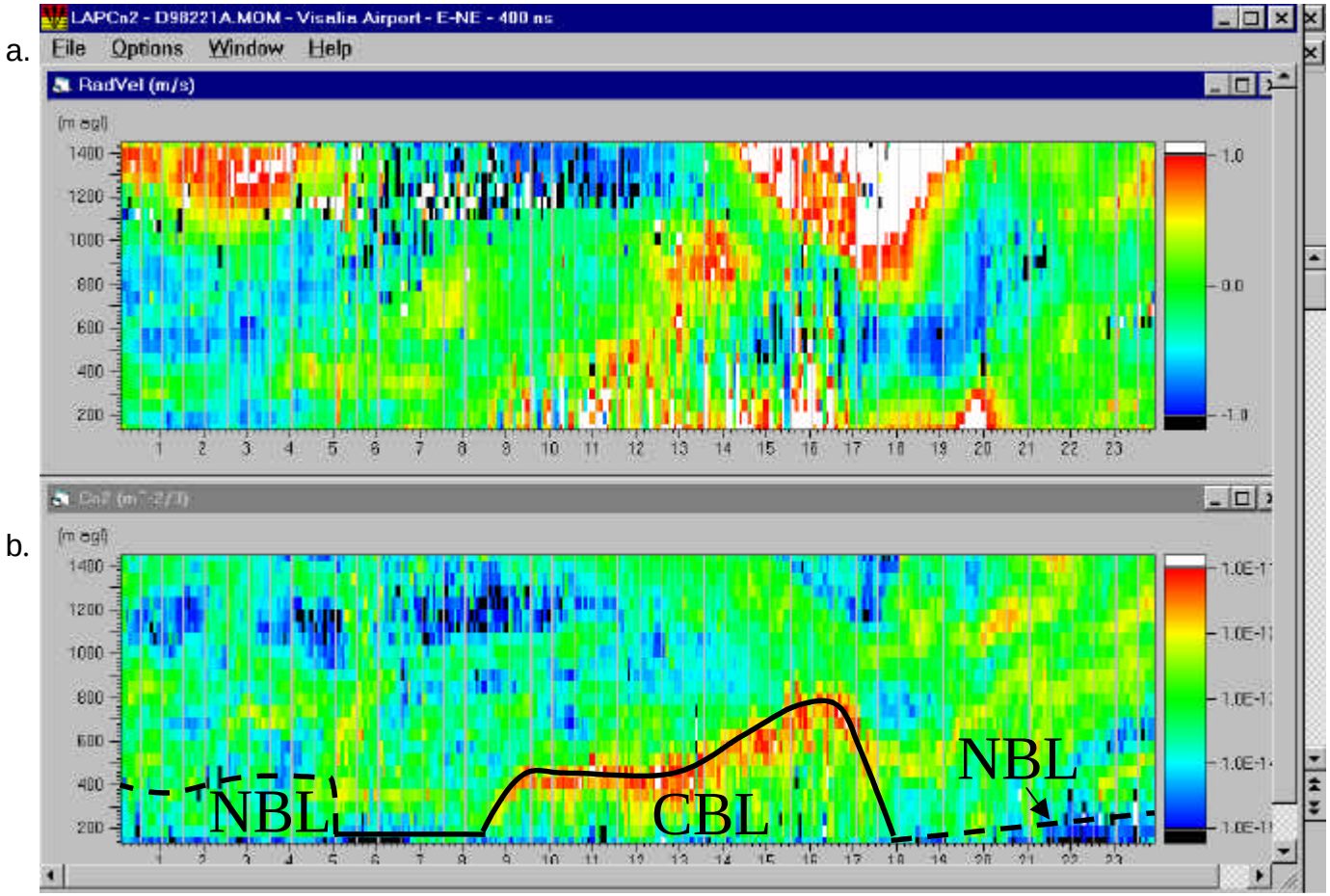

Time (PST)

Figure 4-12. Time/height cross section of radar profiler a) radial velocity and b) C_n^2 data at Visalia on August 9, 1998. The top of the CBL is shown as the black solid line and the top of the NBL is shown as the black dashed line. Note that the NBL and the CBL from 0500 to 0800 PST were estimated from RASS virtual temperature data.

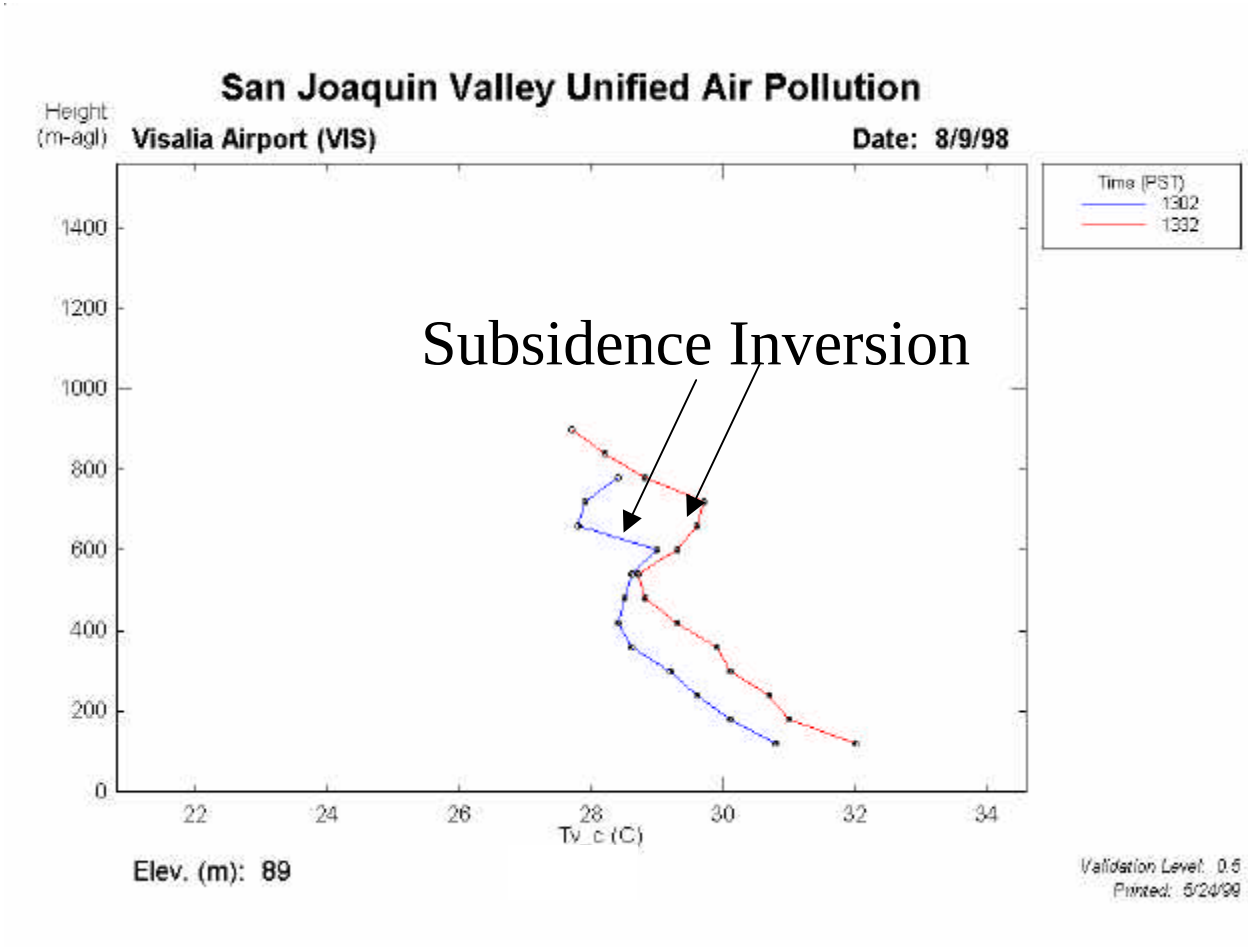

Figure 4-13. RASS virtual temperature data at Visalia on August 9, 1998 showing a subsidence inversion at about 700 m.

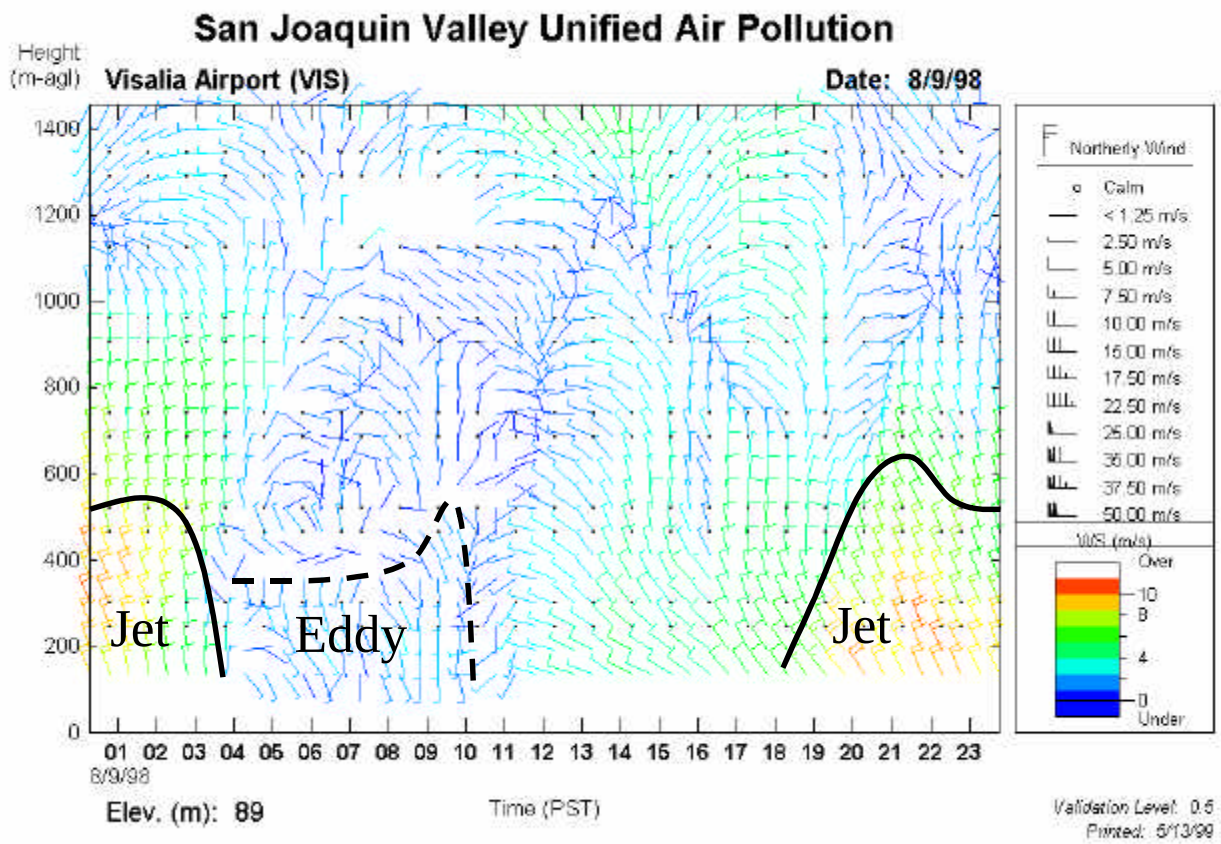

Figure 4-14. Radar profiler wind data at Visalia on August 9, 1998 showing the nocturnal jet and eddy flow. This wind pattern was observed on the majority of the episode days.

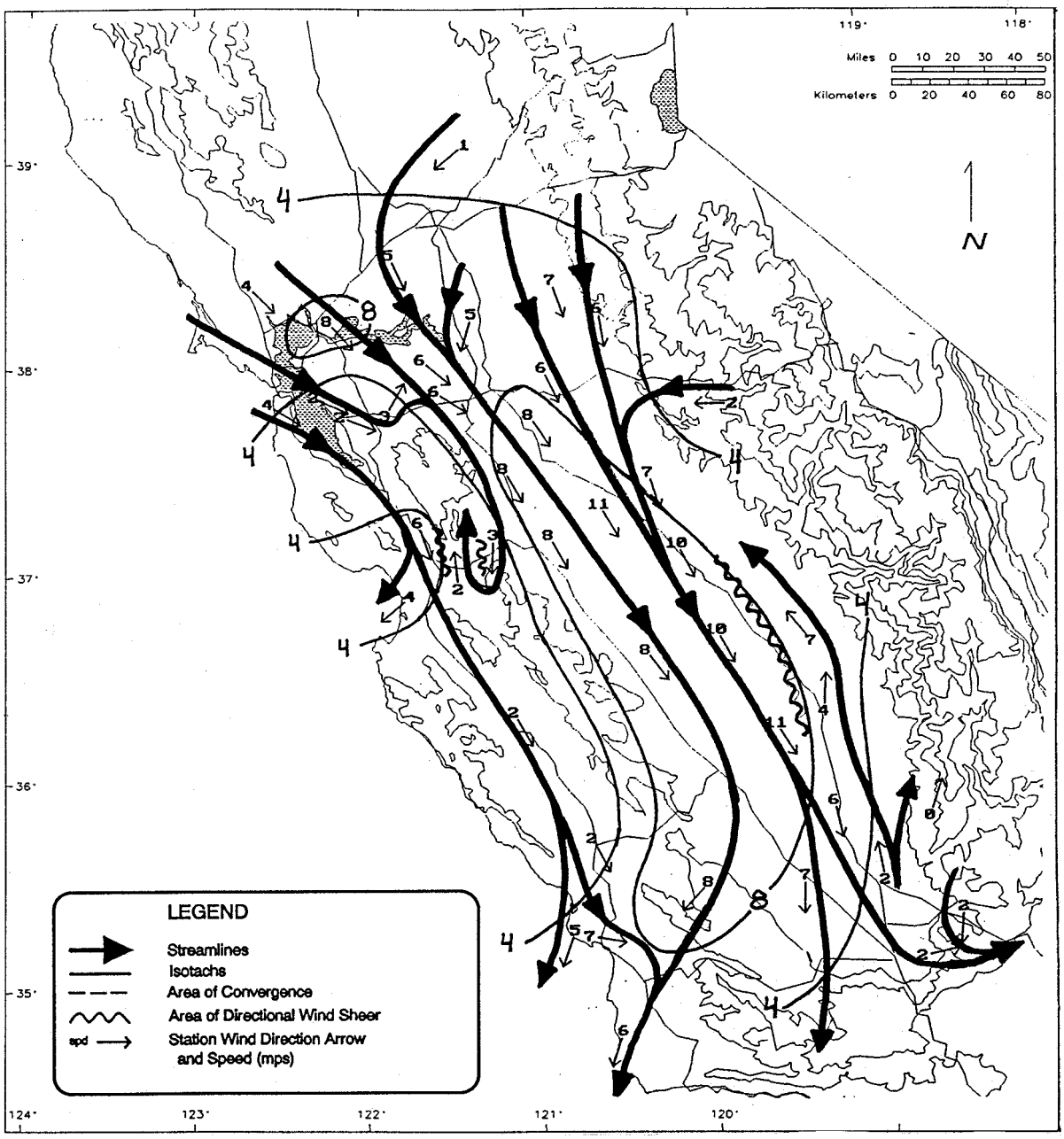

Figure 4-15. Winds at 400 m agl for August 5, 1990 at 0400 PDT (from Lehrman et al., 1994).

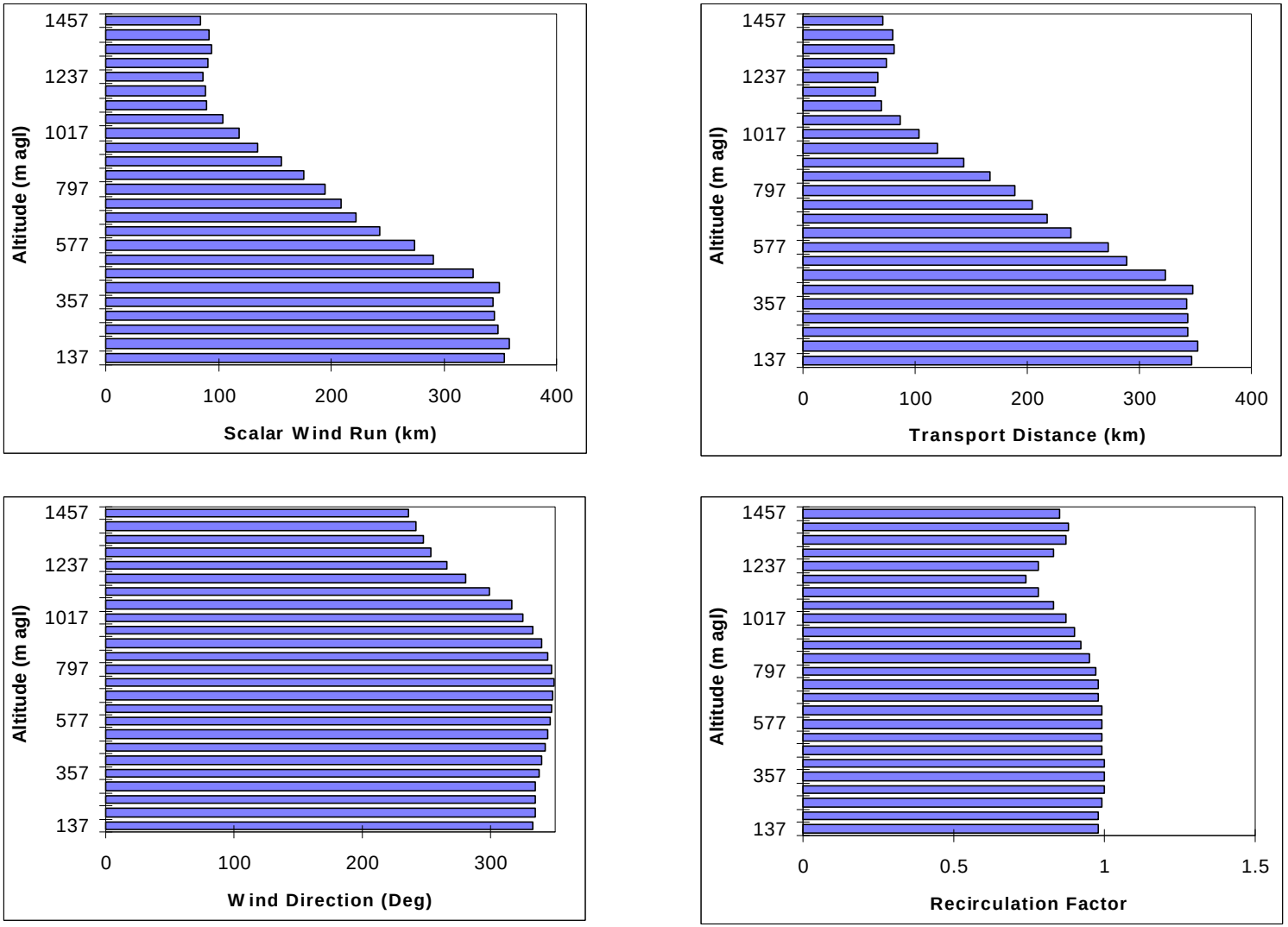

Figure 4-16. Twelve-hour nighttime transport statistics at Visalia from August 8, 1998 at 1600 PST to August 9, 1998 at 0400 PST.

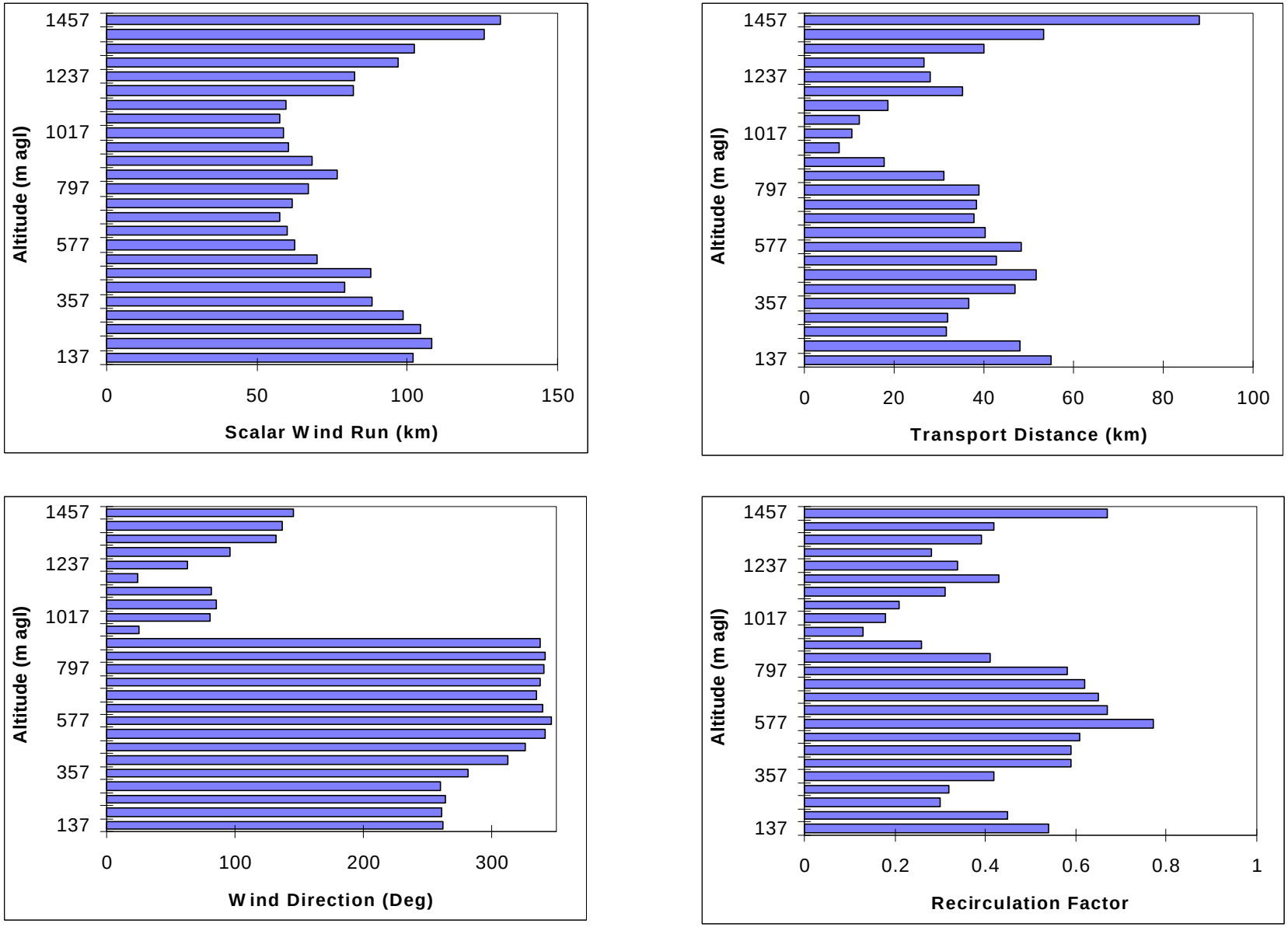

Figure 4-17. Twelve-hour daytime transport statistics at Visalia from 0400 to 1600 PST on August 9, 1998.

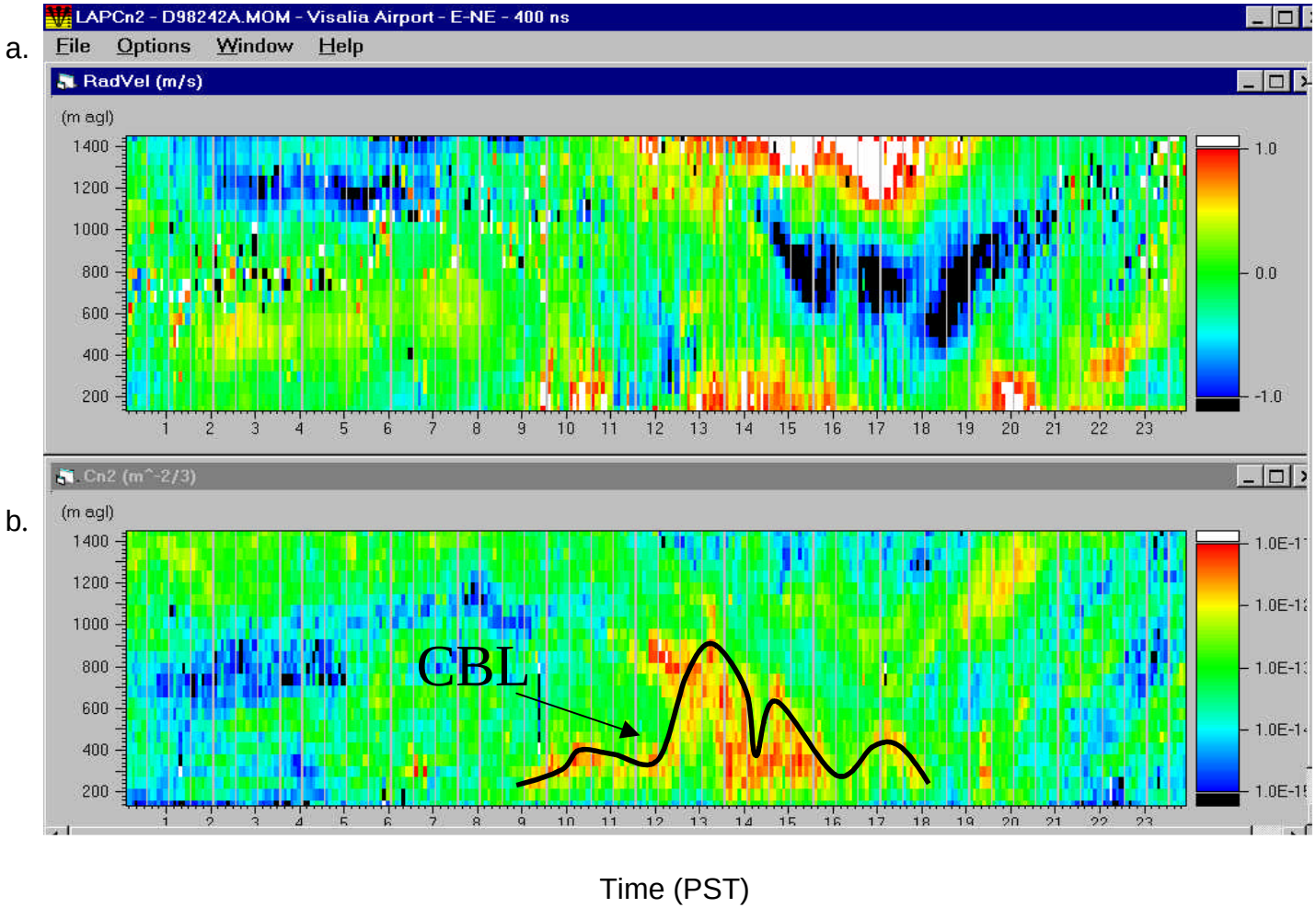

Figure 4-18. Time/height cross section of radar profiler a) radial velocity and b) C_n^2 data at Visalia on August 30, 1998. The top of the CBL is shown as the black solid line.

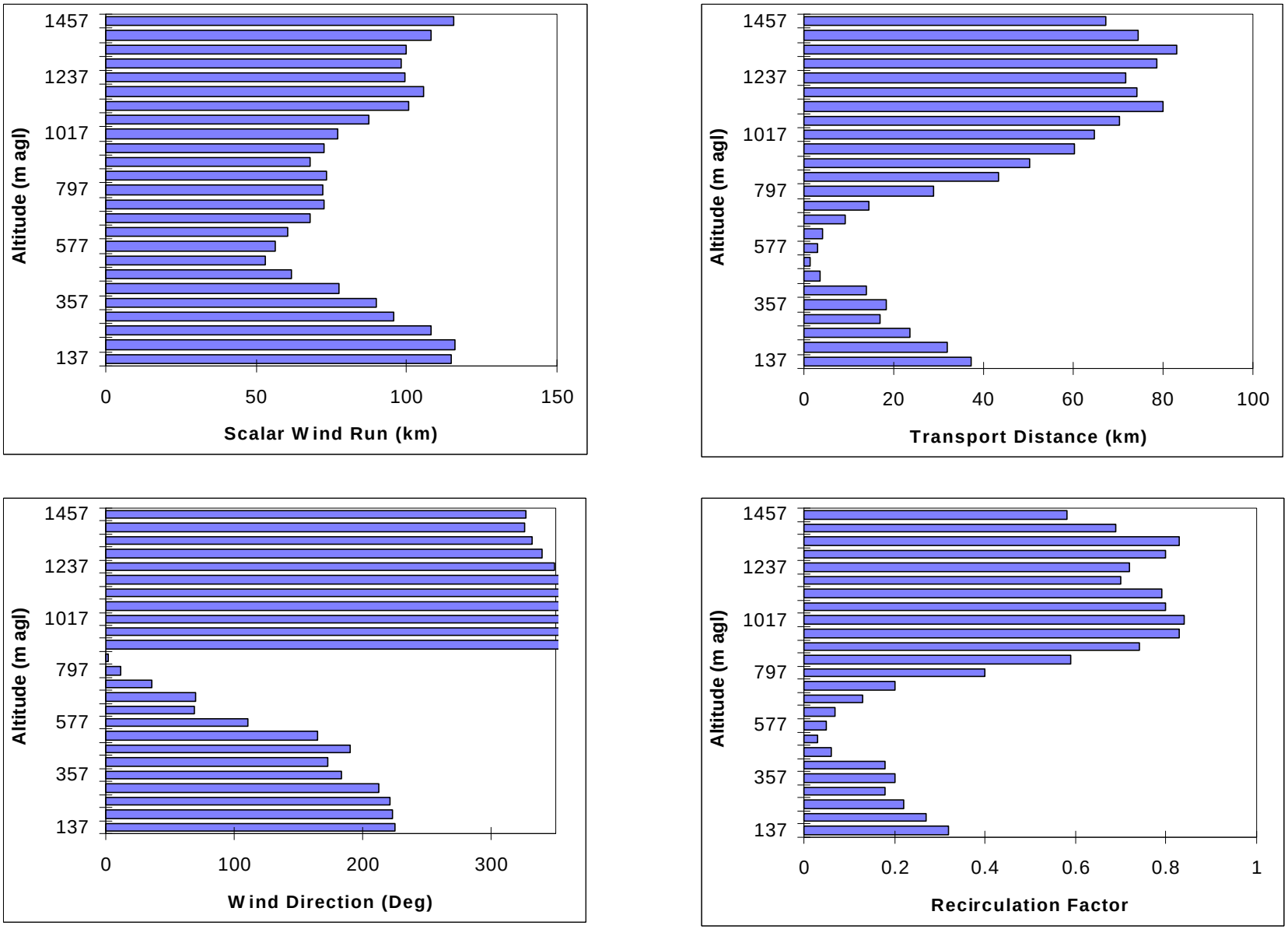

Figure 4-19. Twelve-hour daytime transport statistics at Visalia from 0400 to 1600 PST on August 30, 1998.

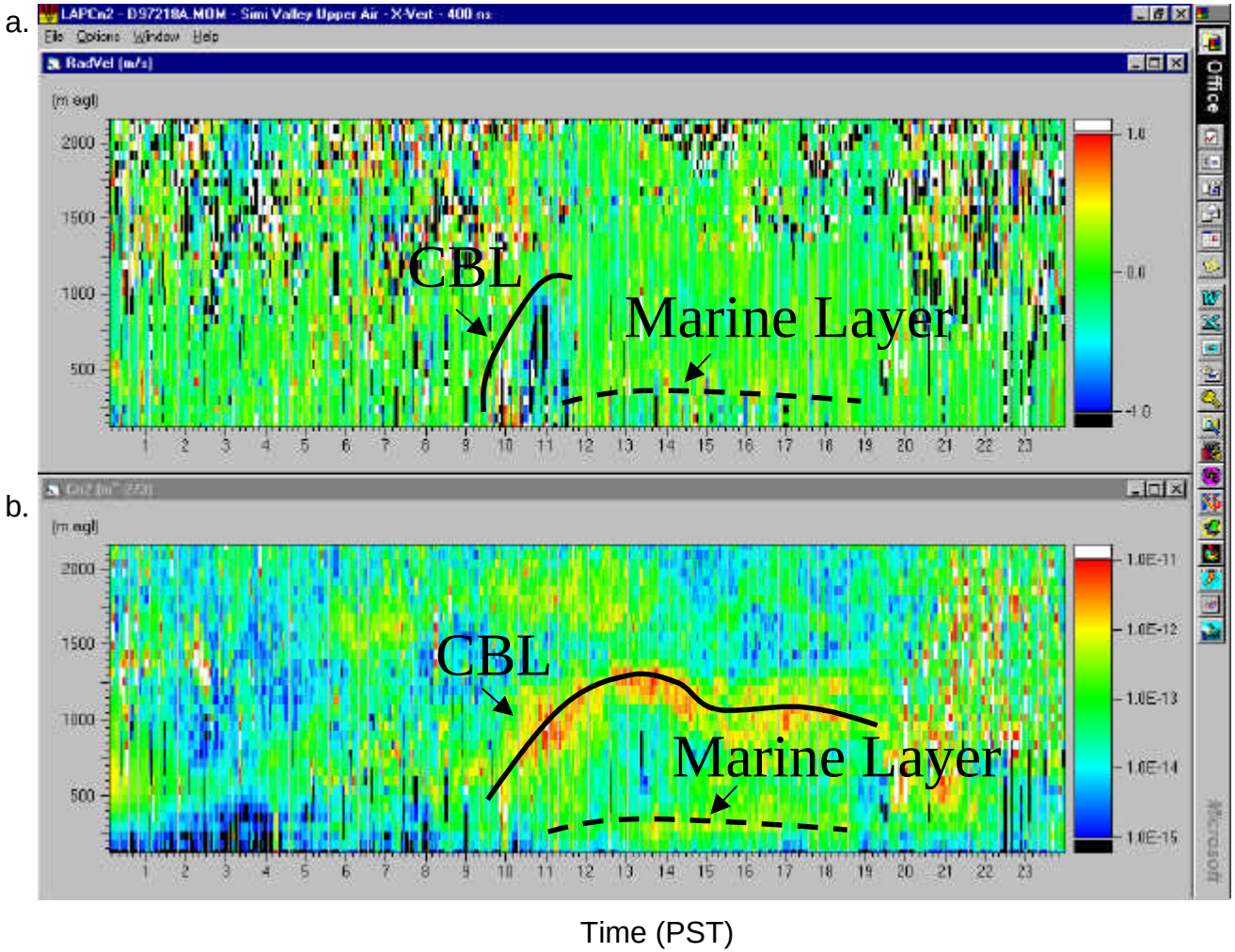

Figure 4-20. Time/height cross section of radar profiler a) vertical velocity and b) C_n^2 data at Simi Valley on August 6, 1997. The top of the CBL is shown as the black solid line and the top of the marine layer is shown as the black dashed line.

a.

b.

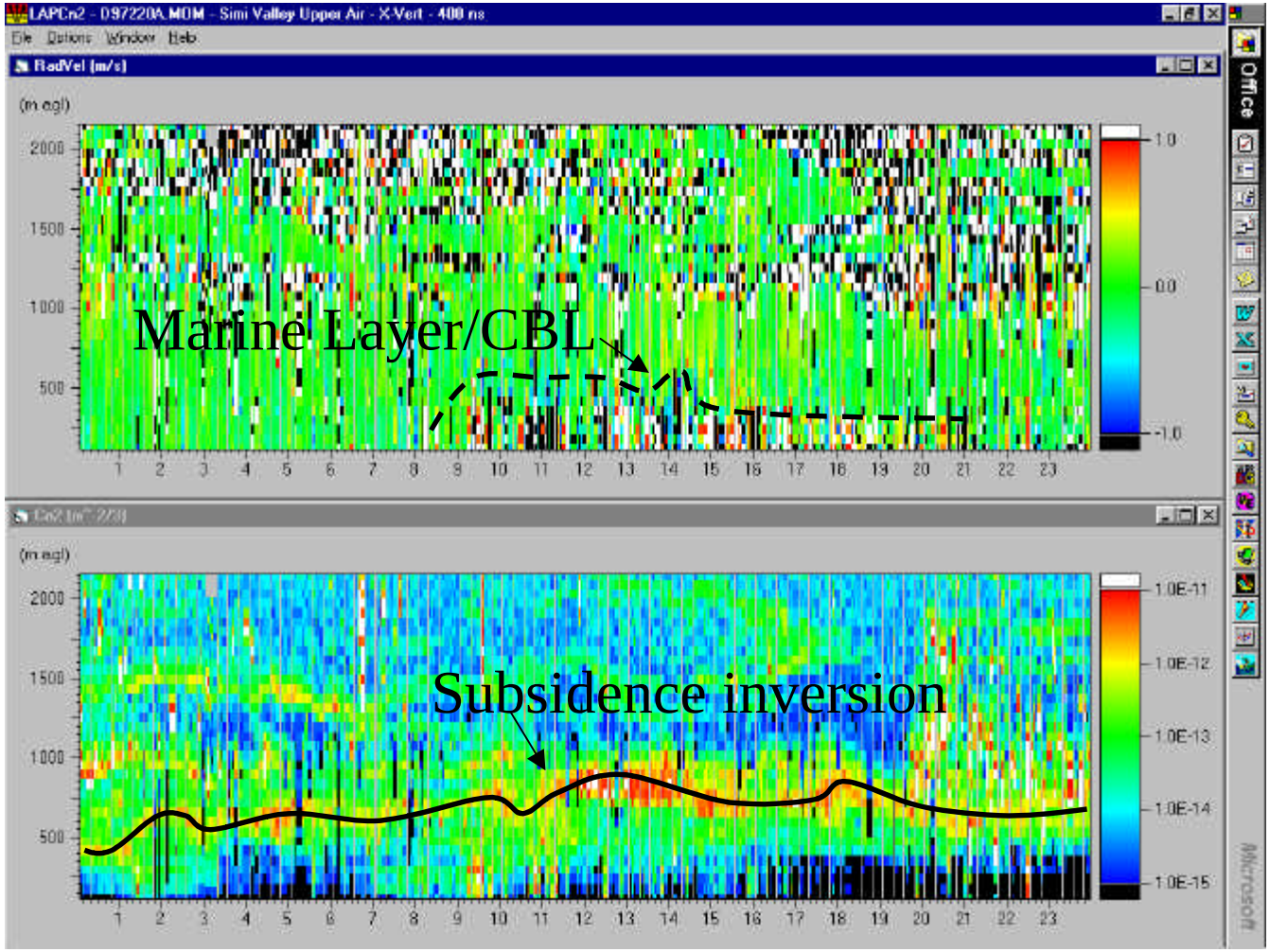

Time (PST)

Figure 4-21. Time/height cross section of radar profiler a) vertical velocity and b) C_n^2 data at Simi Valley on August 8, 1997. The top of the marine layer/CBL is shown as the dashed black line. And what appears to be a subsidence inversion is shown as a black solid line.

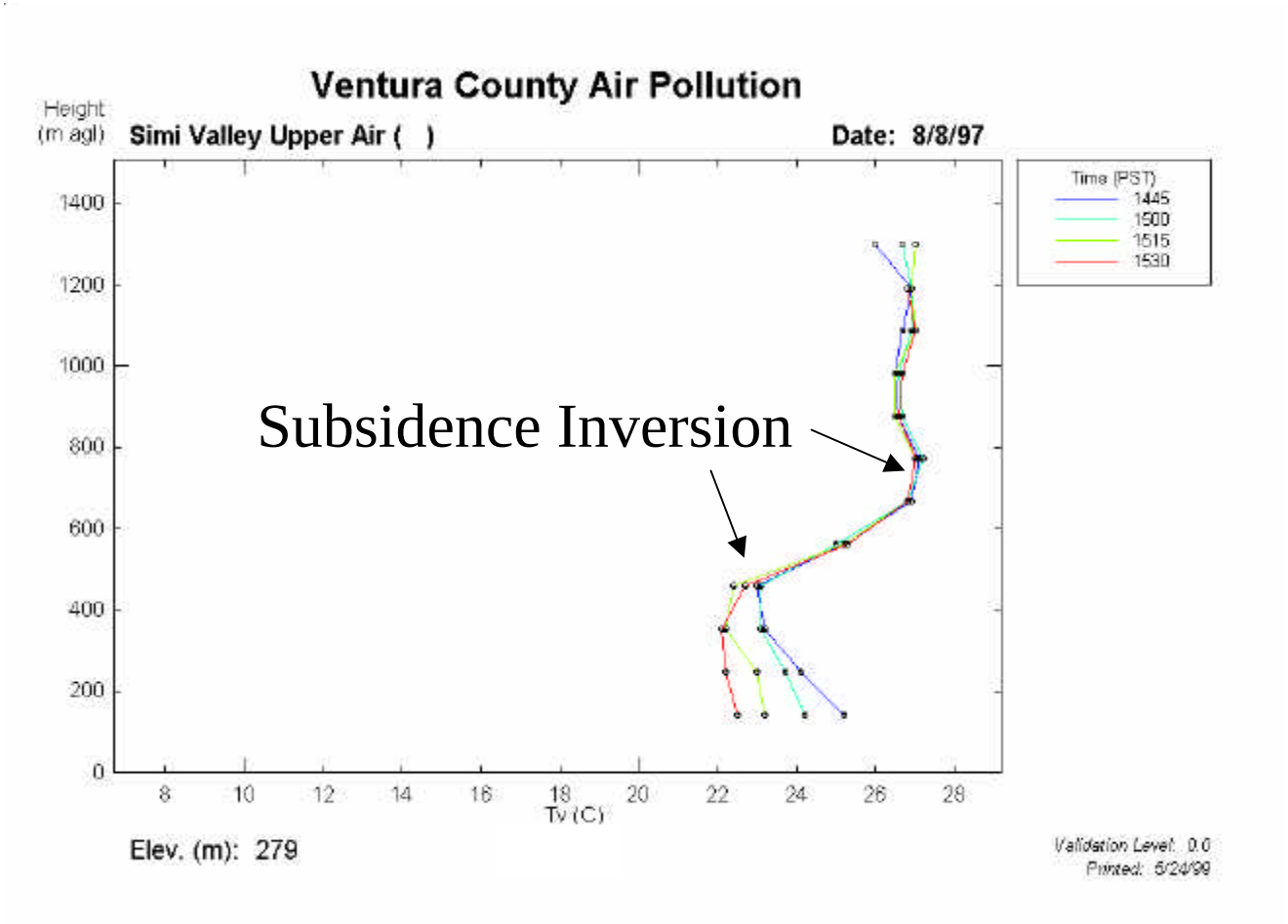

Figure 4-22. RASS virtual temperature data at Simi Valley on August 8, 1997 showing a strong inversion from 450 m to about 650 m. Below about 450 m is the MBL or CBL.

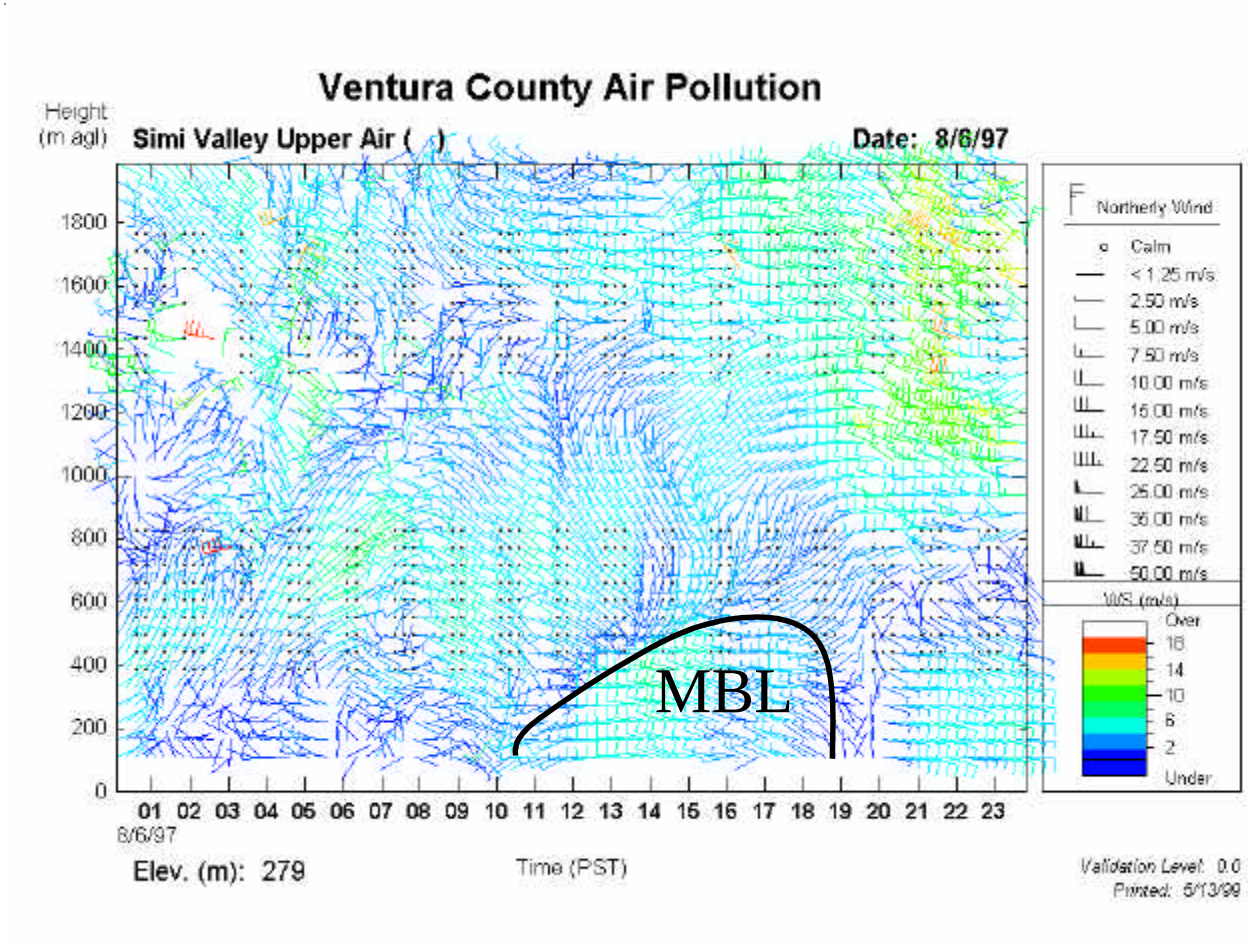

Figure 4-23. Radar profiler wind data at Simi Valley on August 6, 1997 showing the MBL.

a.

b.

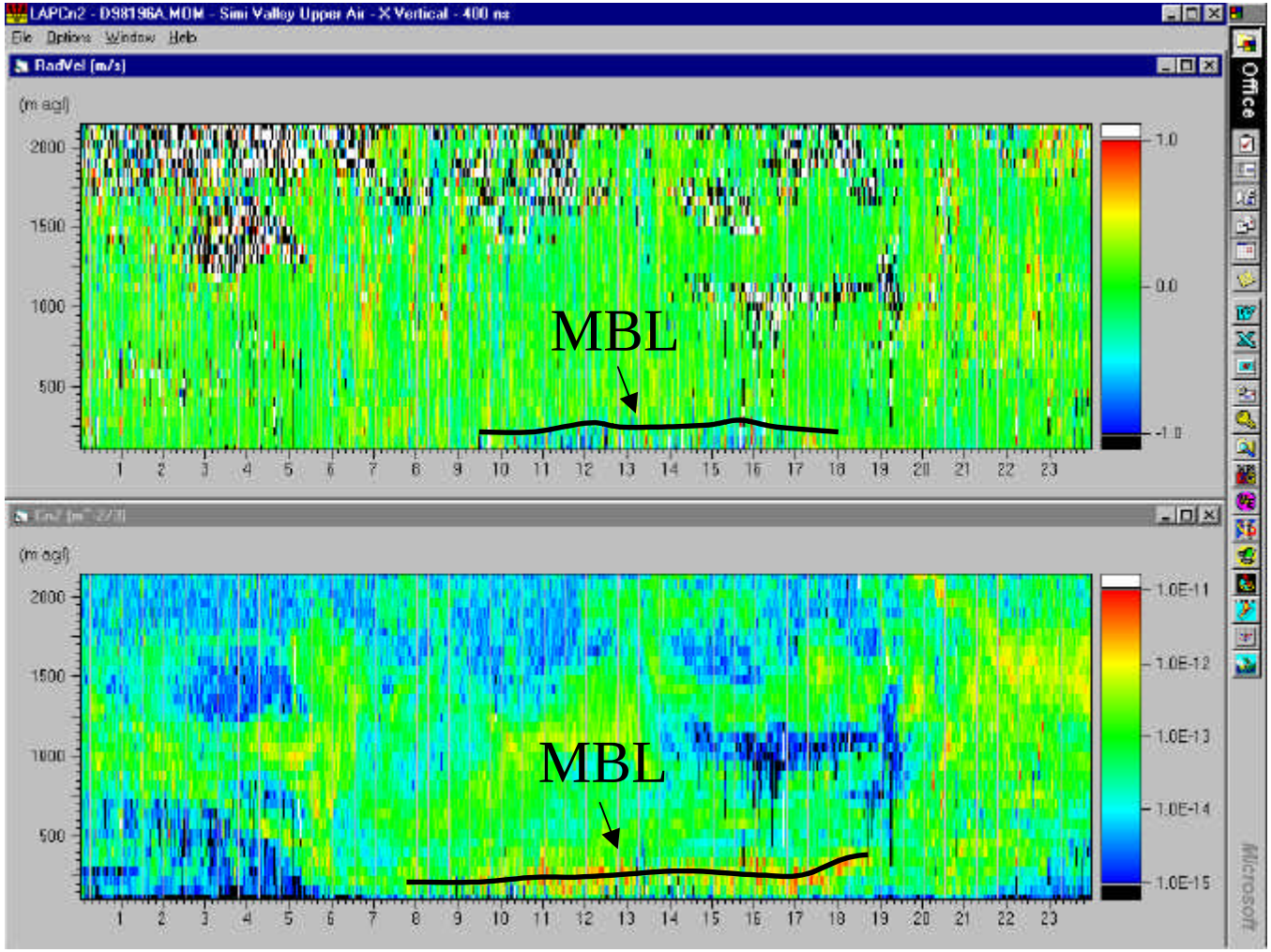

Time (PST)

Figure 4-24. Time/height cross section of radar profiler a) vertical velocity and b) C_n^2 data at Simi Valley on July 15, 1998. The top of the marine layer is shown as a black solid line.

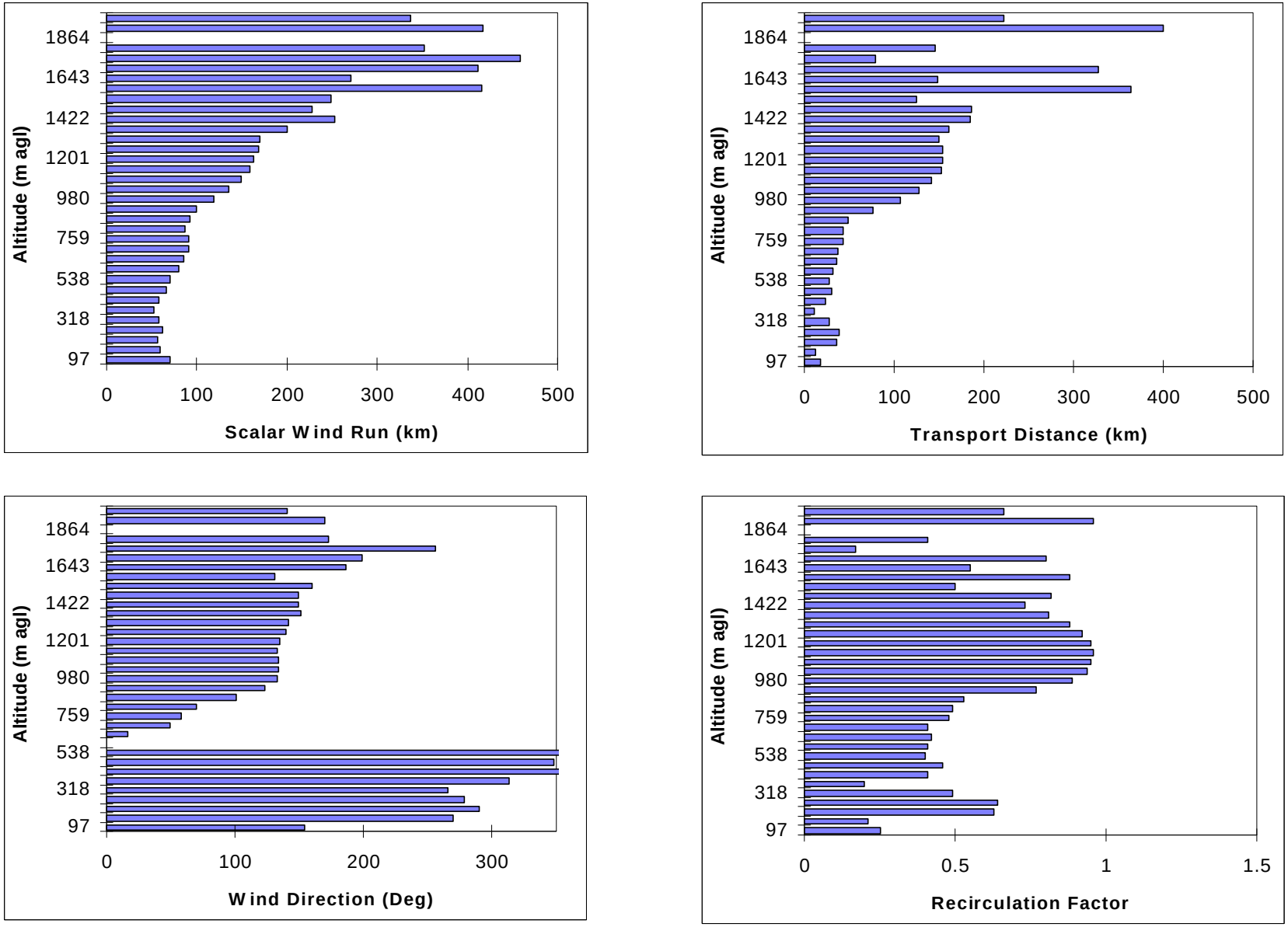

Figure 4-25. Twelve-hour overnight transport statistics at Simi Valley from July 16, 1998 at 1600 PST to July 17, 1998 at 0400 PST.

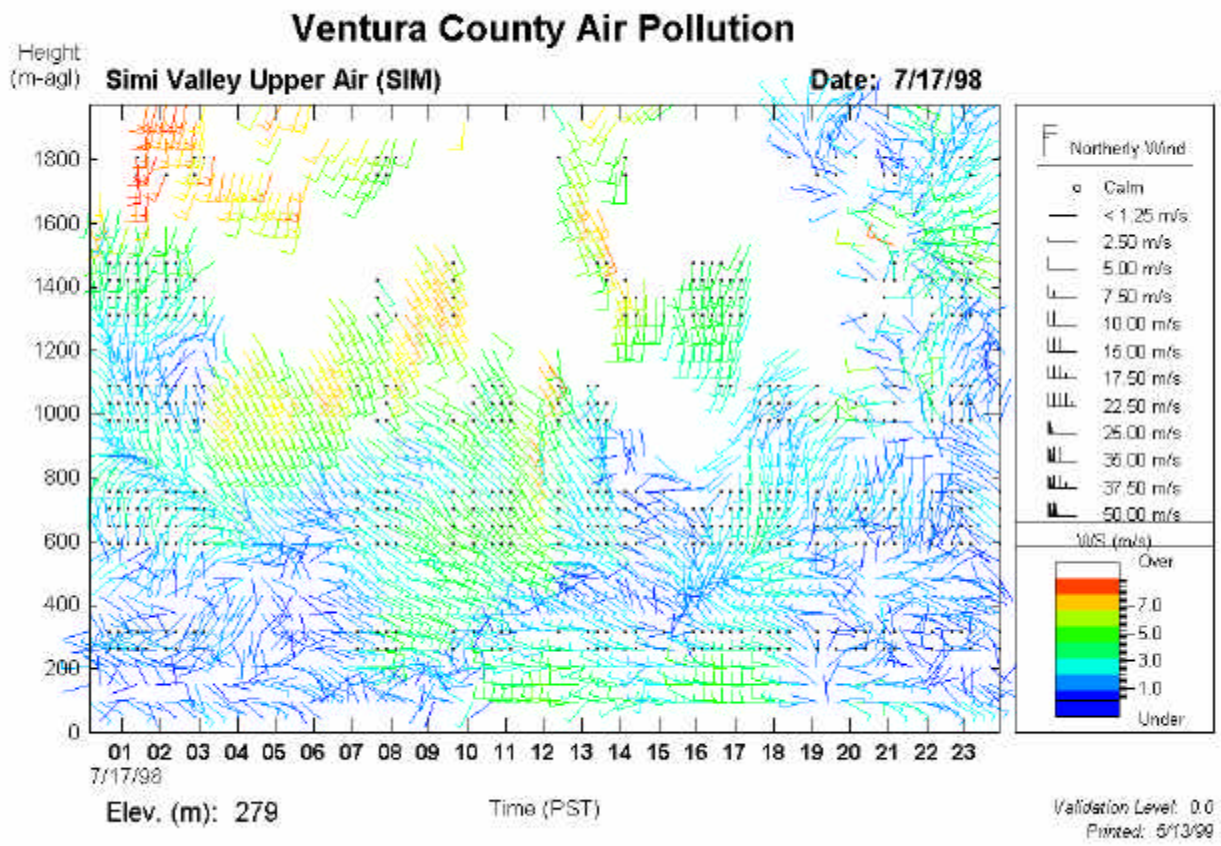

Figure 4-26. Radar profiler wind data at Simi Valley on July 17, 1998.

5. REFERENCES

Allwine K.J. and Whiteman C.D. (1994) Single-station integral measures of atmospheric stagnation, re-circulation, and ventilation. *Atmos. Environ.* **28**, 713-721.

Angevine W.M., Trainer M., McKeen S.A., and Berkowitz C.M. (1996) Mesoscale meteorology of the New England coast, Gulf of Maine, and Nova Scotia: overview. *J. Geophys. Res.* **101**, 28,893-28,901.

Baxter R.A. (1991) Determination of mixing heights from data collected during the 1985 SCCCAMP field program. *J. Appl. Meteorol.* **30**, 598-606.

Berman S., Ku J.-Y., Zhang J., and Rao S.T. (1997) Uncertainties in estimating the mixing depth--comparing three mixing-depth models with profiler measurements. *Atmos. Environ.* **31**, 3023-3039.

Beyrich F. and Weill A. (1993) Some aspects of determining the stable boundary layer depth from sodar data. *Bound.-Layer Meteorol.* **63**, 97-116.

Blumenthal D.L., Smith T.B., Lehrman D.E., Alexander N.L., Lurmann F., and Godden D. (1986) Analysis of aerometric and meteorological data for the Ventura County Region. Final report prepared for the Western Oil and Gas Association (WOGA), Los Angeles, CA by Sonoma Technology, Inc., Santa Rosa, CA and Environmental Research & Technology, Inc., Newbury Park, CA, STI-90094-511-FR, Contract No. 83-8.0.05(3)-14-01-SOT.

Blumenthal D.L., Lurmann F.W., Roberts P.T., Main H.H., MacDonald C.P., Knuth W.R., and Niccum E.M. (1997) Three-dimensional distribution and transport analyses for SJVAQS/AUSPEX. Final report prepared for San Joaquin Valley Air Pollution Study Agency, Sacramento, CA by Sonoma Technology, Inc., Santa Rosa, CA, Technical & Business Systems, Santa Rosa, CA, and California Air Resources Board, Sacramento, CA, STI-91060-1705-FR, February.

Blumenthal D.L., Ray S.E., Dye T.S., Korc M., Moore G., and Londergan R. (1998) Transport phenomena related to ozone episodes in the northeast U.S. Preprints from the *10th Joint Conference on the Applications of Air Pollution Meteorology, January 11-16*, (STI 1756), pp. 182-186.

Carroll J.J. and Baskett R.L. (1979) Dependence of air quality in a remote location on local and mesoscale transports: a case study. *J. Appl. Meteorol.* 18,4.

Clark R.D. (1997) Vertical profiles of meteorological variables and ozone concentrations in the nocturnal boundary layer at Gettysburg, PA. Proceedings of the *12th Symposium on Boundary Layers and Turbulence, Vancouver, BC, August, 1997*, pp. 417-418.

Dye T.S., Lindsey C.G., and Anderson J.A. (1995) Estimates of mixing depths from "boundary layer" profilers. Preprints from the *9th Symposium on Meteorological Observations and Instrumentation, Charlotte, NC, March 27-31*, STI-94212-1451, pp. 156-160.

Holzworth G. (1972) Mixing heights, wind speeds, and potential for urban air pollution throughout the contiguous United States. Prepared by Office of Air Programs, U.S. Environmental Protection Agency, Research Triangle Park, NC, Publication No. AP-101.

Lehrman D.E., Smith T.B., Knuth W.R., and Dorman C.E. (1994) Meteorological analysis of the San Joaquin Valley Air Quality Study, Atmospheric Utilities Signatures, Predictions and Experiments Program (SJVAQS/AUSPEX). Final report prepared for California Air Resources Board, Sacramento, CA by Technical & Business Systems, Santa Rosa, CA.

MacDonald C.P. (1998) Effects of synoptic and mesoscale weather on air pollution in Central California. MS Thesis, University of California, Davis.

MacDonald C.P., Dye T.S., and Chinkin L.R. (1997) Forecasting guidelines for winds and ozone air quality in the Sacramento Region. Technical memo prepared for the Sacramento Air Quality Management District, Sacramento, CA by Sonoma Technology, Inc., Santa Rosa, CA, STI-997121-1734-TM, June.

MacDonald C.P., Roberts P.T., Main H.H., and Dye T.S. (1998) Phenomena that influence high ozone concentrations in the Paso del Norte area. Paper presented at the *Air and Waste Management Association 1998 Annual Meeting and Exhibition, San Diego, CA, June 14-18*.

MacDonald C.P., Kwiatkowski J.J., and Dye T.S. (1999) Photochemical assessment monitoring stations (PAMS) data analysis for Southern California. Tasks III.1 to III.3: Meteorological data analysis. Report prepared for South Coast Air Quality Management District, Diamond Bar, CA by Sonoma Technology, Inc., Petaluma, CA, STI-997524-1871-DFR, March.

National Research Council (1992) *Rethinking the Ozone Problem in Urban and Regional Air Pollution*. National Academy of Science Press, Washington, DC, 489 pp.

Neff W.D. (1994) Mesoscale air quality studies with meteorological remote sensing systems. *Int. J. Remote Sensing* **10**, 393-426.

Neiburger M., Edinger J.G., and Bonner W.D. (1971) *Understanding Our Atmospheric Environment*, 2nd Edition. W.H. Freeman and Company, San Francisco, 453 pp.

Ray S.E., Dye T.S., Roberts P.T., and Blumenthal D.L. (1998) Analysis of nocturnal low-level jets in the Northeastern United States during the summer of 1995. Paper No. 5A.4 presented at the *10th Joint Conference on the Applications of Air Pollution Meteorology, Phoenix, AZ, January 11-16*, (STI 1750).

Roberts P.T., Anderson J.A., Main H.H. (1993) Pollutant concentrations aloft as measured by aircraft during the Gulf of Mexico Air Quality Study and the coastal oxidant assessment for southwest Texas. Paper presented at the *Air & Waste Management Association Regional Photochemical Measurement and Modeling Studies Conference, San Diego, CA, November 8-12*.

Roberts P.T., MacDonald C.P., Main H.H., Dye T.S., Coe D., and Haste T.L. (1997) Analysis of meteorological and air quality data for the 1996 Paso del Norte ozone study. Final report prepared for U.S. Environmental Protection Agency, Region 6, Dallas TX under subcontract to SAIC, McLean, VA by Sonoma Technology, Inc., Santa Rosa, CA, STI-997330-1754-FR, EPA Contract No. 68-D3-0030, Work Assignments III-102 and III-130, September.

Stull R.B. (1989) *An Introduction to Boundary Layer Meteorology*. *Kluwer Academic Publishers*, Boston.

Uno I., Wakamatsu S., Ueda H., and Nakamura A. (1992) Observed structure of the nocturnal urban boundary layer and its evolution into a convective mixed layer. *Atmos. Environ*. **26B**, 45-47.

White A.B., Fairall C.W., and Wolfe D.E. (1991) Use of 915 MHz wind profiler data to describe the diurnal variability of the mixed layer. In Preprints from the *AMS and A&WMA 7th Joint Conference on Applications of Air Pollution Meteorology, New Orleans, LA January 14-18*, American Meteorological Society, Boston, MA.

Wyngaard J.C. and LeMone M.A. (1980) Behavior of the refractive index structure parameter in the entraining convective boundary layer. *J. Atmos. Sci*. **37**, 1573-1585.

[BLANK PAGE]

APPENDIX A

NESTED GRID MODEL ANALYSIS WEATHER CHARTS

This appendix provides Nested Grid Model analysis weather charts for the 1997 and 1998 episode days analyzed in this report. These charts were used to characterize the synoptic meteorology during ozone episodes. The characterization of the episodes is presented in Section 4 of this report. Note that the charts are in UTC time.

(Note: This electronic version of the original report contains the first page of forty-nine pages of Nested Grid Model (NGM) analysis weather charts presented in the original Appendix A. The first page is provided as an example of the data used to support the analysis discussed in the report. The historic NGM meteorological data can be acquired by requesting a hard copy of the original report or viewing individual days for areas discussed at http://www.arl.noaa.gov/ready/arlplota.html.)

[BLANK PAGE]

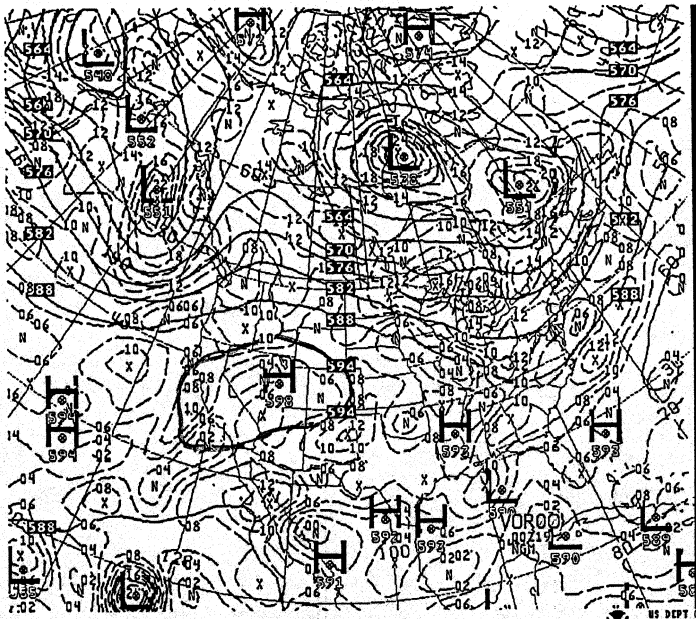

D033 .. 00HR FCST 500MB HEIGHTS/VORTICITY VALID 00Z SUN 19 JUL 1998

US DEPT OF COMMERCE
NOAA/NWS/NCEP WASHINGTON

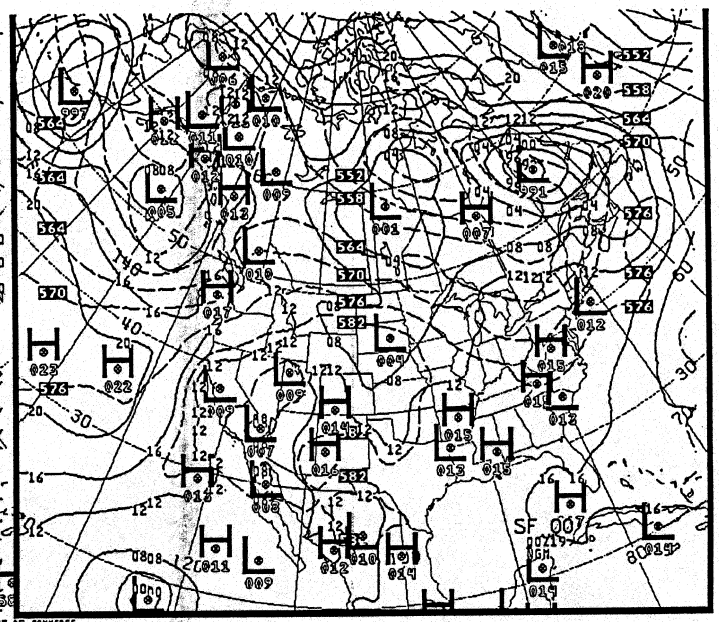

D033 .. 00HR FCST MSL PRES/1000-500MB THICKNESS VALID 00Z SUN 19 JUL 1998

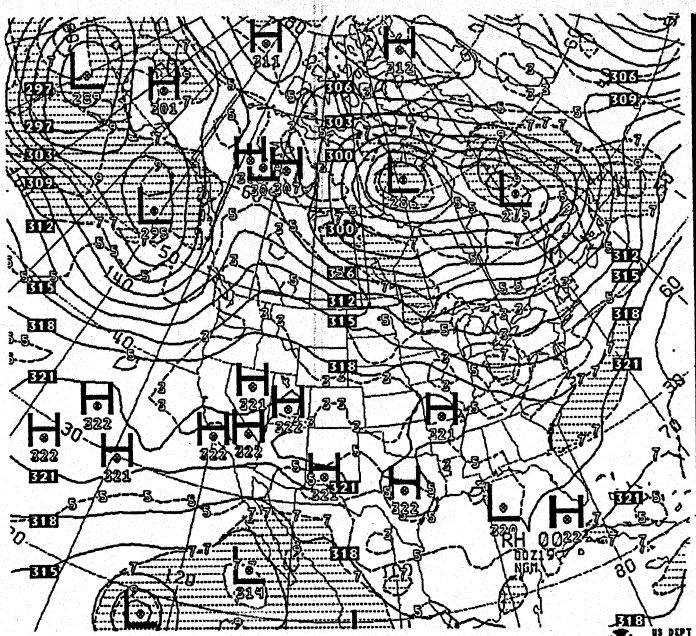

D033 .. 00HR FCST 700MB HEIGHT/REL HUMIDITY VALID 00Z SUN 19 JUL 1998

US DEPT OF COMMERCE
NOAA/NWS/NCEP WASHINGTON

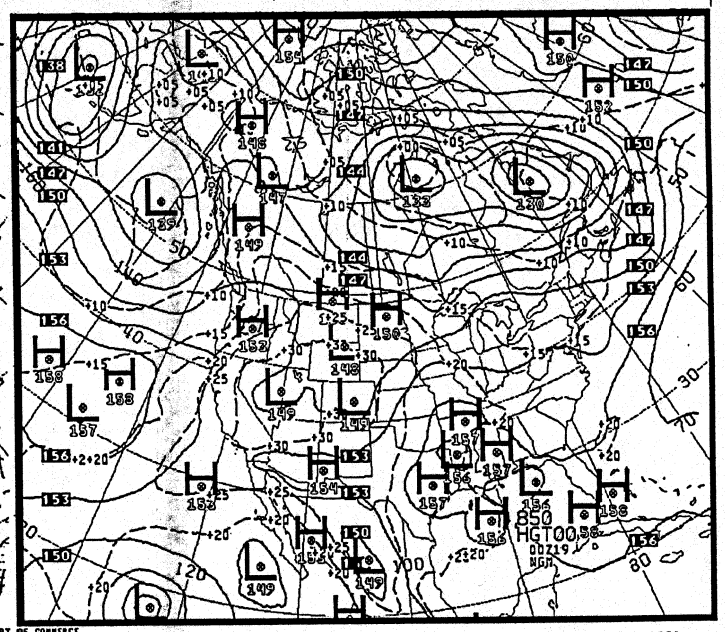

D033 .. 00HR FCST 850MB HEIGHTS/TEMPERATURE VALID 00Z SUN 19 JUL 1998

00H HT/RH/THK 7/19/98 02:37:00

[BLANK PAGE]

APPENDIX B

RADAR PROFILER WIND PLOTS

This appendix provides time/height cross sectional plots of radar profiler winds measured at Simi Valley (Ventura), Franklin Field (Sacramento), and Visalia (San Joaquin Valley) for the 1997 and 1998 episode days analyzed in this report. These plots were used to characterize the various wind flow patterns during ozone episodes. The characterization of the flow patterns during the ozone episodes is presented in Section 4 of this report. Note that the wind data are reported by Pacific Standard Time begin hour.

[BLANK PAGE]

Sacramento Air Quality

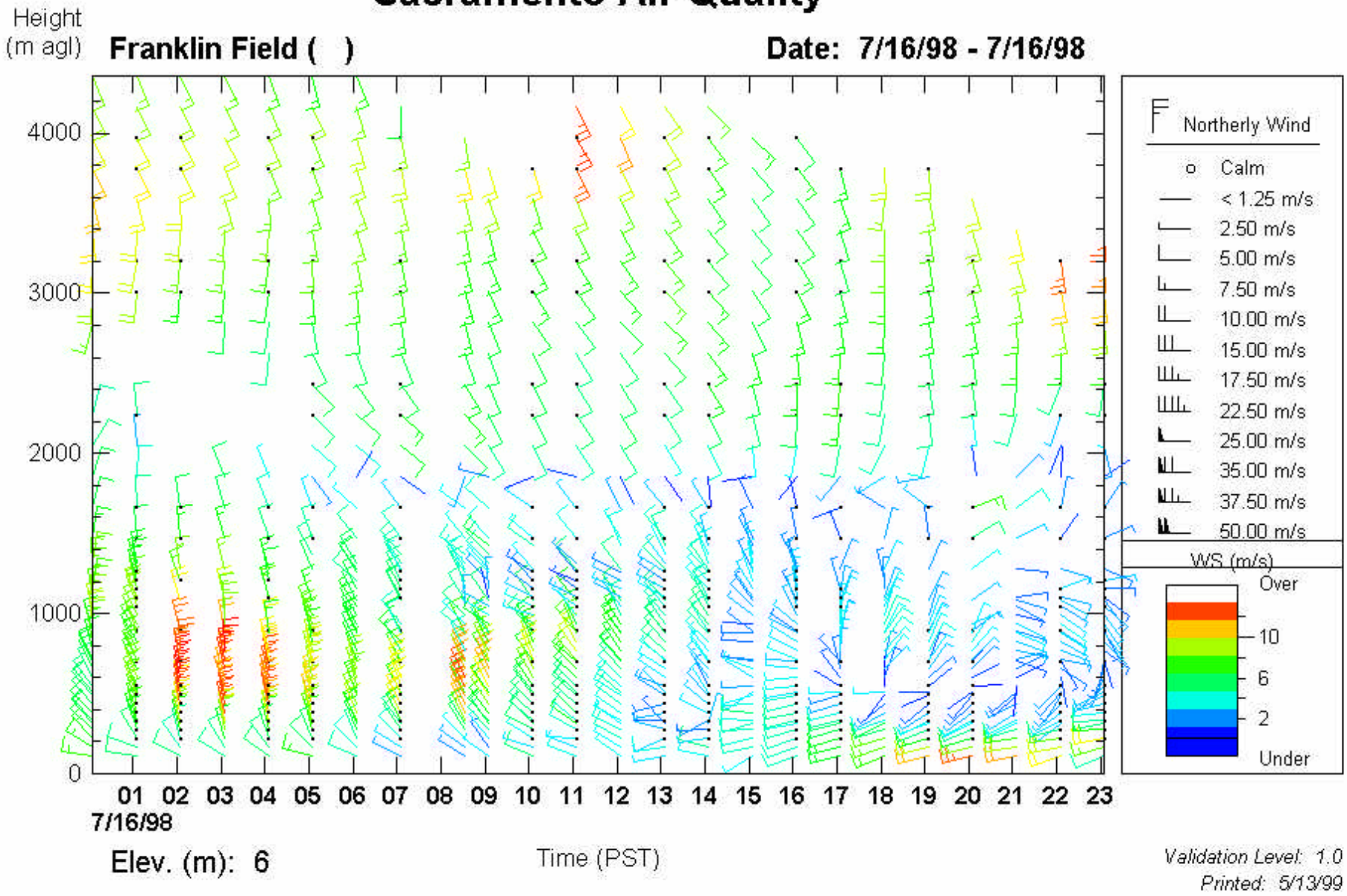

Elev. (m): 6

Validation Level: 1.0
Printed: 5/13/99

Sacramento Air Quality

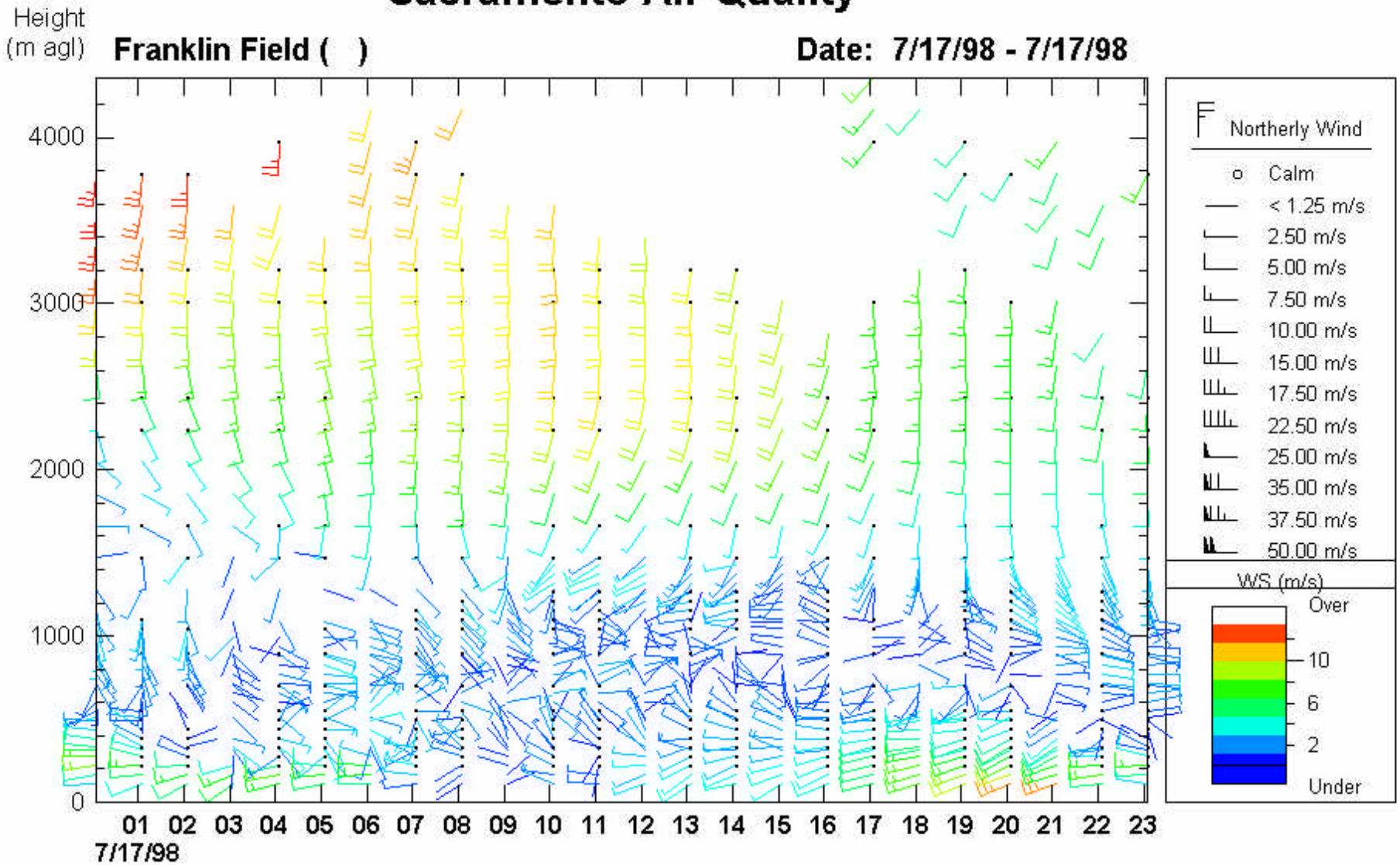

Elev. (m): 6

Validation Level: 1.0
Printed: 5/13/99

Sacramento Air Quality

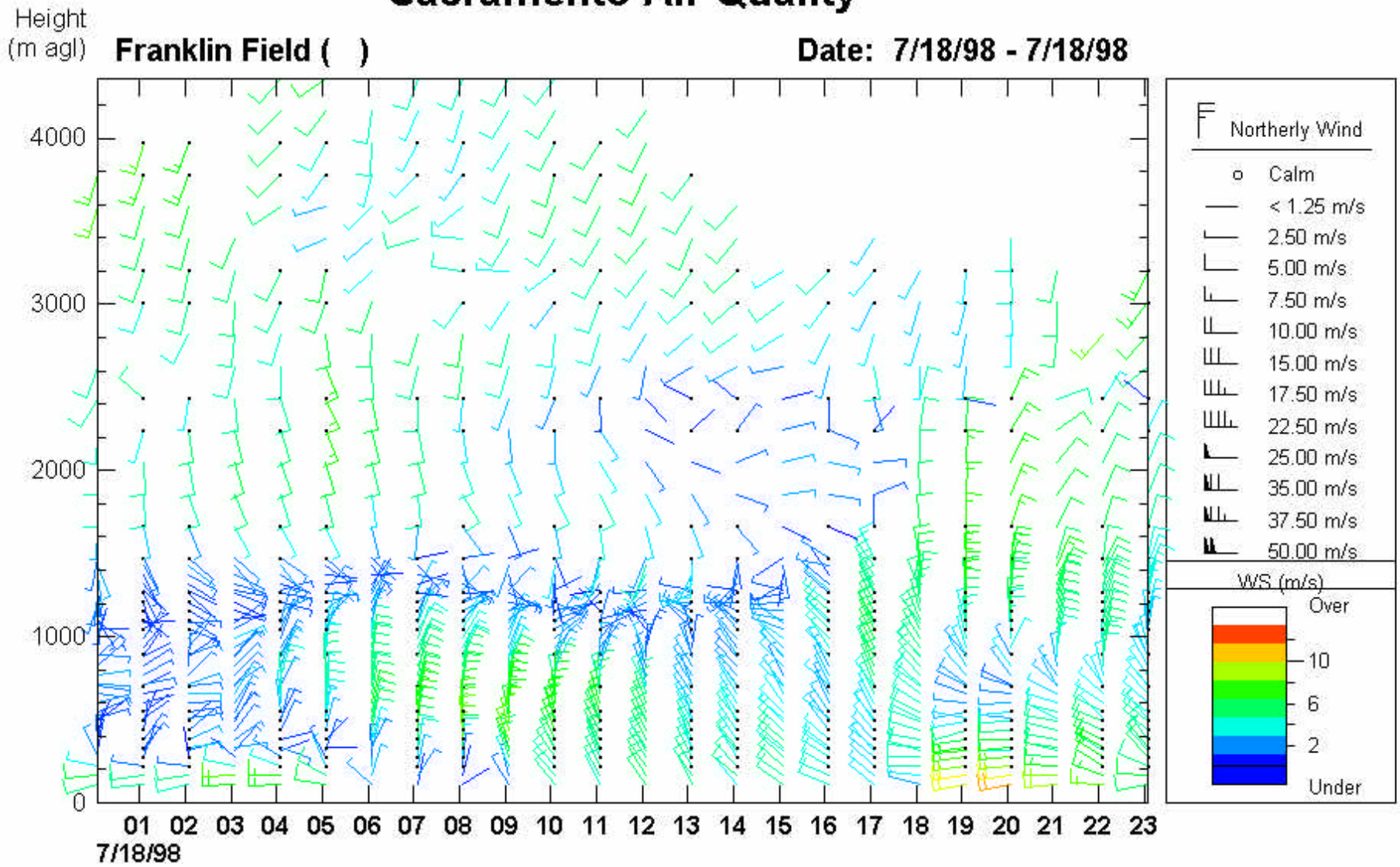

Elev. (m): 6

Validation Level: 1.0
Printed: 5/13/99

Sacramento Air Quality

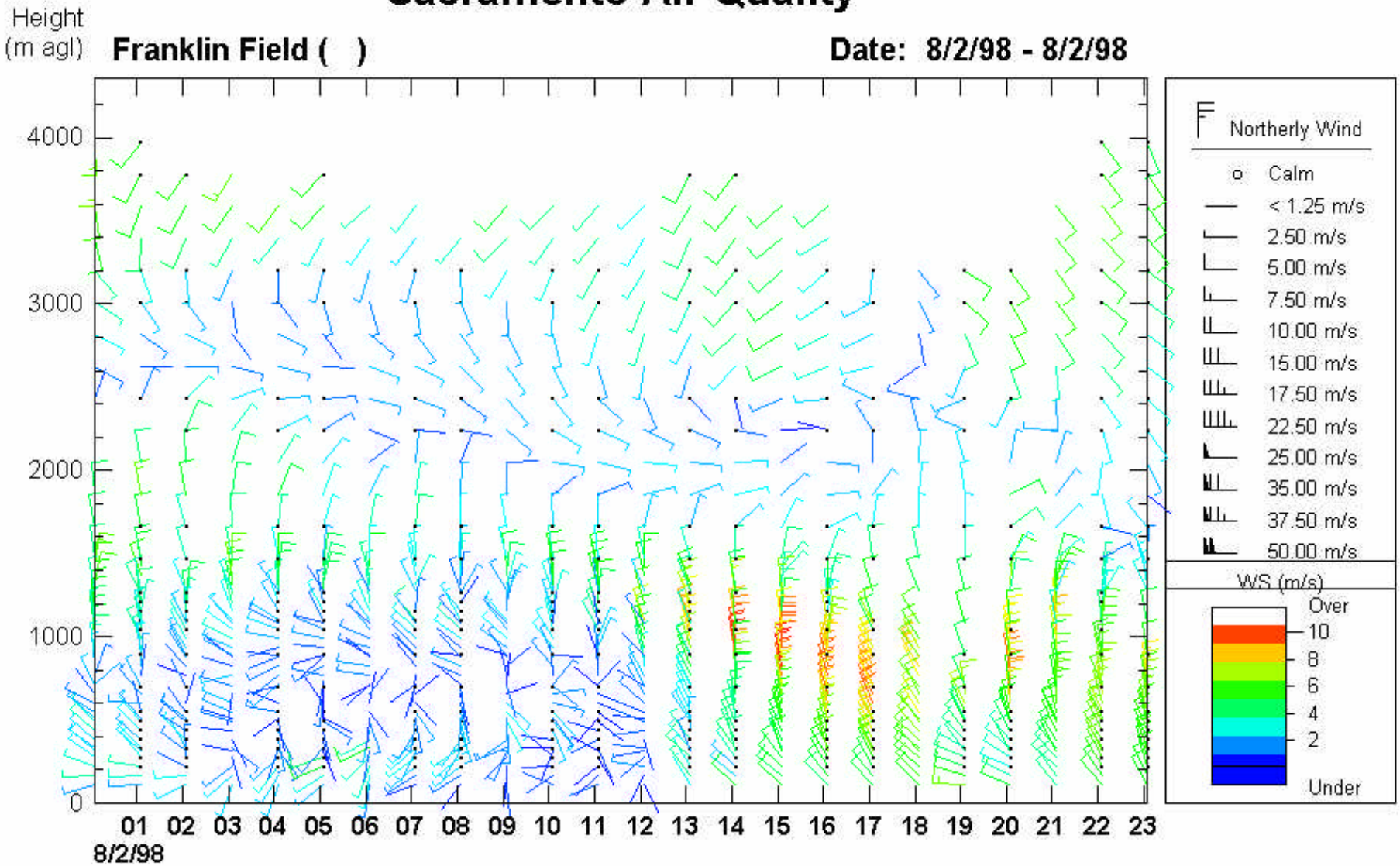

Elev. (m): 6

Validation Level: 1.0
Printed: 5/13/99

Sacramento Air Quality

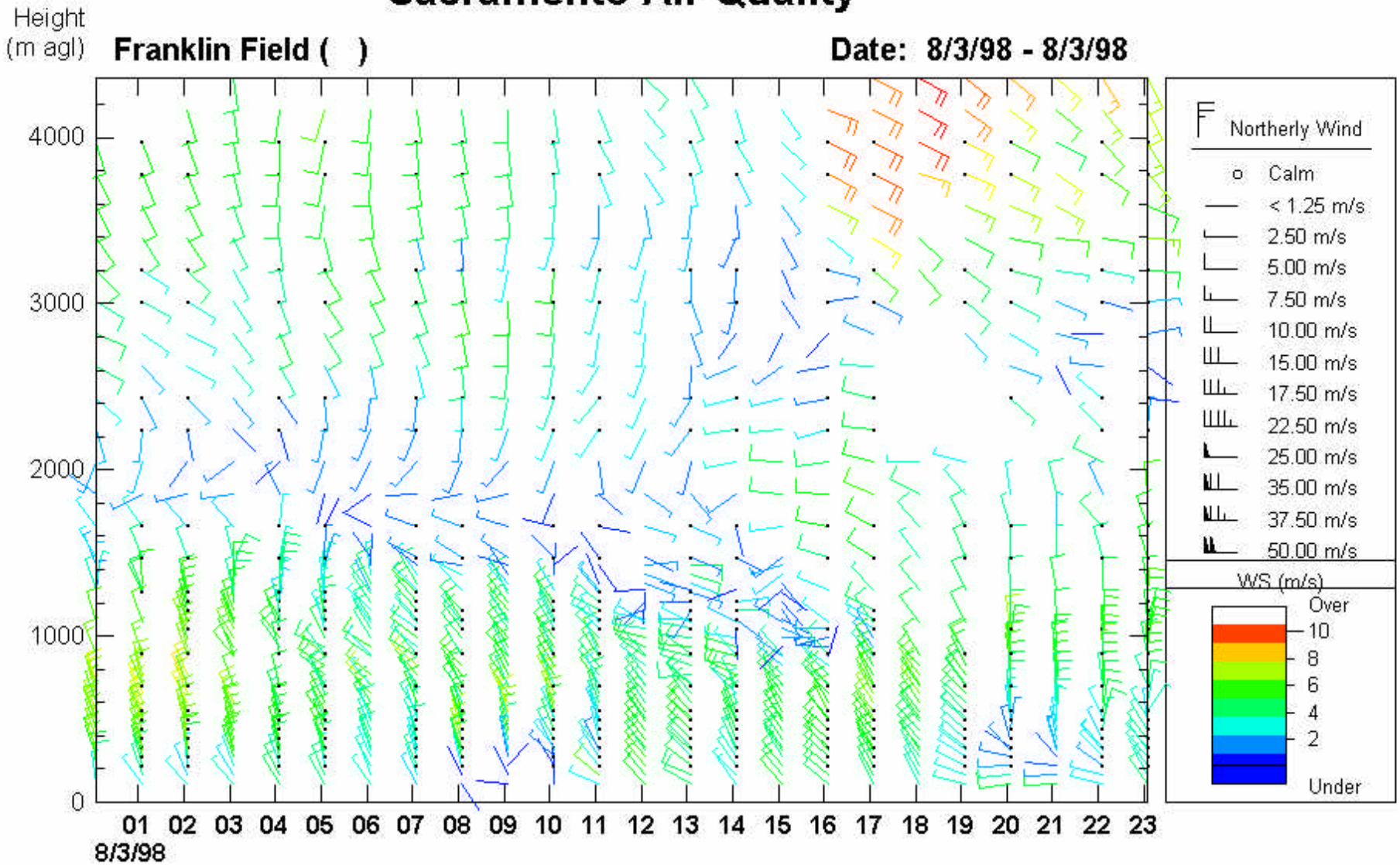

Elev. (m): 6

Validation Level: 1.0
Printed: 5/13/99

Sacramento Air Quality

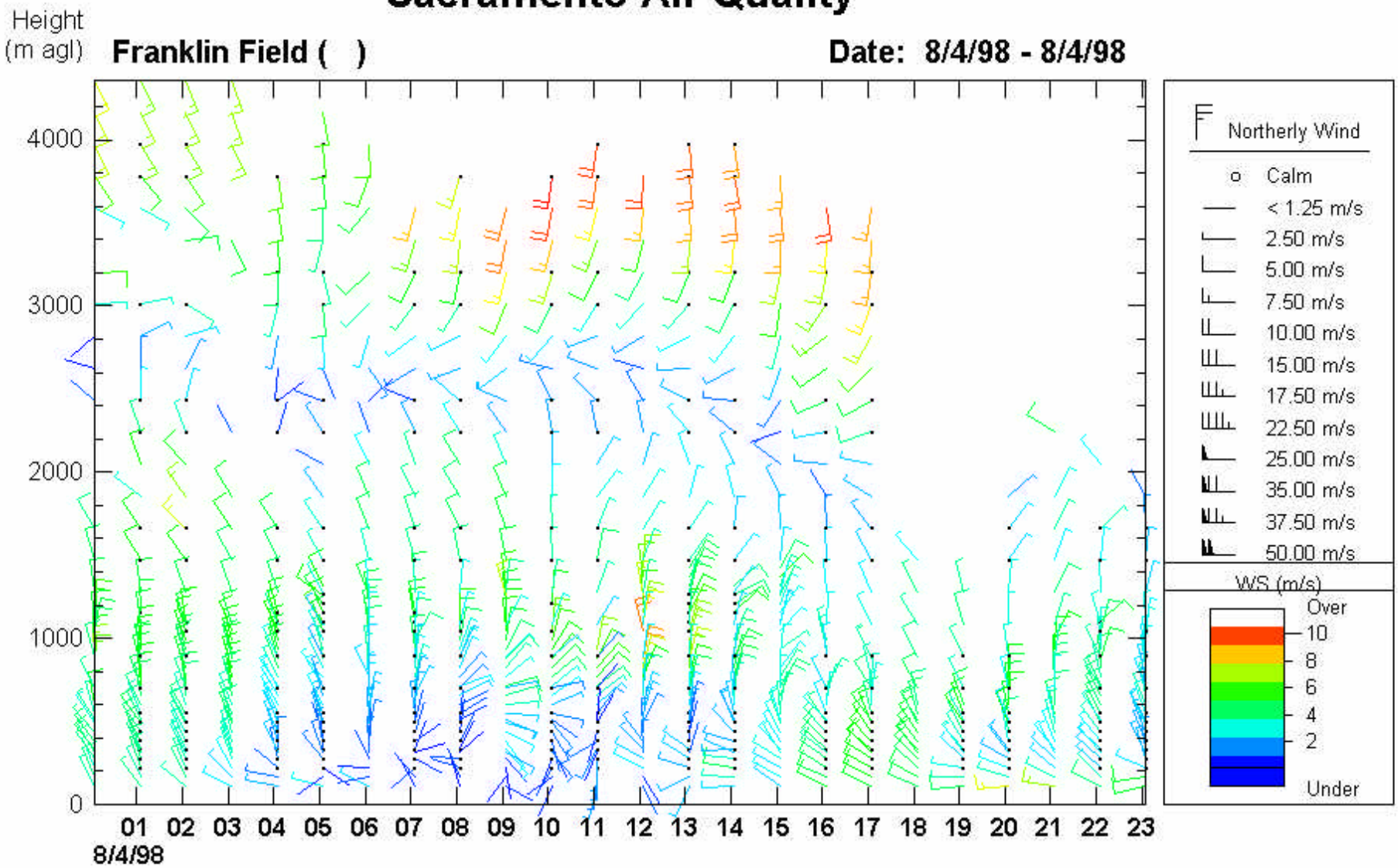

Elev. (m): 6

Validation Level: 1.0
Printed: 5/13/99

Sacramento Air Quality

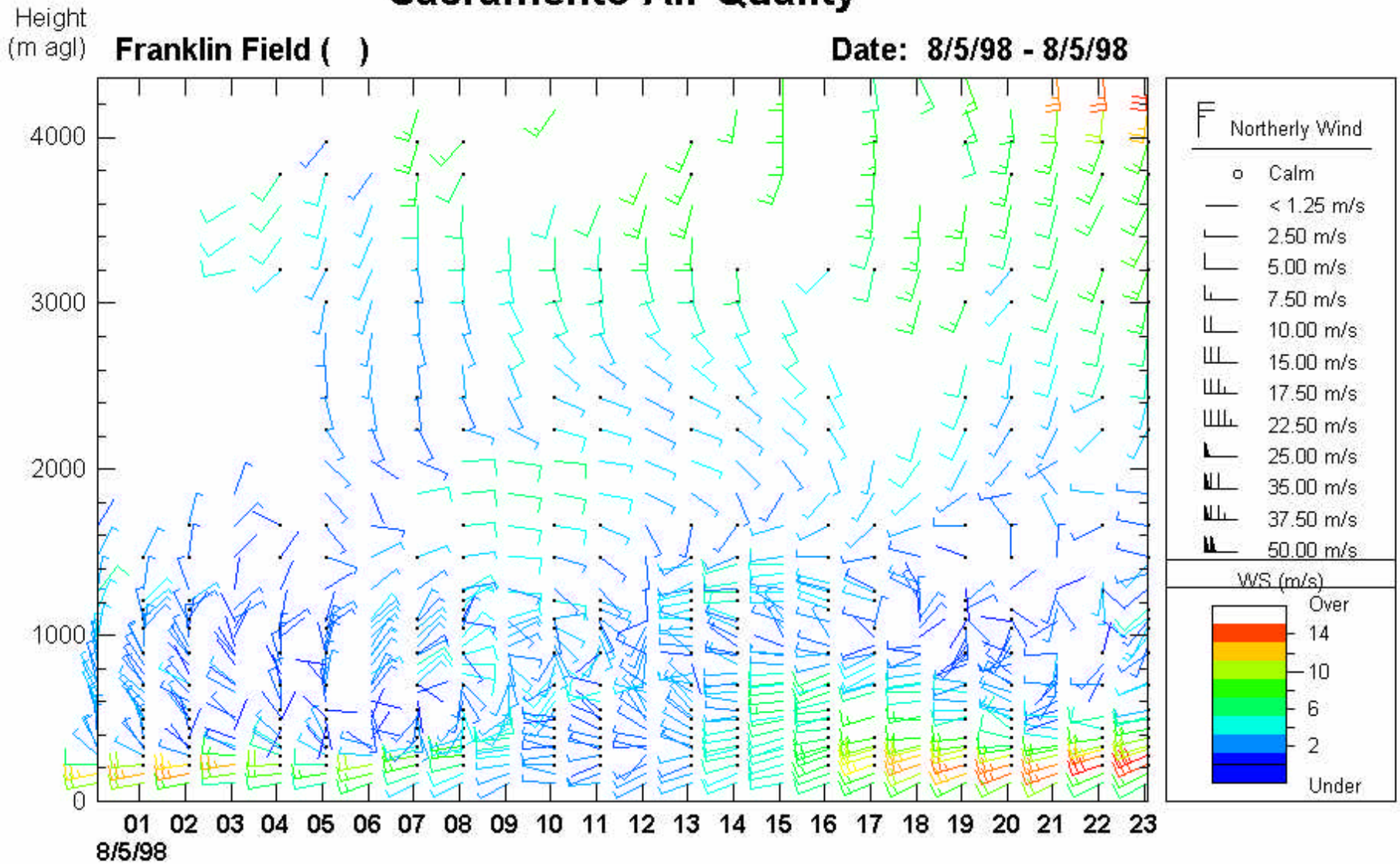

Elev. (m): 6

Validation Level: 1.0
Printed: 5/13/99

Sacramento Air Quality

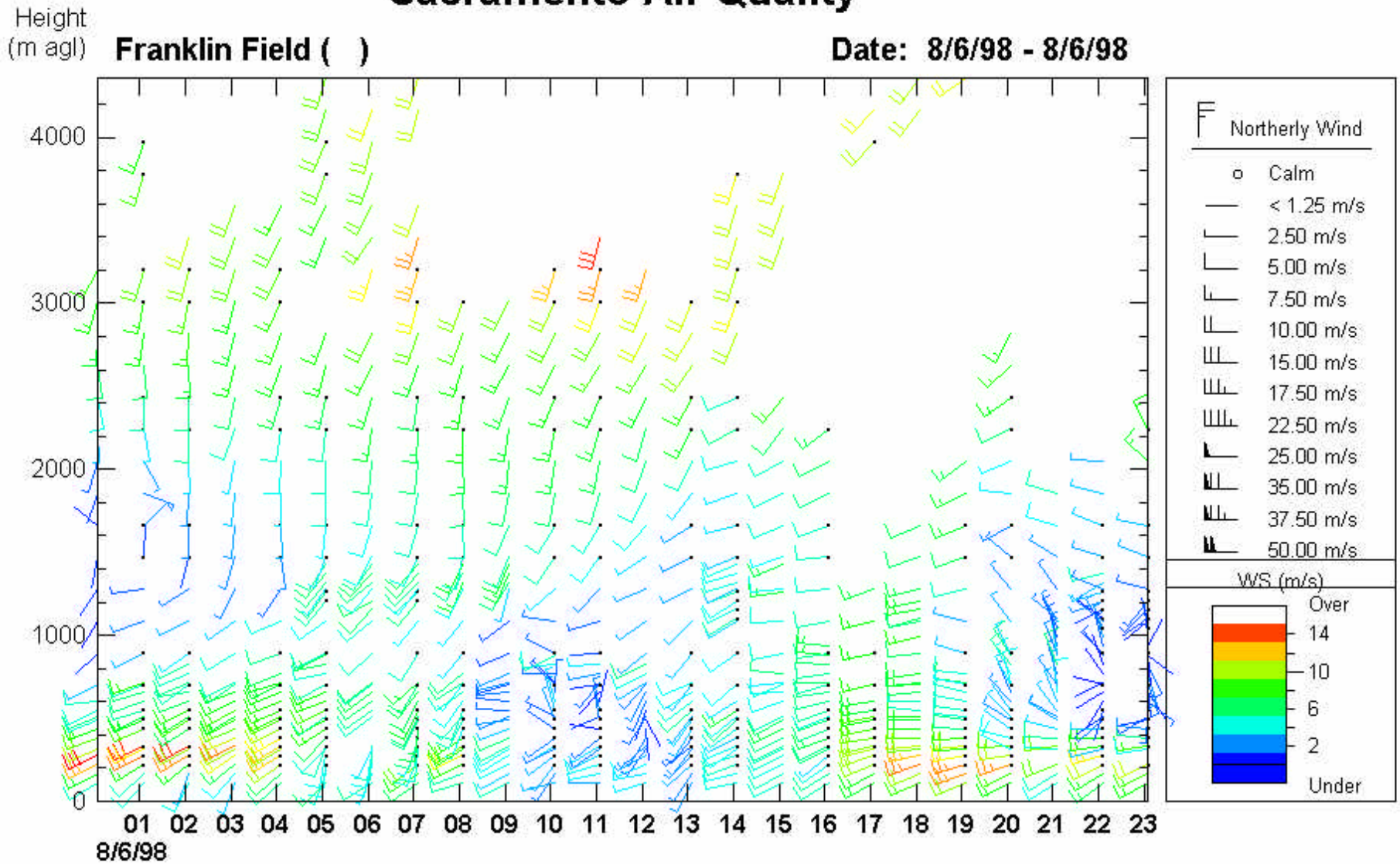

Elev. (m): 6

Validation Level: 1.0
Printed: 5/13/99

San Joaquin Valley Unified Air Pollution

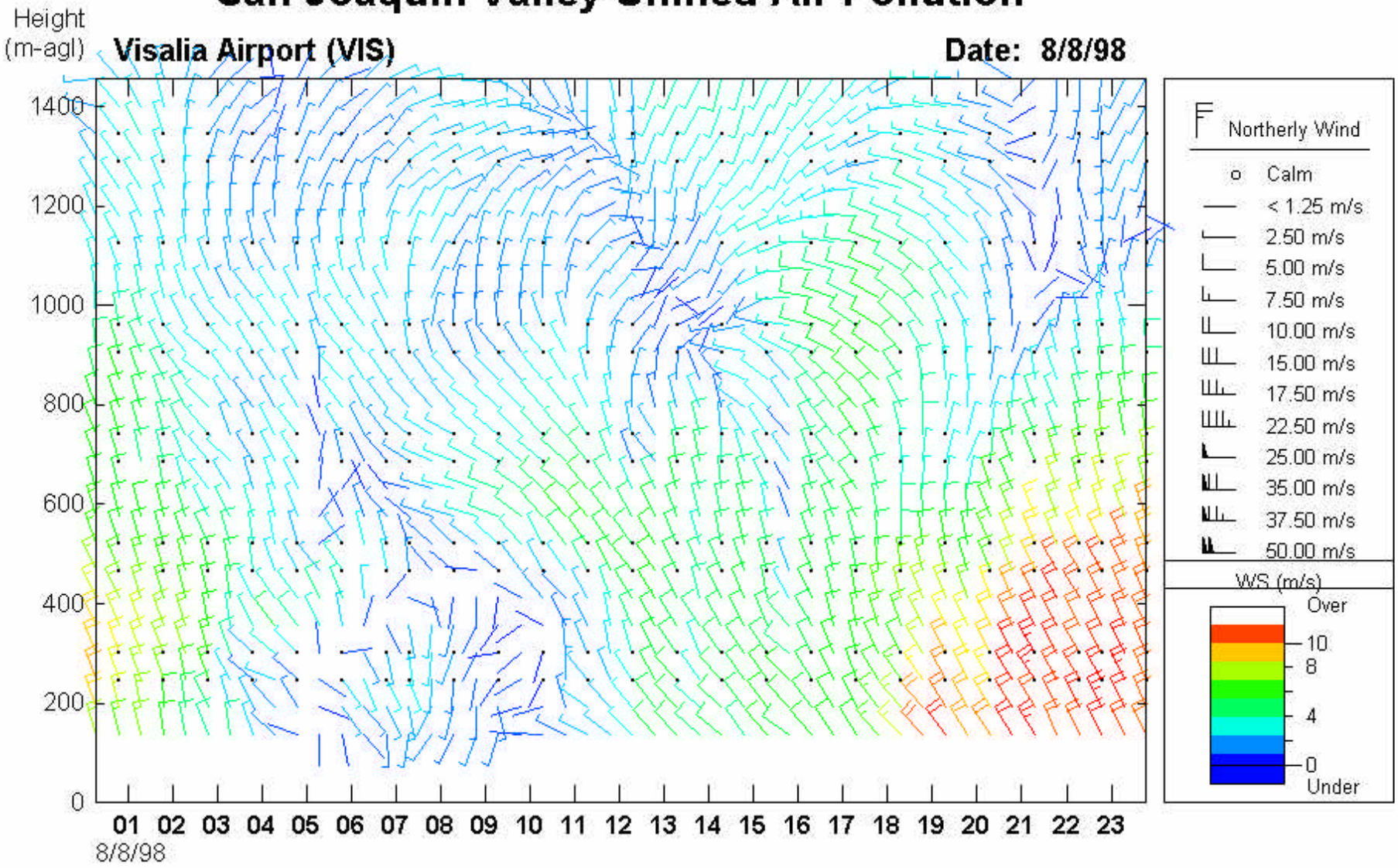

Elev. (m): 89

Time (PST)

Validation Level: 0.5
Printed: 5/13/99

San Joaquin Valley Unified Air Pollution

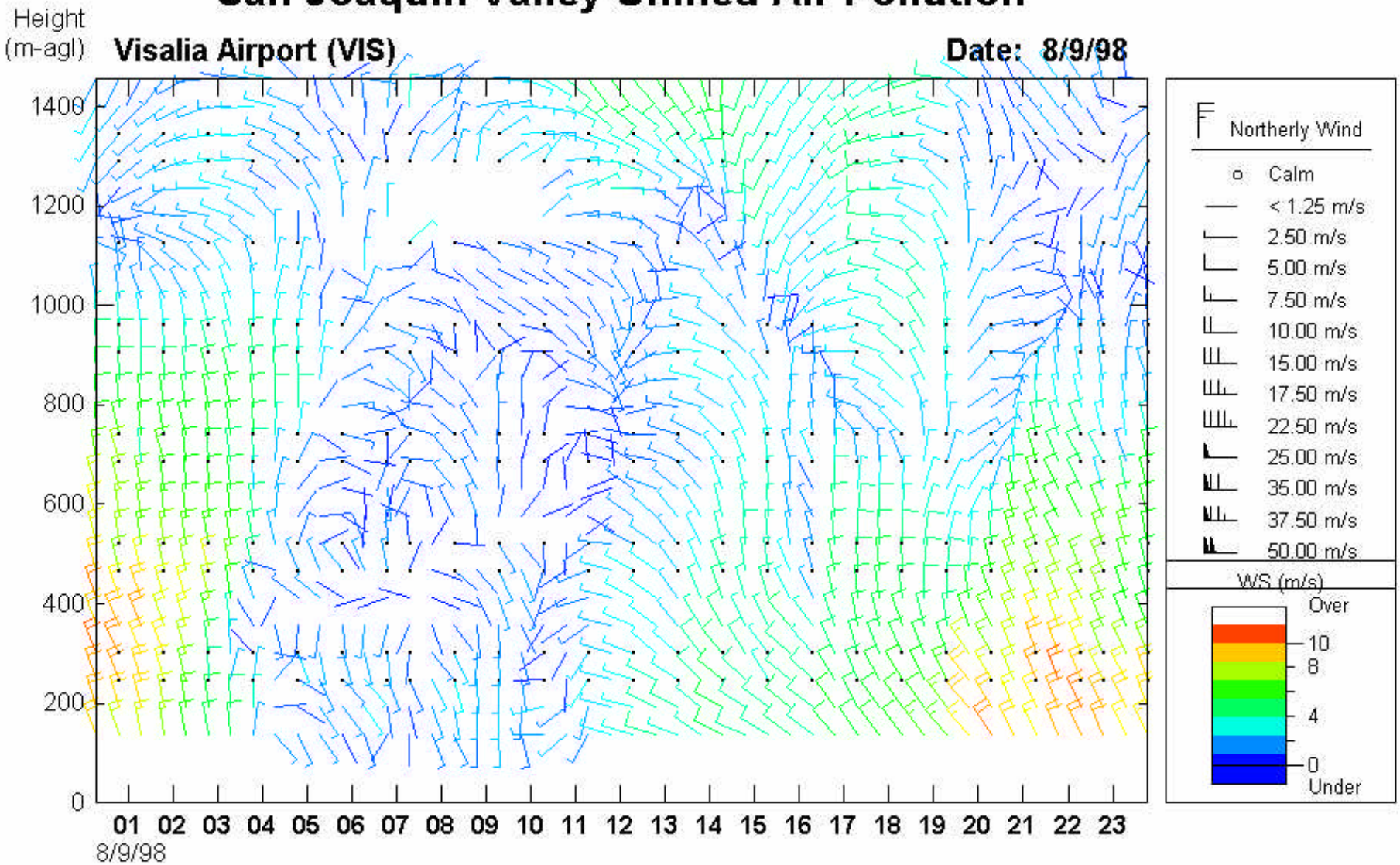

Elev. (m): 89

Validation Level: 0.5
Printed: 5/13/99

San Joaquin Valley Unified Air Pollution

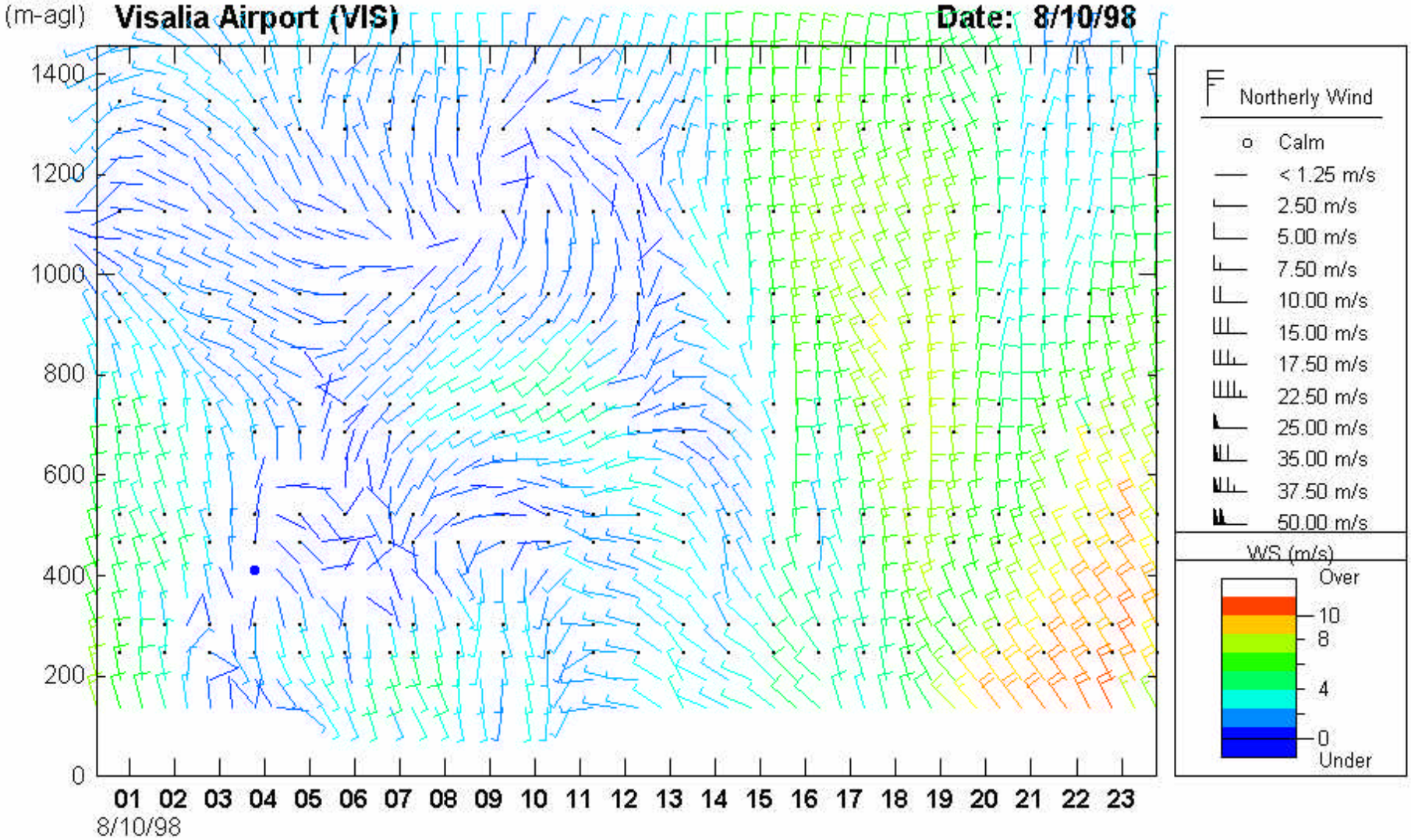

Elev. (m): 89

Validation Level: 0.5
Printed: 5/13/99

San Joaquin Valley Unified Air Pollution

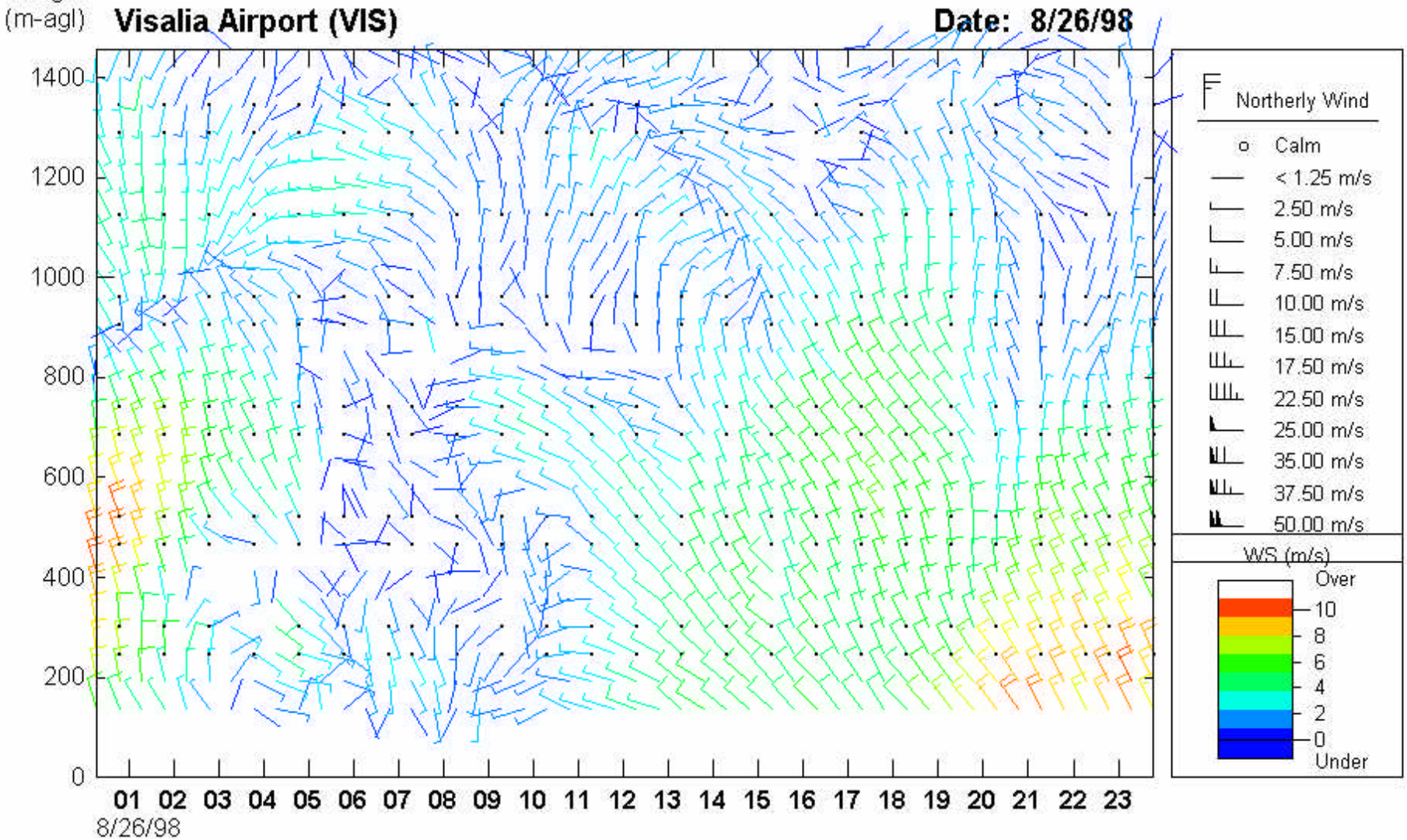

Elev. (m): 89

Validation Level: 0.5
Printed: 5/13/99

San Joaquin Valley Unified Air Pollution

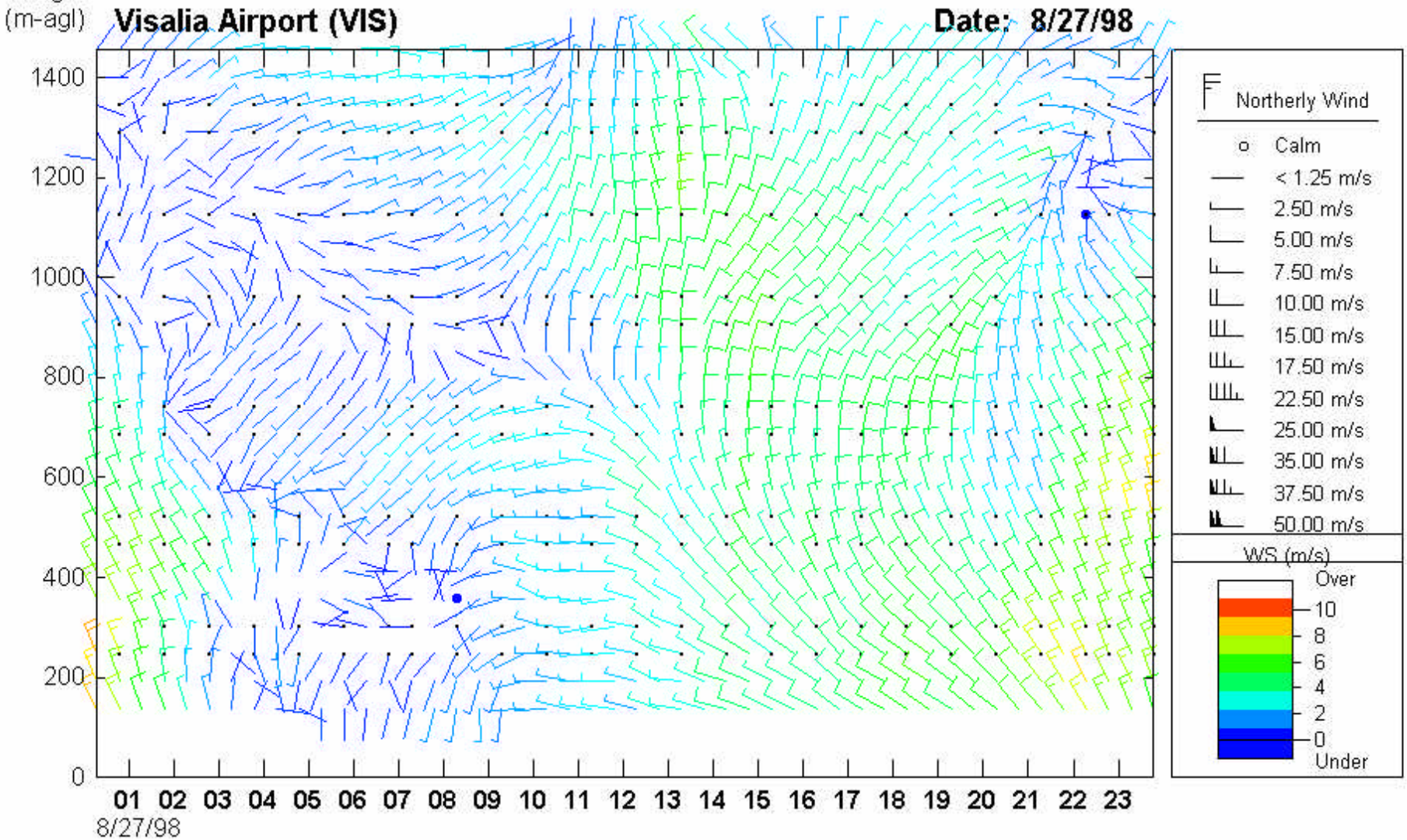

Elev. (m): 89

Validation Level: 0.5
Printed: 5/13/99

San Joaquin Valley Unified Air Pollution

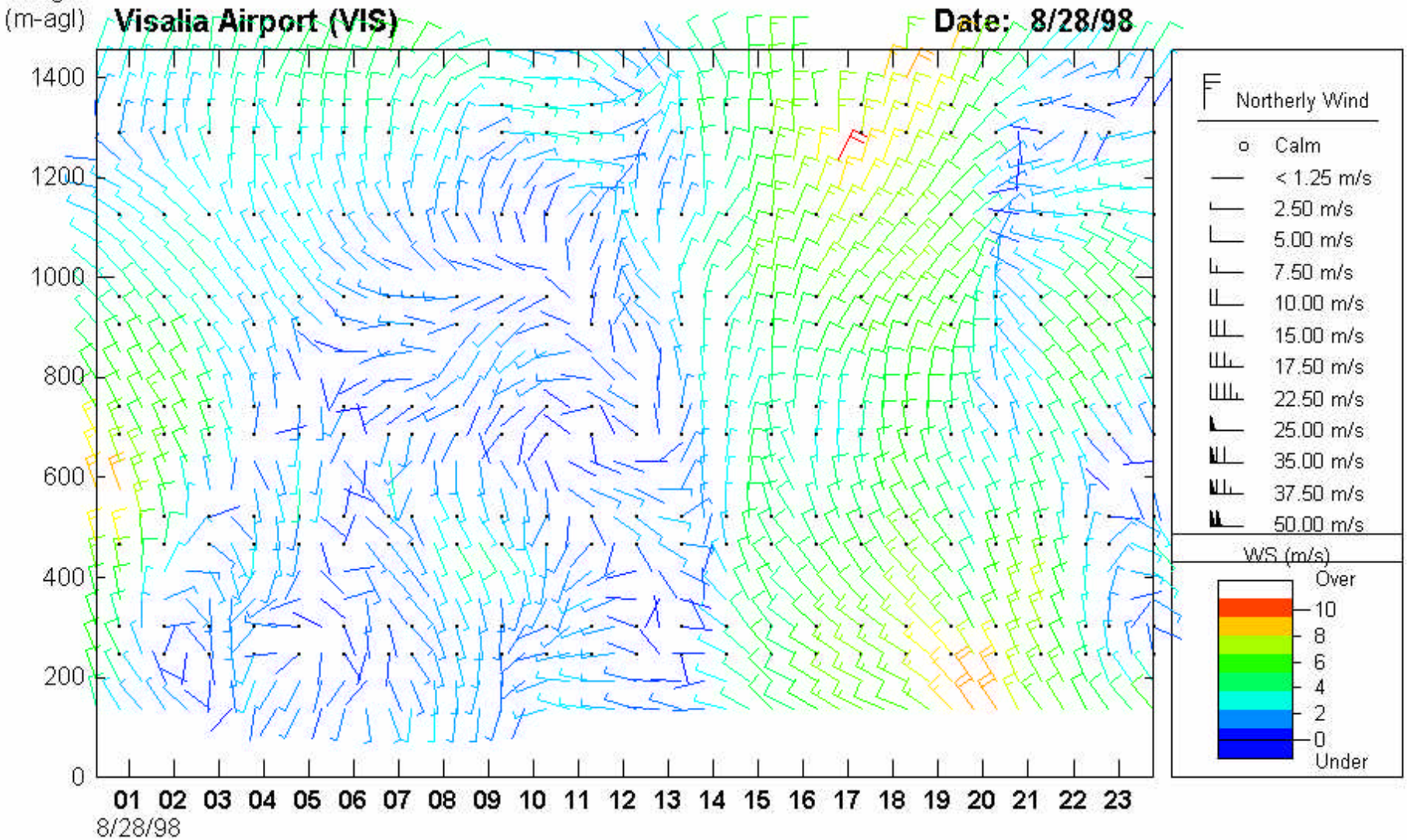

Elev. (m): 89

Validation Level: 0.5
Printed: 5/13/99

San Joaquin Valley Unified Air Pollution

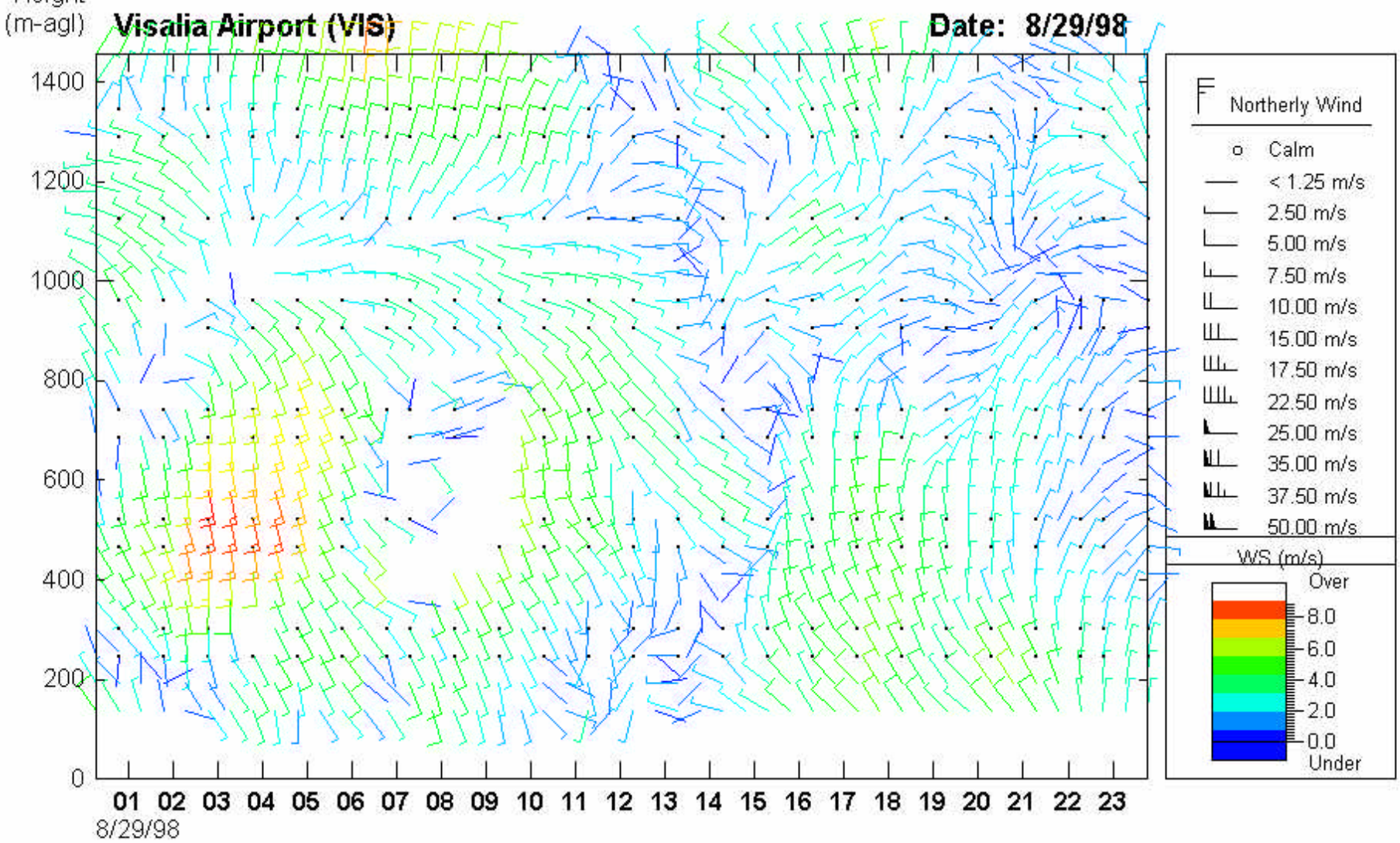

Elev. (m): 89

Validation Level: 0.5
Printed: 5/13/99

San Joaquin Valley Unified Air Pollution

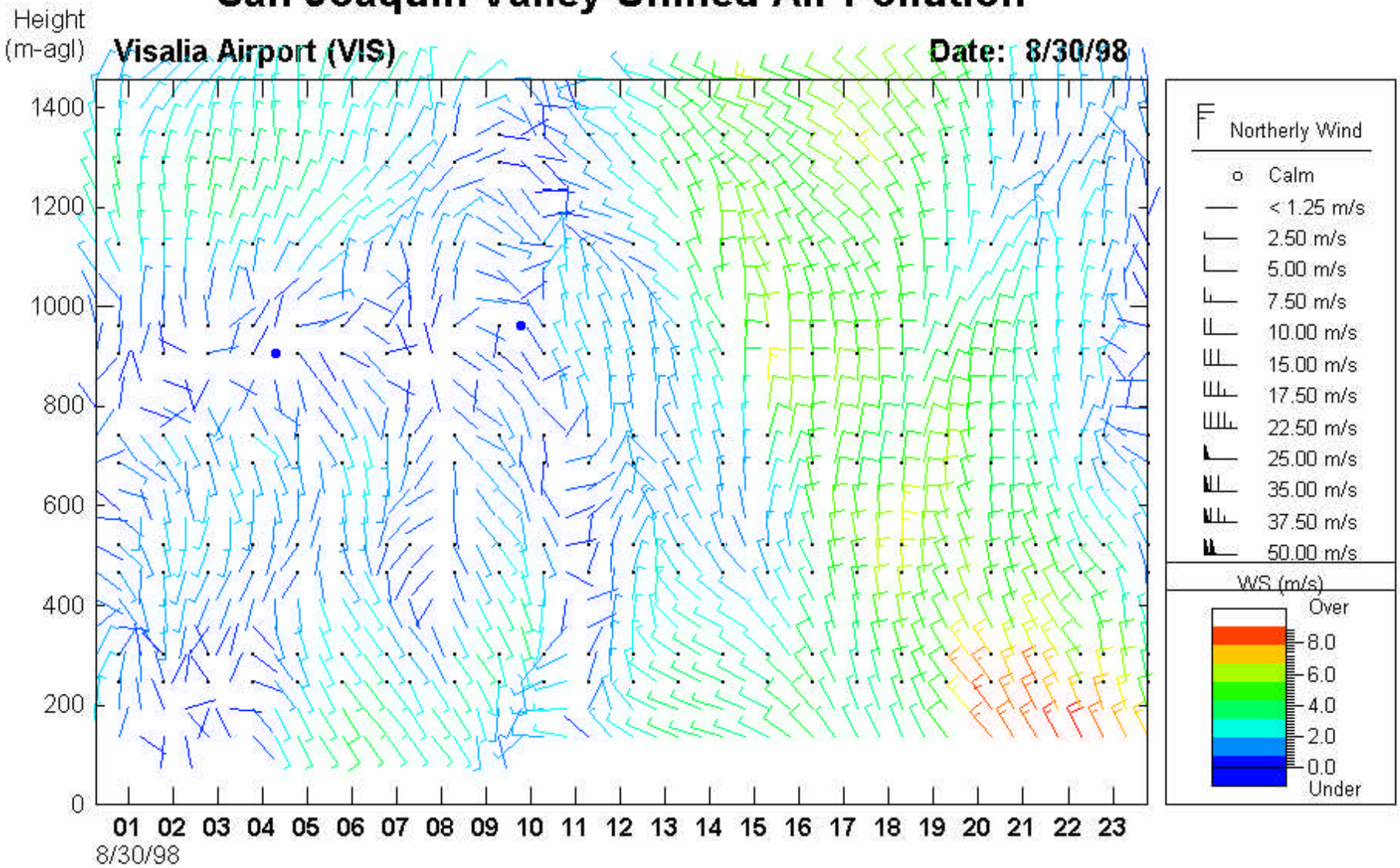

Elev. (m): 89

Validation Level: 0.5
Printed: 5/13/99

San Joaquin Valley Unified Air Pollution

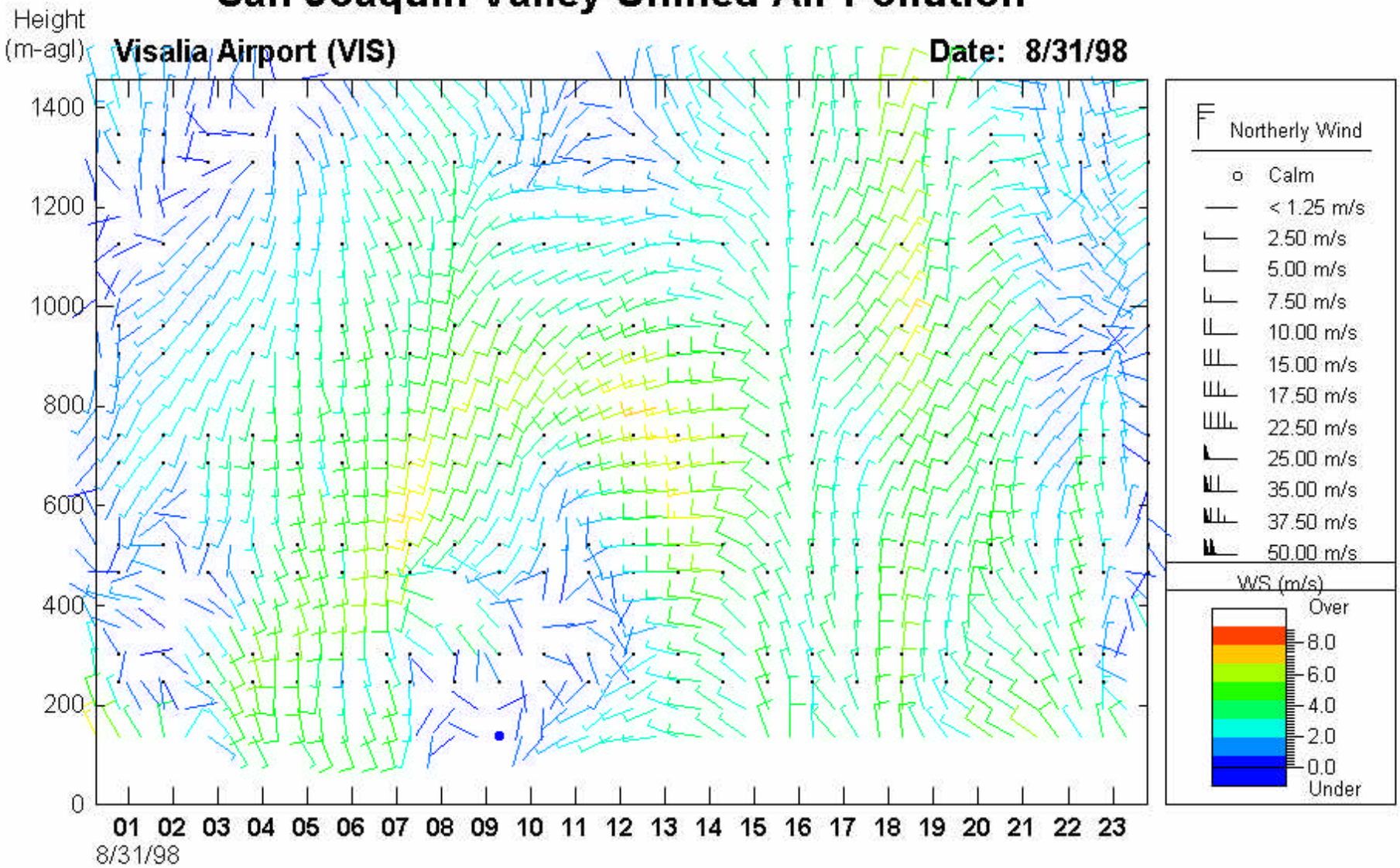

Elev. (m): 89

Validation Level: 0.5
Printed: 5/13/99

San Joaquin Valley Unified Air Pollution

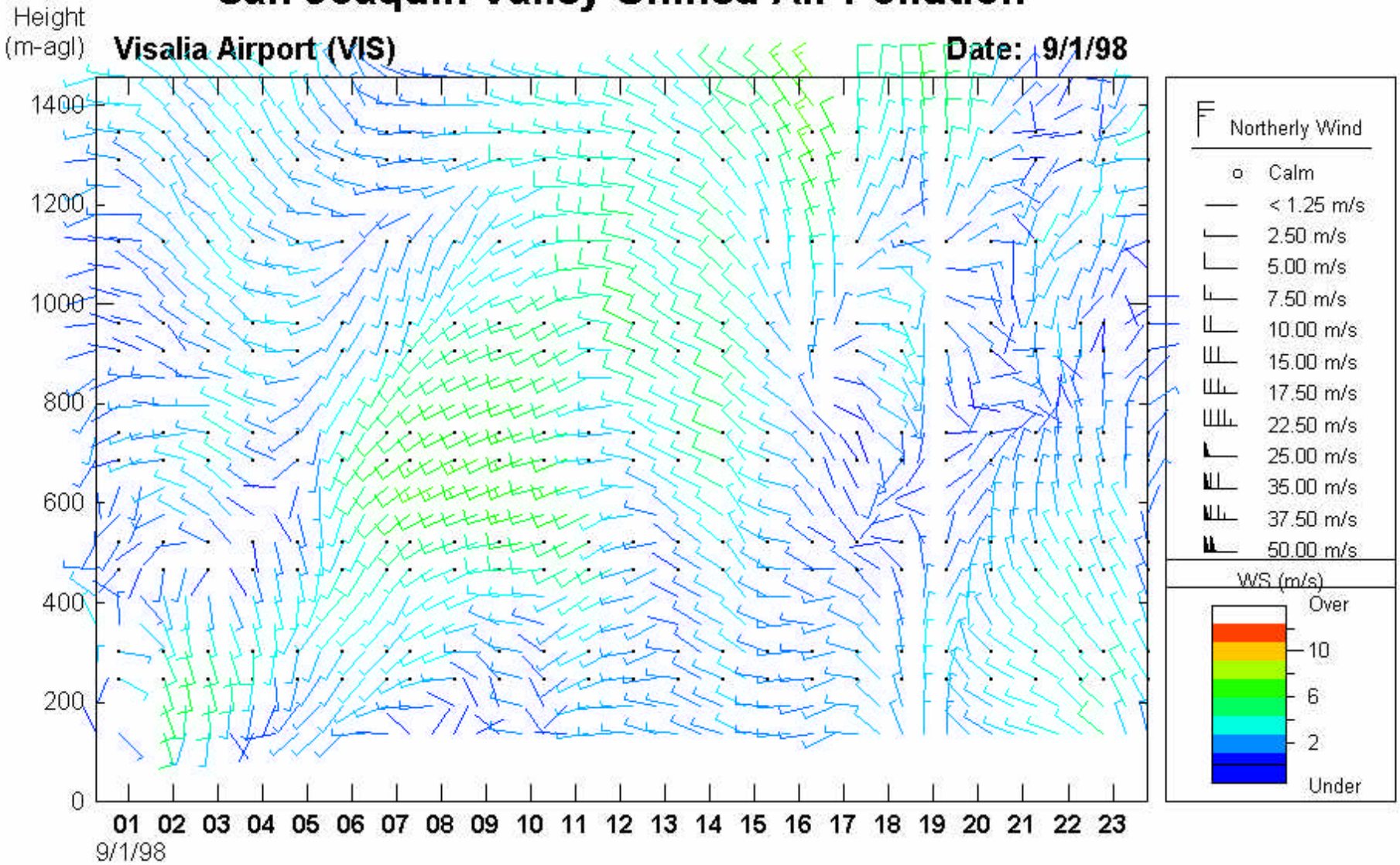

Elev. (m): 89

Time (PST)

Validation Level: 0.5
Printed: 5/13/99

San Joaquin Valley Unified Air Pollution

Visalia Airport (VIS) **Date: 9/2/98**

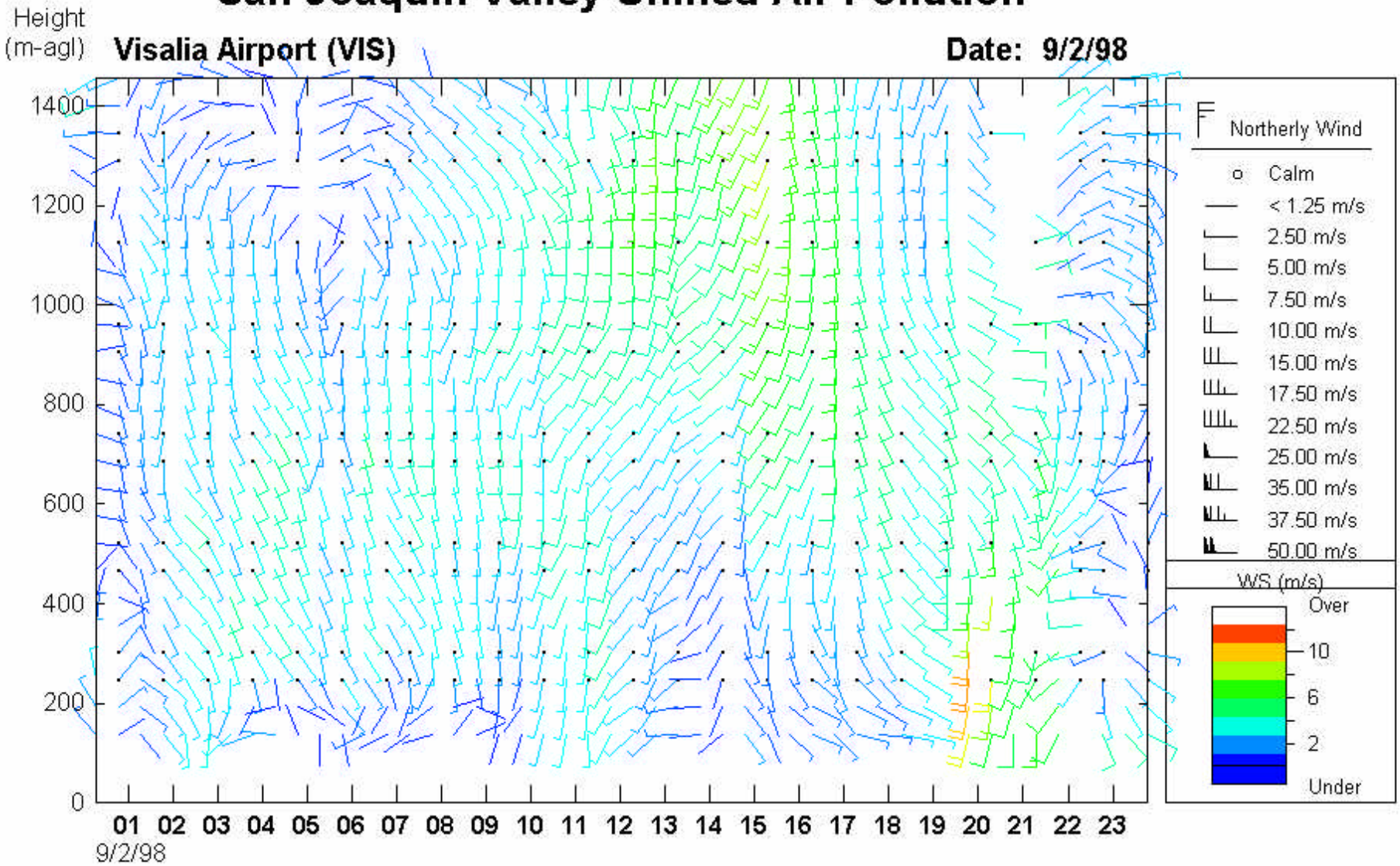

Elev. (m): 89

Validation Level: 0.5
Printed: 5/13/99

San Joaquin Valley Unified Air Pollution

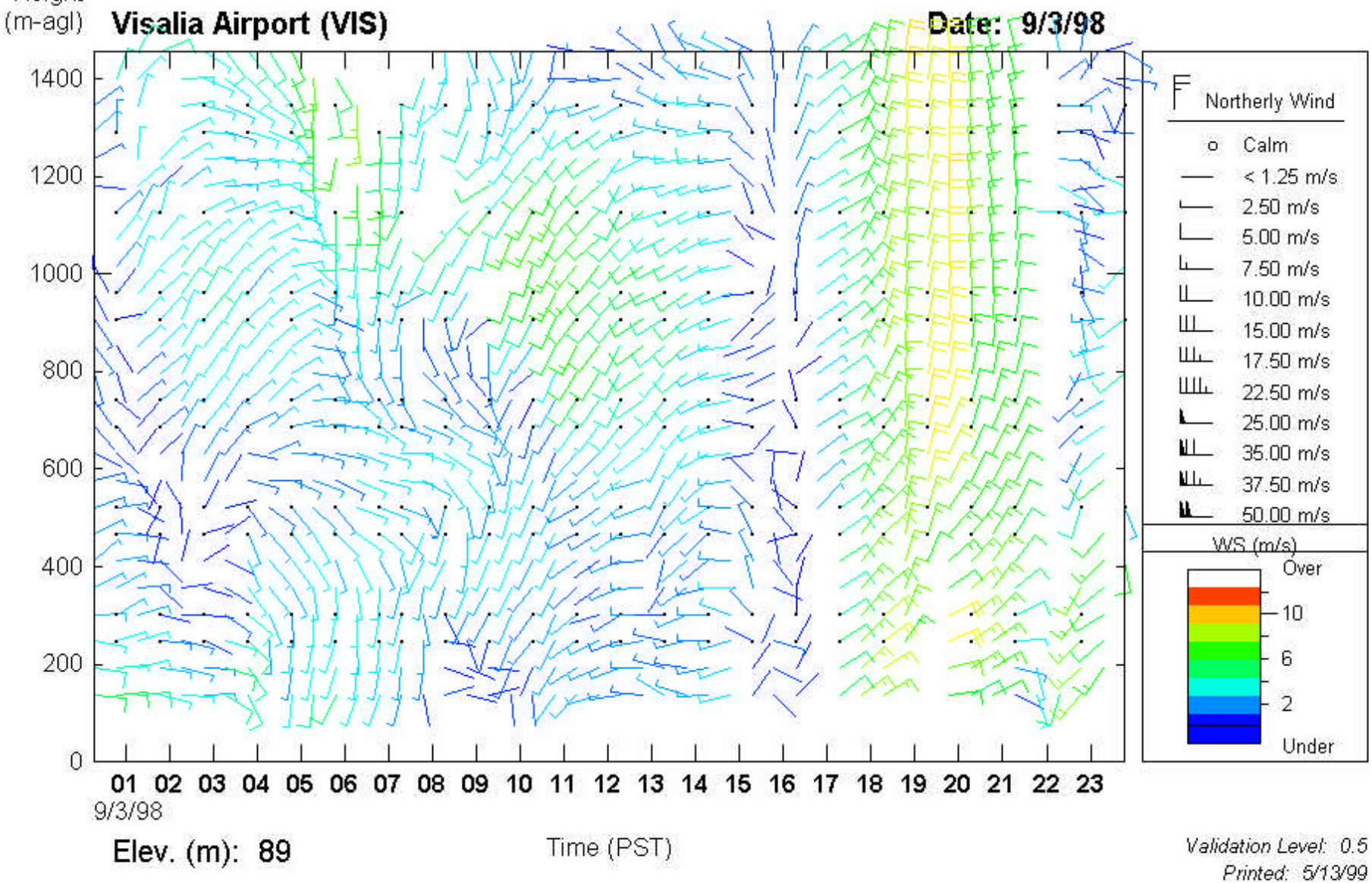

Elev. (m): 89

Time (PST)

Validation Level: 0.5
Printed: 5/13/99

Ventura County Air Pollution

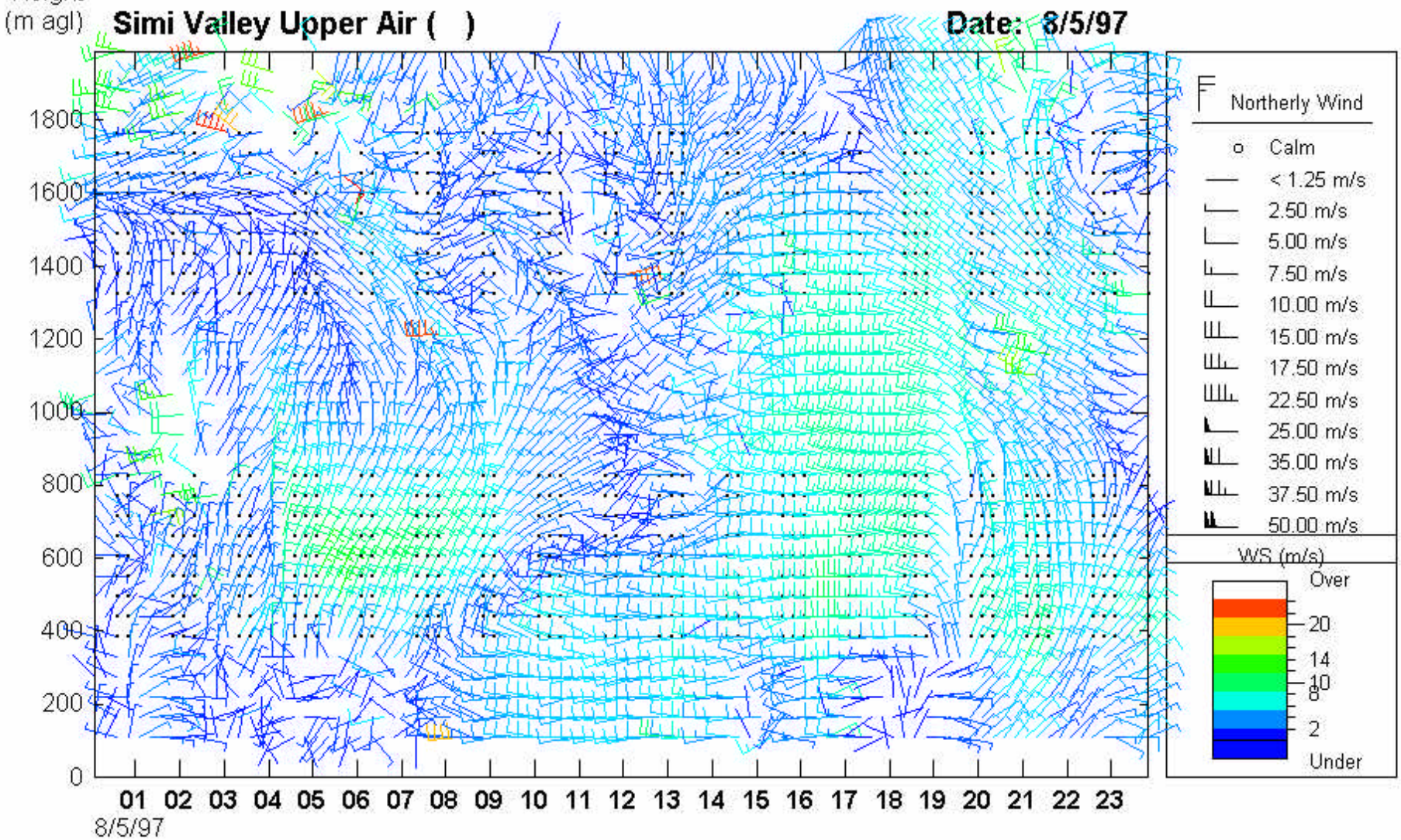

Elev. (m): 279

Time (PST)

Validation Level: 0.0
Printed: 5/13/99

Ventura County Air Pollution

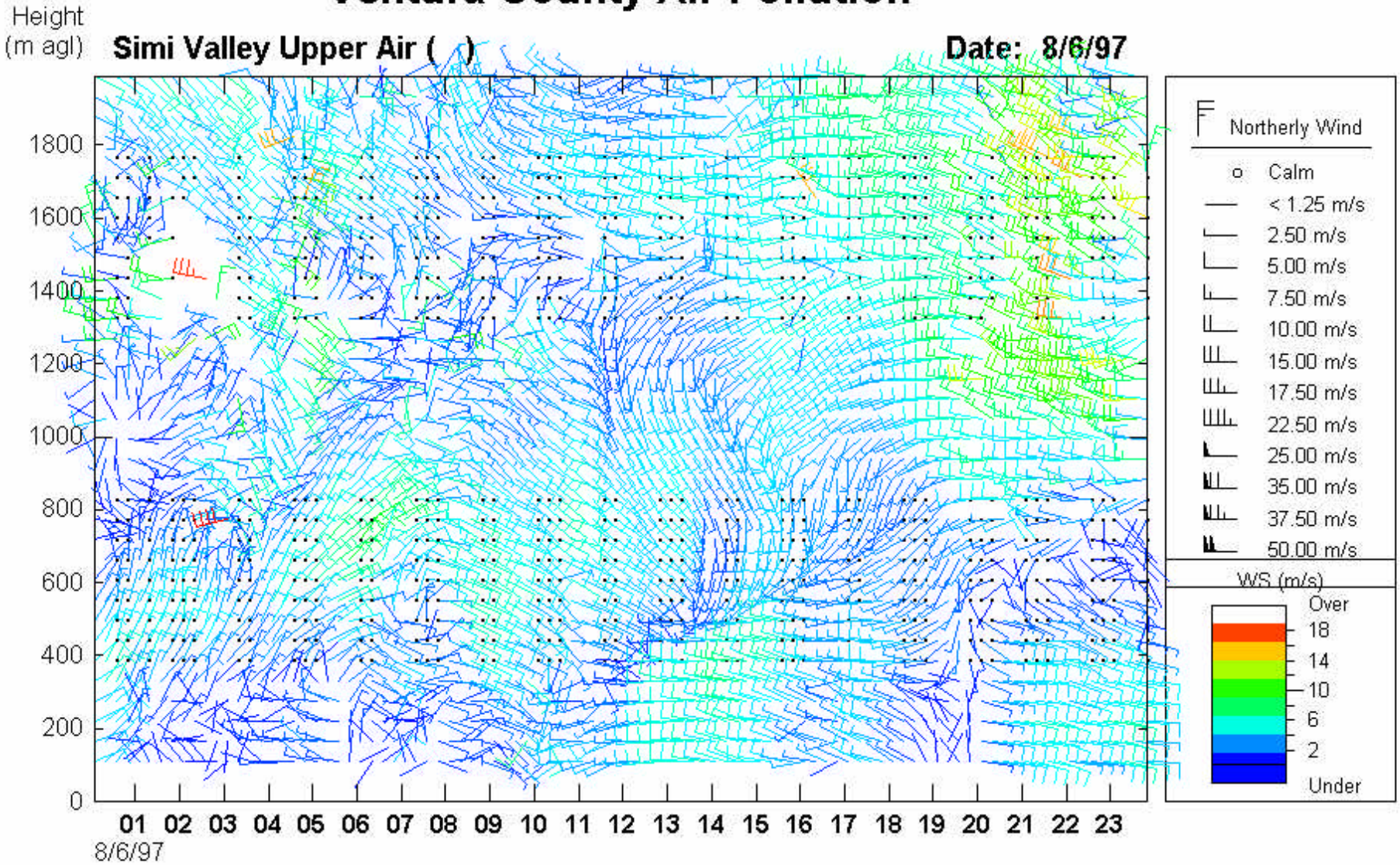

Elev. (m): 279

Validation Level: 0.0
Printed: 5/13/99

Ventura County Air Pollution

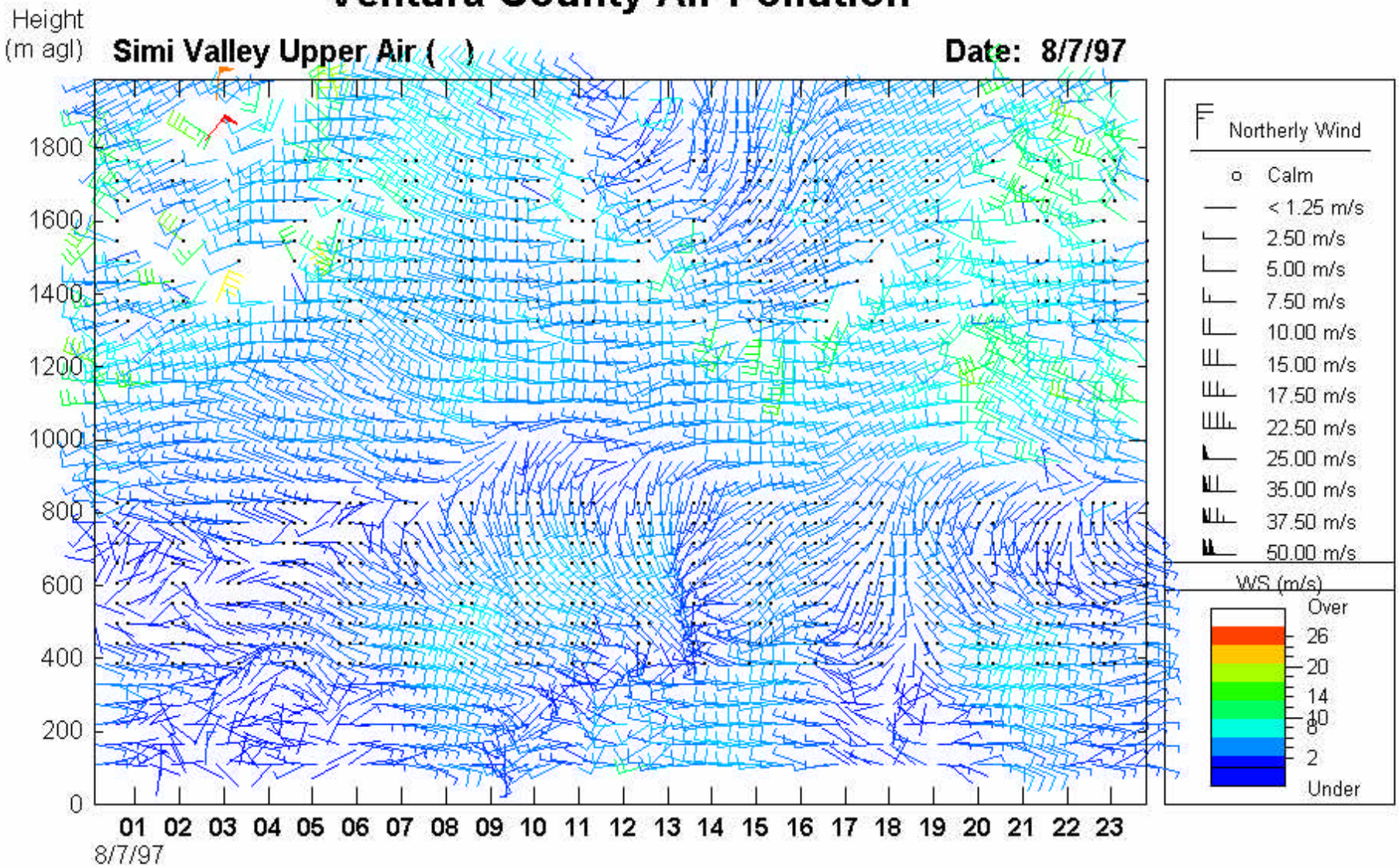

Elev. (m): 279

Validation Level: 0.0
Printed: 5/13/99

Ventura County Air Pollution

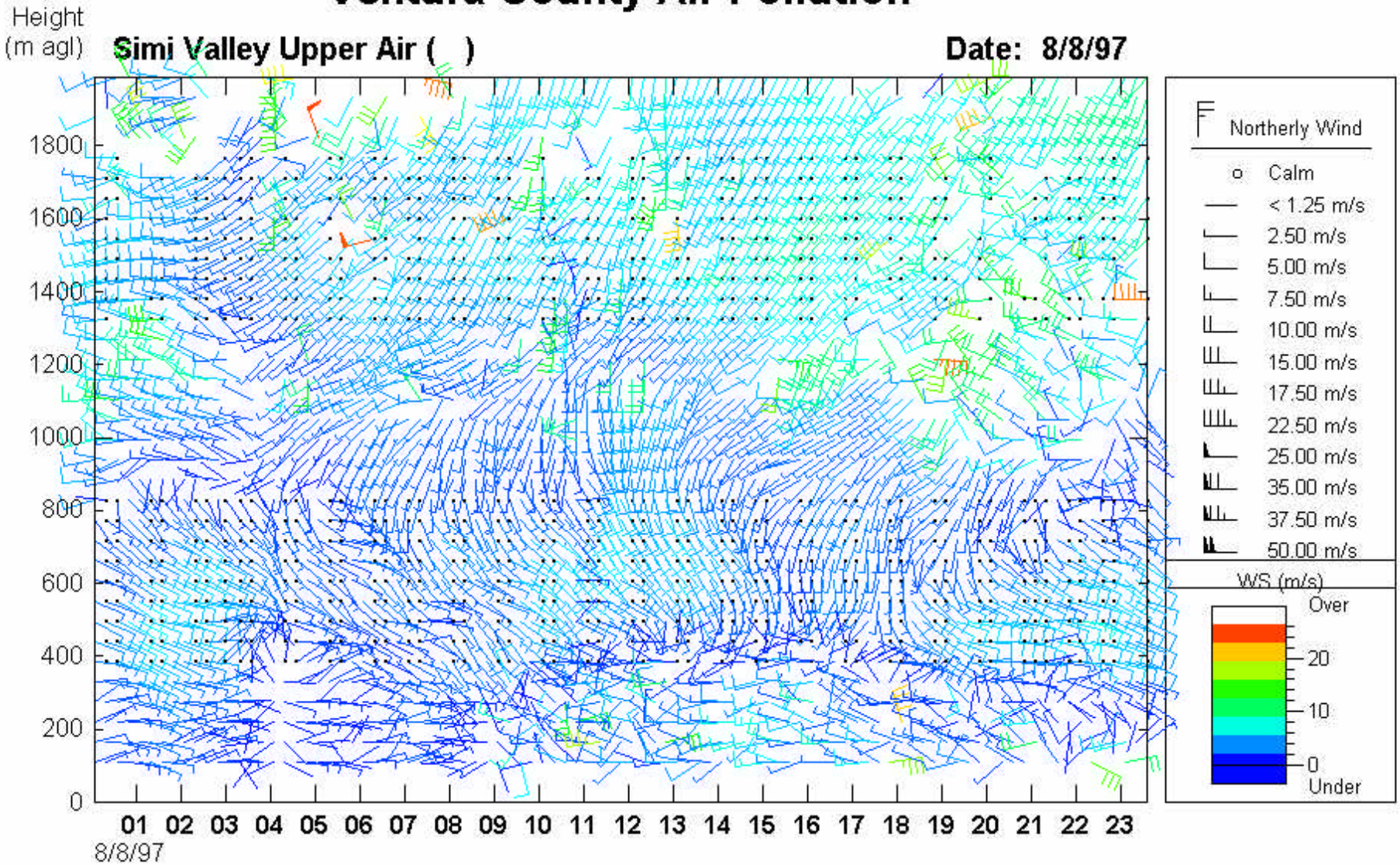

Elev. (m): 279

Validation Level: 0.0
Printed: 5/13/99

Ventura County Air Pollution

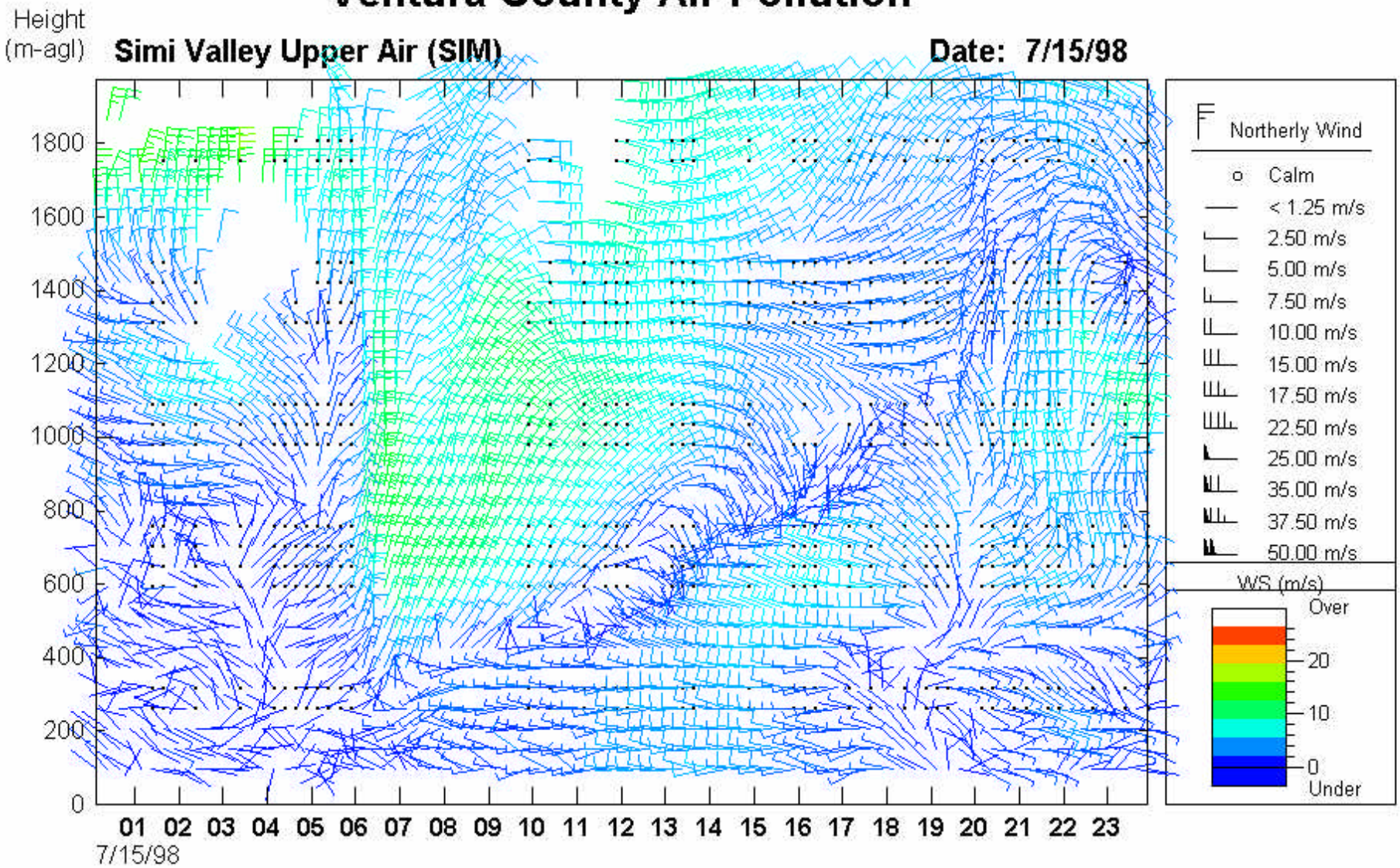

Elev. (m): 279

Time (PST)

Validation Level: 0.0
Printed: 5/13/99

Ventura County Air Pollution

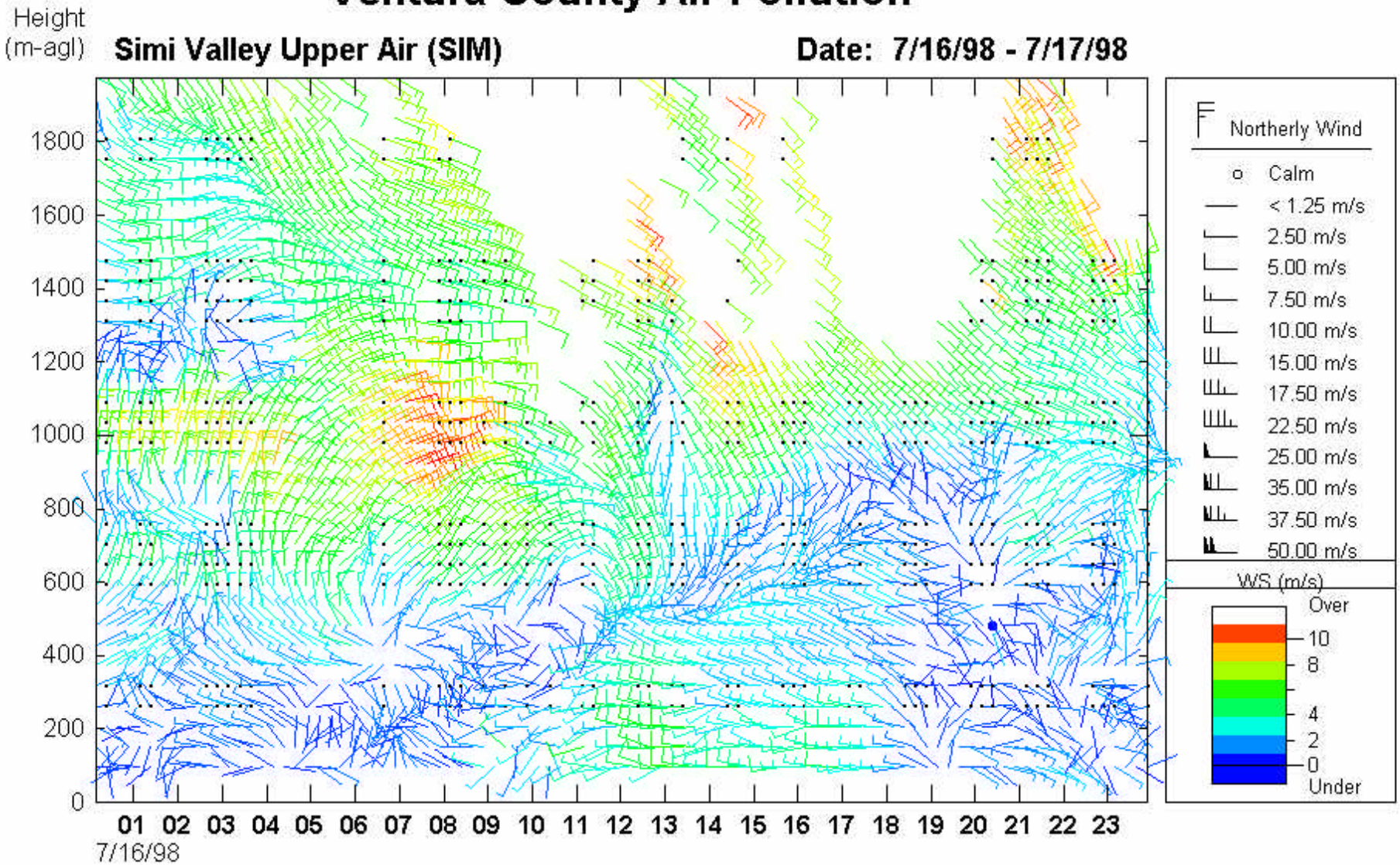

Elev. (m): 279

Validation Level: 0.0
Printed: 5/13/99

Ventura County Air Pollution

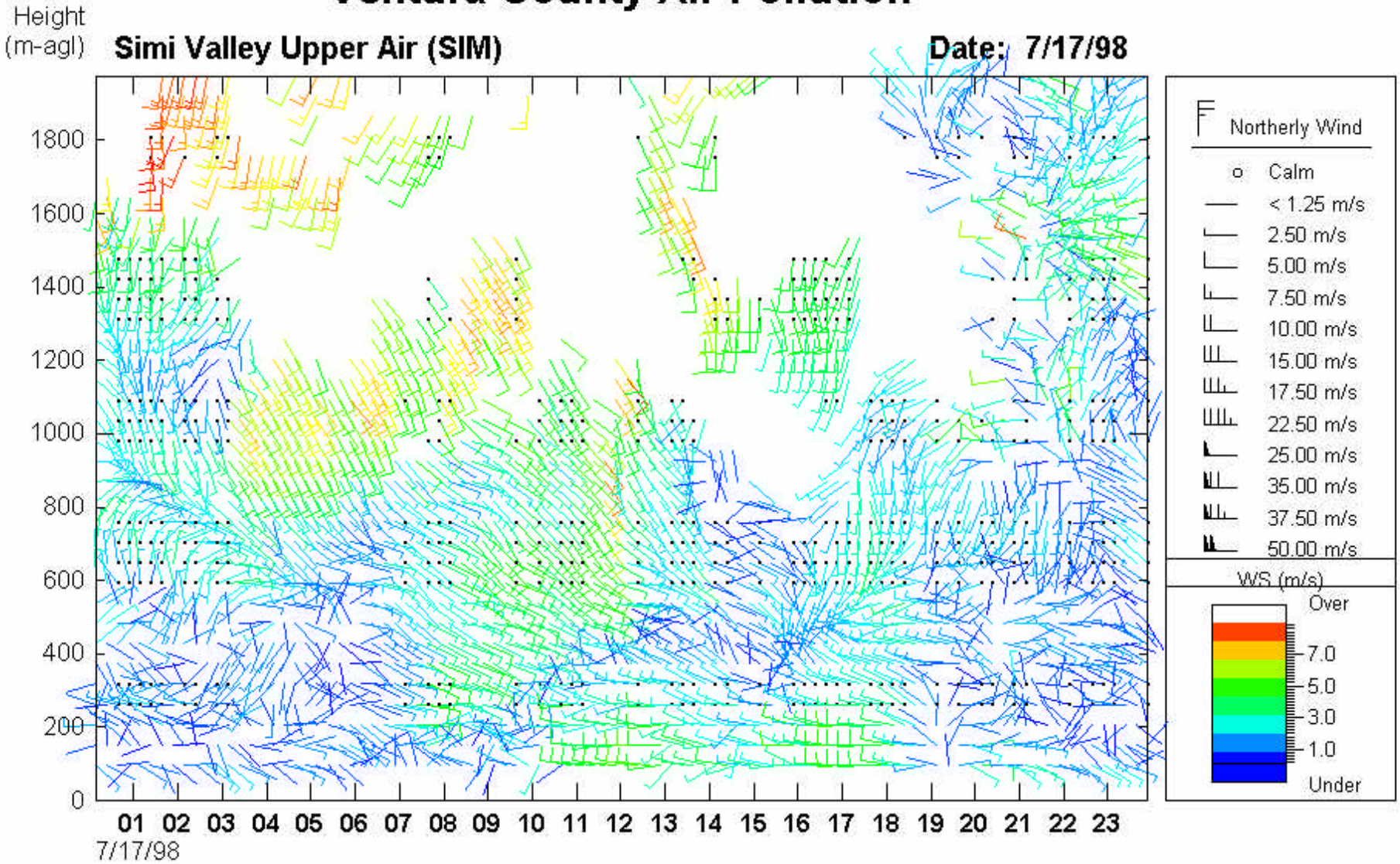

Elev. (m): 279

Validation Level: 0.0
Printed: 5/13/99

Ventura County Air Pollution

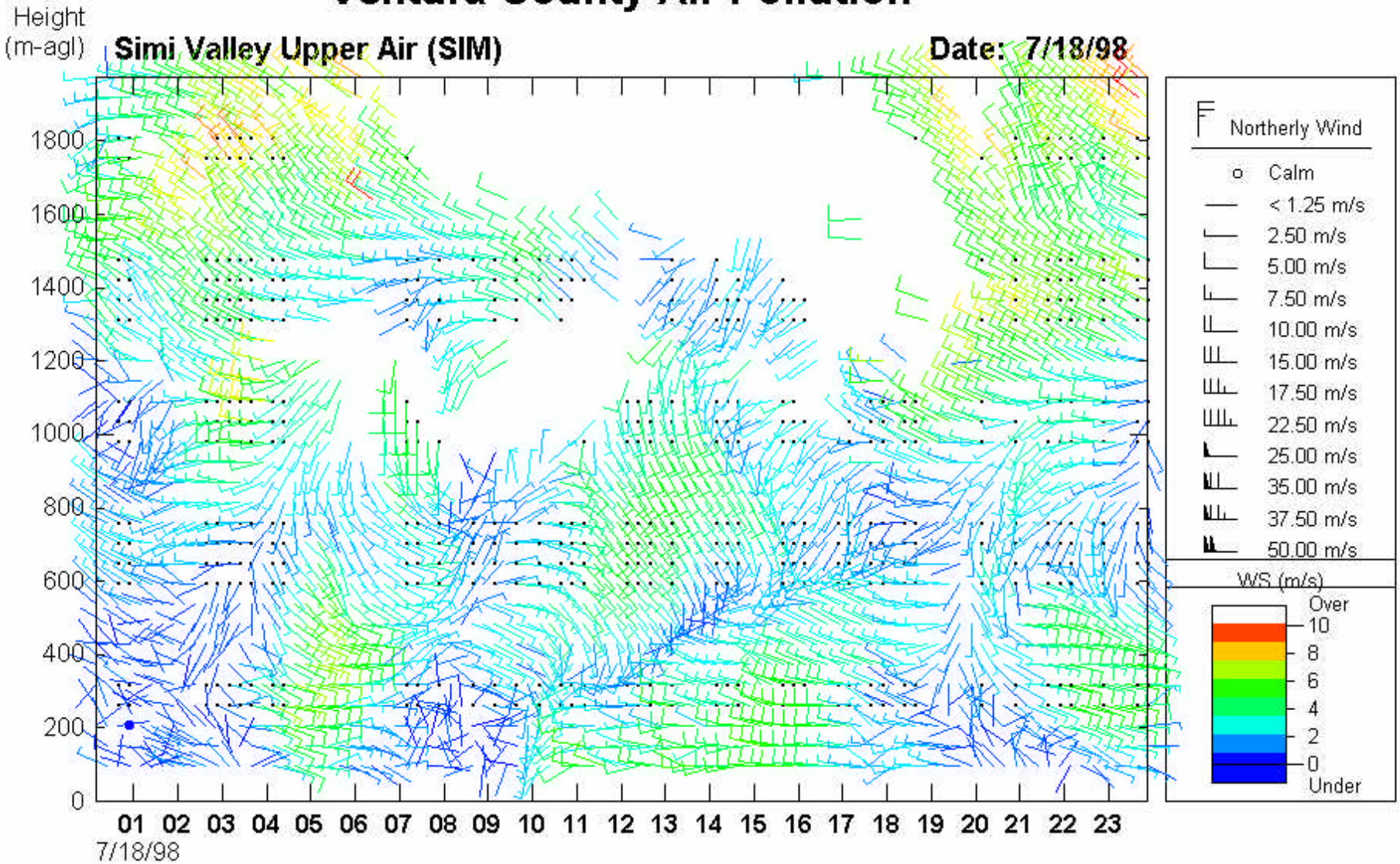

Elev. (m): 279

Validation Level: 0.0
Printed: 5/13/99

Ventura County Air Pollution

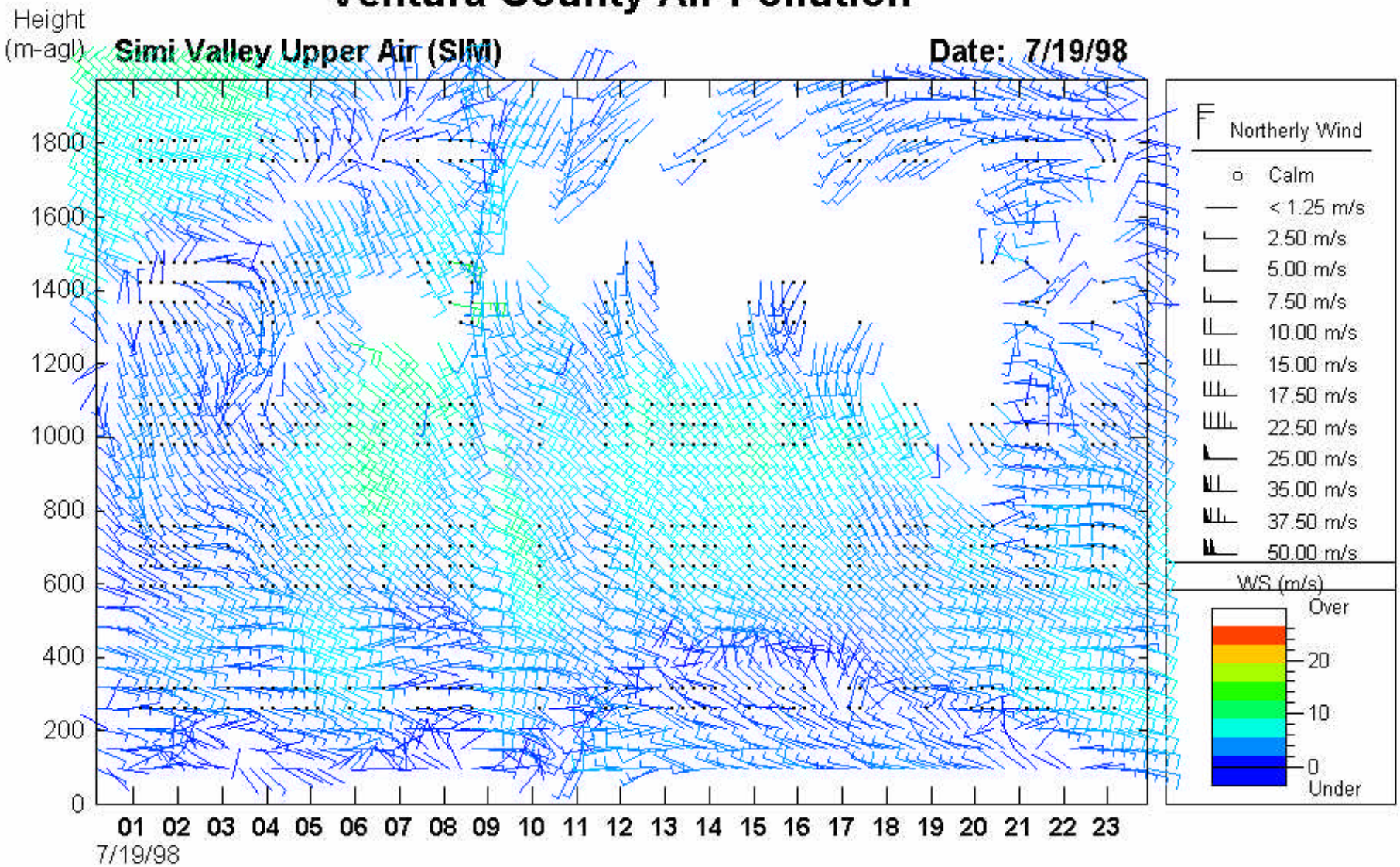

Elev. (m): 279

Time (PST)

Validation Level: 0.0
Printed: 5/13/99

Ventura County Air Pollution

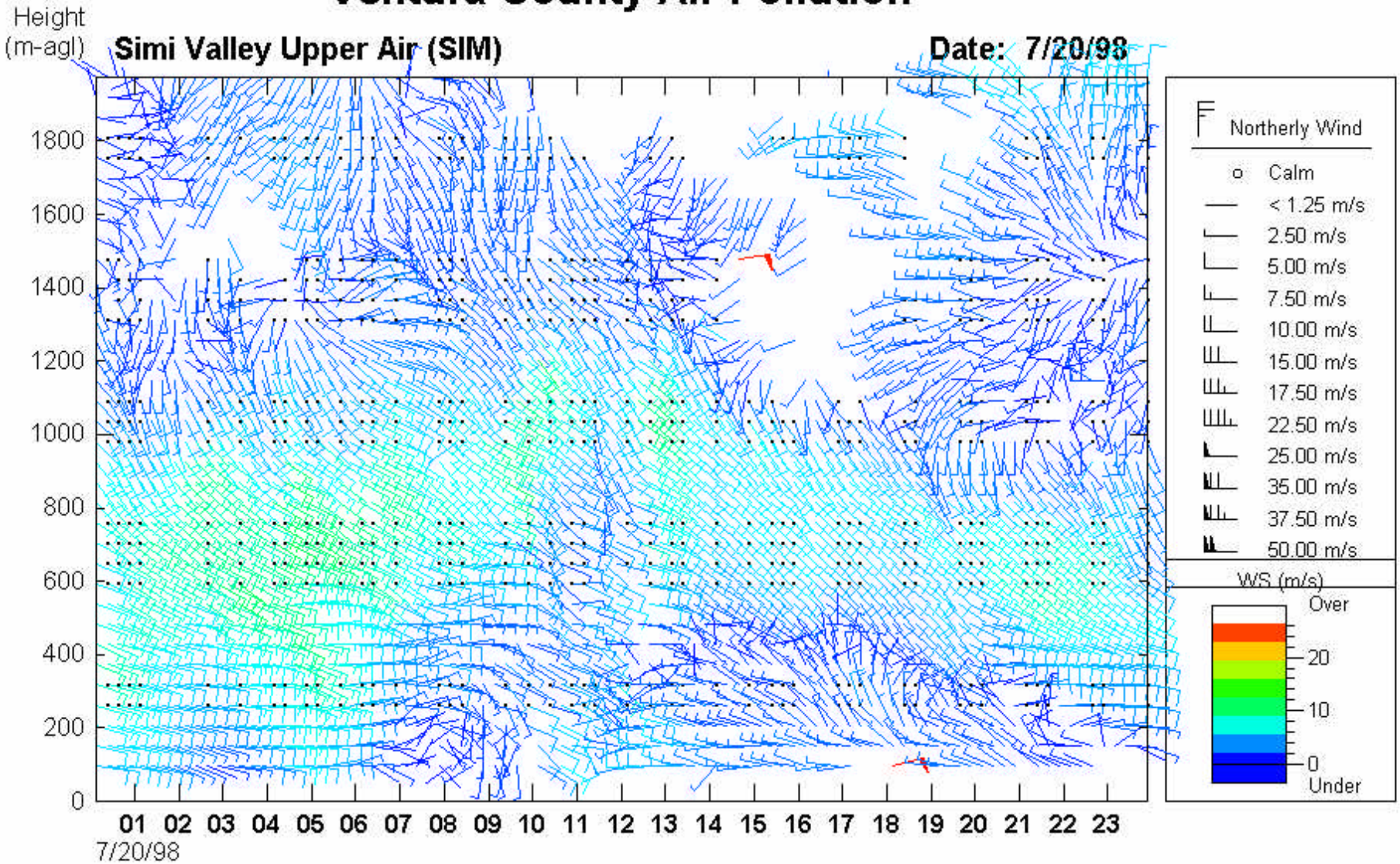

Elev. (m): 279

Validation Level: 0.0
Printed: 5/13/99

APPENDIX C

TRANSPORT STATISTICS

This appendix provides transport statistics calculated from the radar profiler winds measured at Simi Valley (Ventura), Franklin Field (Sacramento), and Visalia (San Joaquin Valley) for the 1997 and 1998 episode days analyzed in this report. Transport statistics are metrics used to help us understand transport, ventilation, and re-circulation throughout the day and at all profiler sampling heights.

The quantities computed using the procedure developed by Allwine and Whiteman (1994) represent the scalar wind run S (km), the resultant (vector) transport distance L (km), the resultant (vector-averaged) wind direction Θ (degrees from true north adjusted to the proper quadrant), and the recirculation factor, R. Note that the vector transport distance is not a trajectory, but a wind run. It quantifies the transport assuming that the wind observed by the profiler is spatially consistent through the maximum transport distance. The recirculation factor is the ratio of the resultant transport distance to the scalar transport distance (wind run). When R is equal to 1, straight-line, steady transport has occurred during the integration period. When R is equal to zero, no net transport has occurred during the integration period. Values of R close to 1, combined with transport distances of a few hundred kilometers, would typically characterize good ventilation conditions. Conversely, low values of R represent periods of stagnation or recirculation. Stagnation would be indicated by short scalar wind runs (i.e., low wind speeds); recirculation would be characterized by low values of the vector transport distance (e.g., L less than 50 km) compared to the scalar wind run. For example, if R were 0.25 and the vector-averaged wind run were 50 km, the scalar wind run would be 200 km. This would be characteristic of recirculation conditions; air must have recirculated in the area of interest.

The integration time, T, was specified as 12 hours and the transport statistics were computed from day 1 at 0400 PST to day 1 at 1600 PST, and from day 1 at 1600 PST to day 2 at 0400 PST. These time periods were selected to capture daytime and nighttime flow patterns, respectively.

[BLANK PAGE]

SAC 07-16-98 0400 to 1600.xls

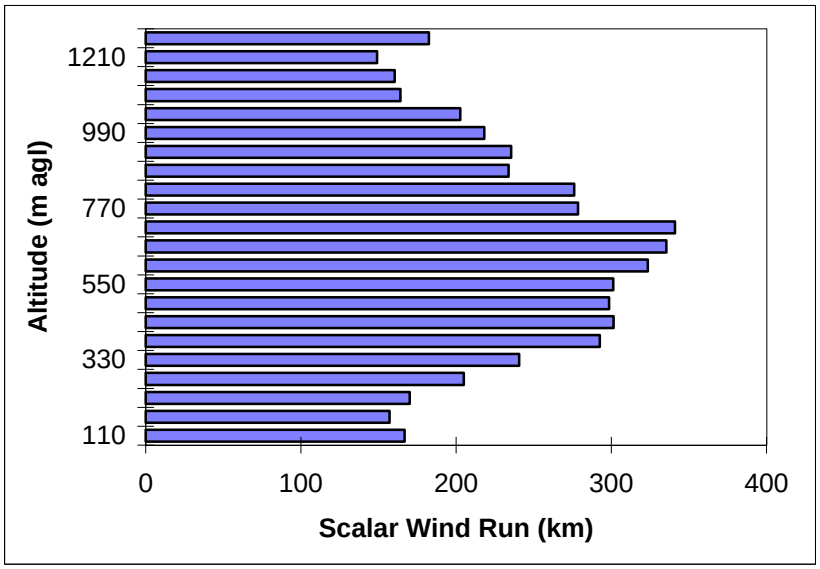

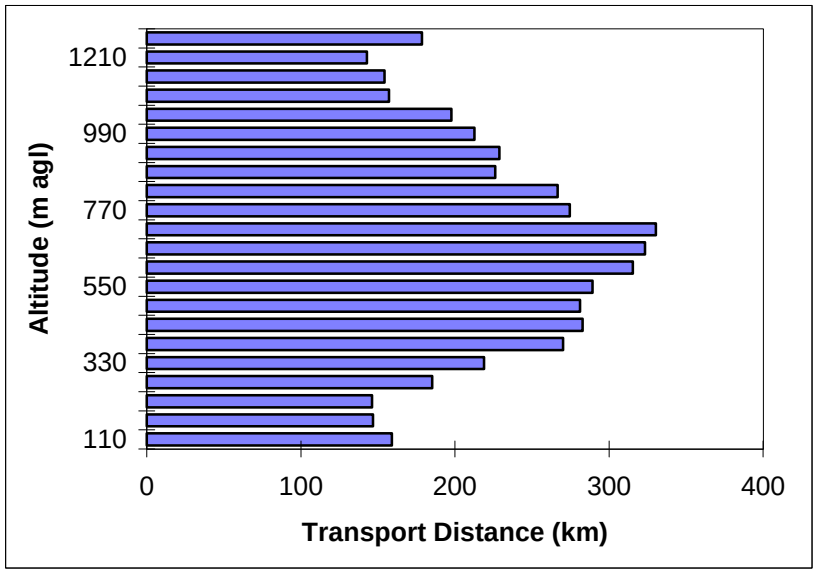

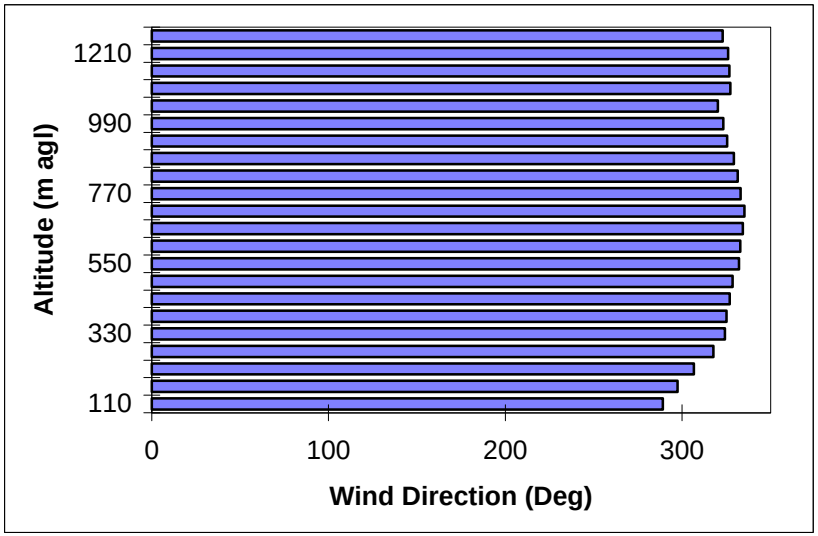

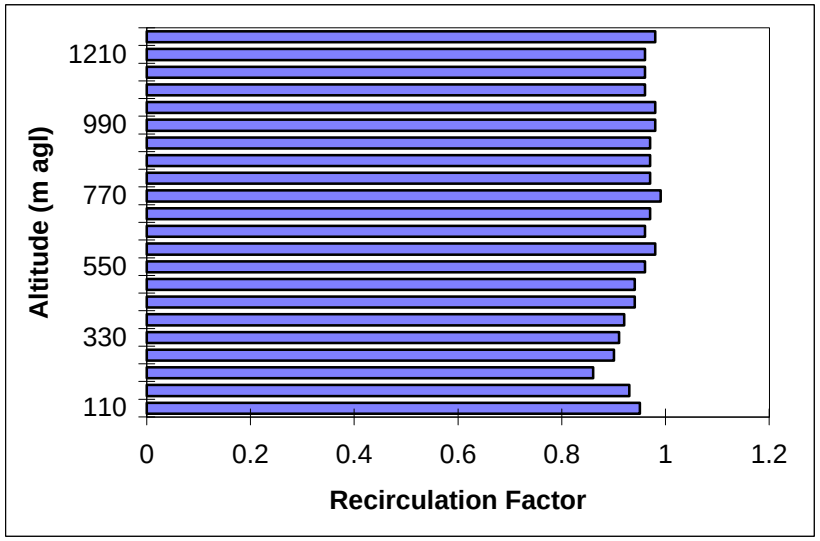

[BLANK PAGE]

SAC 07-16-98 1600 to 0400.xls

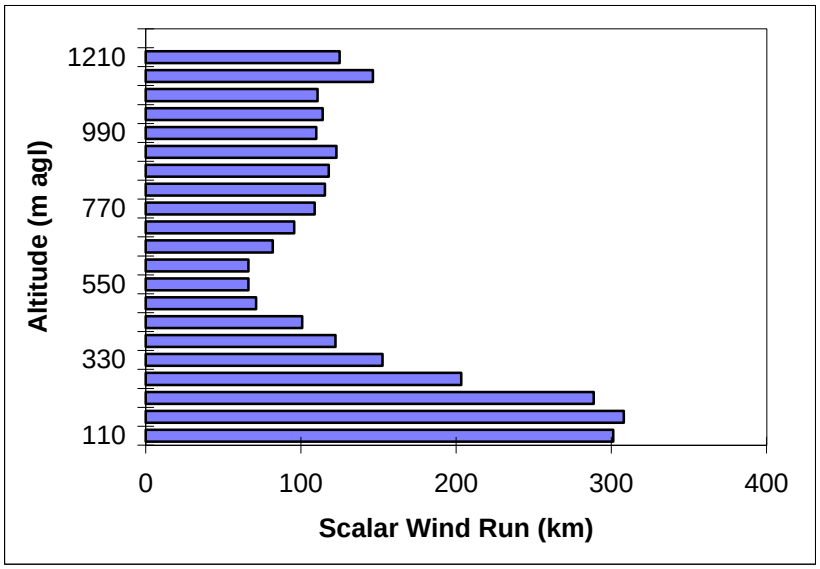

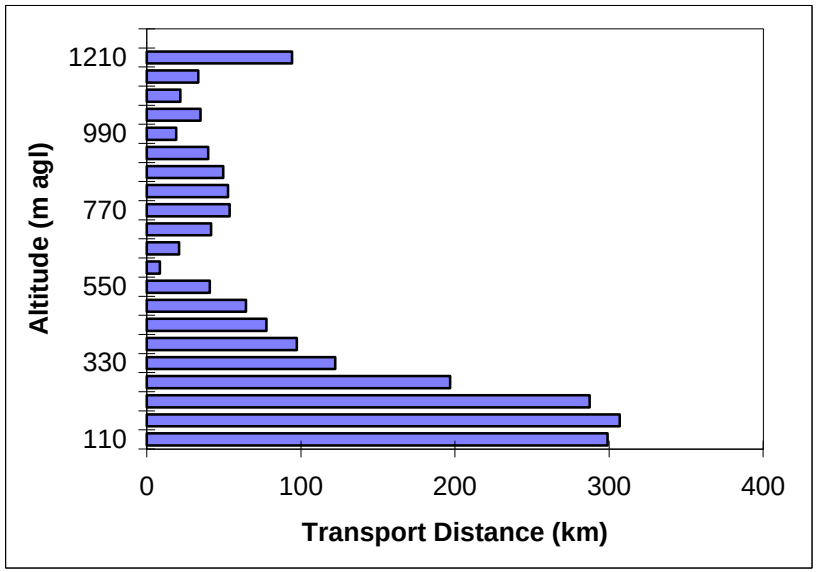

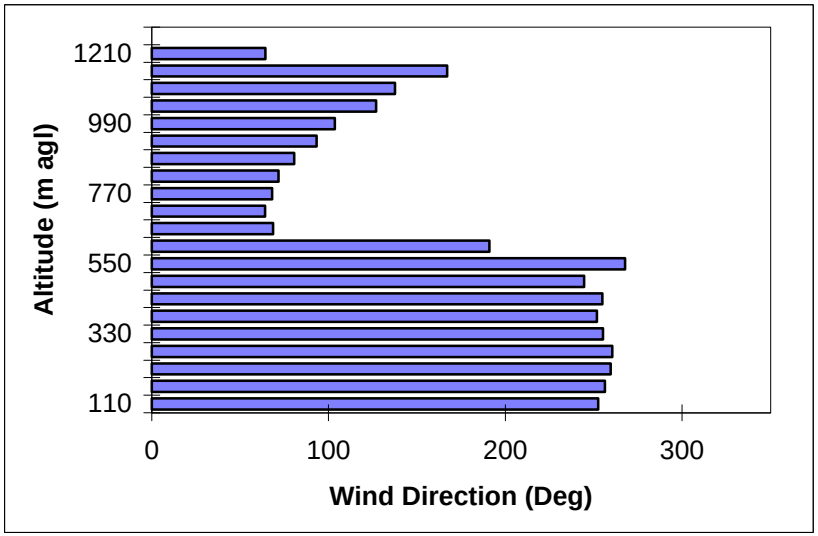

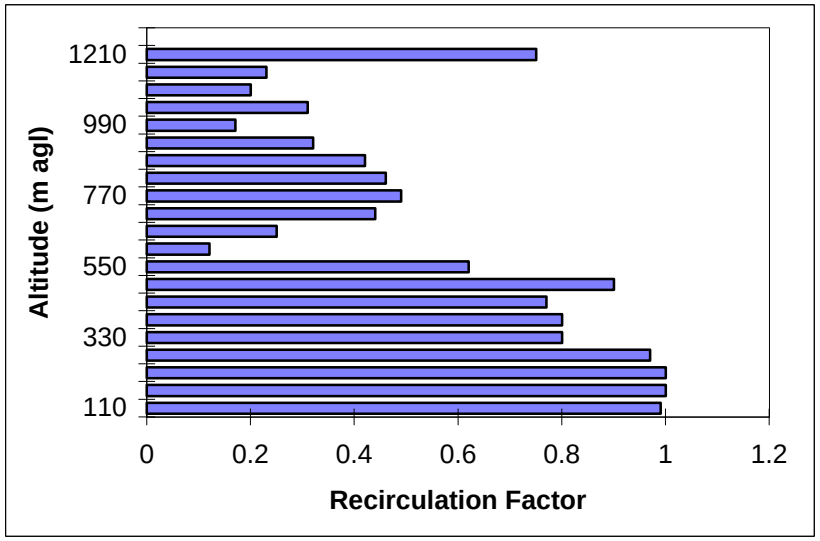

SAC 07-17-98 0400 to 1600.xls

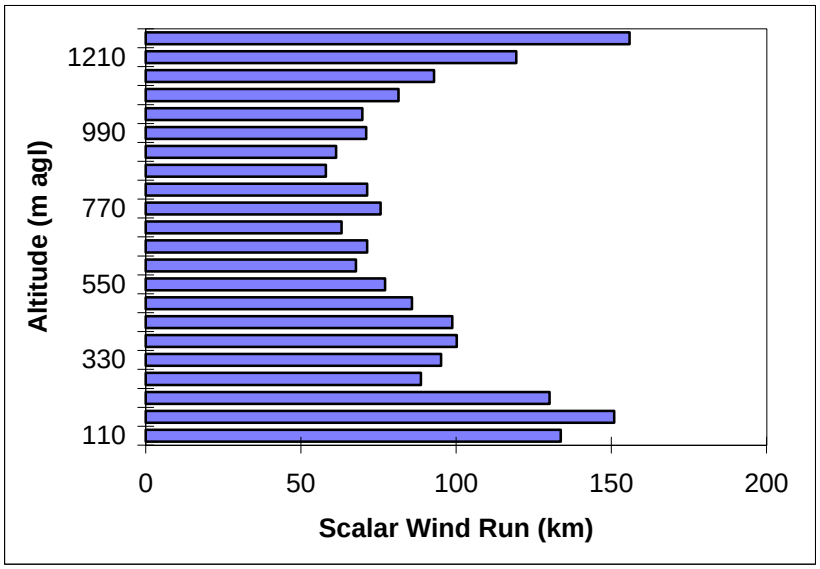

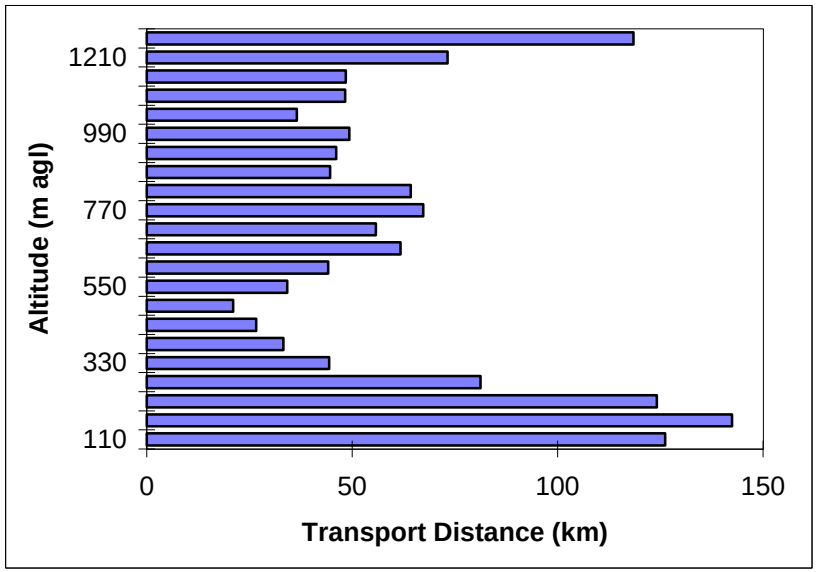

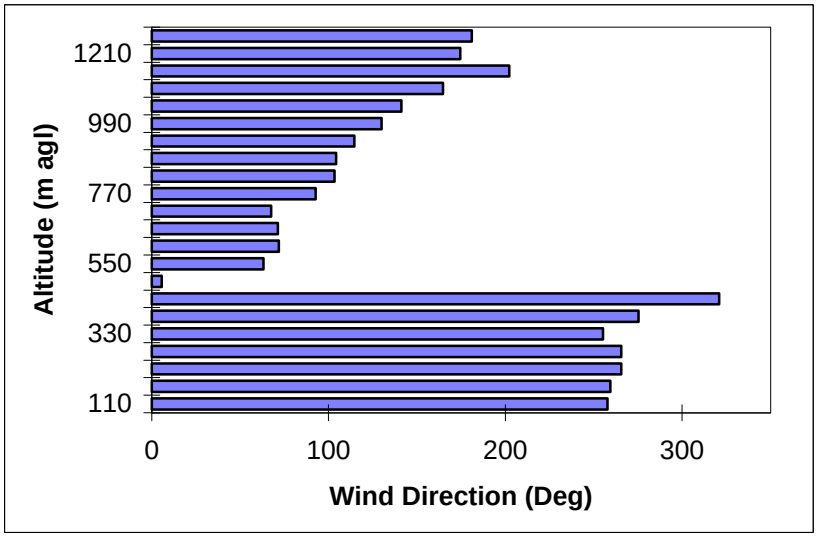

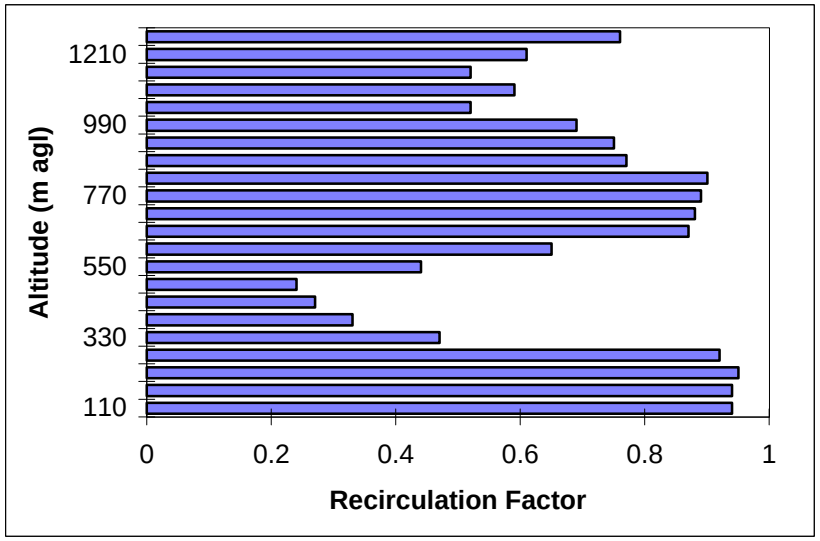

SAC 07-17-98 1600 to 0400.xls

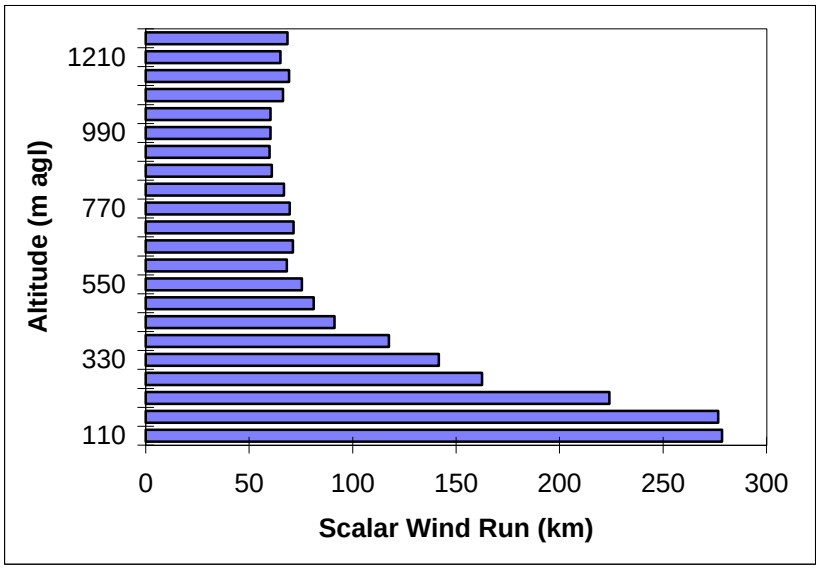

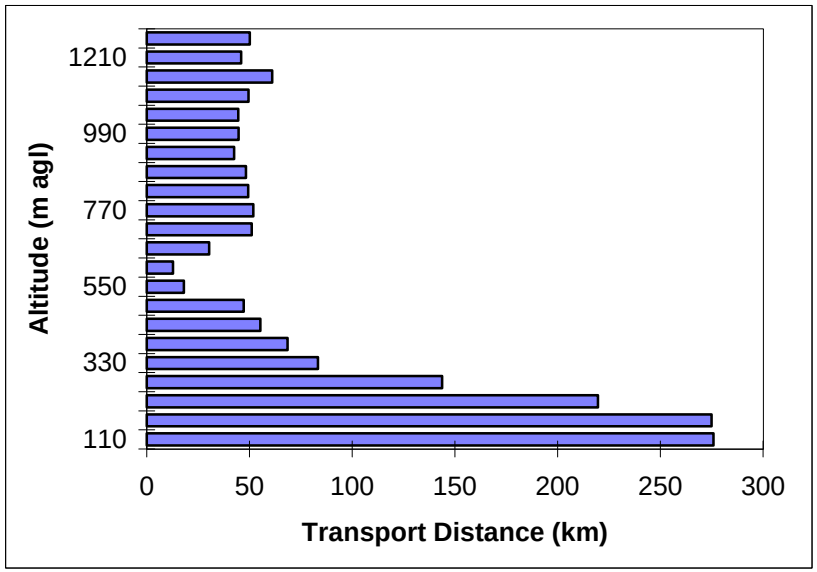

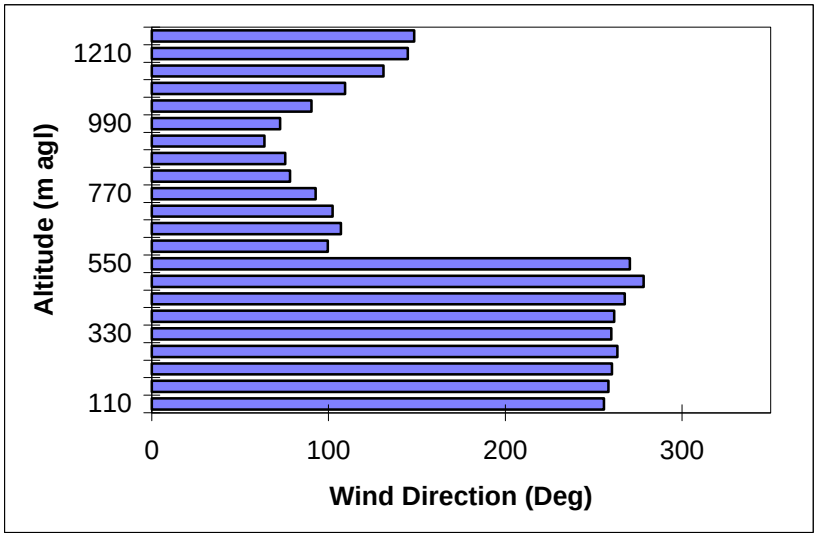

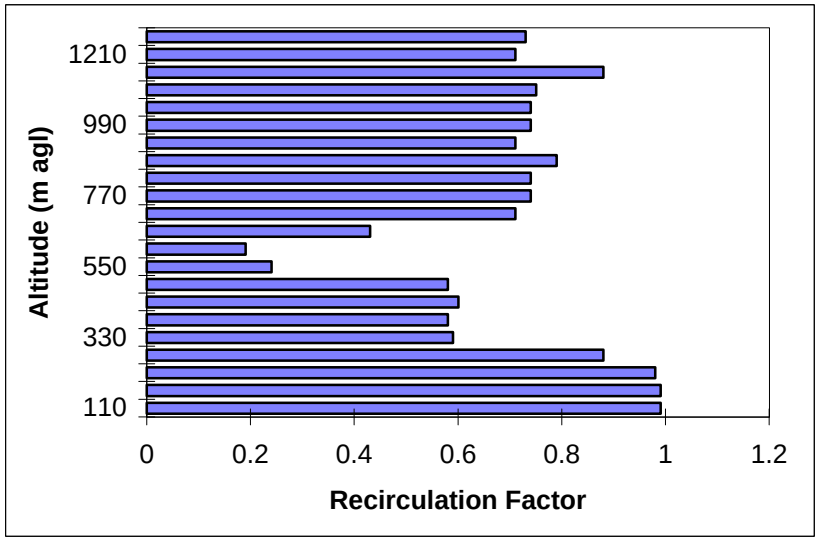

SAC 07-18-98 0400 to 1600.xls

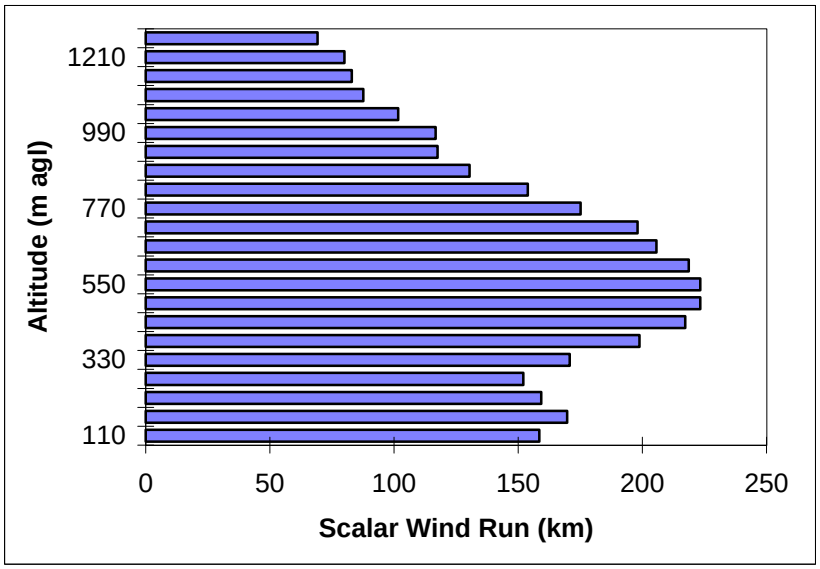

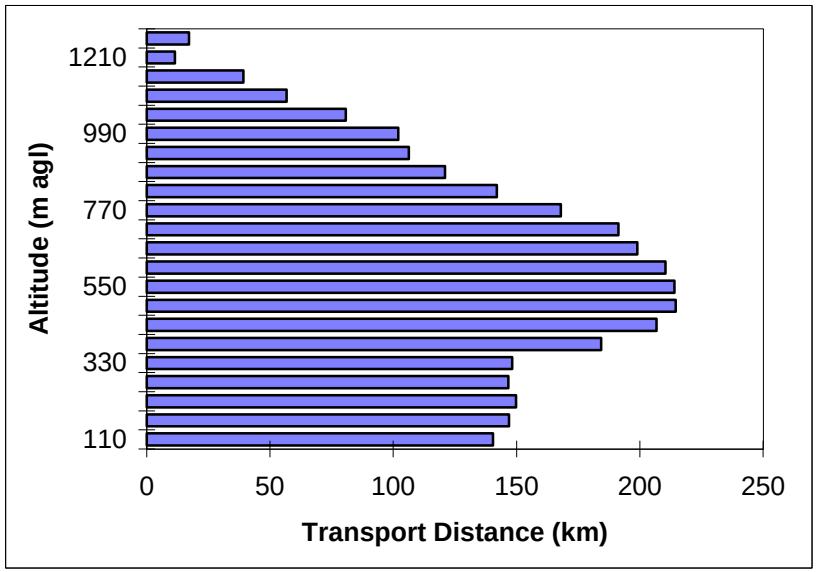

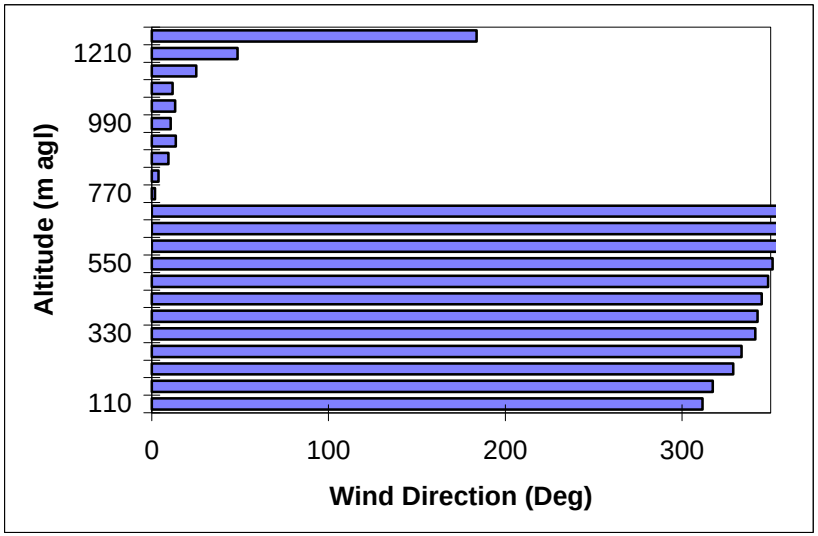

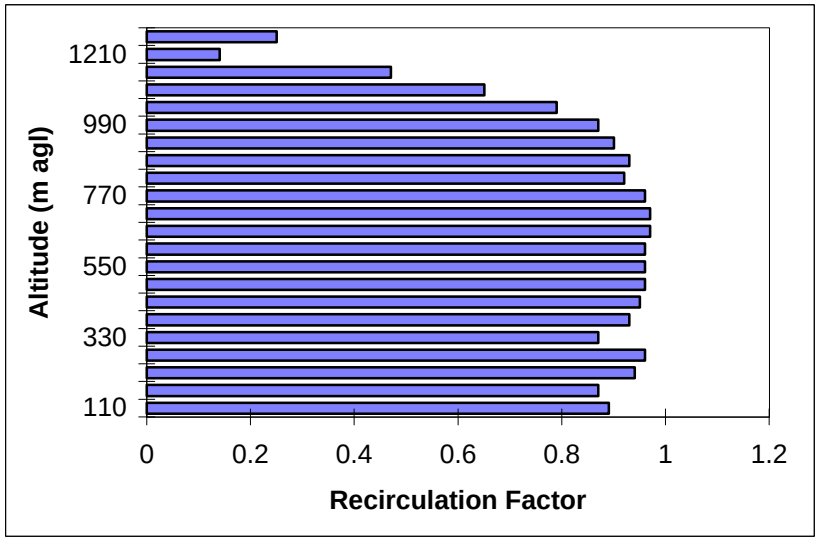

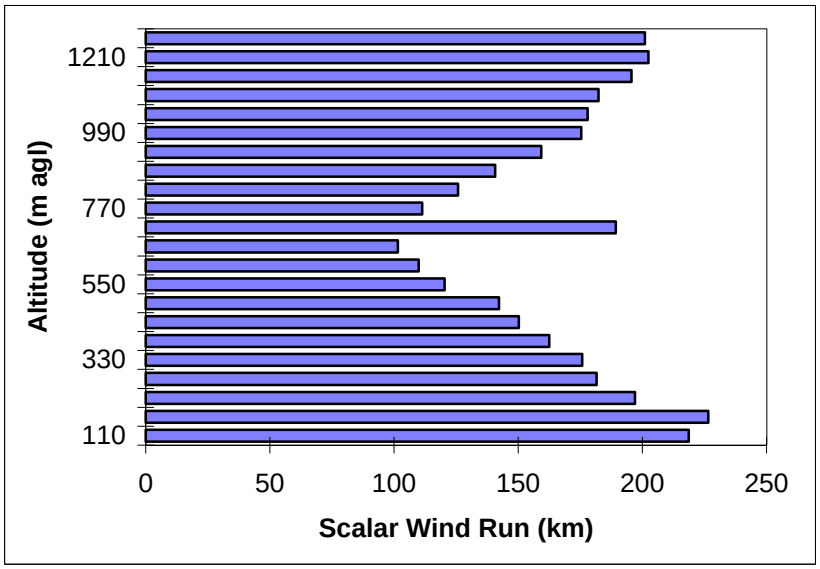
Altitude (m agl)
1210
990
770
550
330
110
0
50
100
150
200
250
Scalar Wind Run (km)

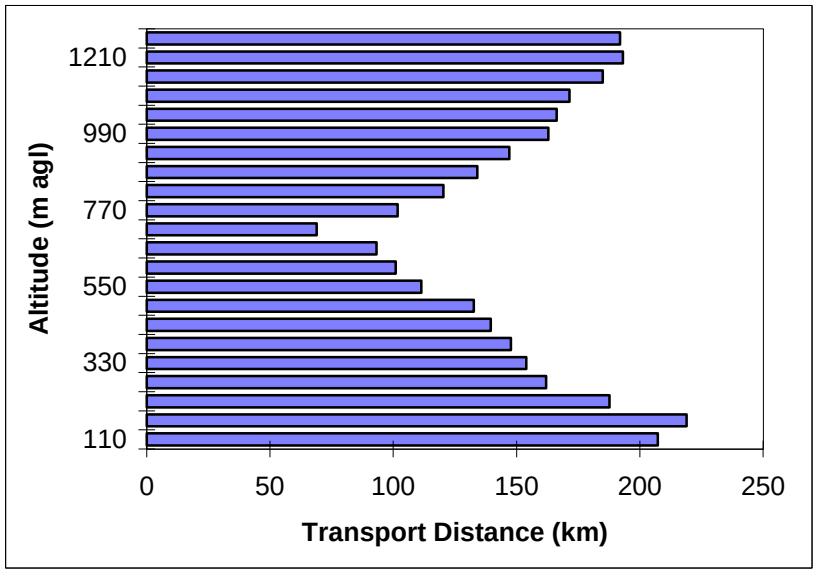
Altitude (m agl)
1210
990
770
550
330
110
0
50
100
150
200
250
Transport Distance (km)

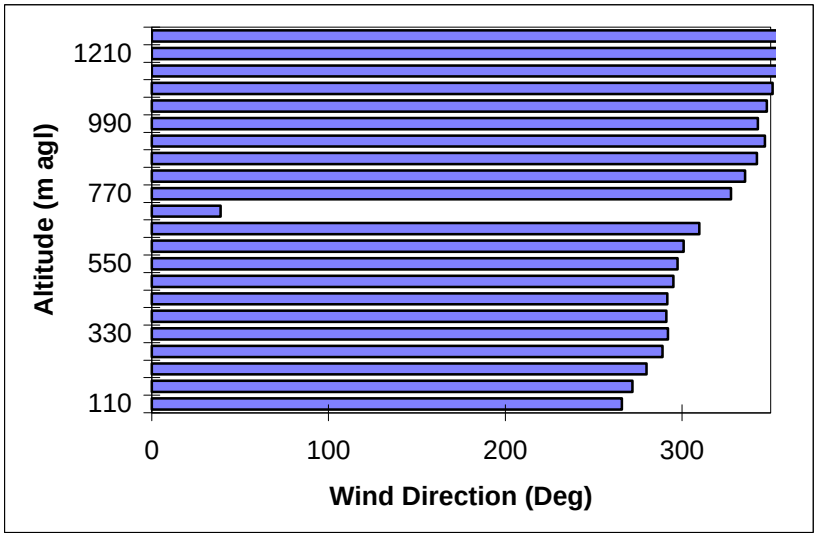
Altitude (m agl)
1210
990
770
550
330
110
0
100
200
300
Wind Direction (Deg)

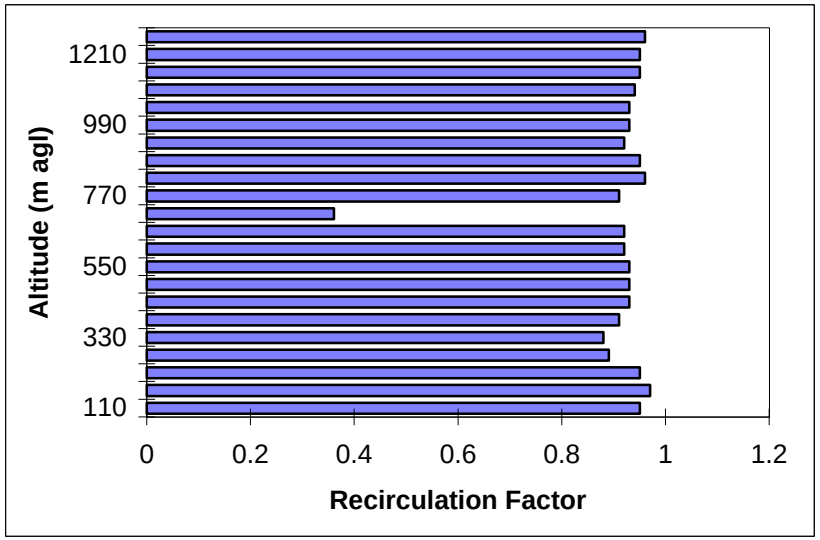
Altitude (m agl)
1210
990
770
550
330
110
0
0.2
0.4
0.6
0.8
1
1.2
Recirculation Factor

SAC 08-02-98 0400 to 1600.xls

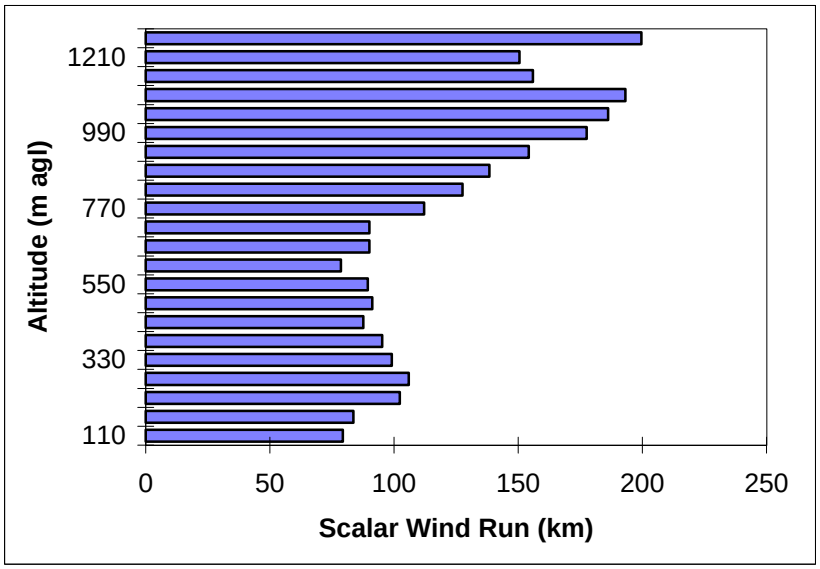

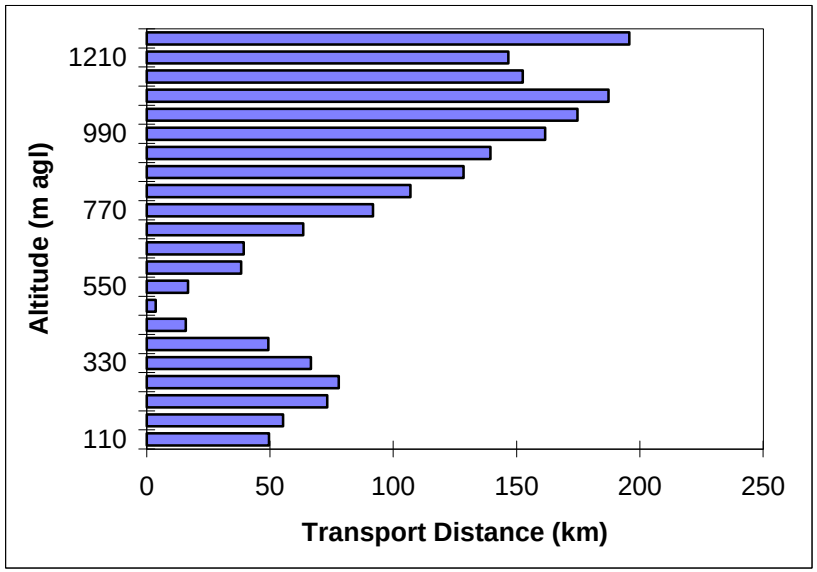

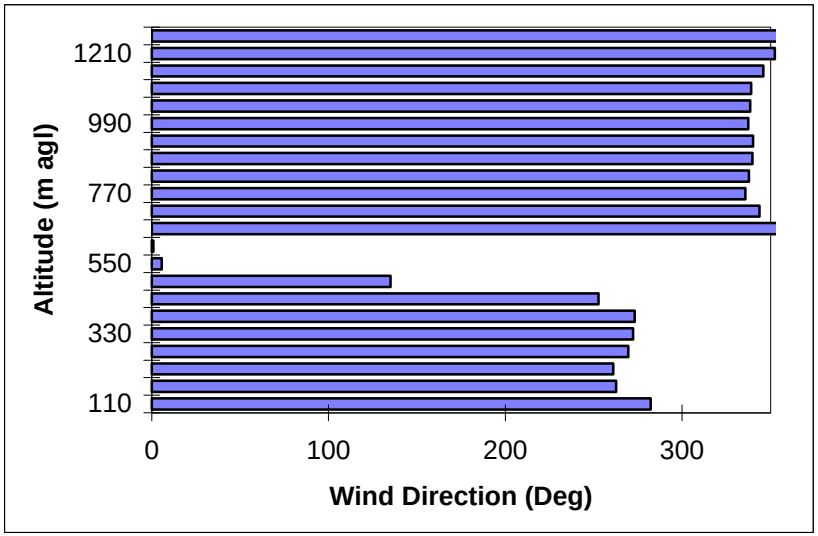

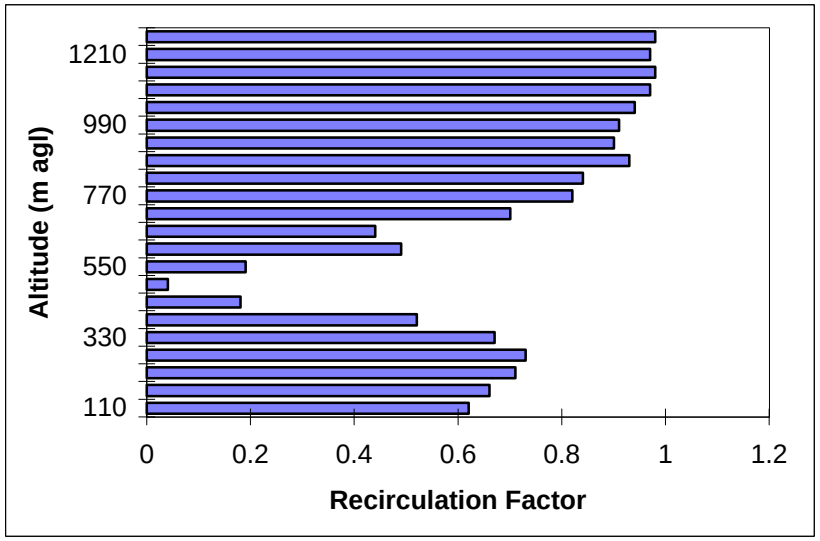

SAC 08-02-98 1600 to 0400.xls

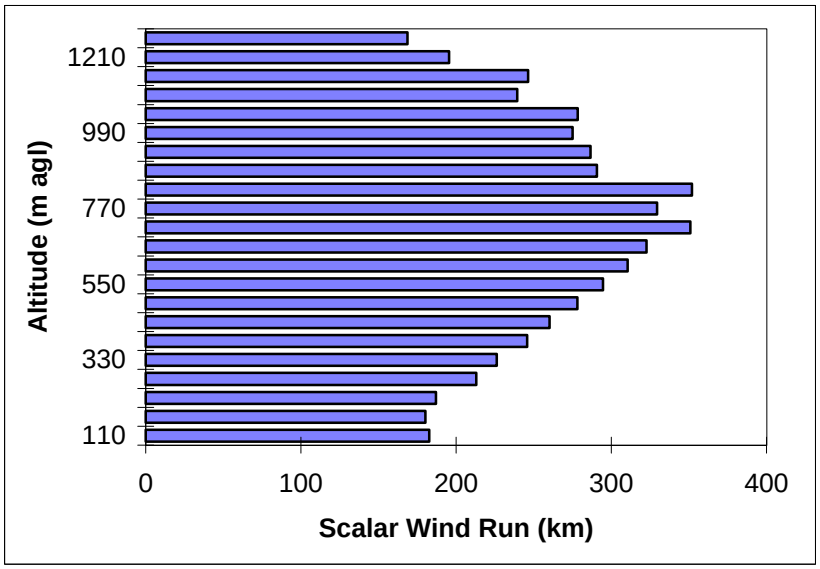

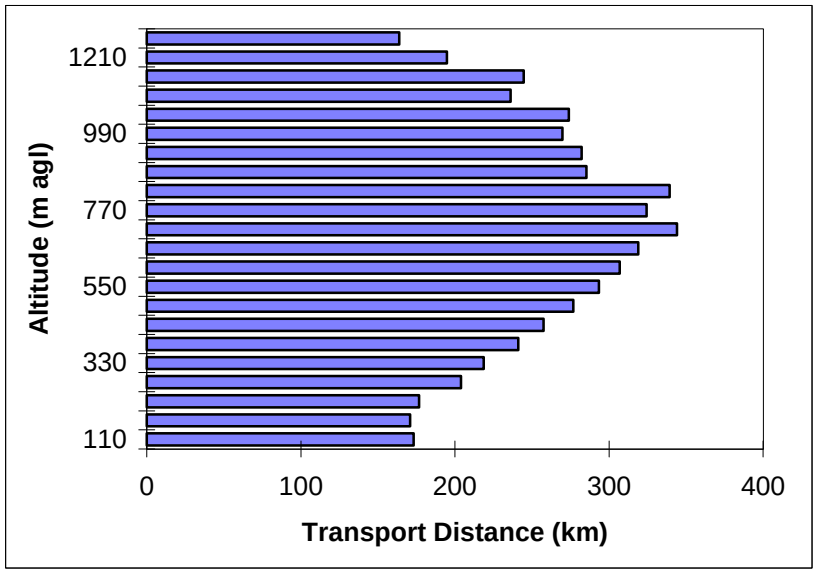

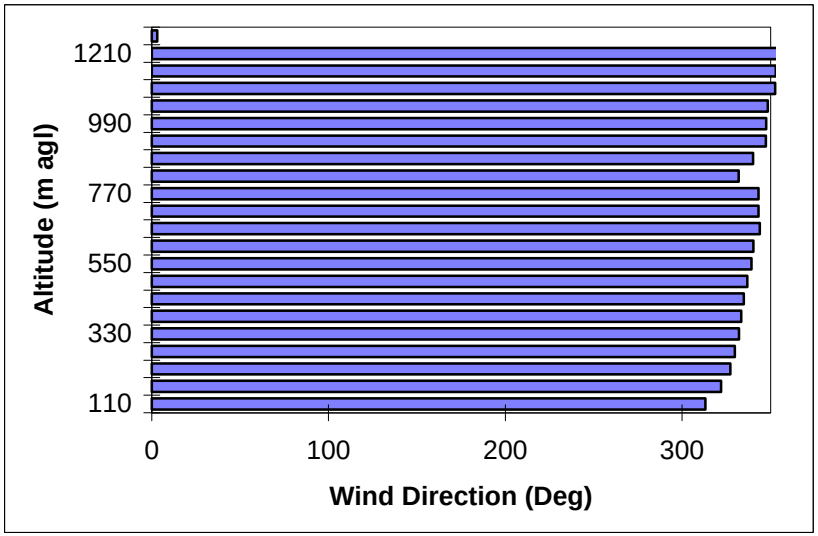

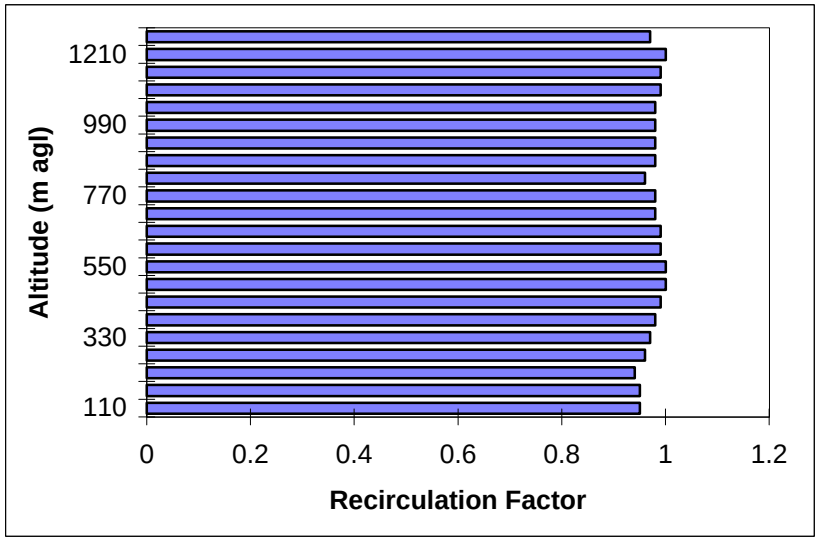

SAC 08-03-98 0400 to 1600.xls

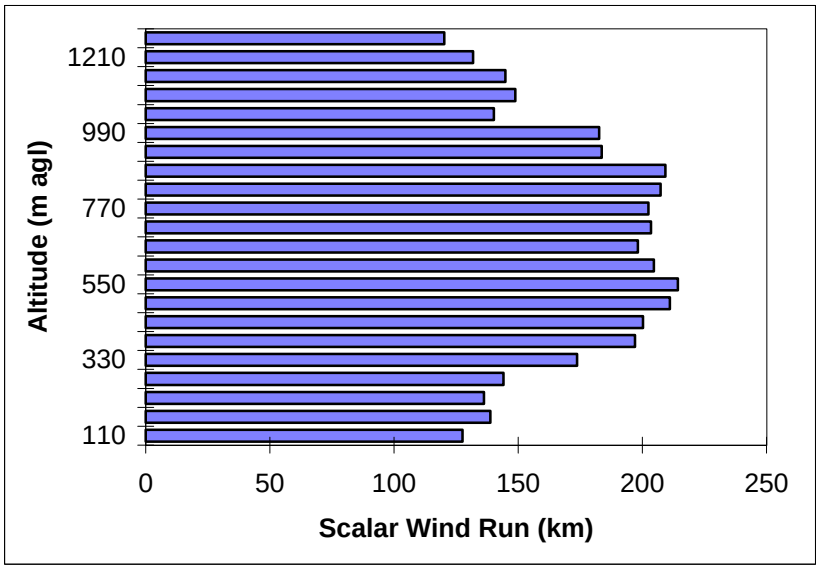

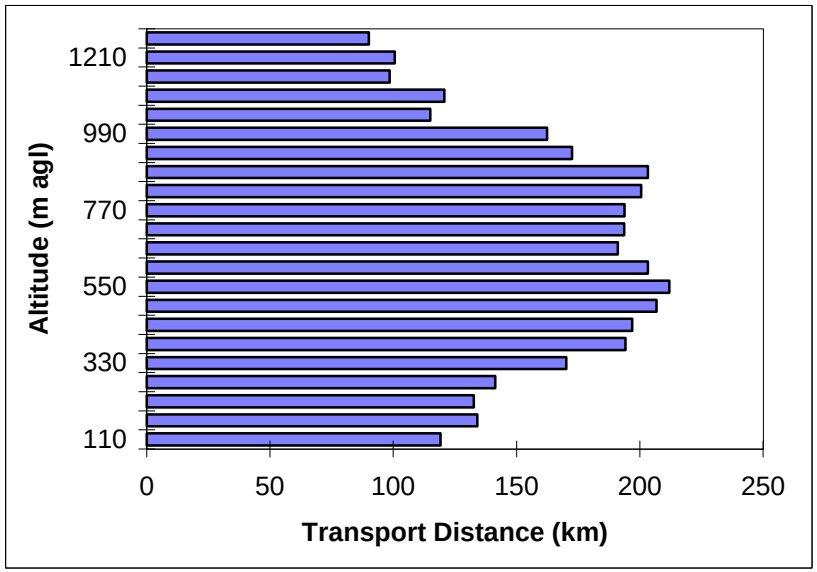

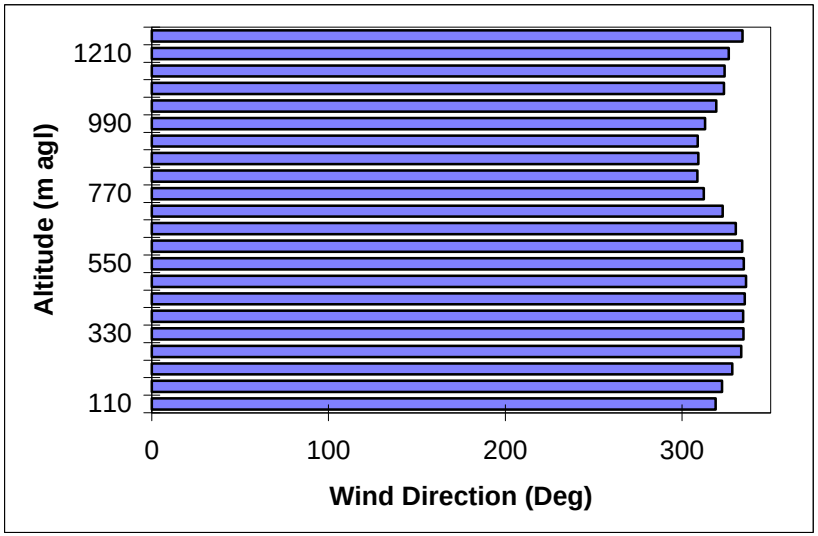

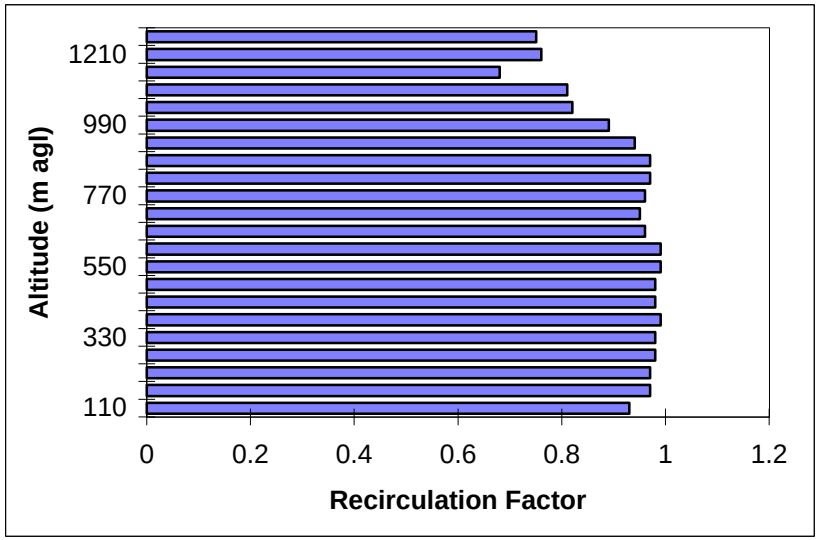

SAC 08-03-98 1600 to 0400.xls

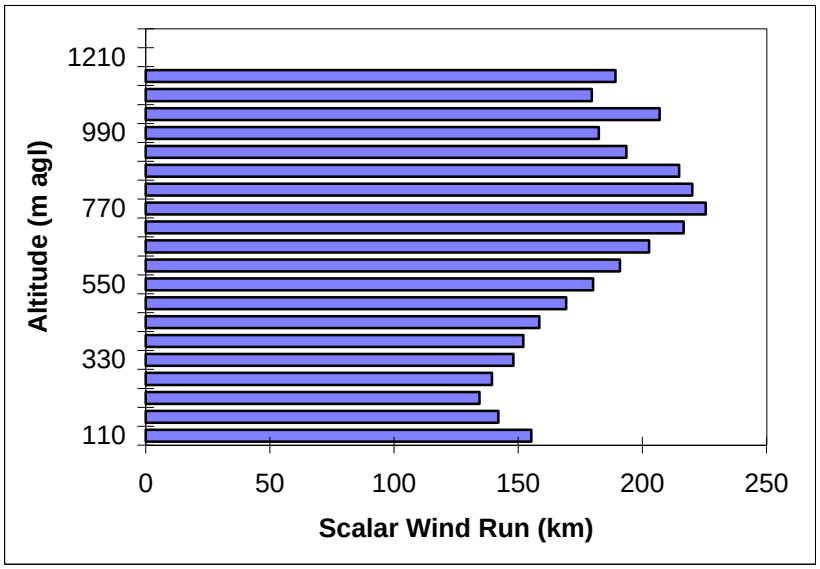

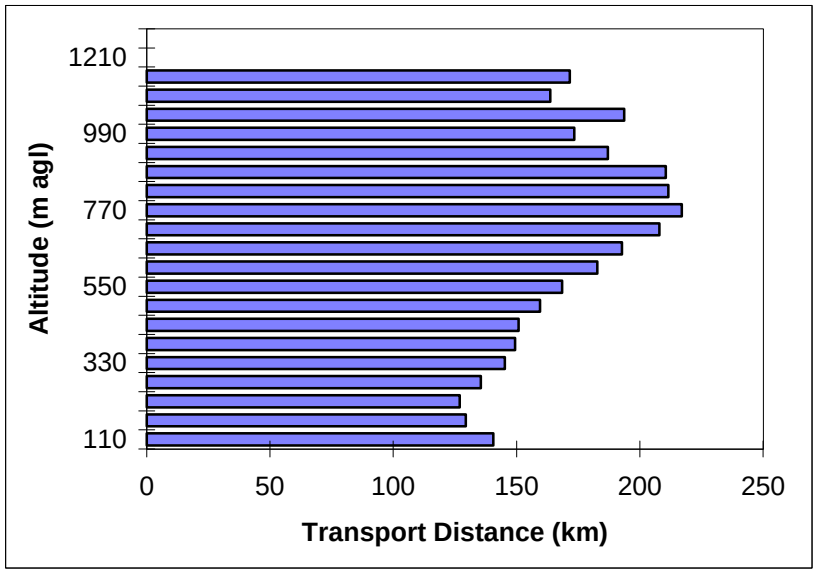

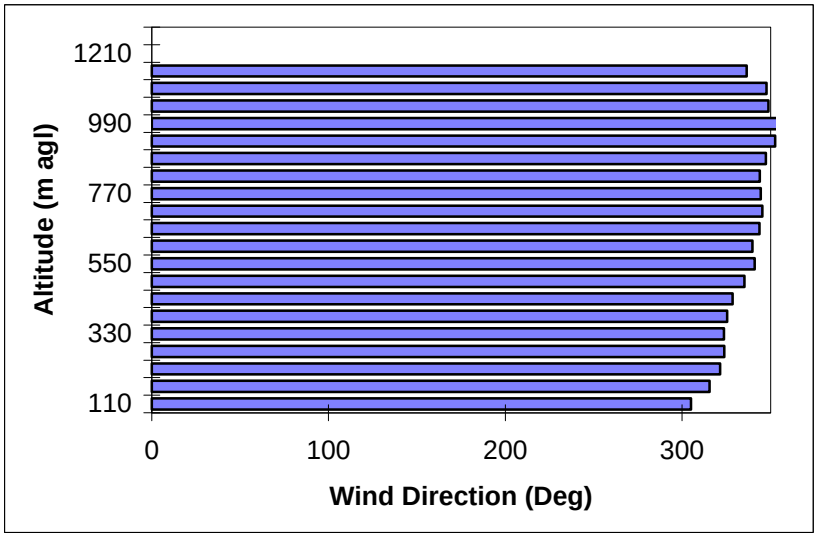

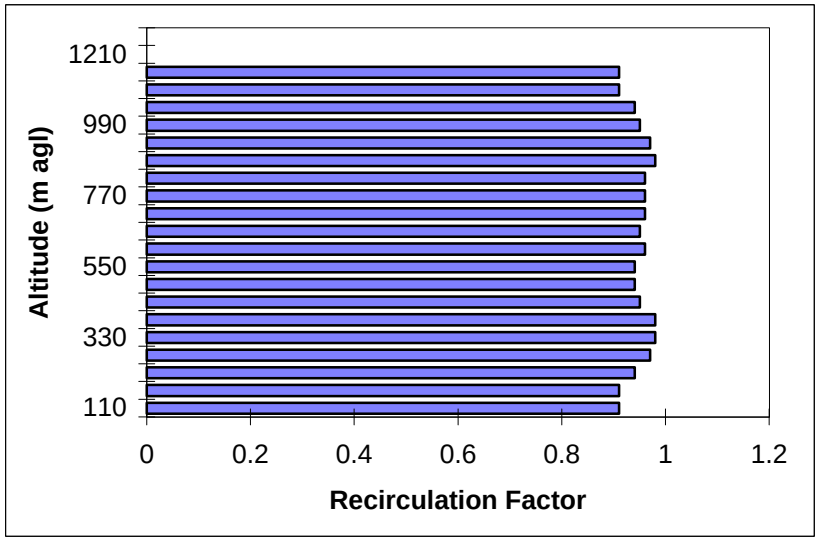

SAC 08-04-98 0400 to 1600.xls

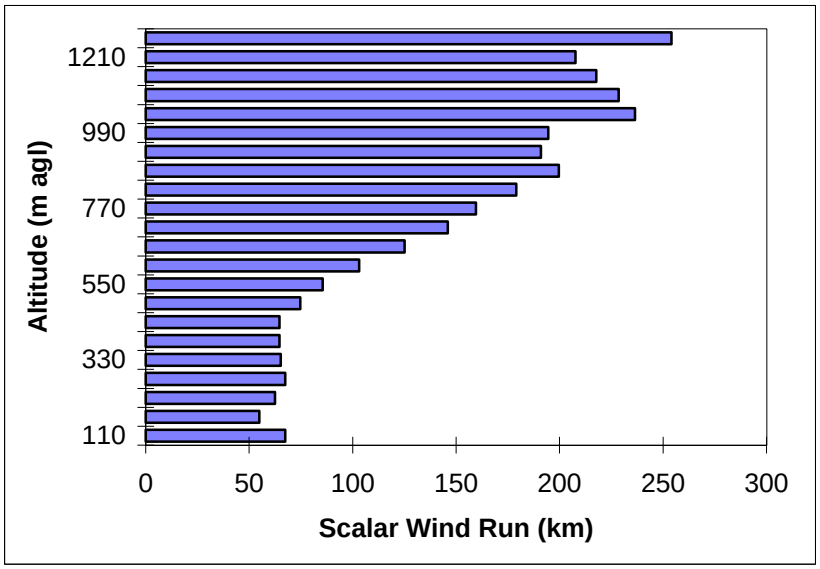

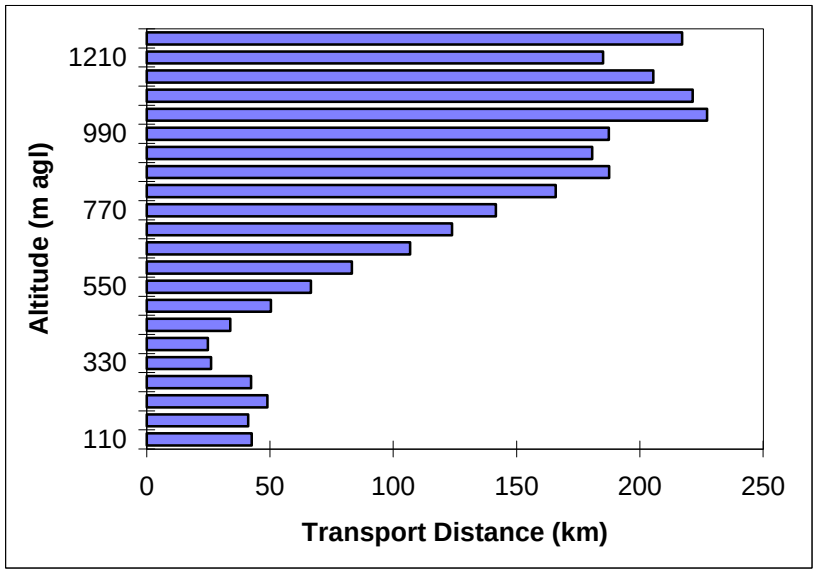

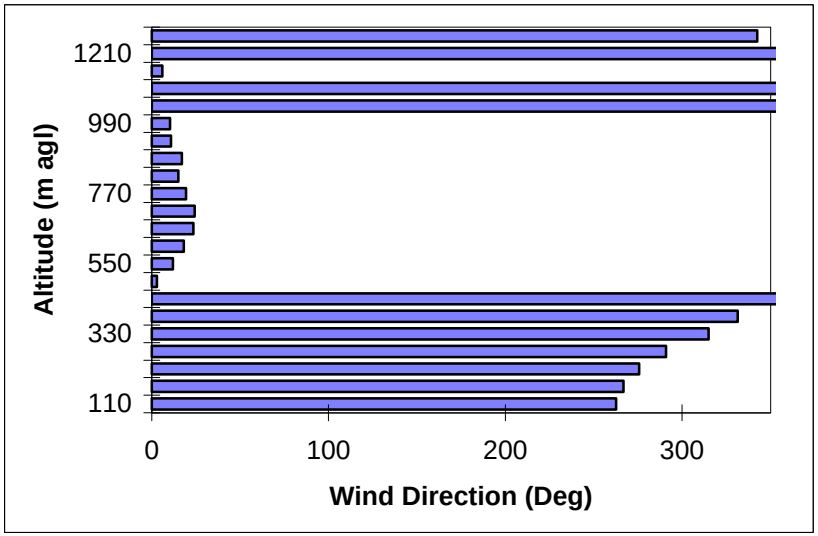

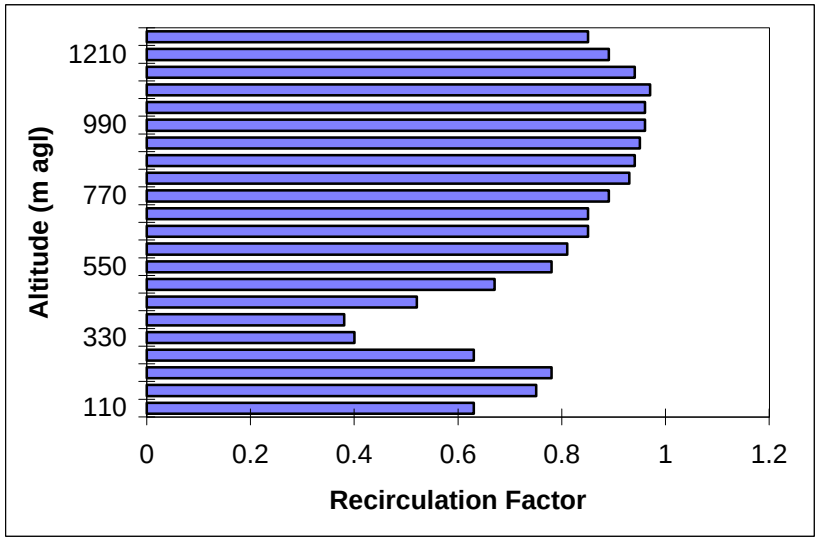

SAC 08-04-98 1600 to 0400.xls

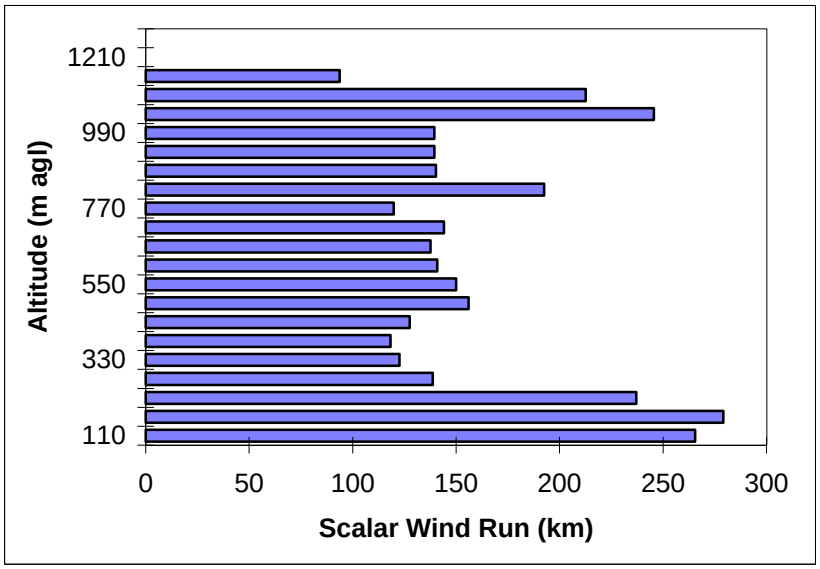

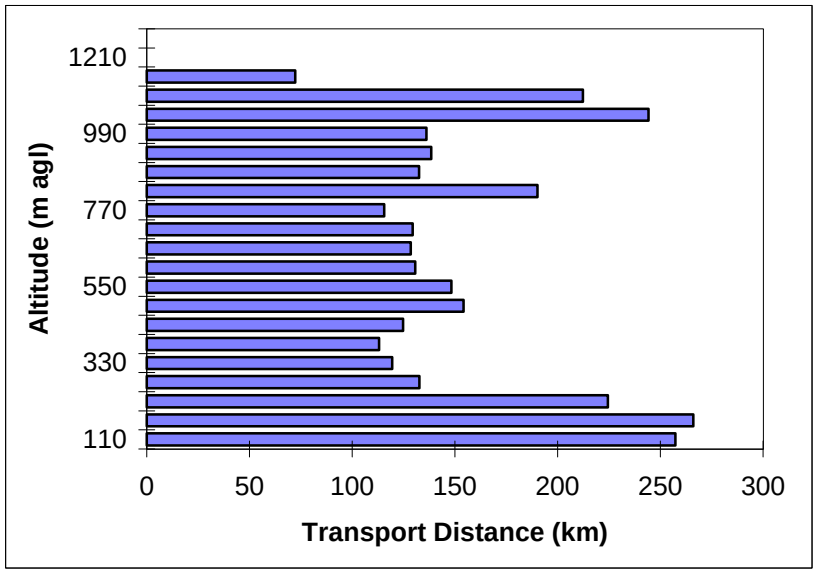

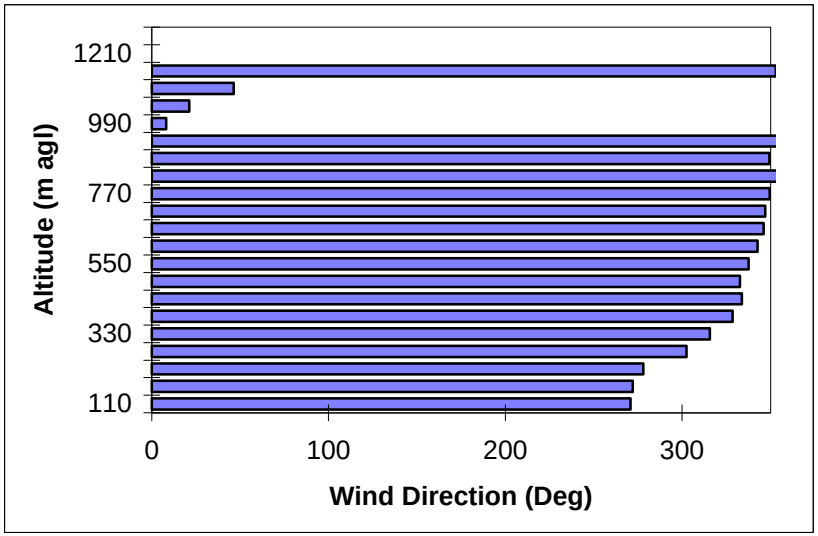

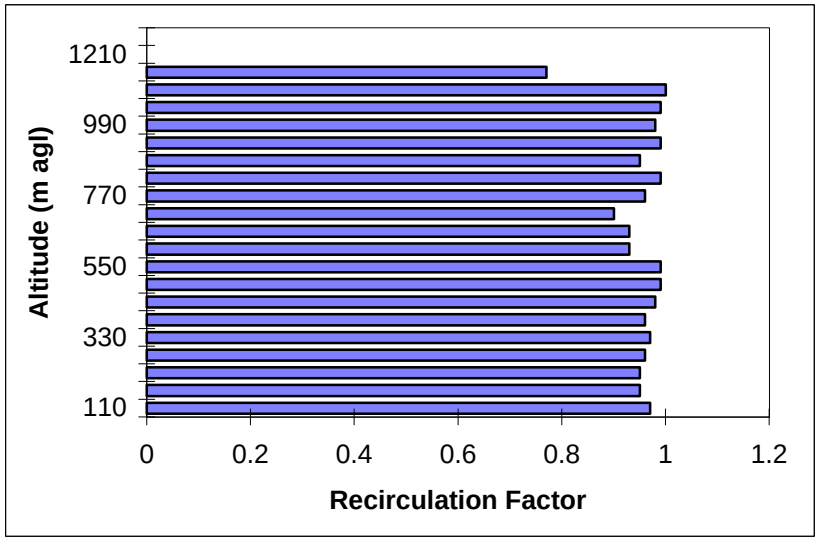

SAC 08-05-98 0400 to 1600.xls

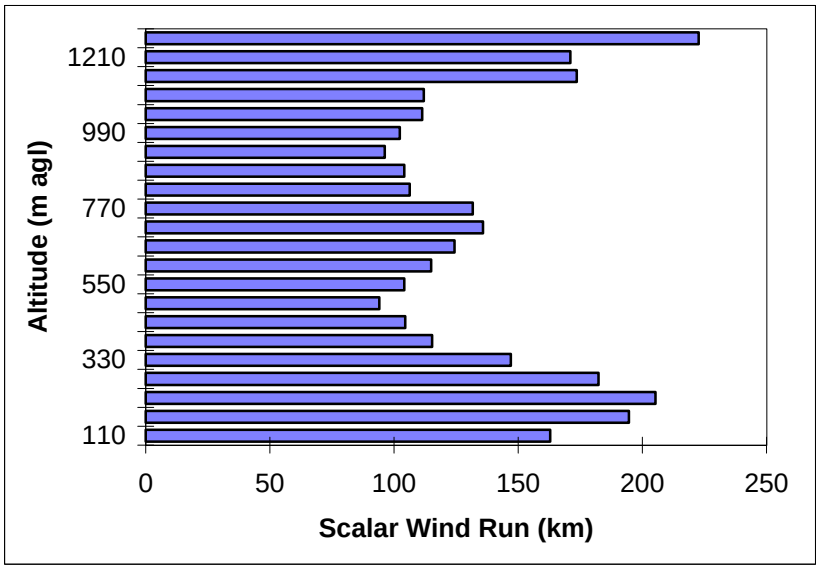

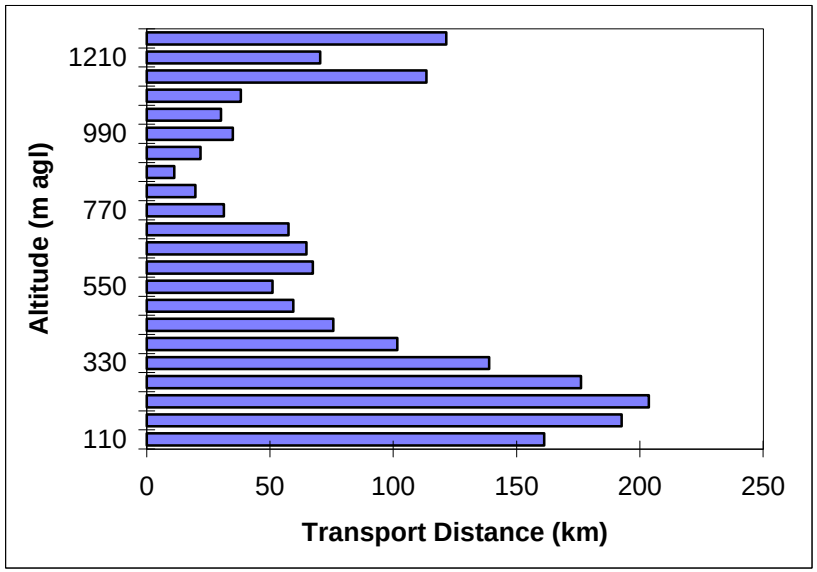

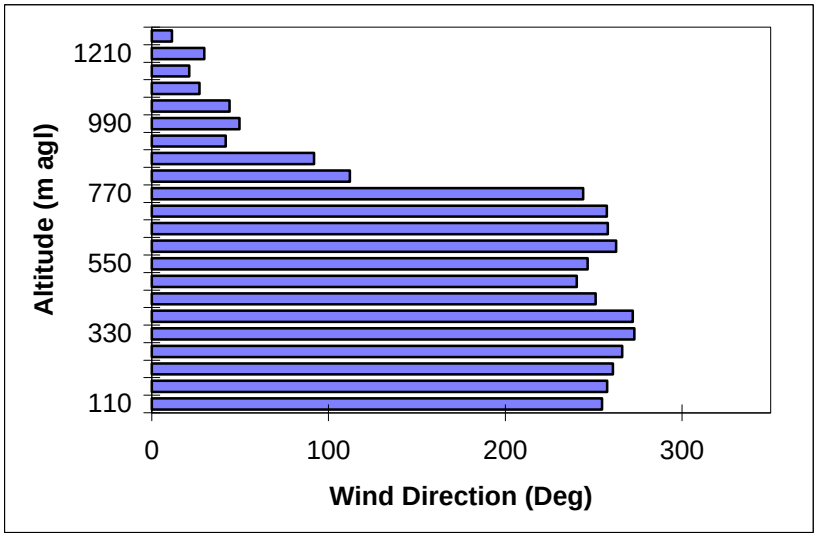

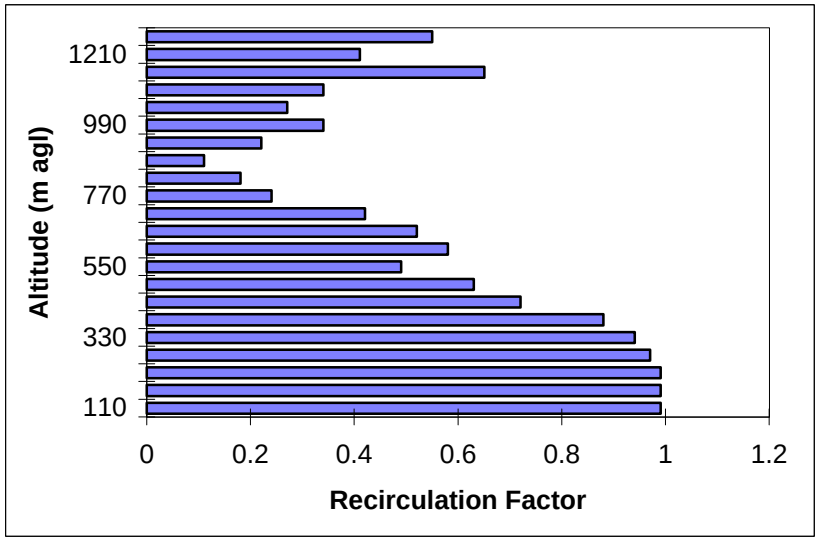

SAC 08-05-98 1600 to 0400.xls

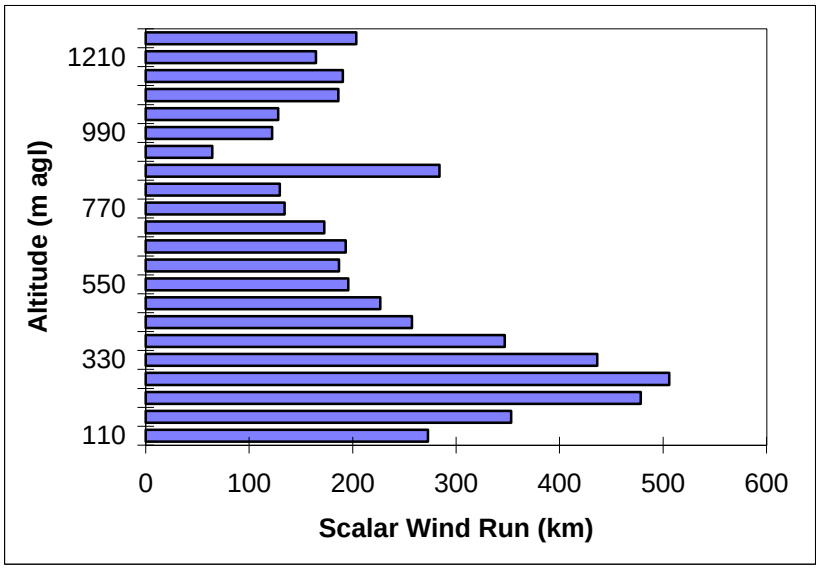

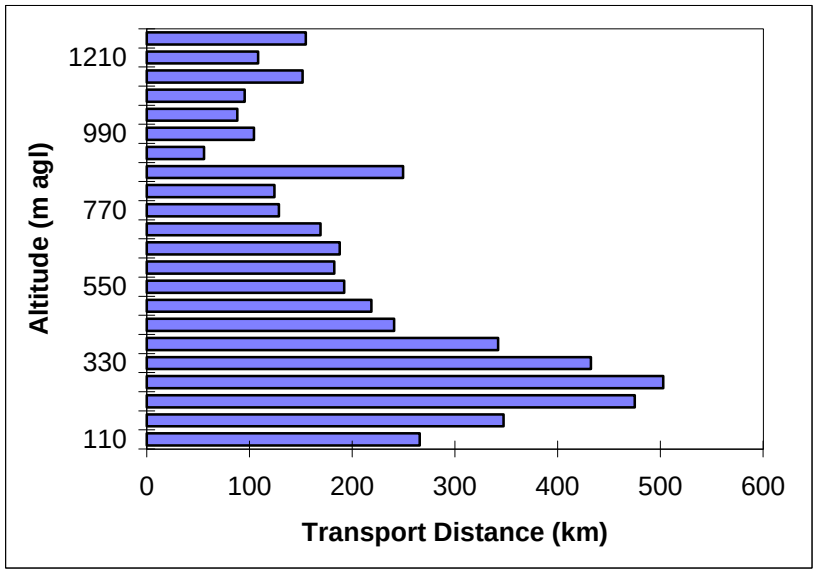

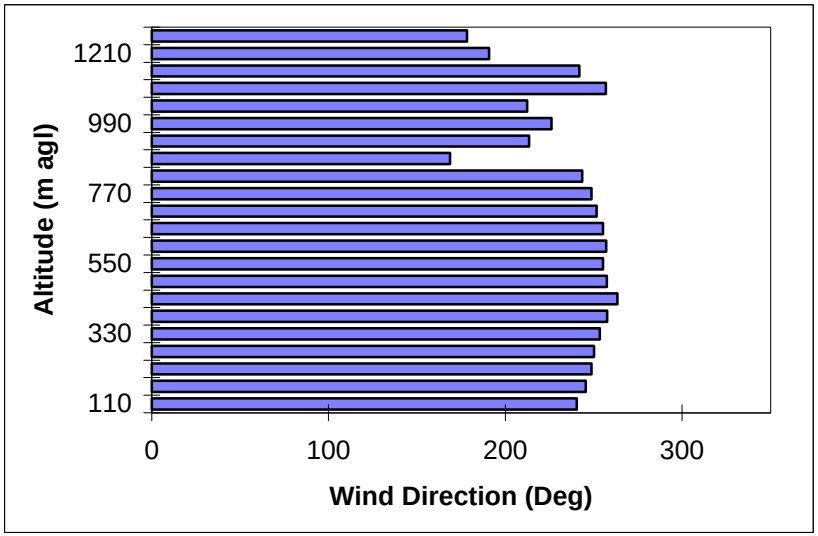

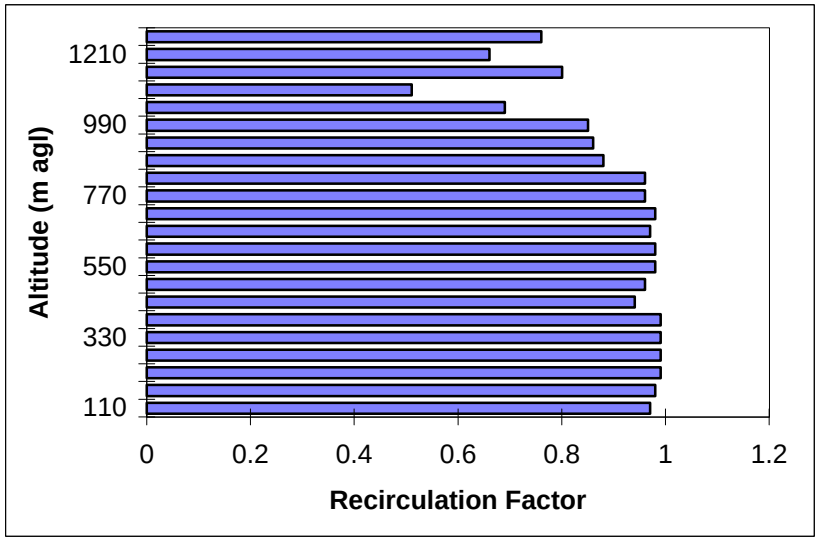

SAC 08-06-98 0400 to 1600.xls

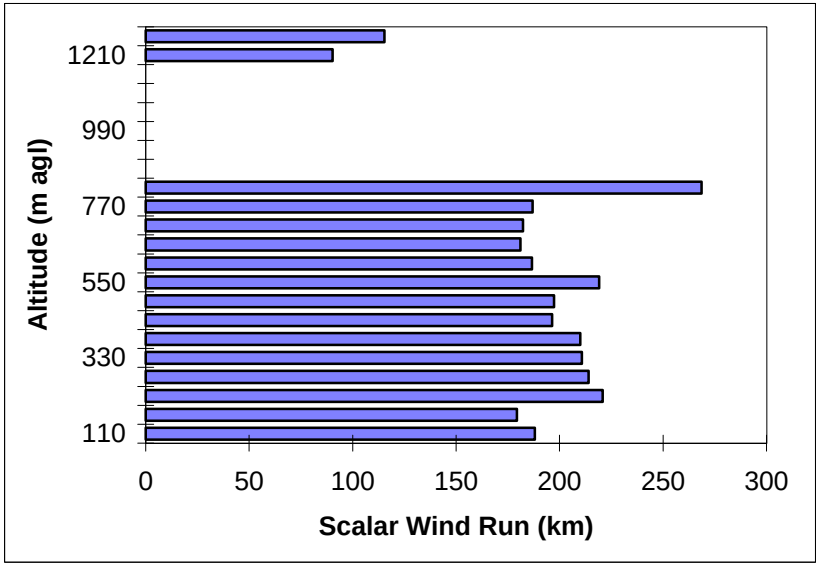

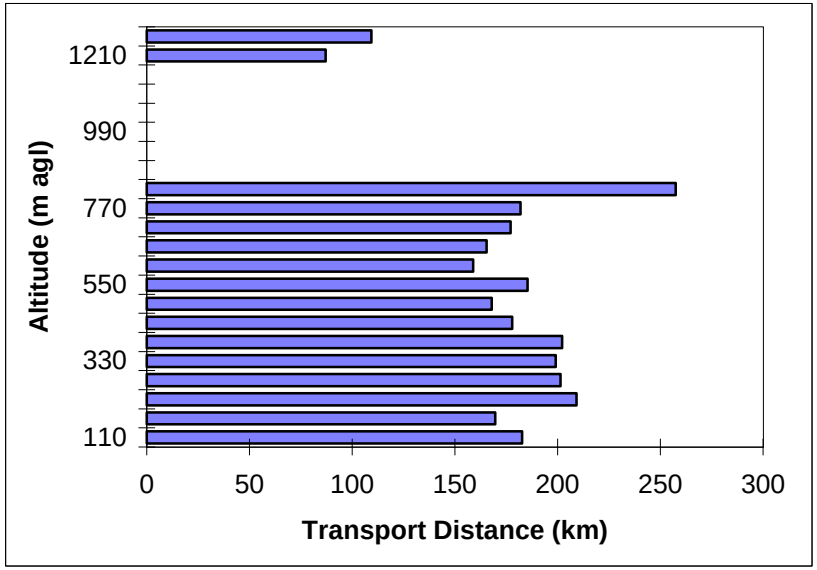

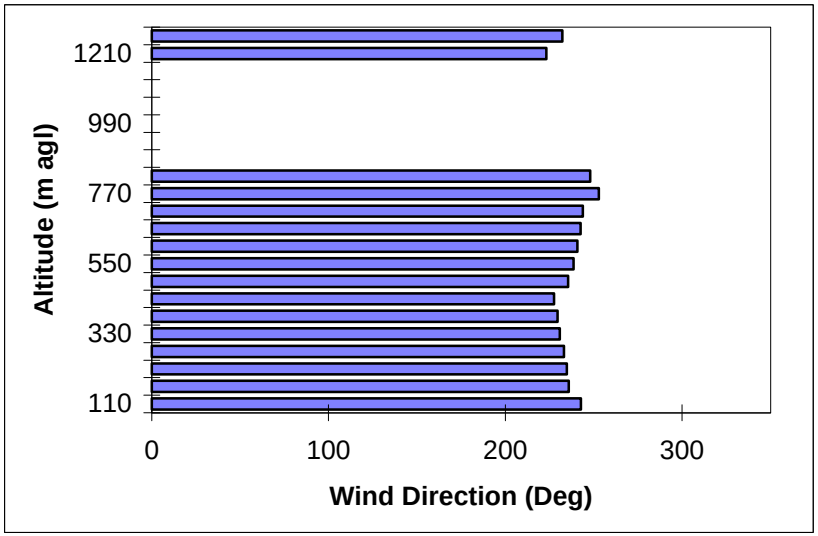

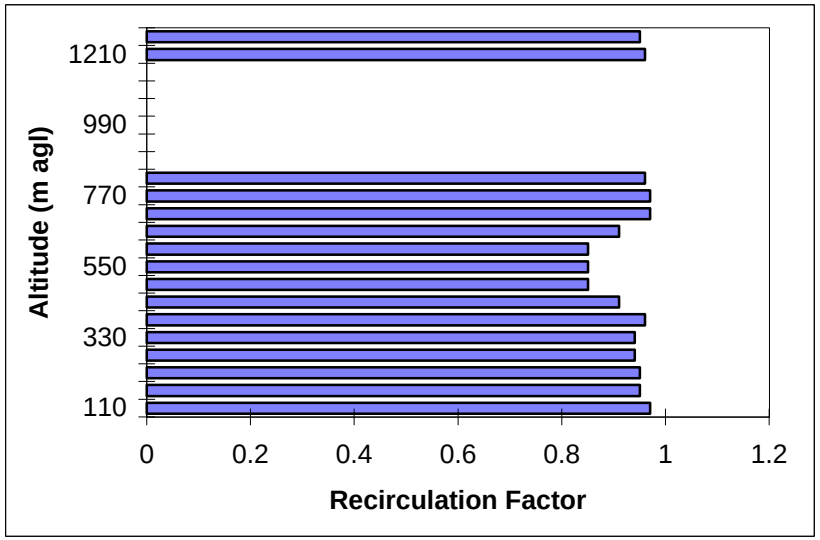

SJV 08-08-98 0400 to 1600.xls

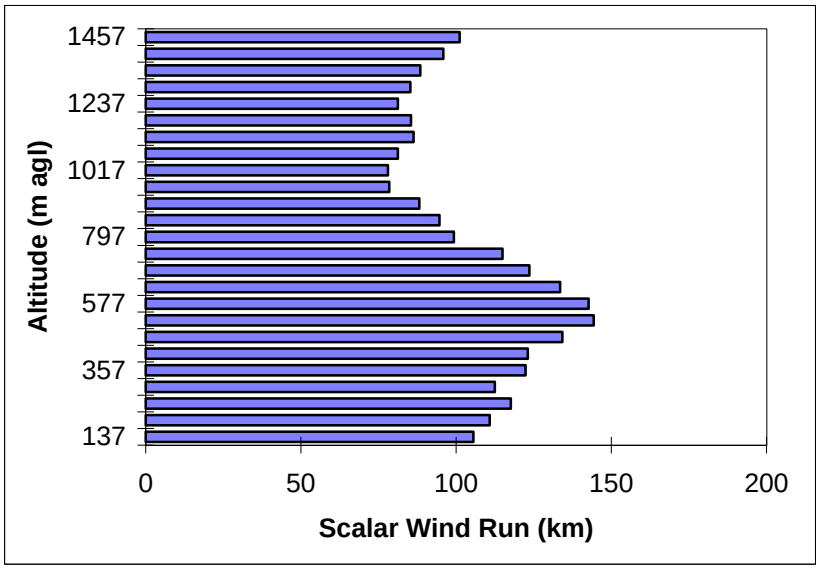

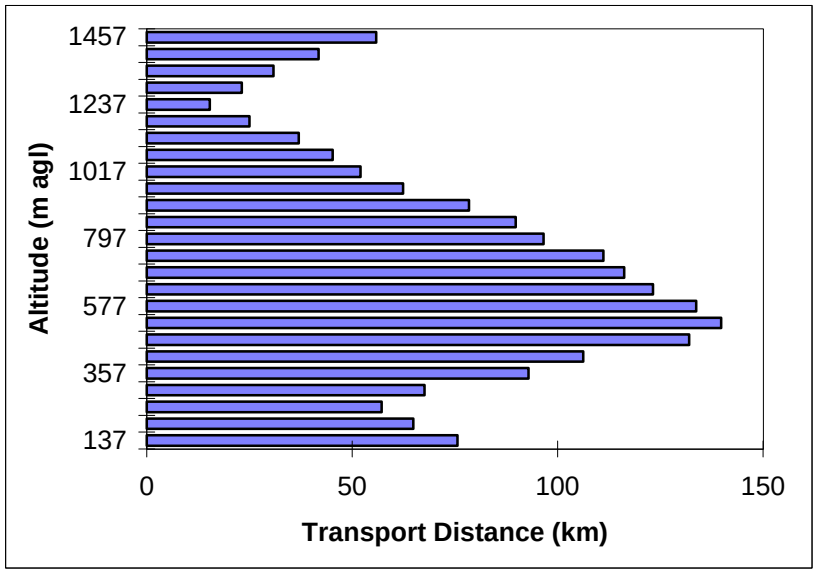

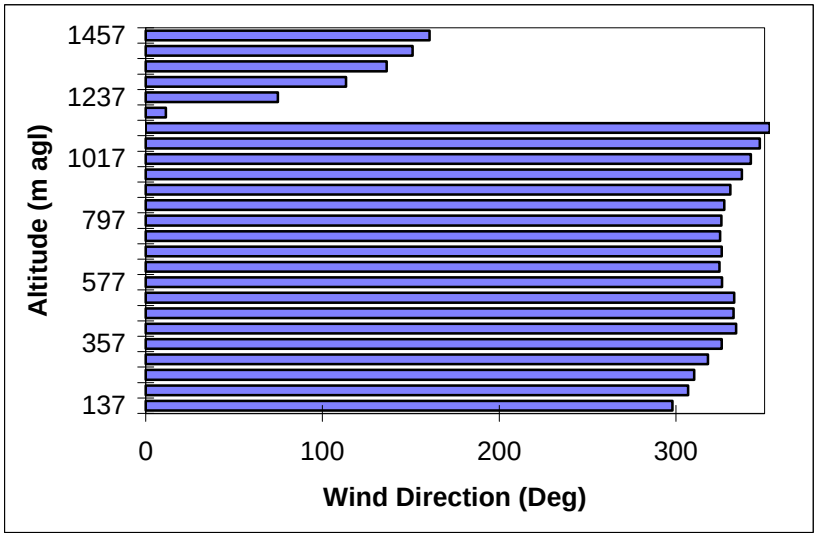

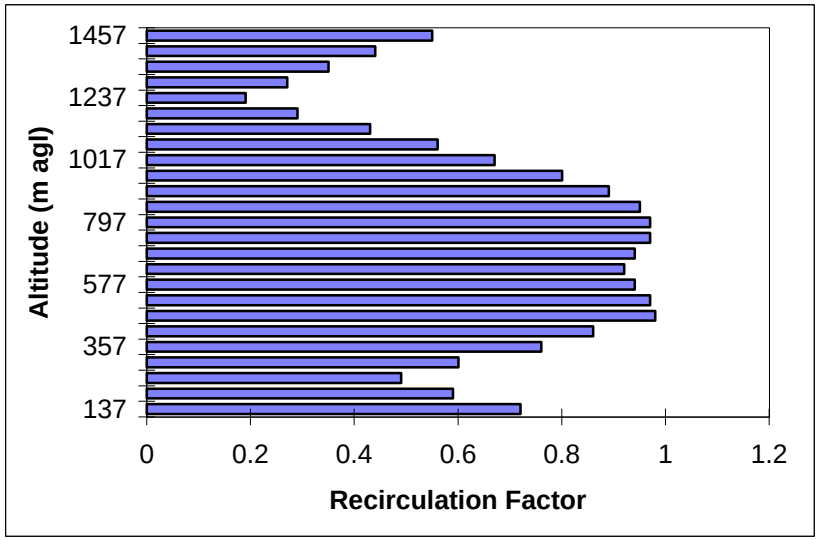

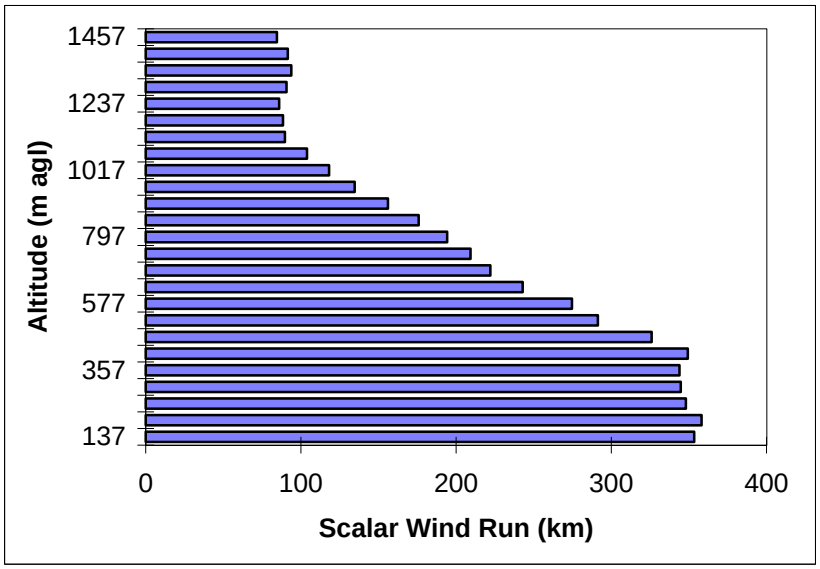
Altitude (m agl)
1457
1237
1017
797
577
357
137
0
100
200
300
400
Scalar Wind Run (km)

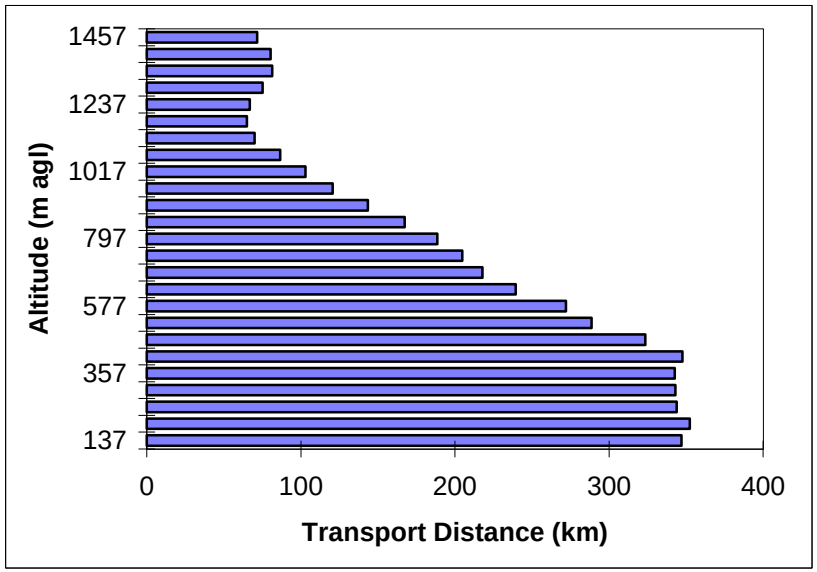
Altitude (m agl)
1457
1237
1017
797
577
357
137
0
100
200
300
400
Transport Distance (km)

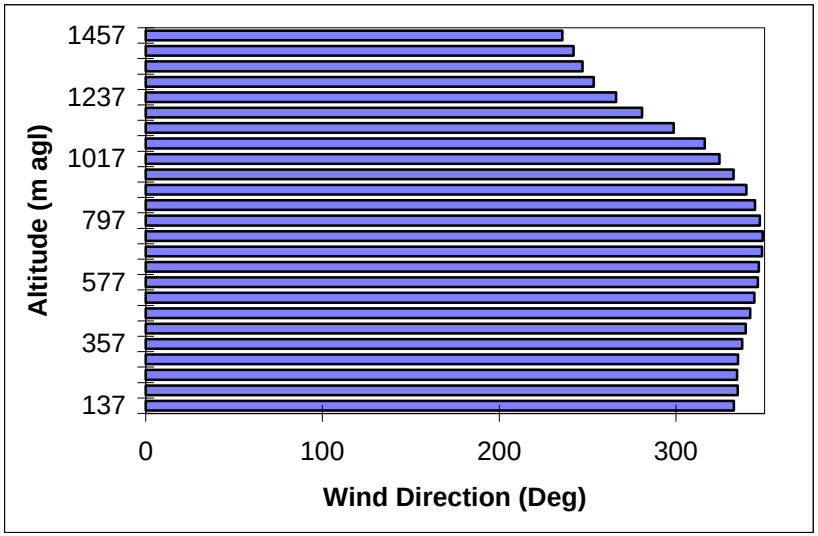
Altitude (m agl)
1457
1237
1017
797
577
357
137
0
100
200
300
Wind Direction (Deg)

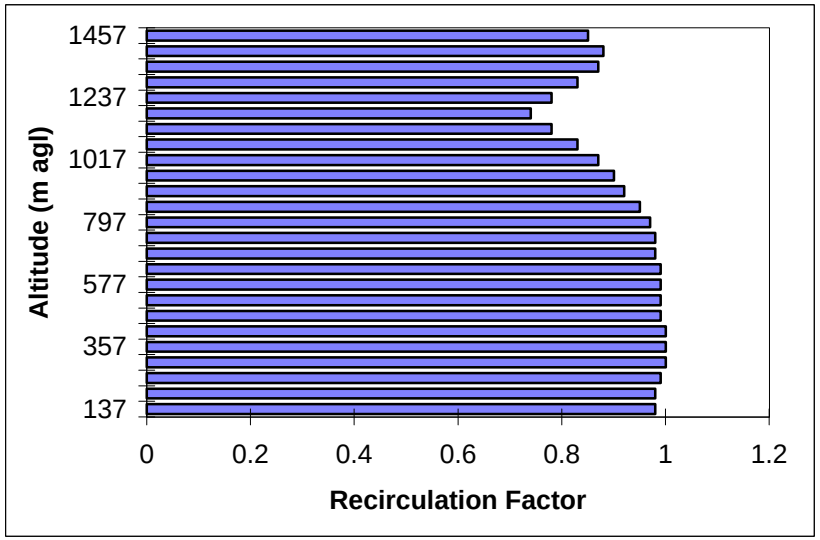
Altitude (m agl)
1457
1237
1017
797
577
357
137
0
0.2
0.4
0.6
0.8
1
1.2
Recirculation Factor

SJV 08-09-98 0400 to 1600.xls

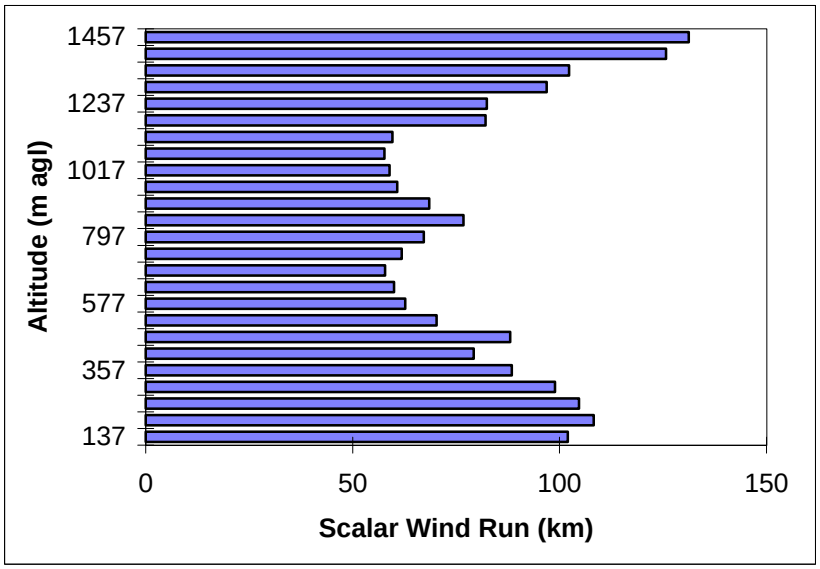

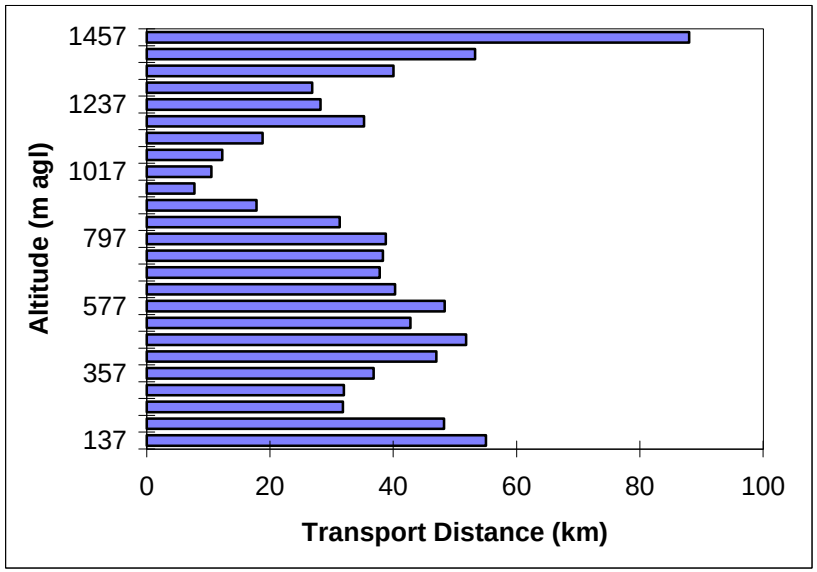

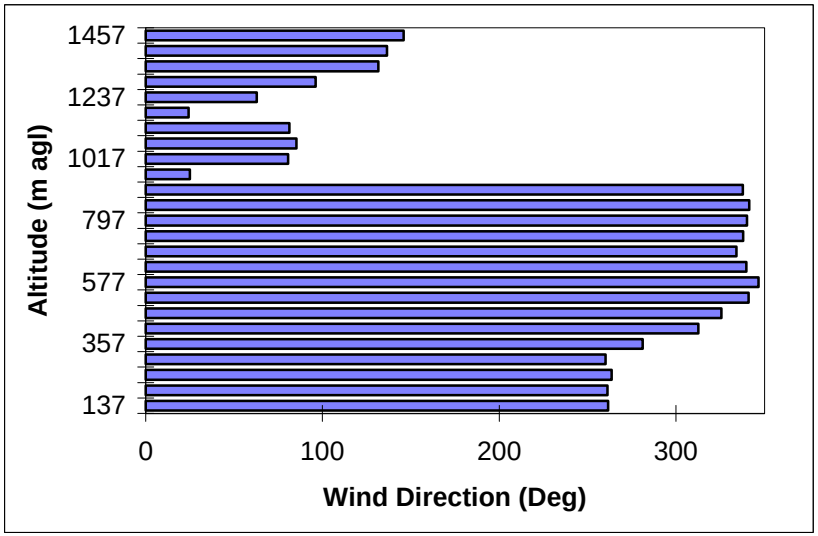

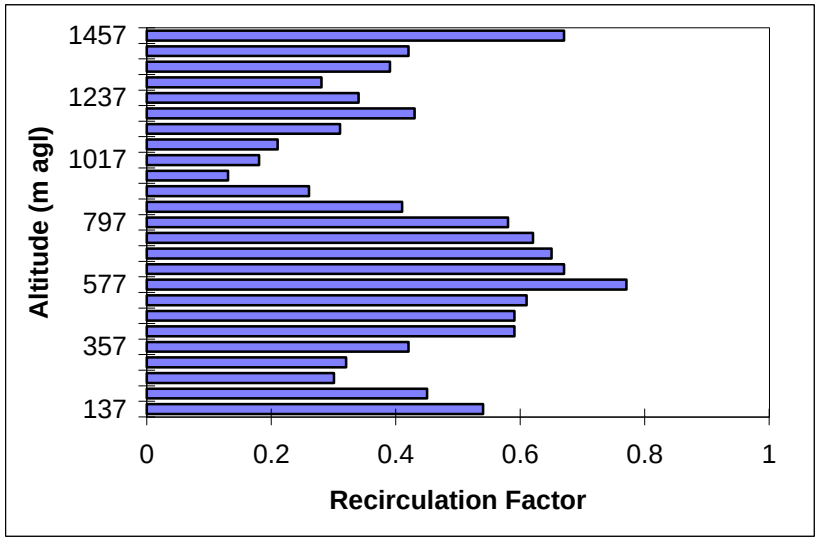

SJV 08-09-98 1600 to 0400.xls

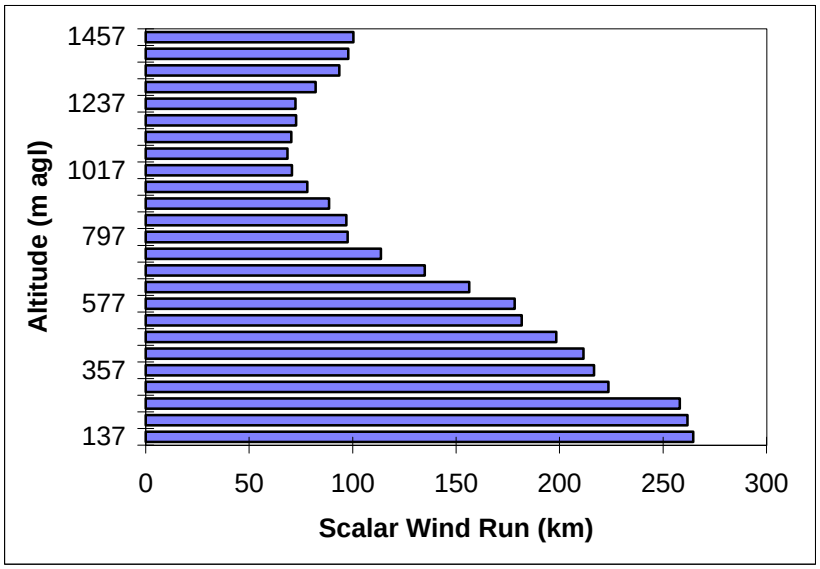

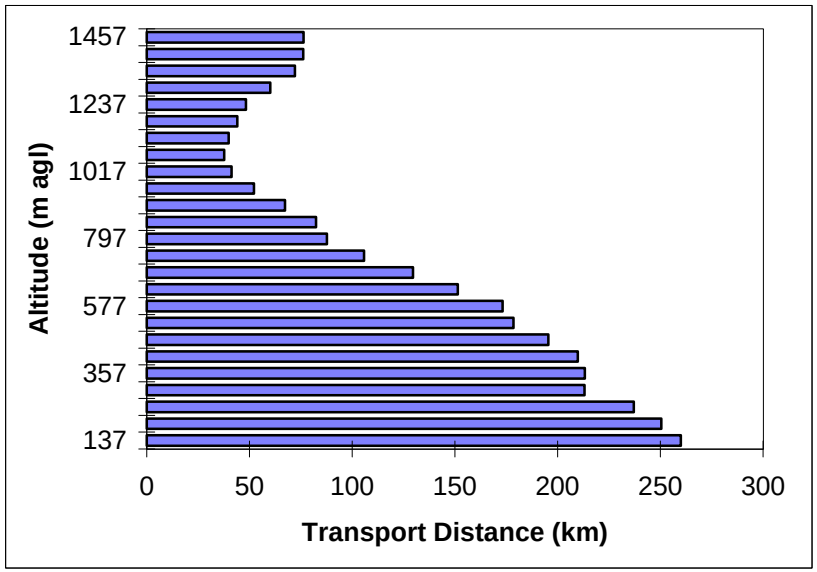

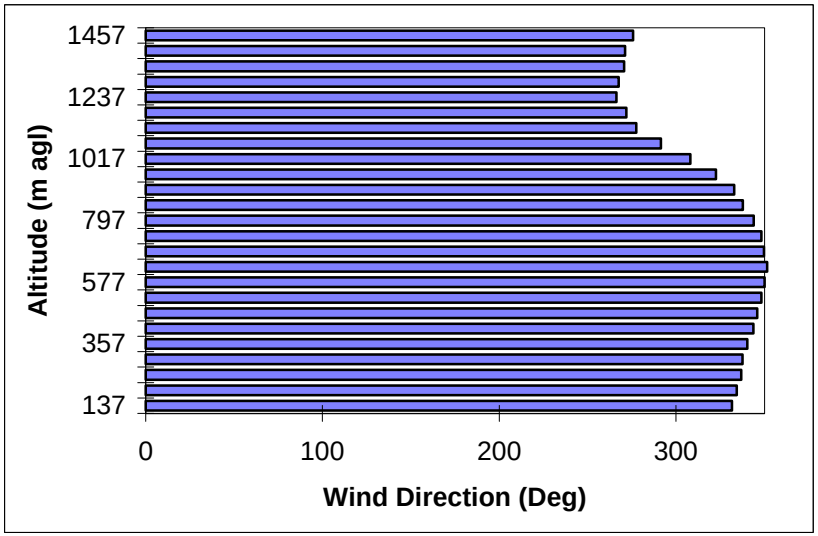

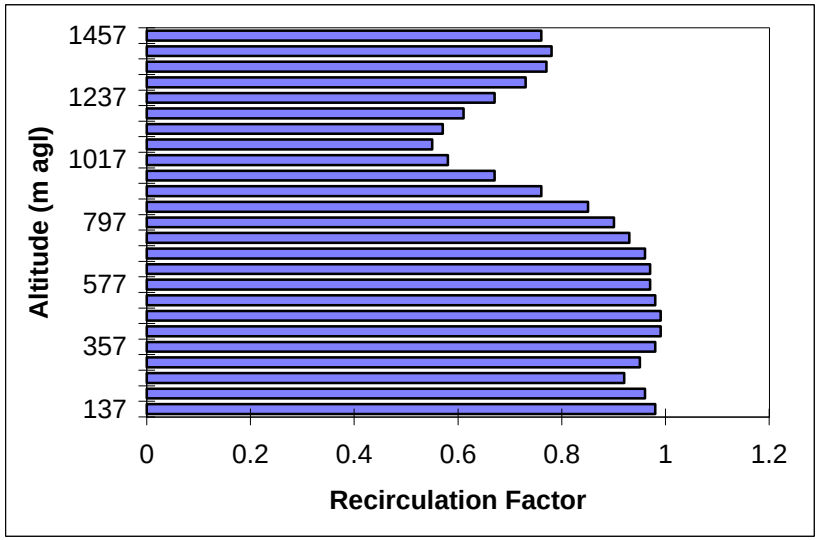

SJV 08-10-98 0400 to 1600.xls

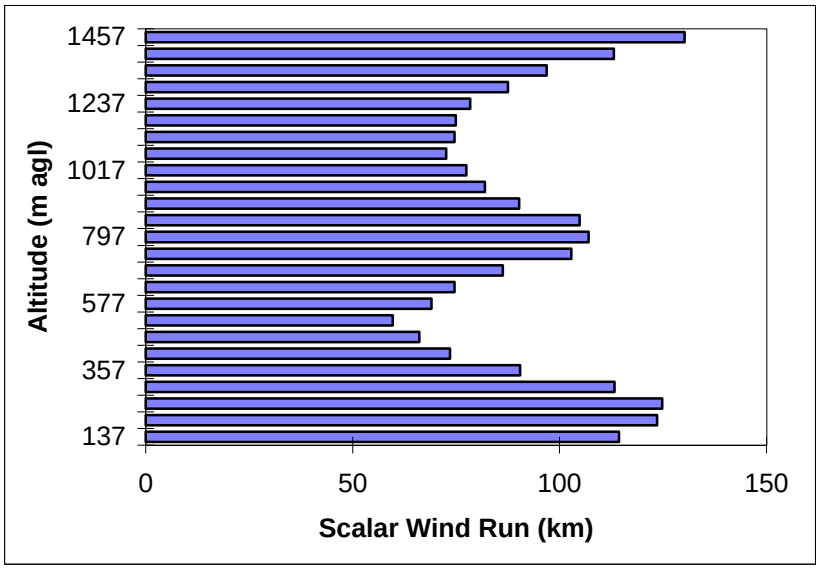

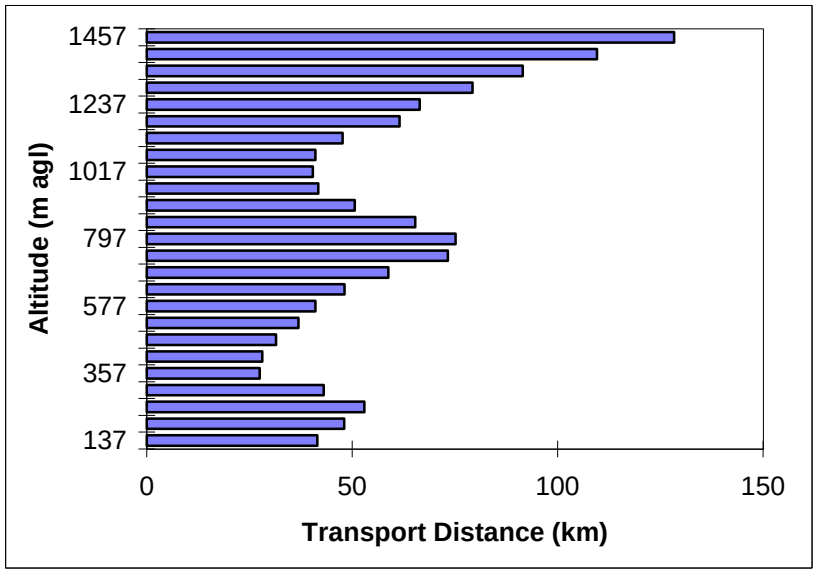

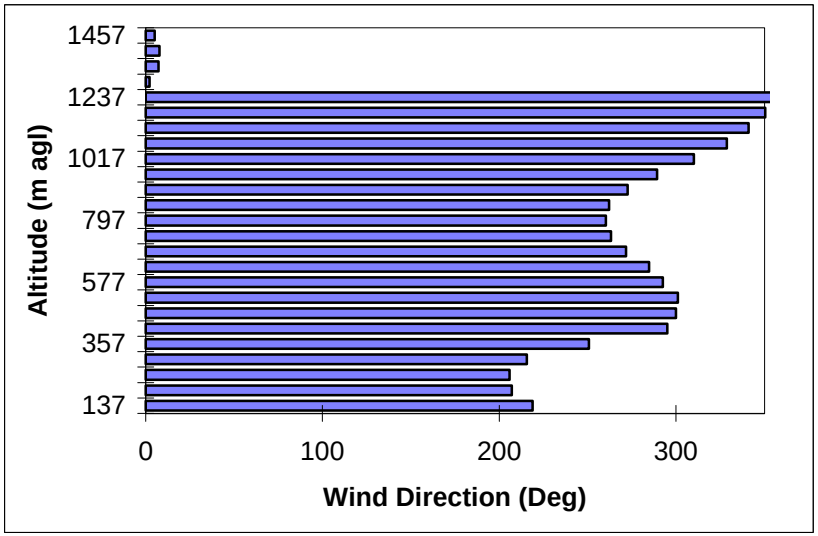

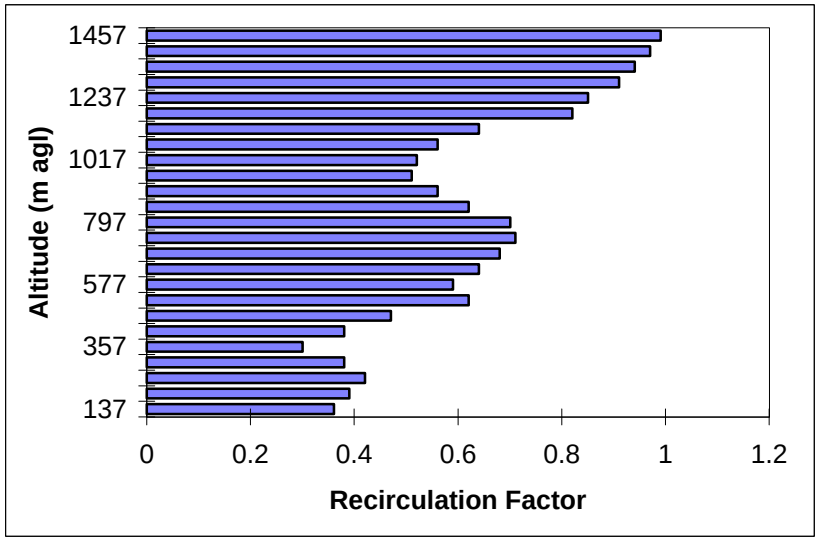

SJV 08-10-98 1600 to 0400.xls

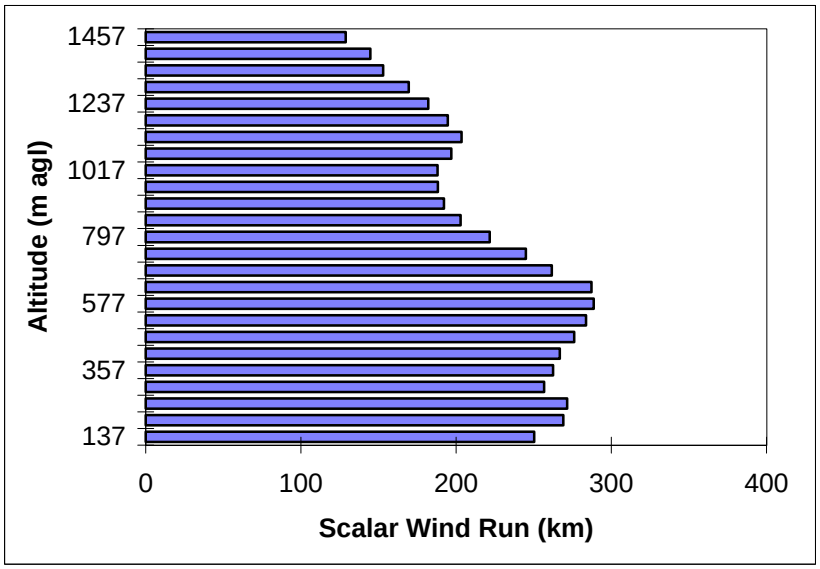

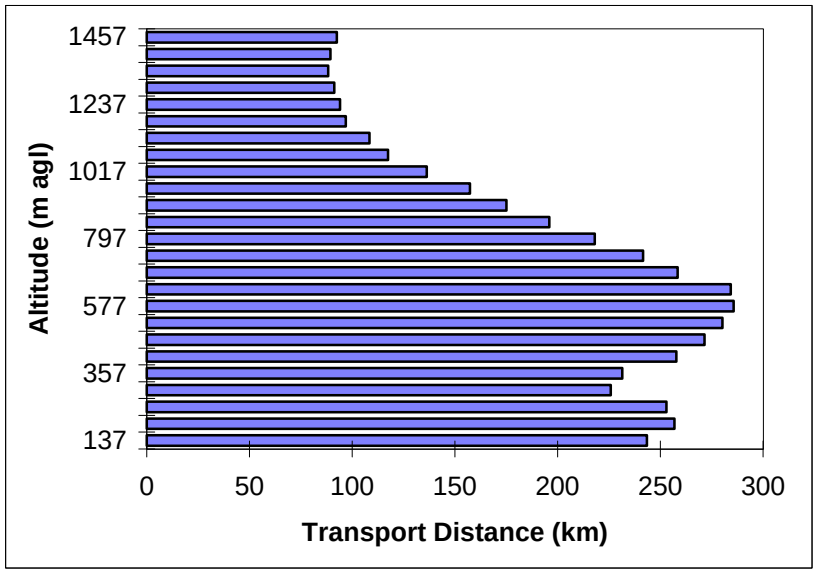

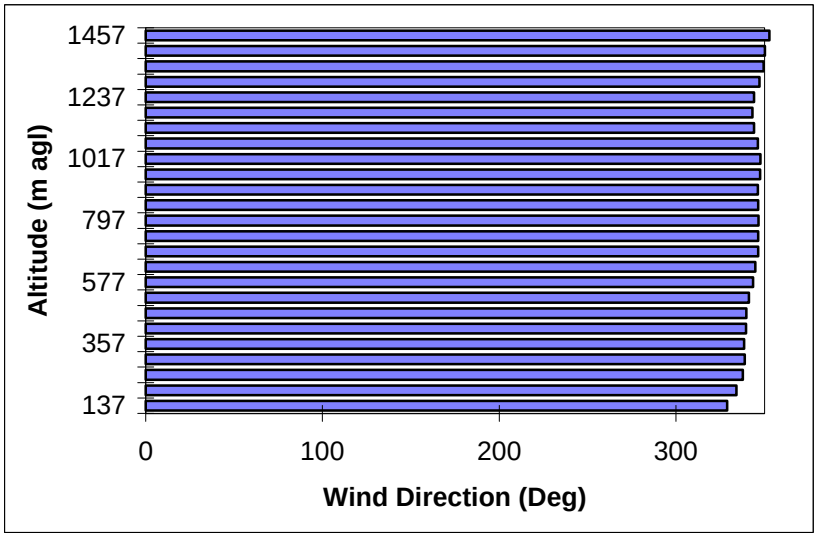

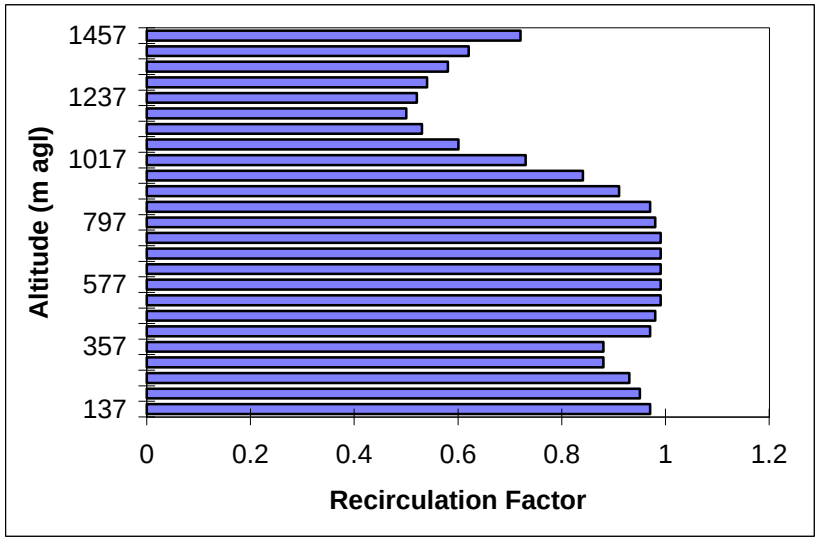

SJV 08-26-98 0400 to 1600.xls

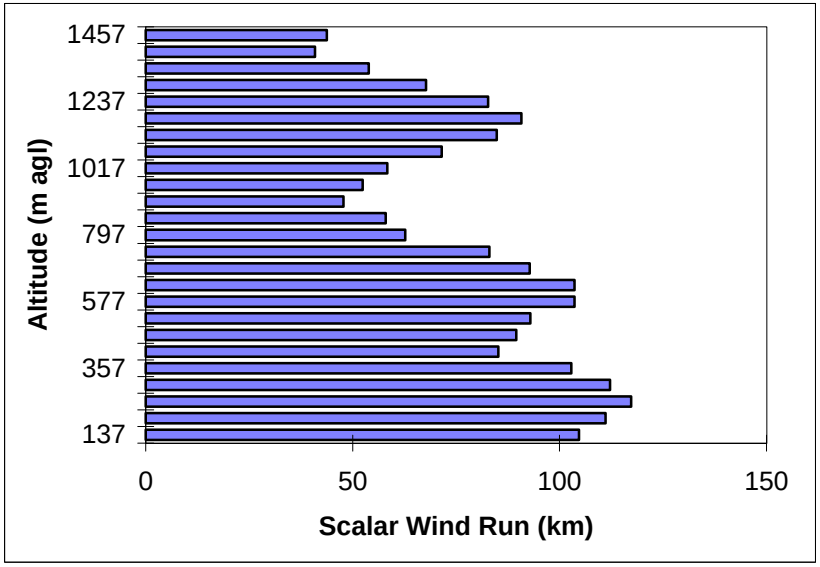

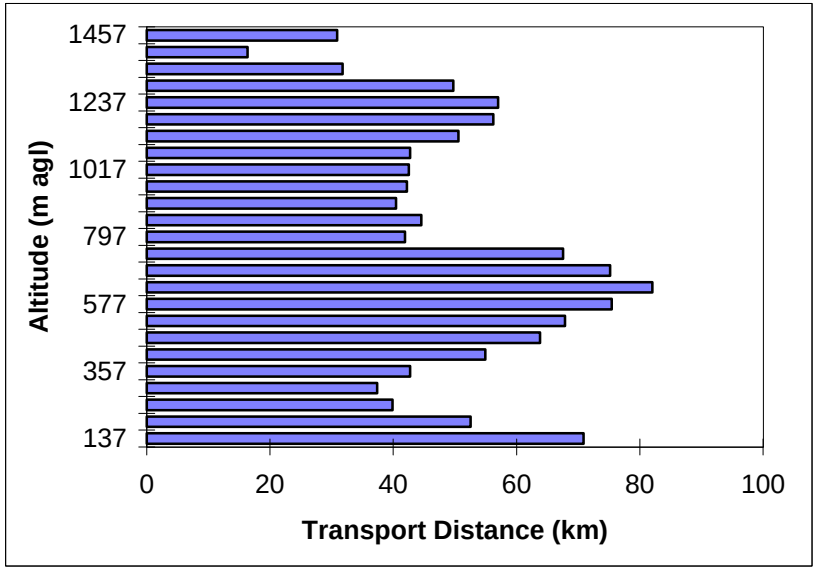

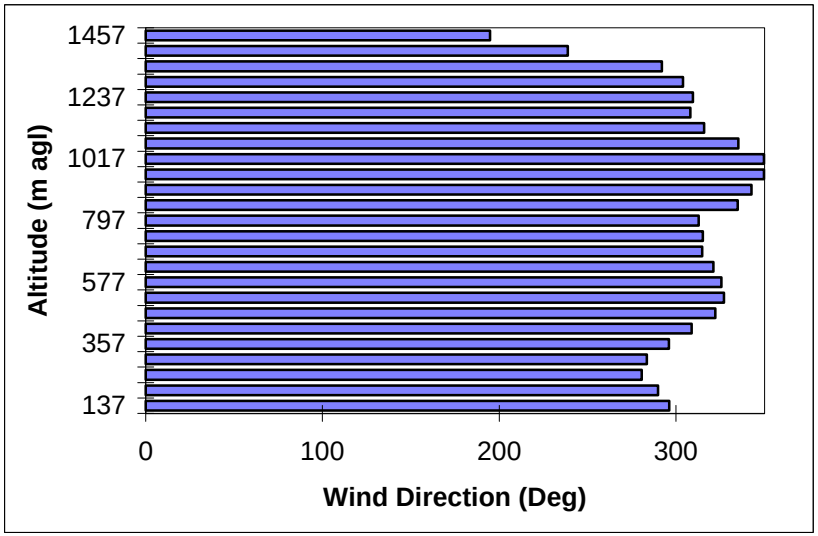

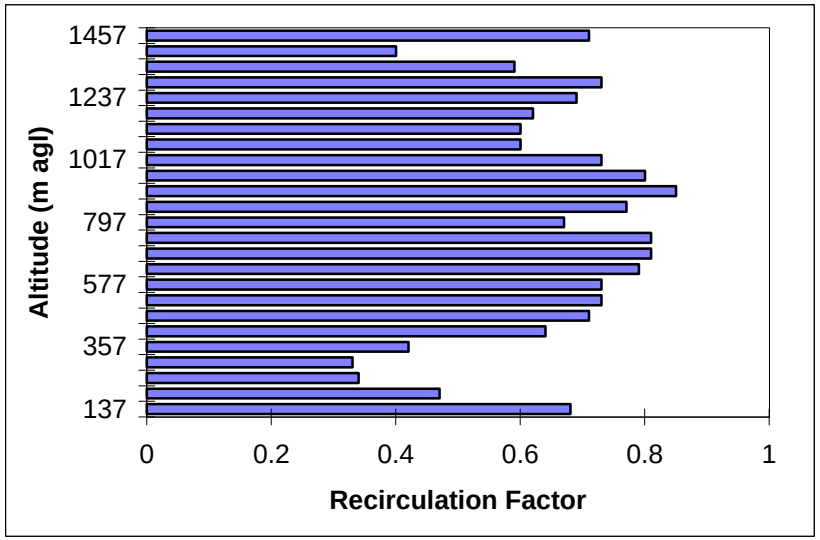

SJV 08-26-98 1600 to 0400.xls

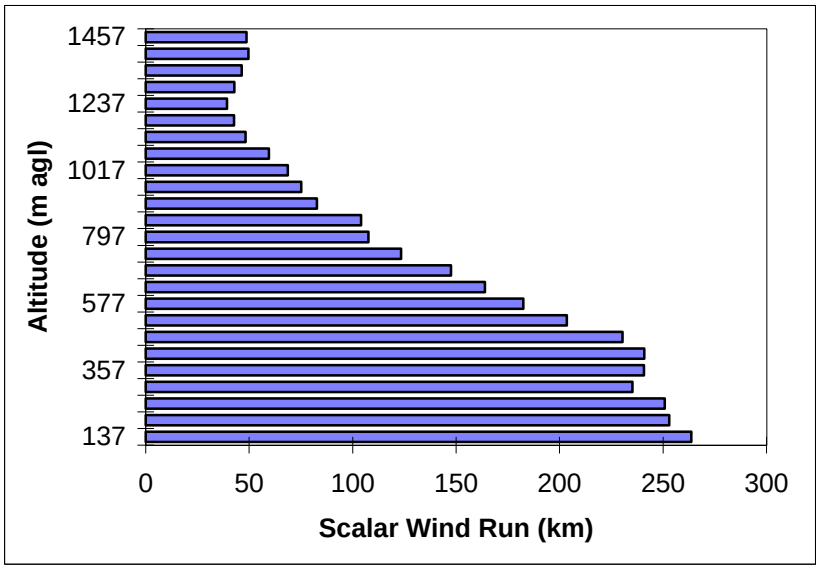

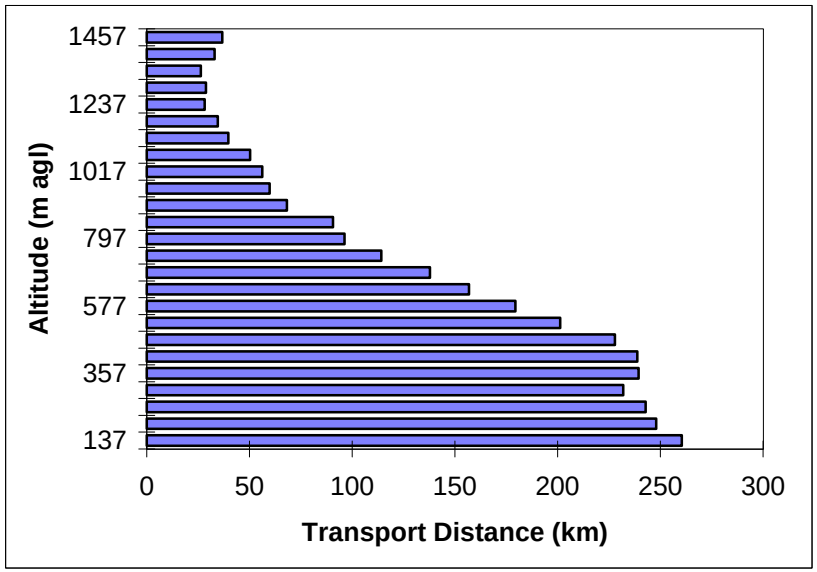

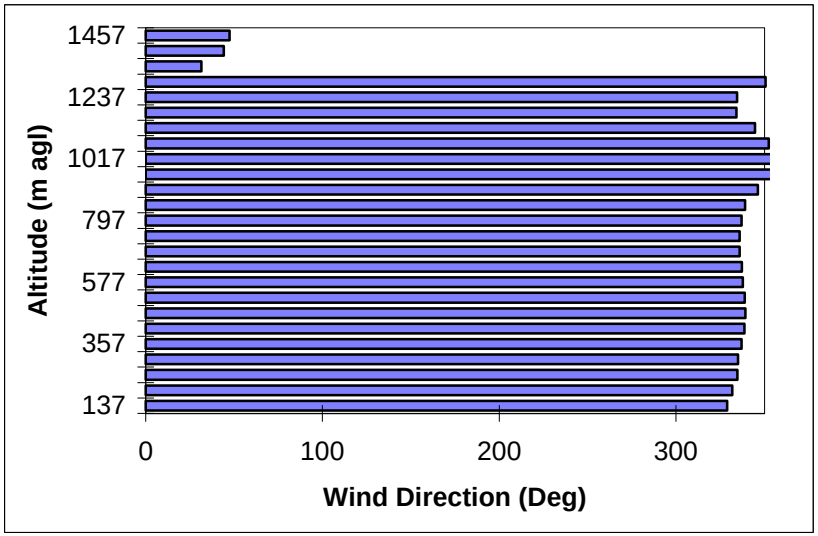

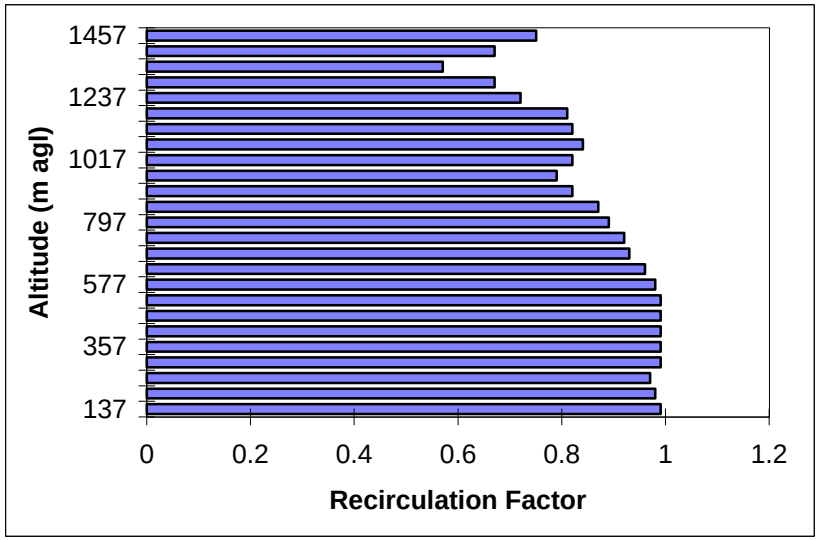

SJV 08-27-98 0400 to 1600.xls

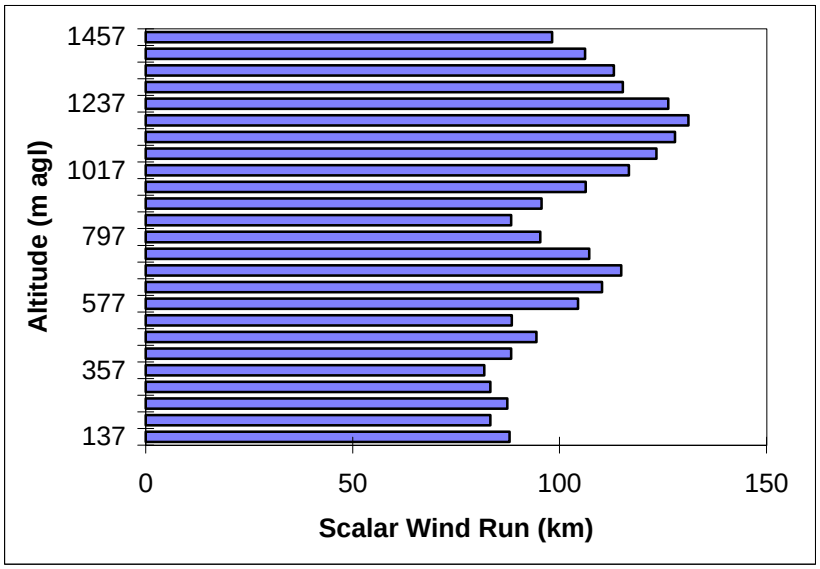

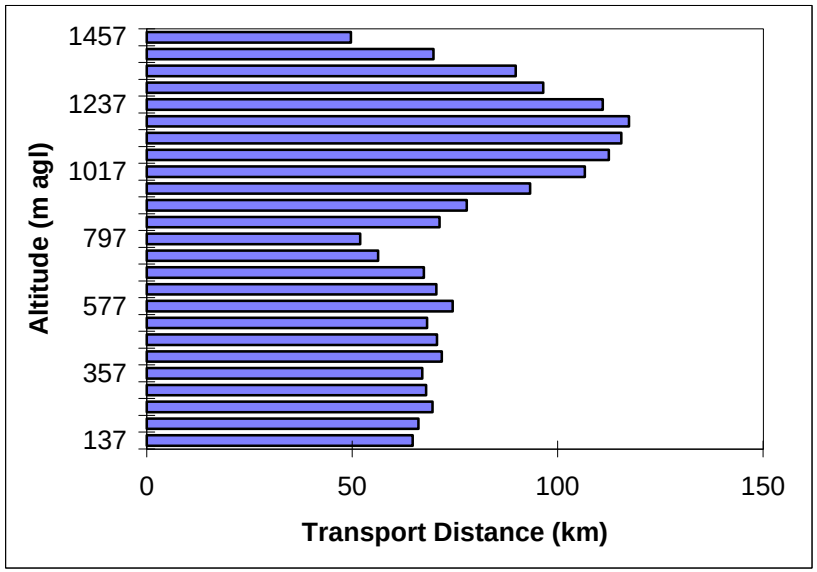

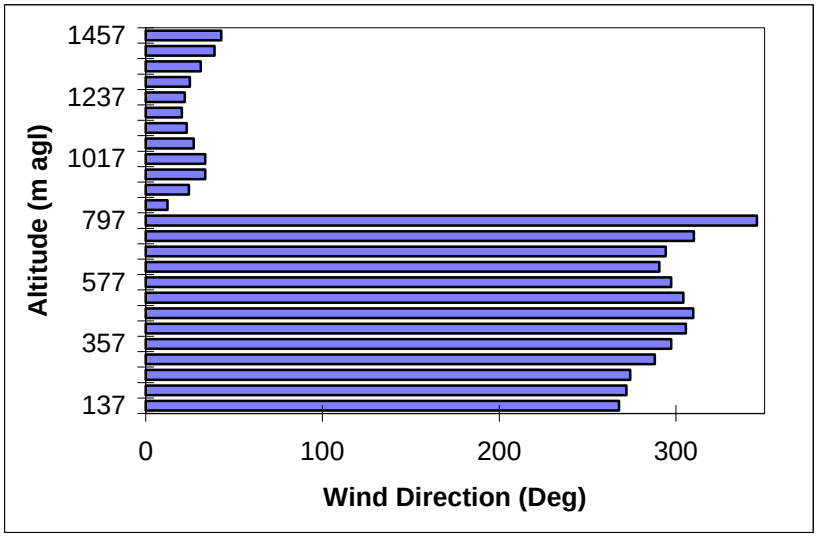

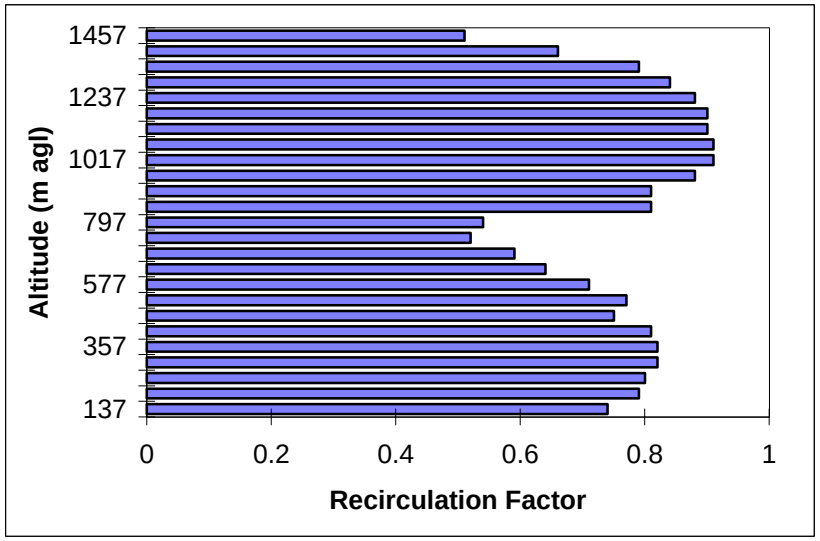

SJV 08-27-98 1600 to 0400.xls

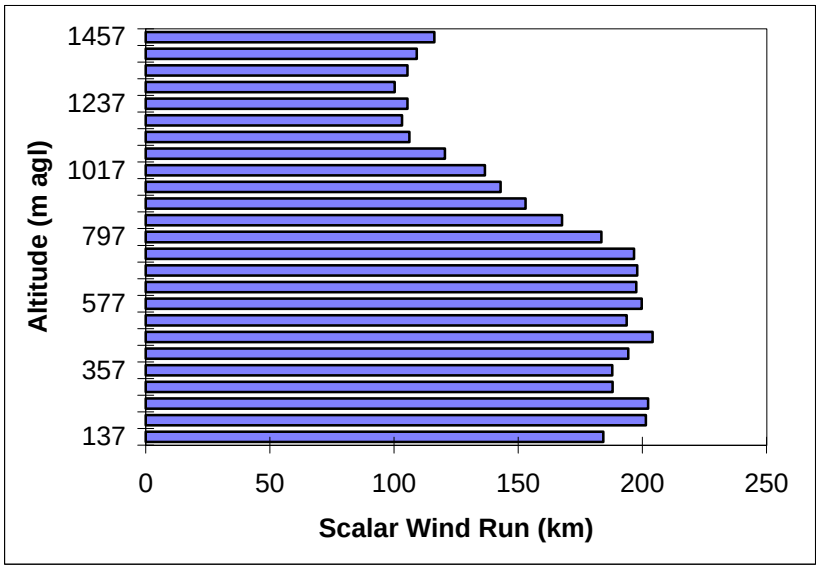

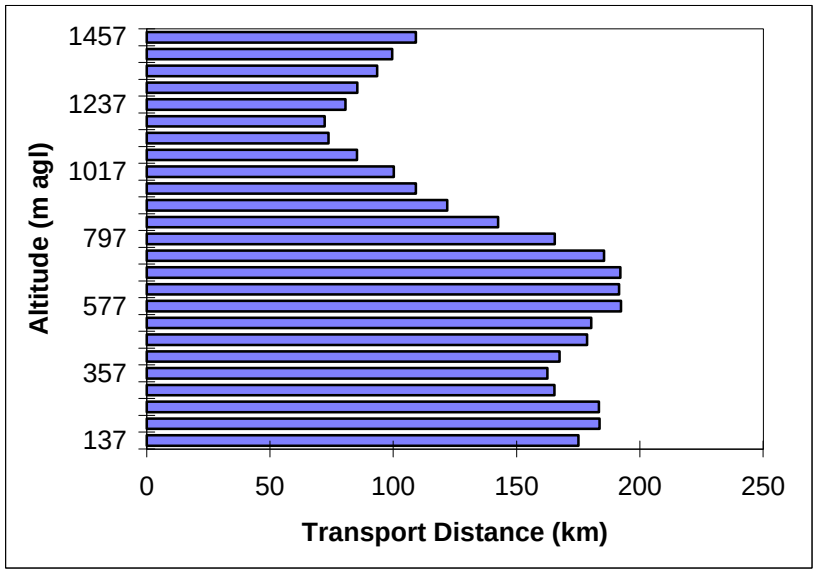

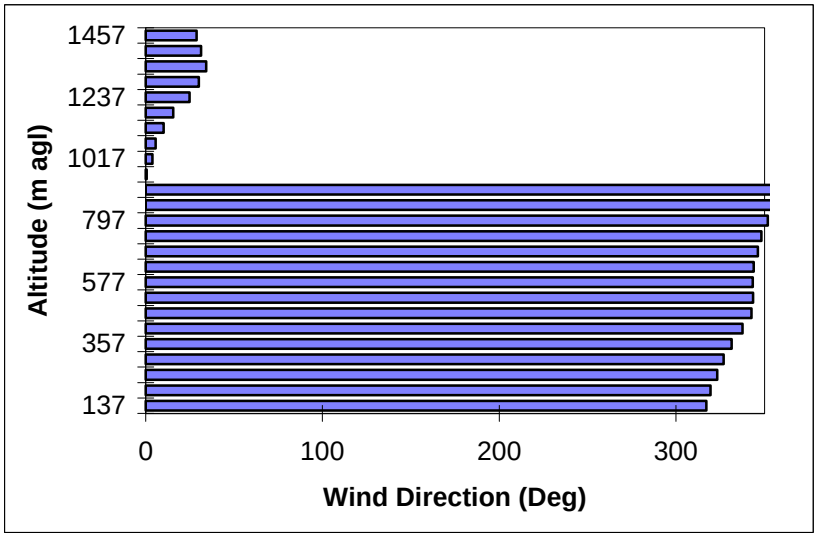

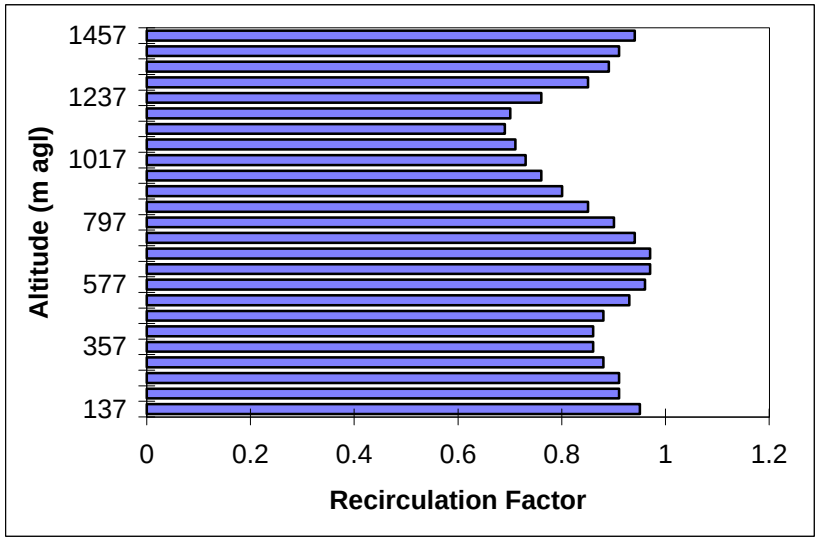

SJV 08-28-98 0400 to 1600.xls

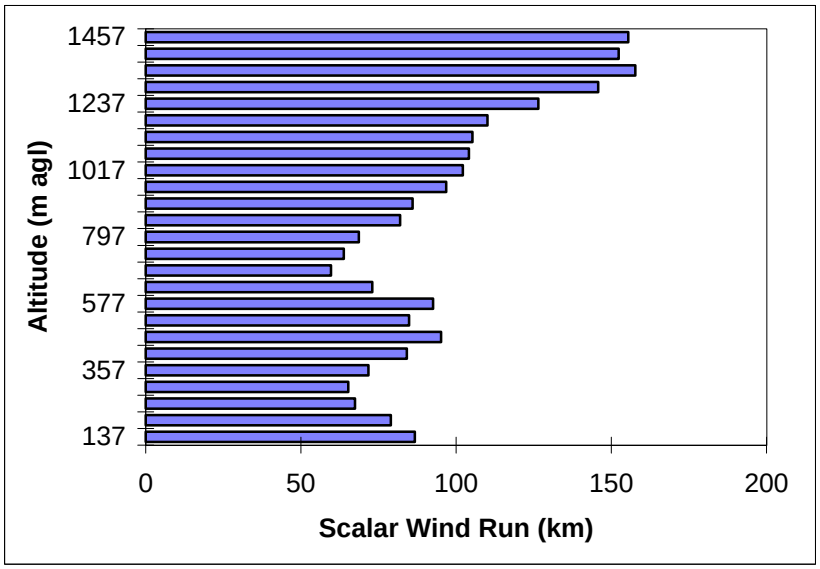

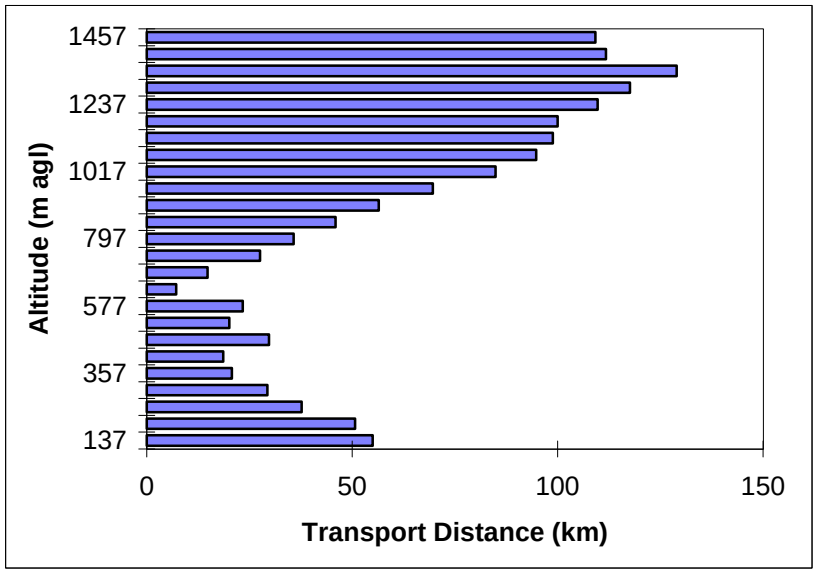

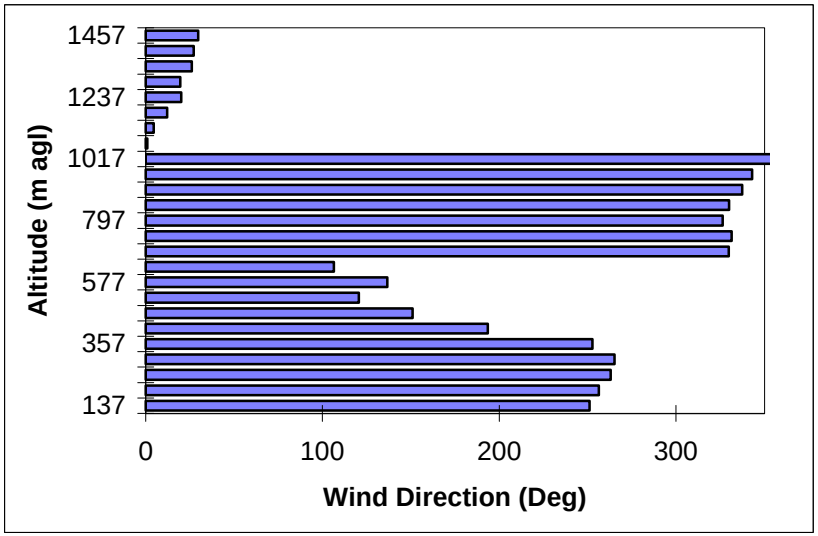

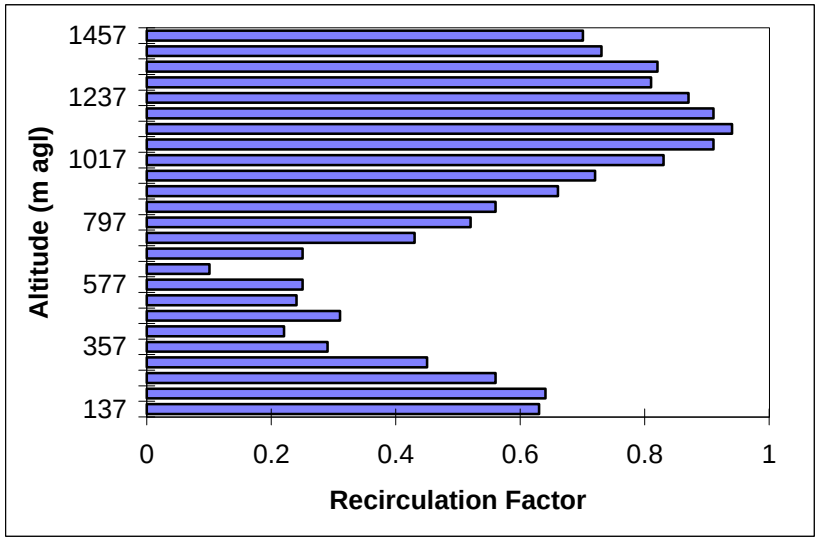

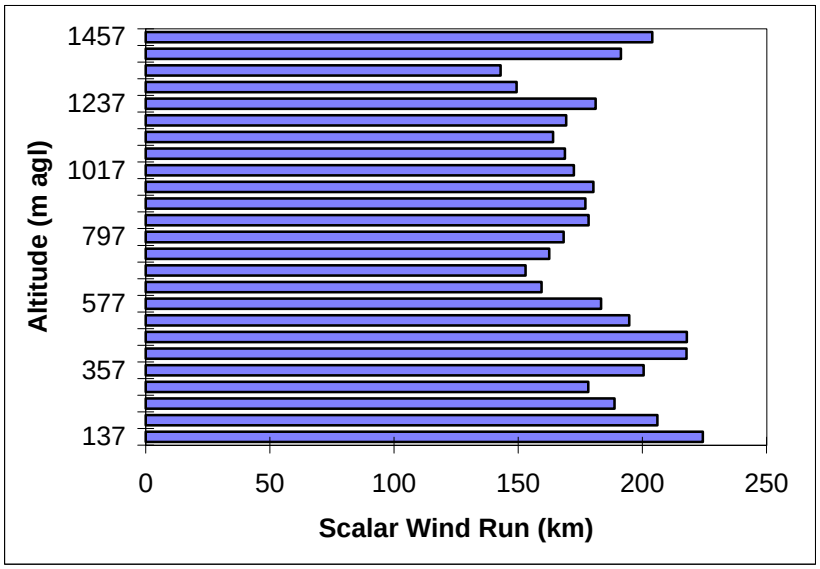
Altitude (m agl)
1457
1237
1017
797
577
357
137
0
50
100
150
200
250
Scalar Wind Run (km)

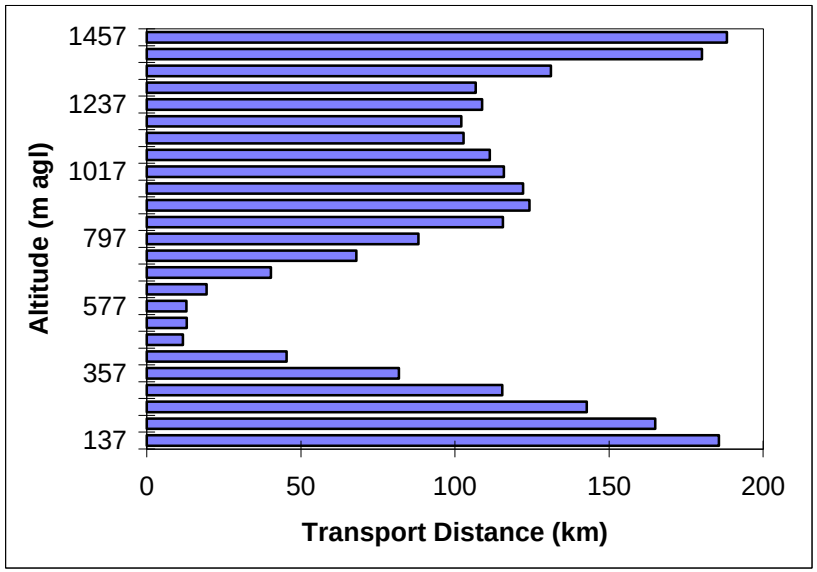
Altitude (m agl)
1457
1237
1017
797
577
357
137
0
50
100
150
200
Transport Distance (km)

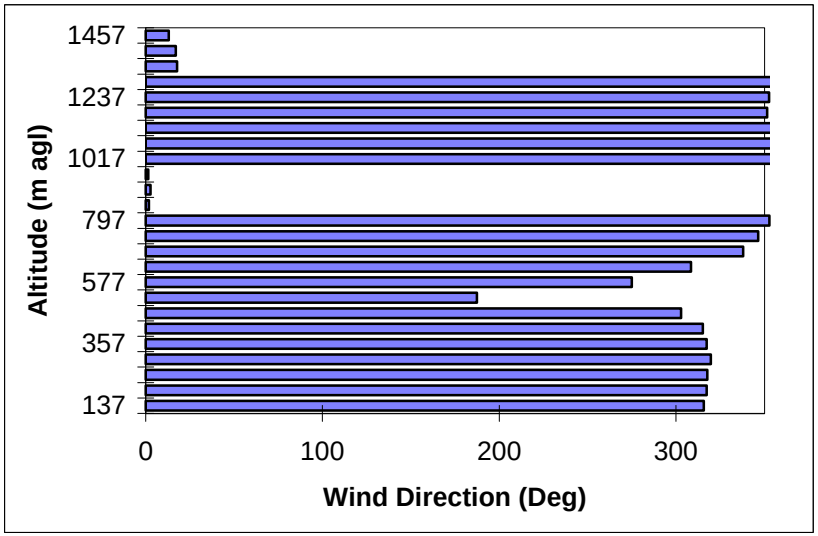
Altitude (m agl)
1457
1237
1017
797
577
357
137
0
100
200
300
Wind Direction (Deg)

Altitude (m agl)
1457
1237
1017
797
577
357
137
0
0.2
0.4
0.6
0.8
1
Recirculation Factor

SJV 08-29-98 0400 to 1600.xls

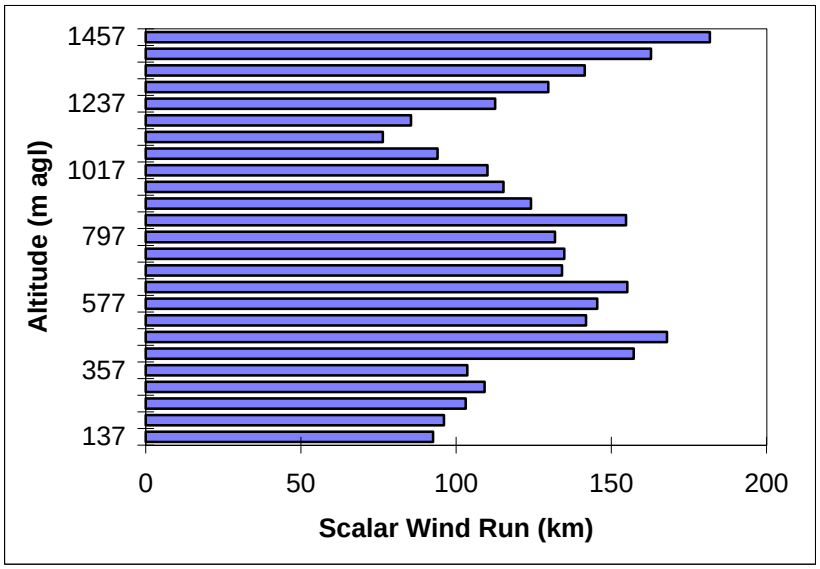

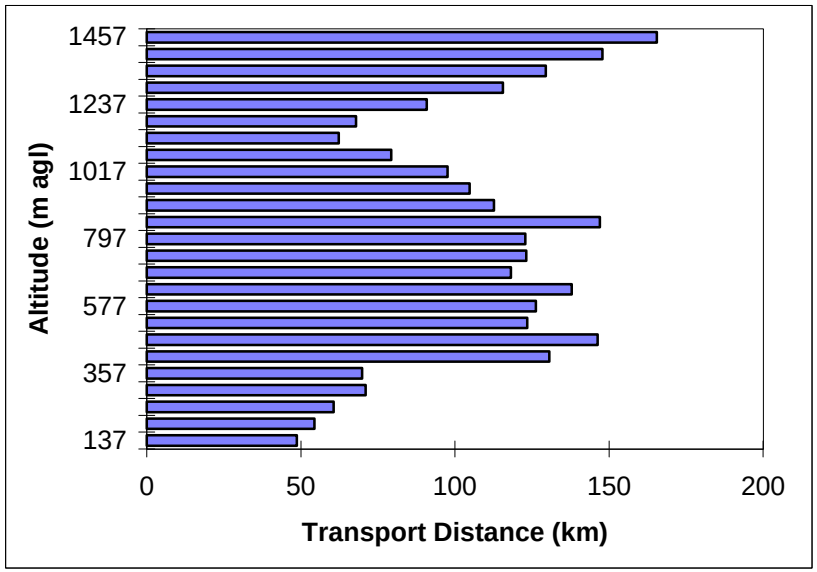

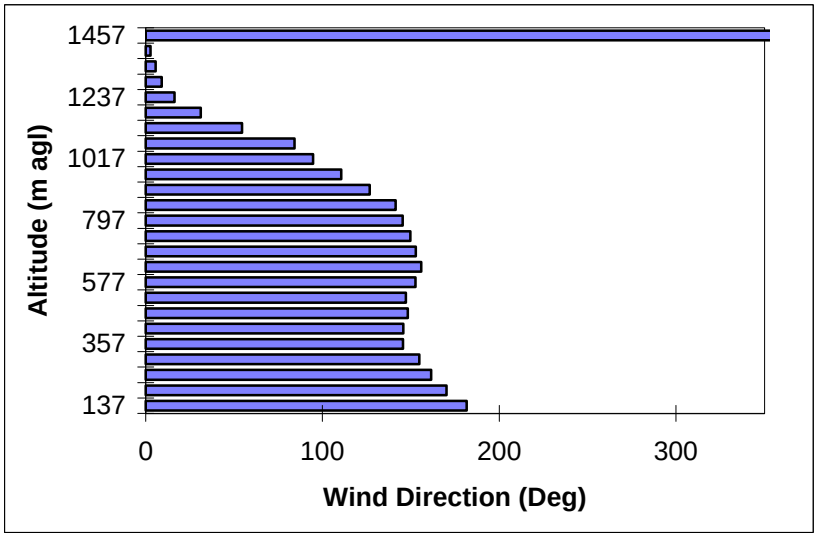

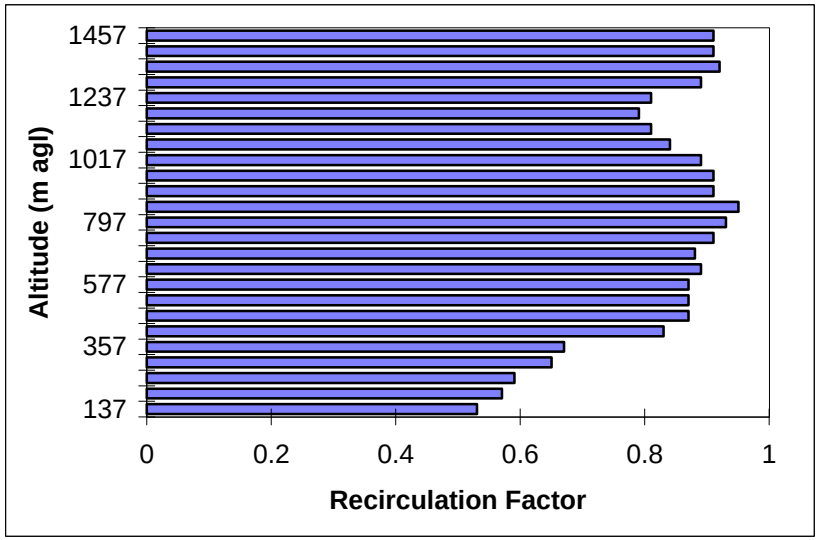

SJV 08-29-98 1600 to 0400.xls

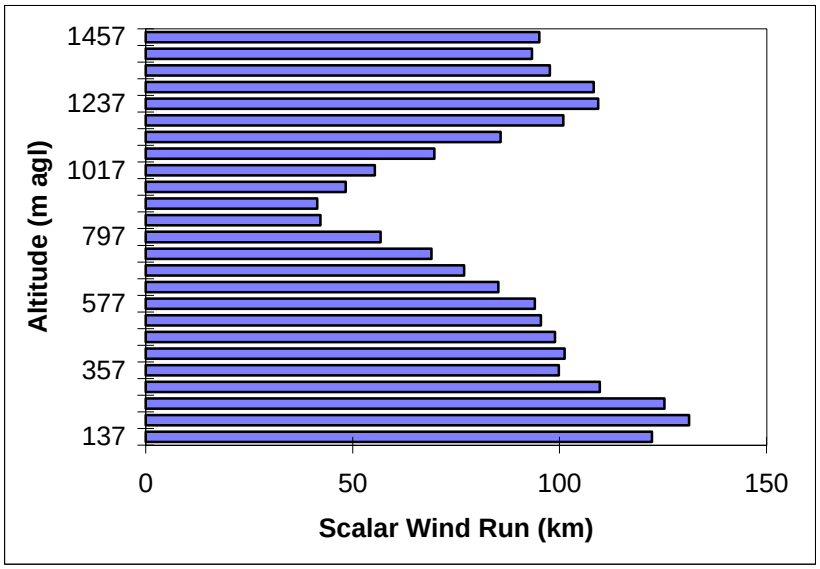

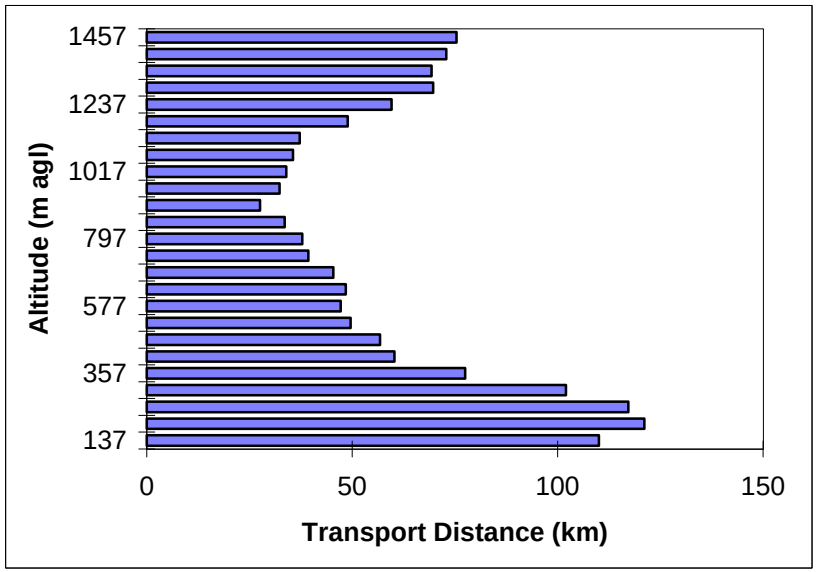

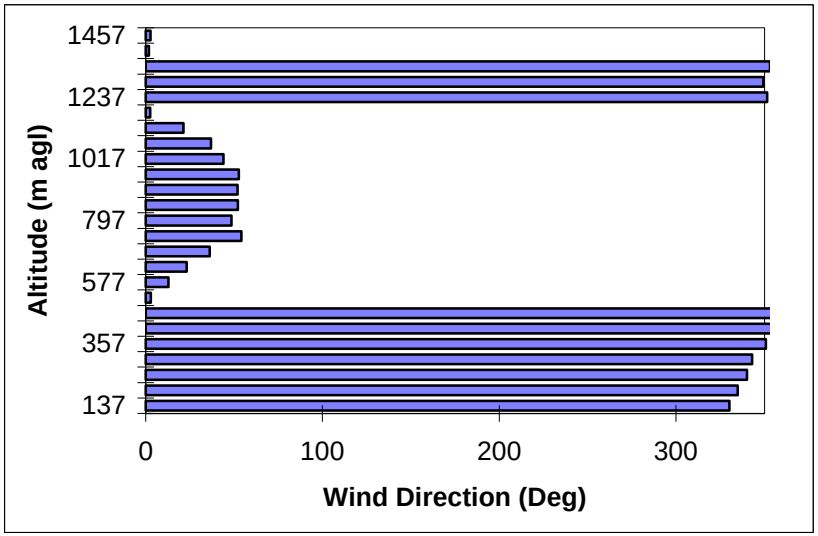

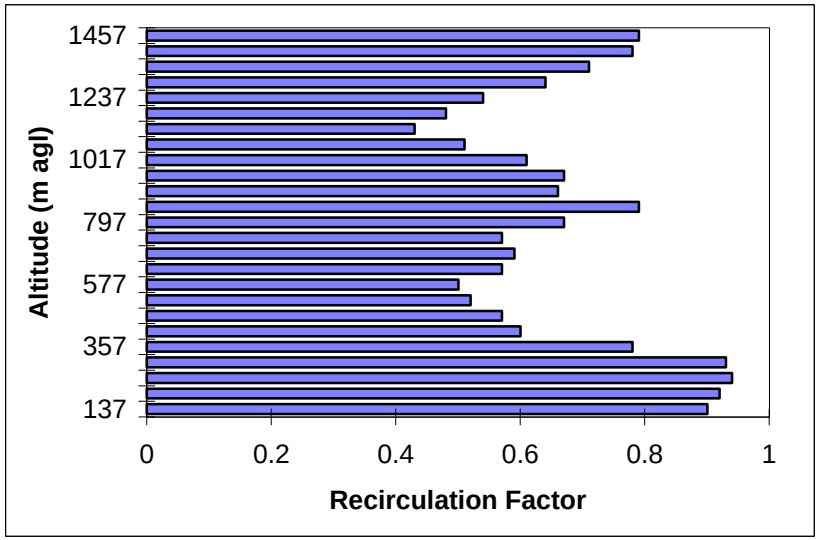

SJV 08-30-98 0400 to 1600.xls

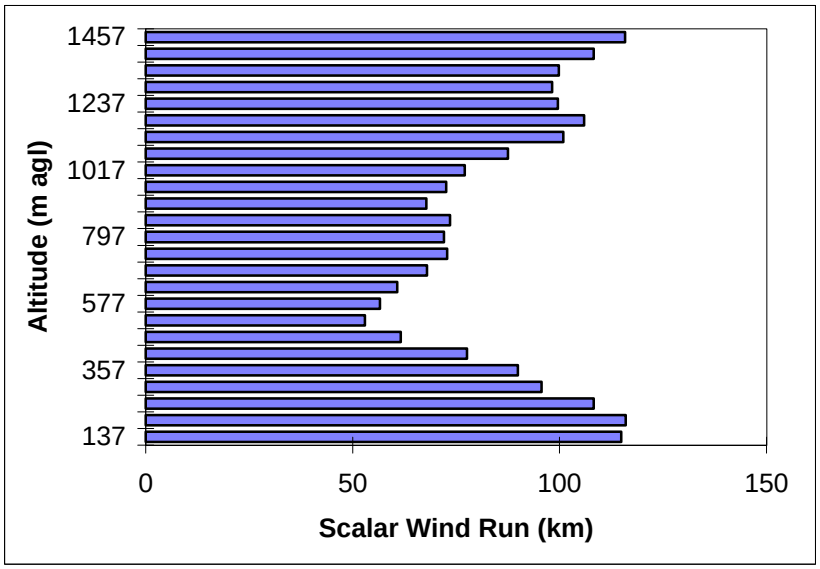

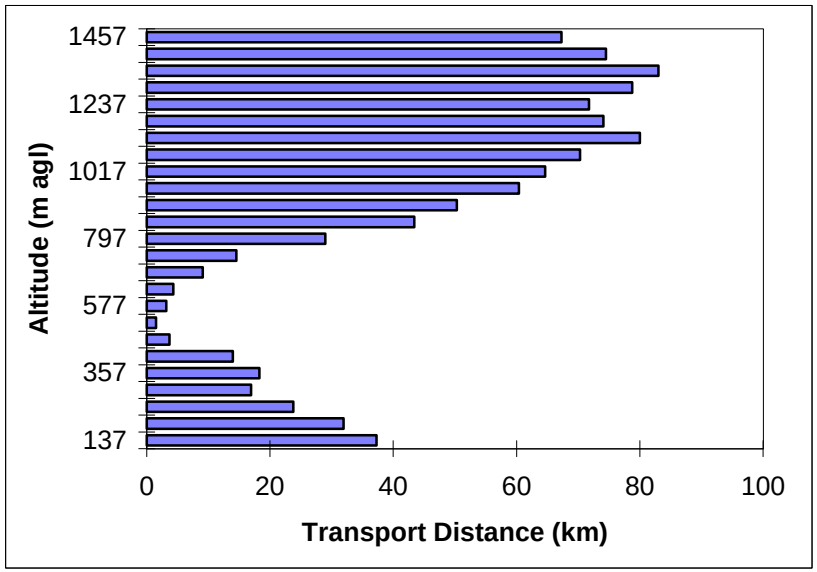

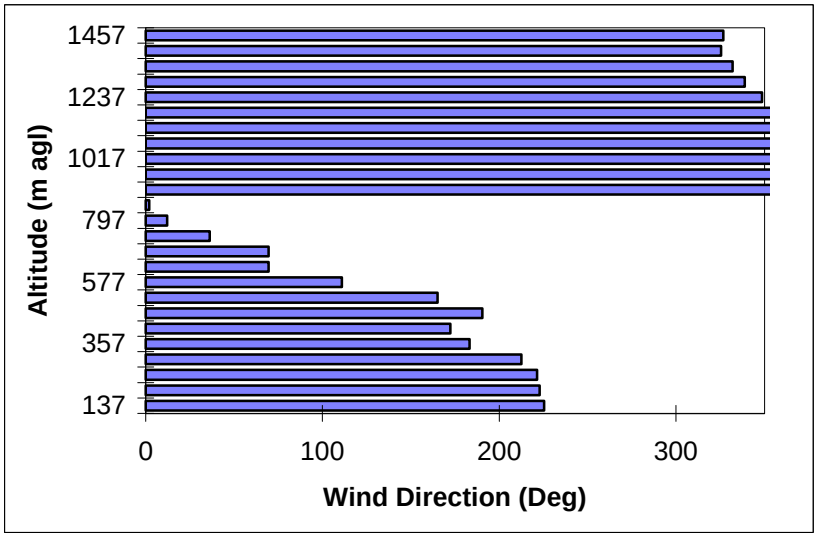

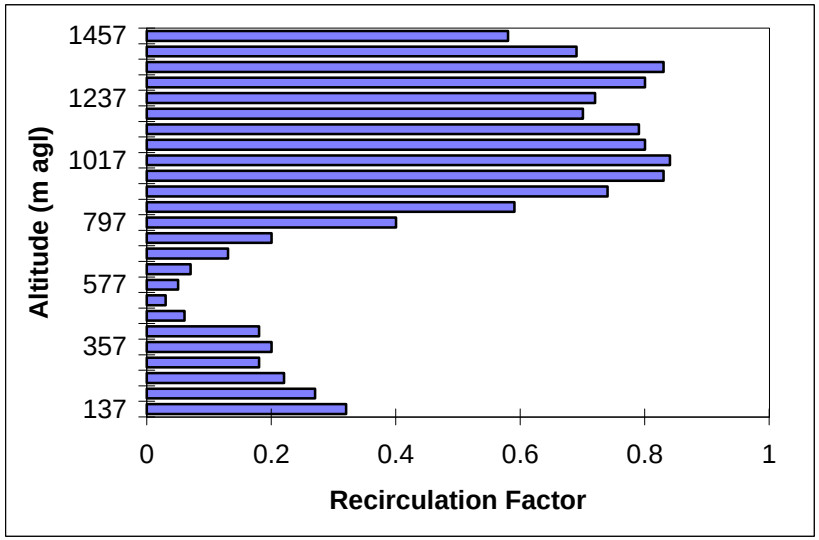

SJV 08-30-98 1600 to 0400.xls

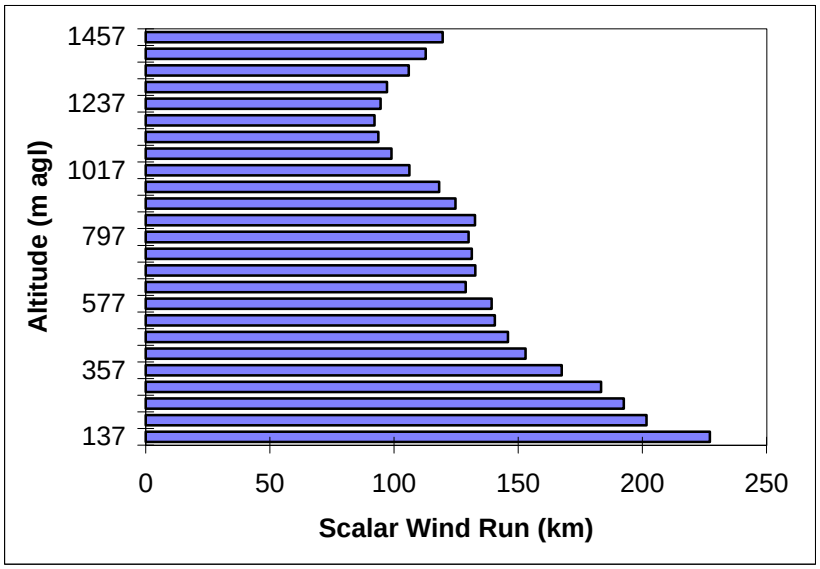

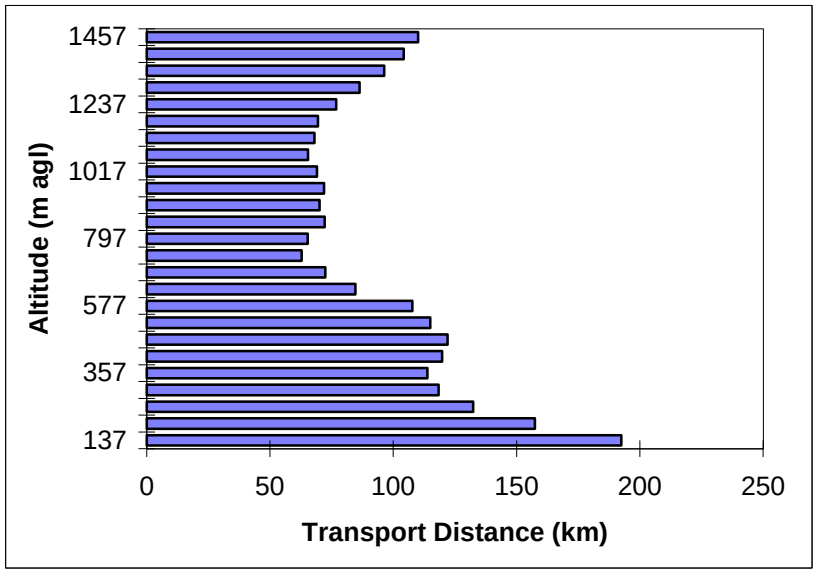

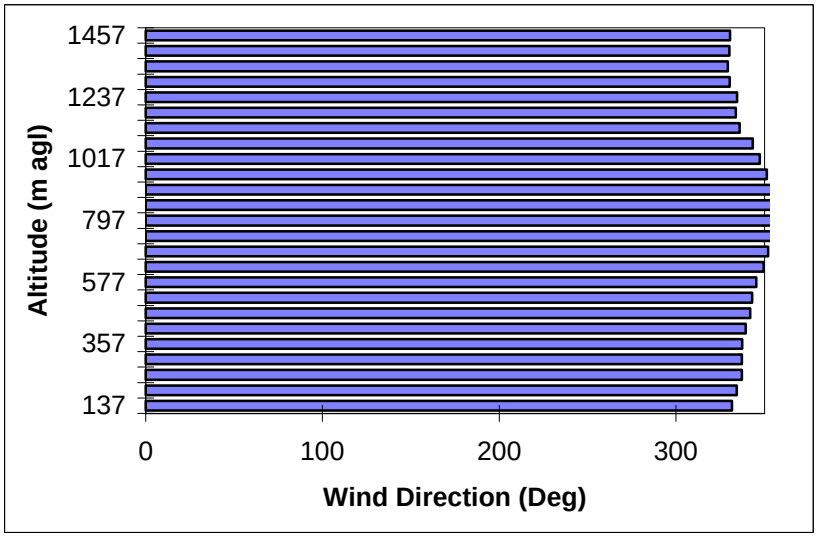

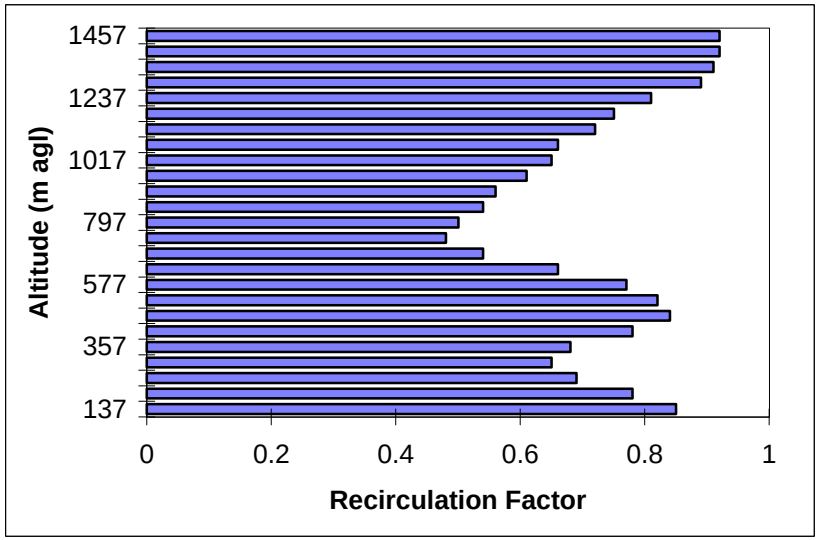

SJV 08-31-98 0400 to 1600.xls

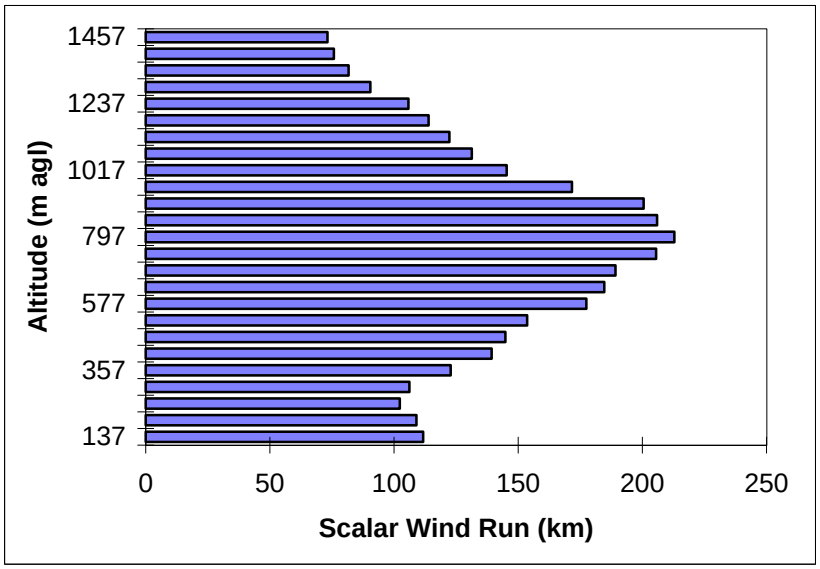

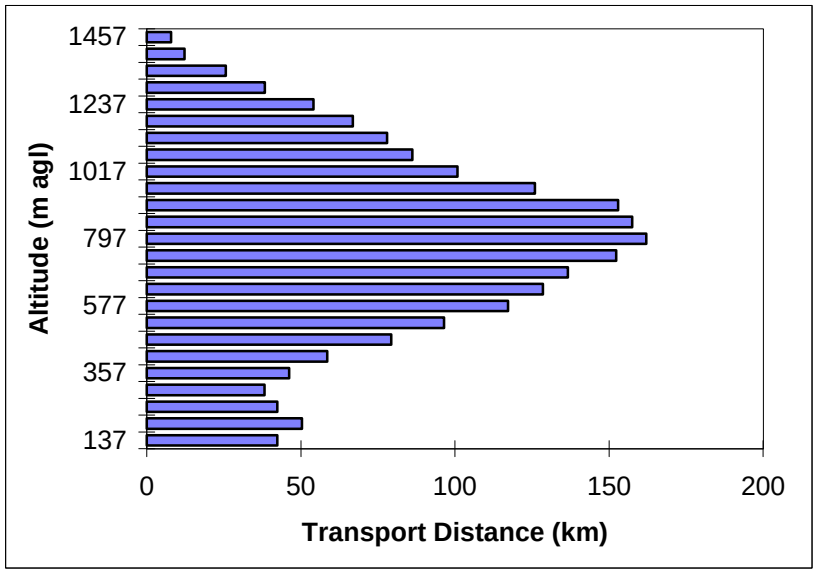

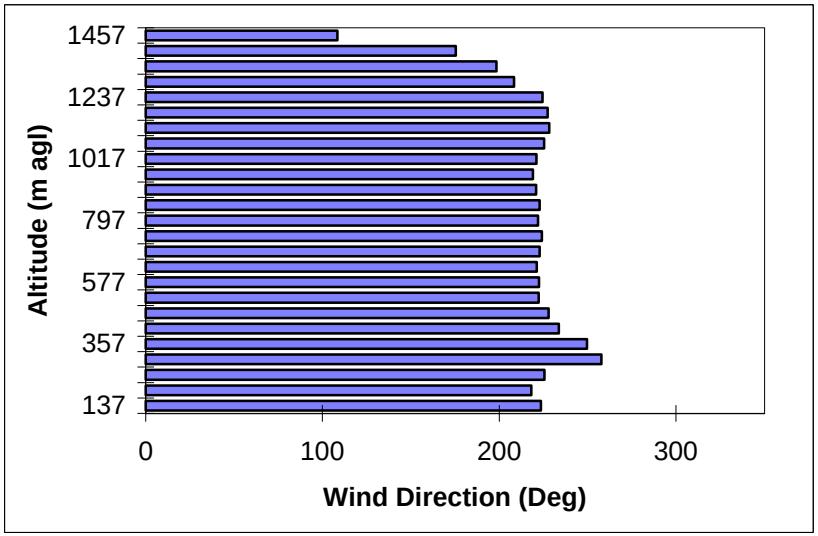

SJV 08-31-98 1600 to 0400.xls

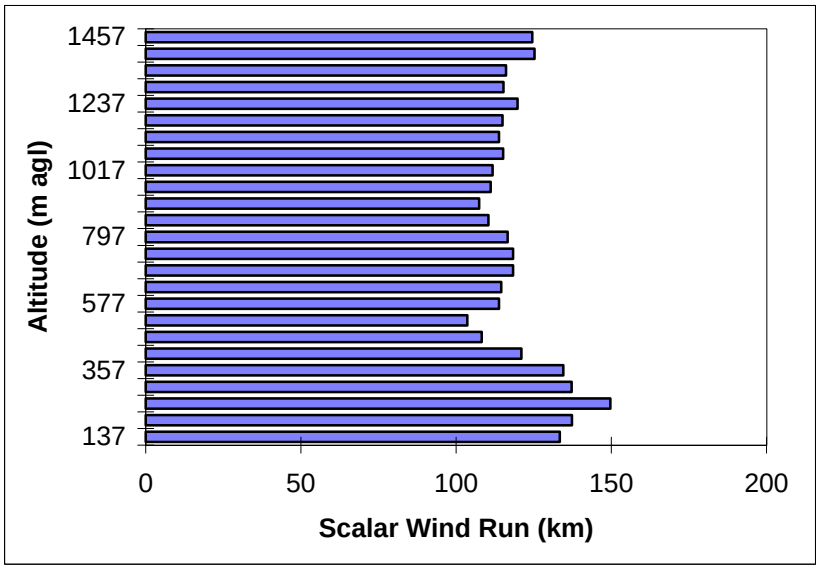

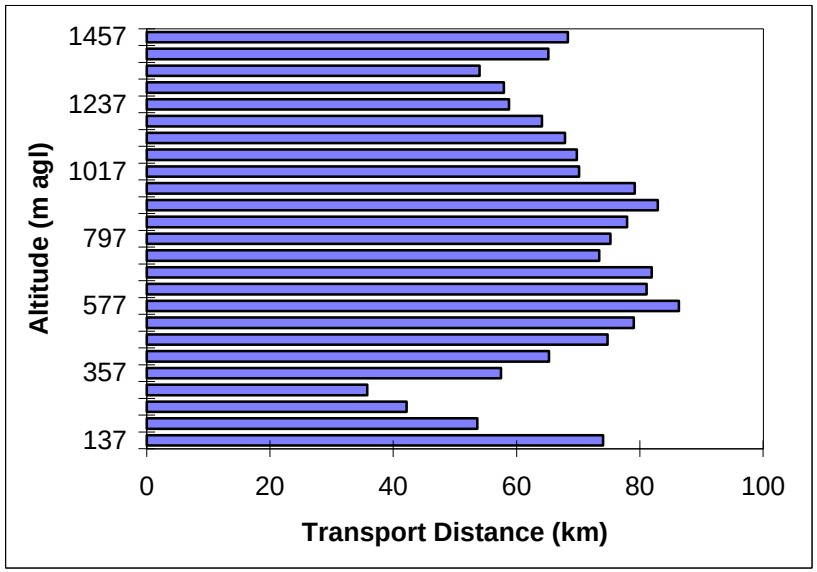

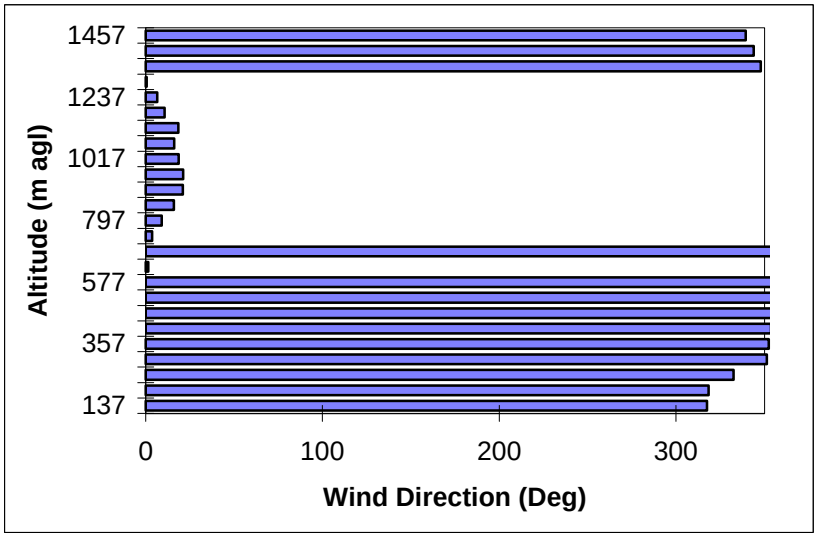

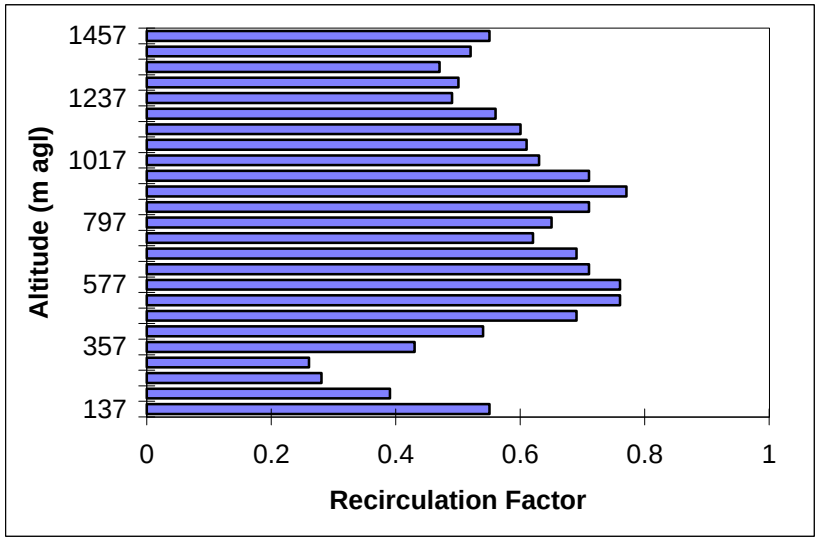

SJV 09-01-98 0400 to 1600.xls

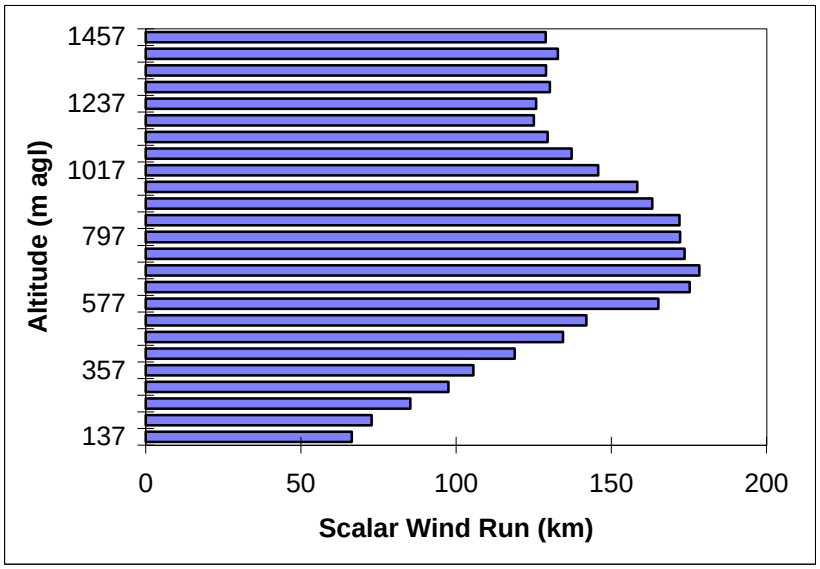

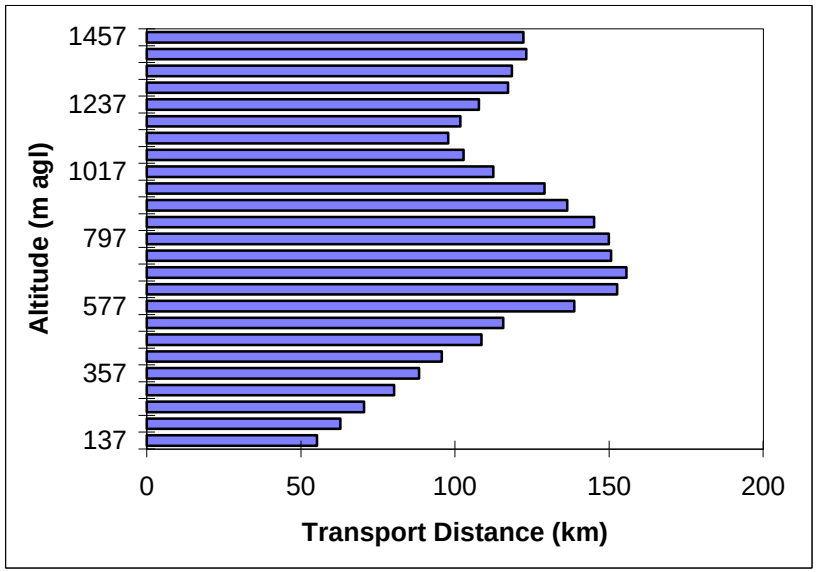

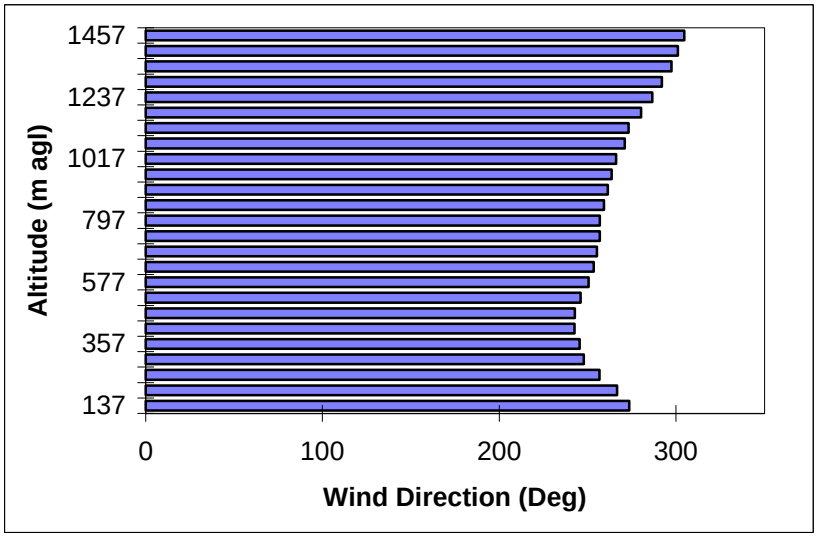

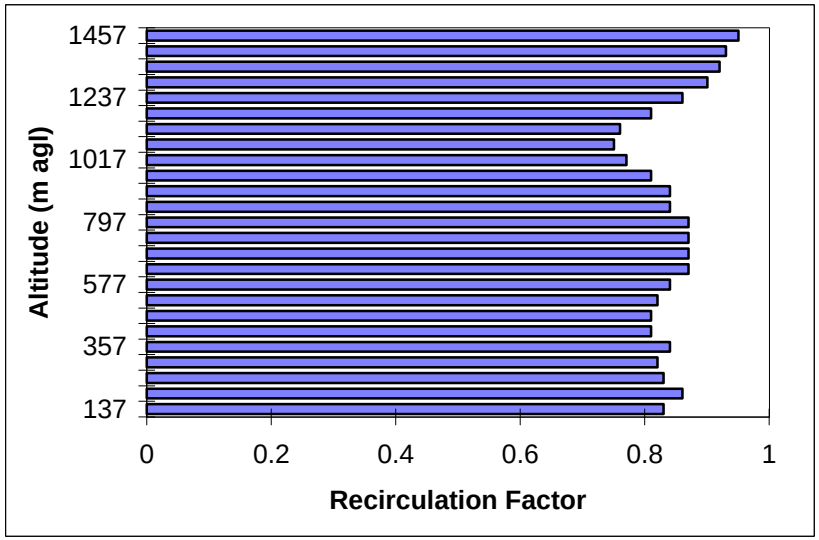

SJV 09-01-98 1600 to 0400.xls

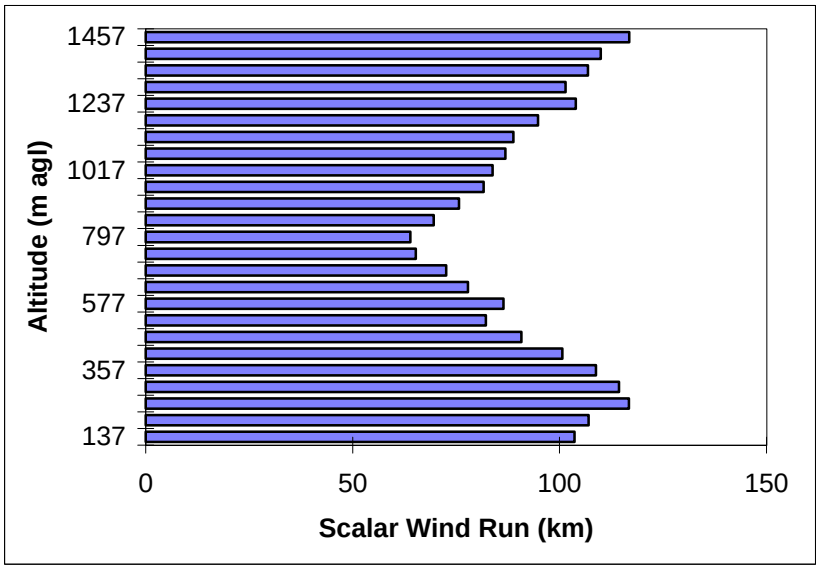

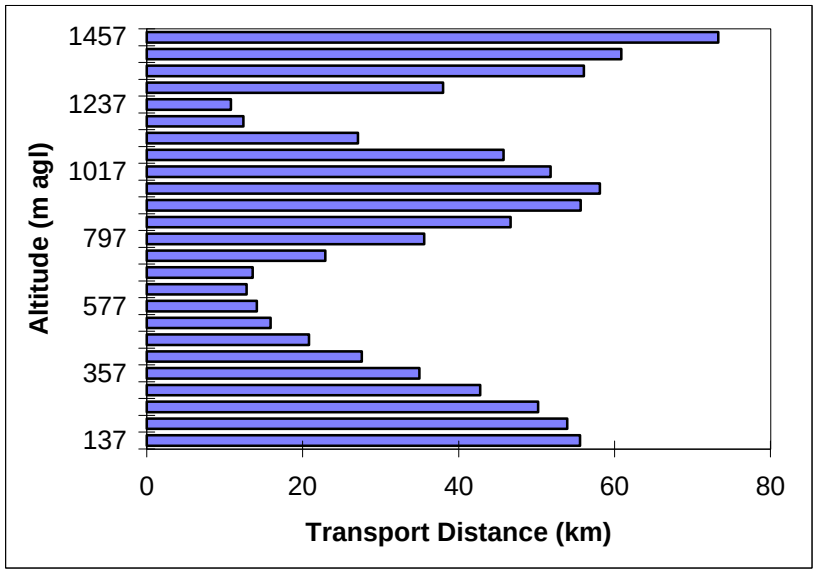

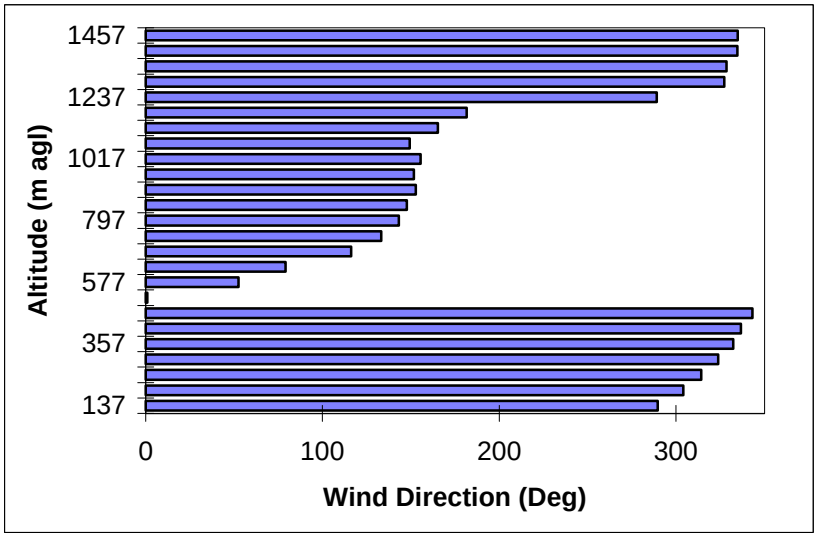

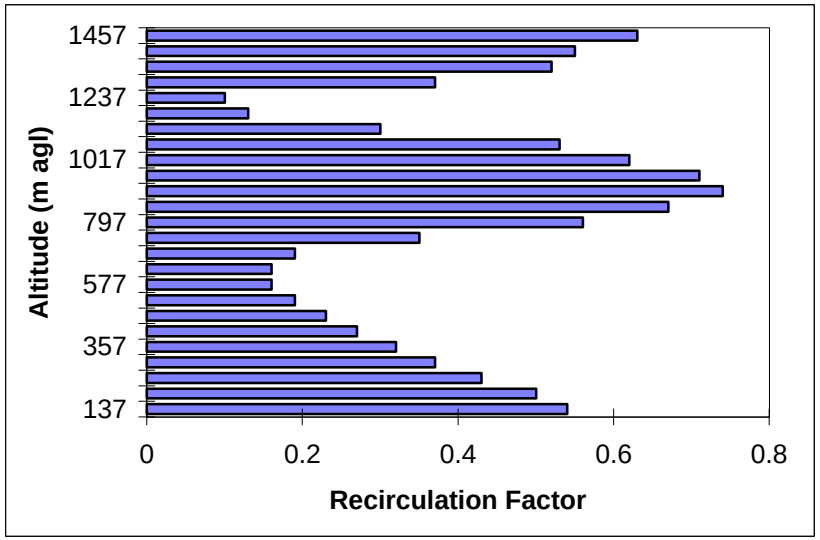

SJV 09-02-98 0400 to 1600.xls

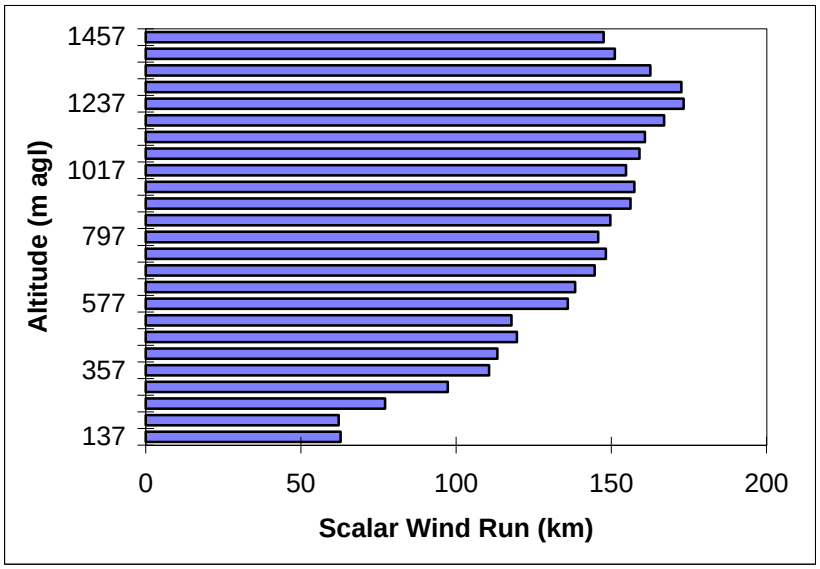

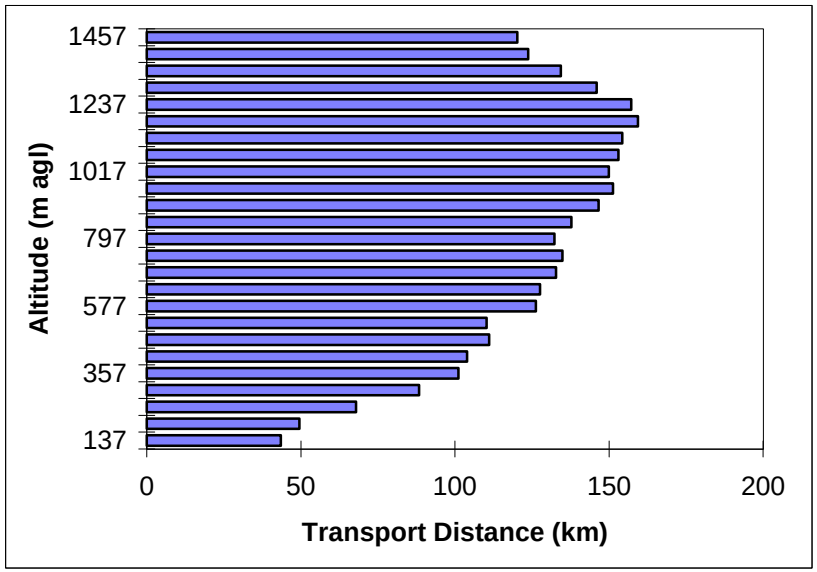

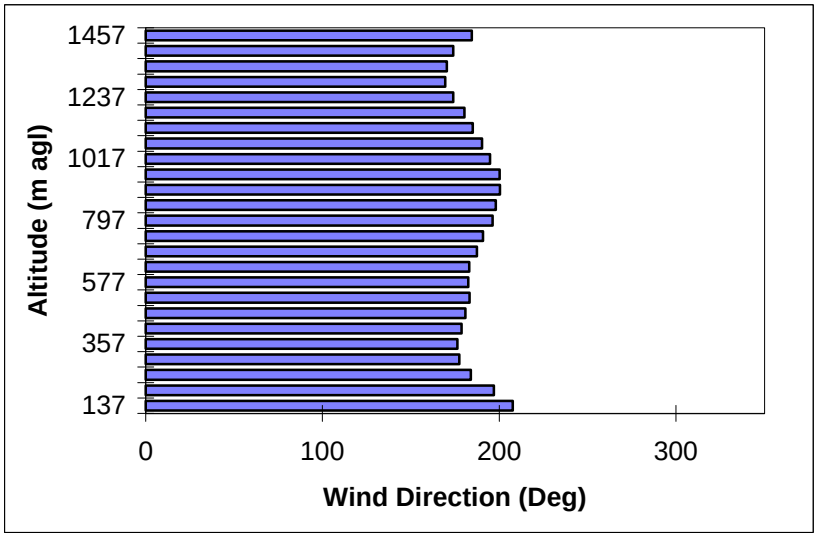

SJV 09-02-98 1600 to 0400.xls

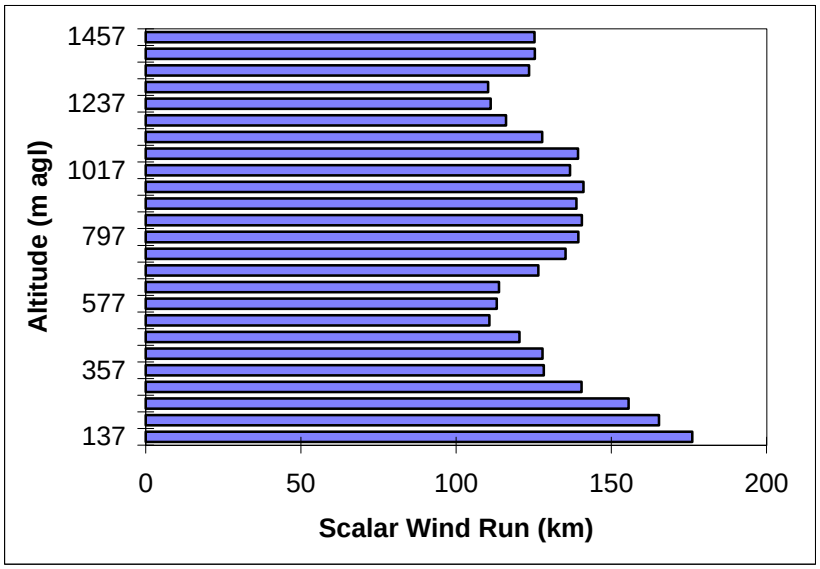

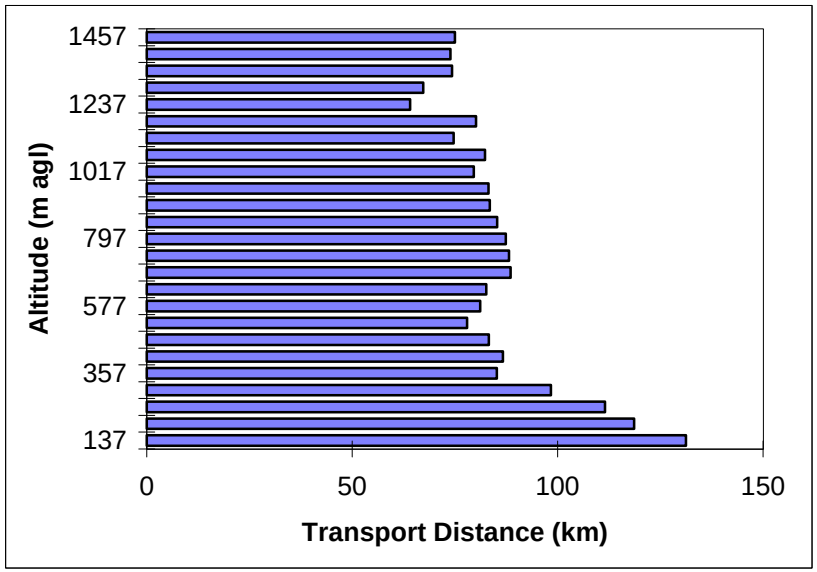

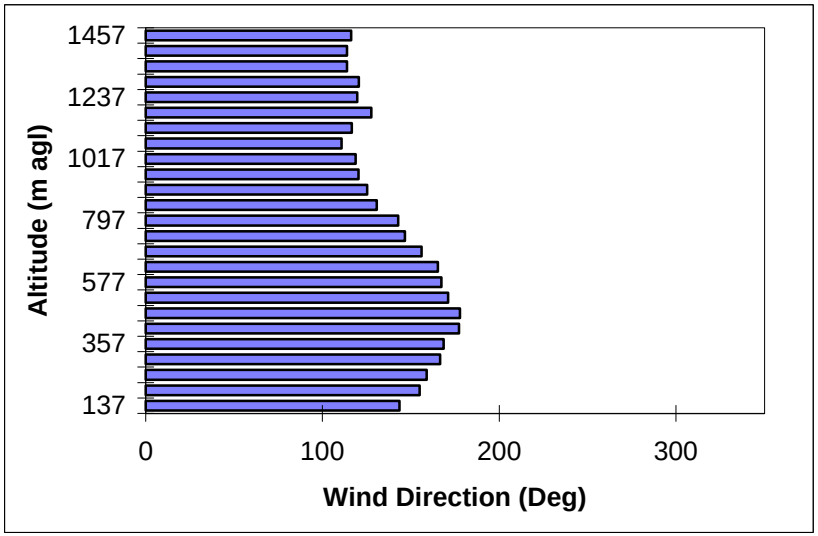

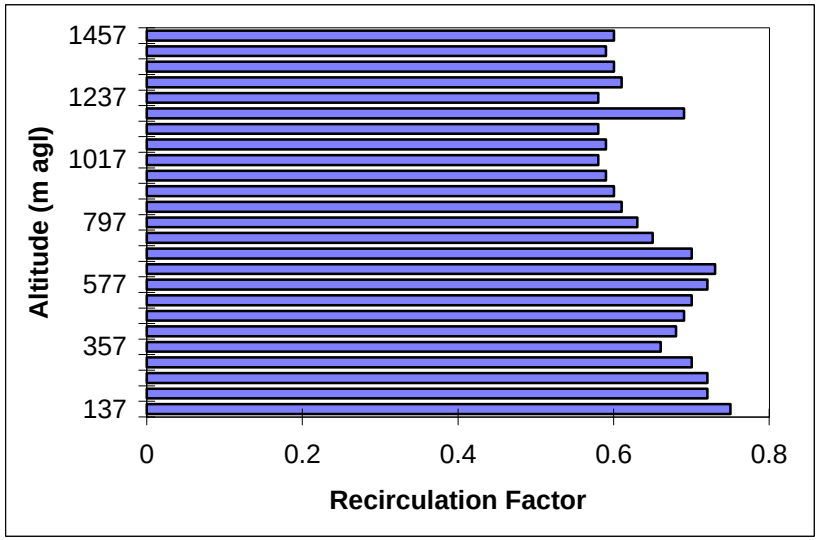

SJV 09-03-98 0400 to 1600.xls

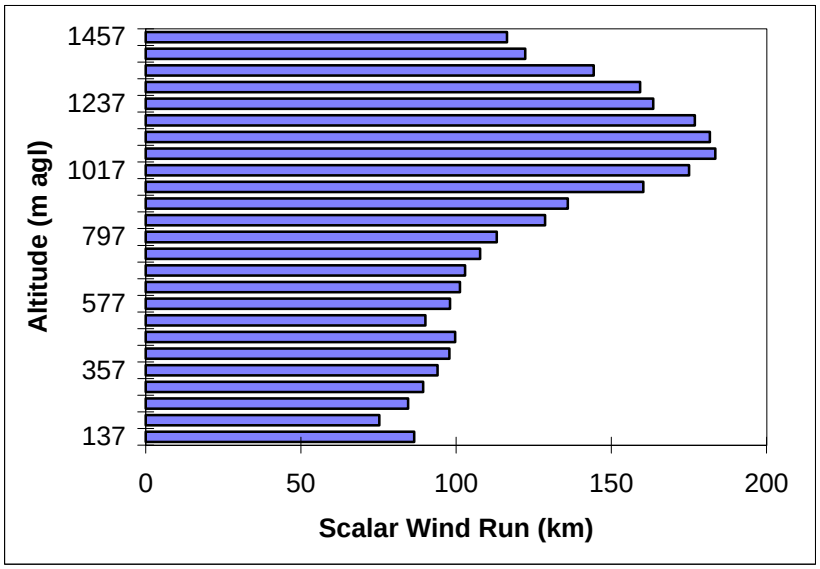

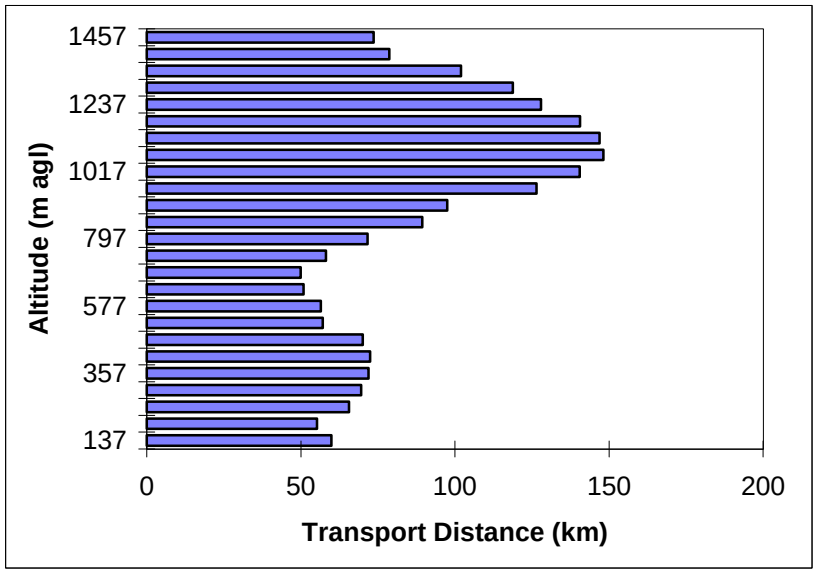

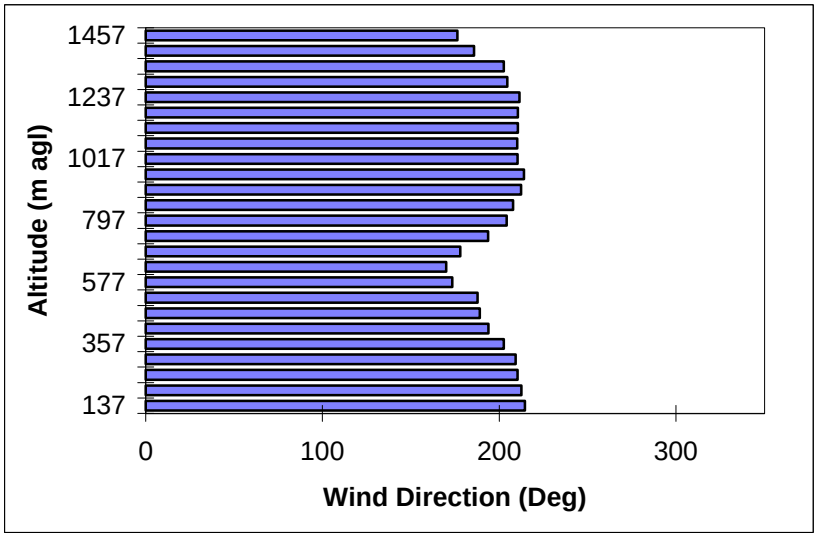

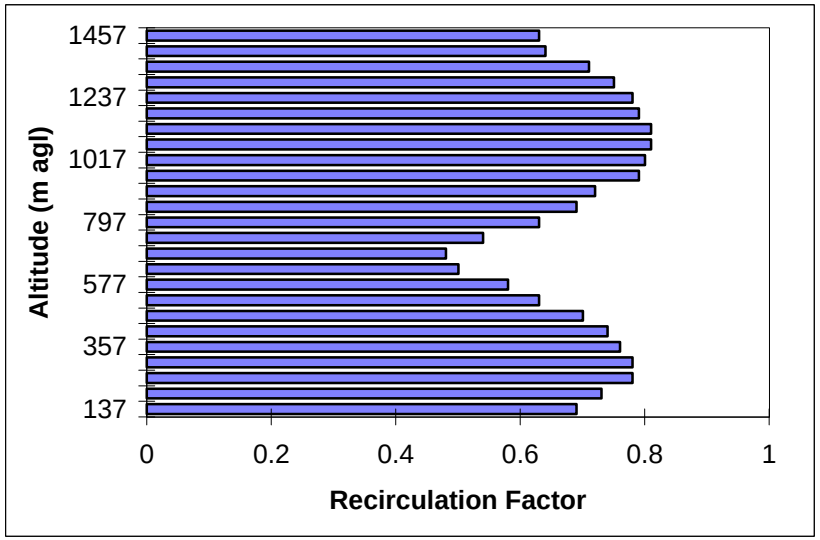

Ventura 08-05-97 0400 to 1600.xls

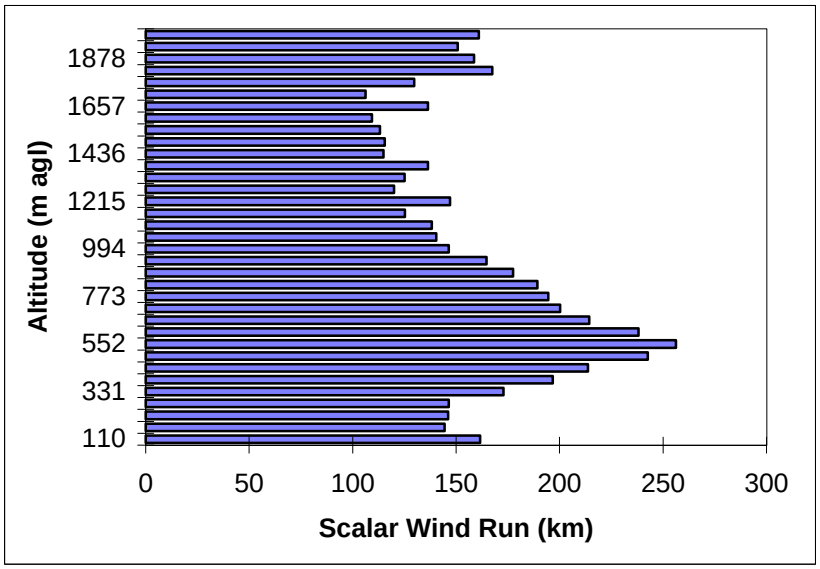

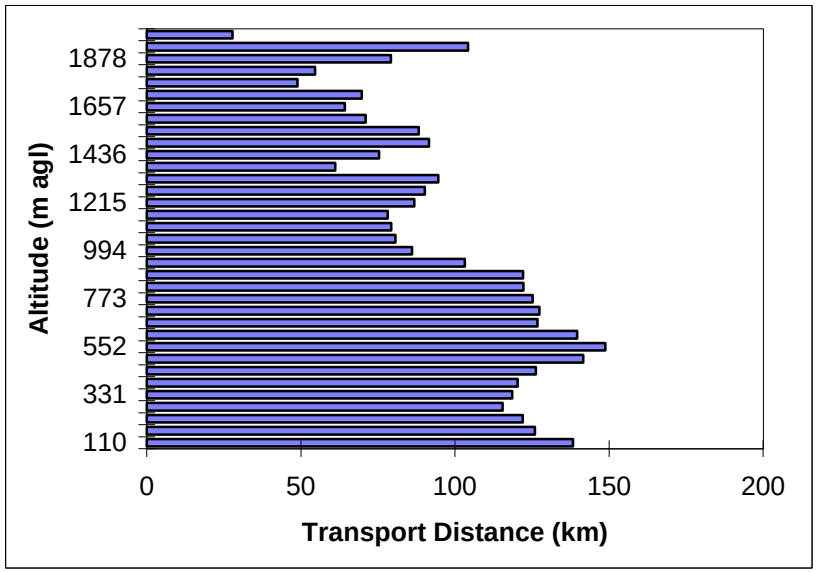

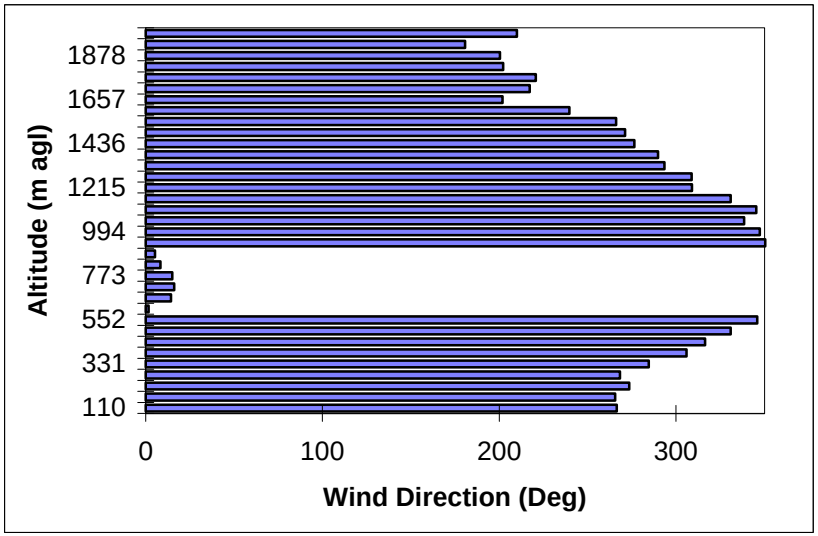

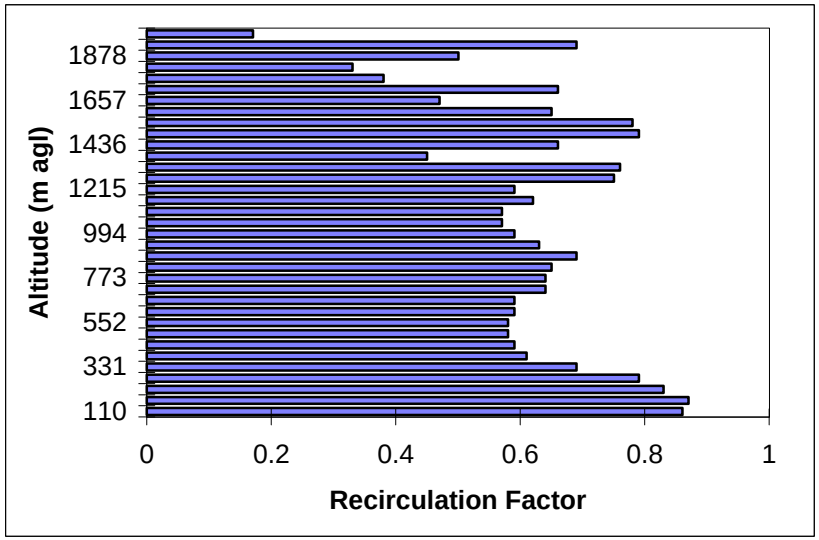

Ventura 08-05-97 1600 to 0400.xls

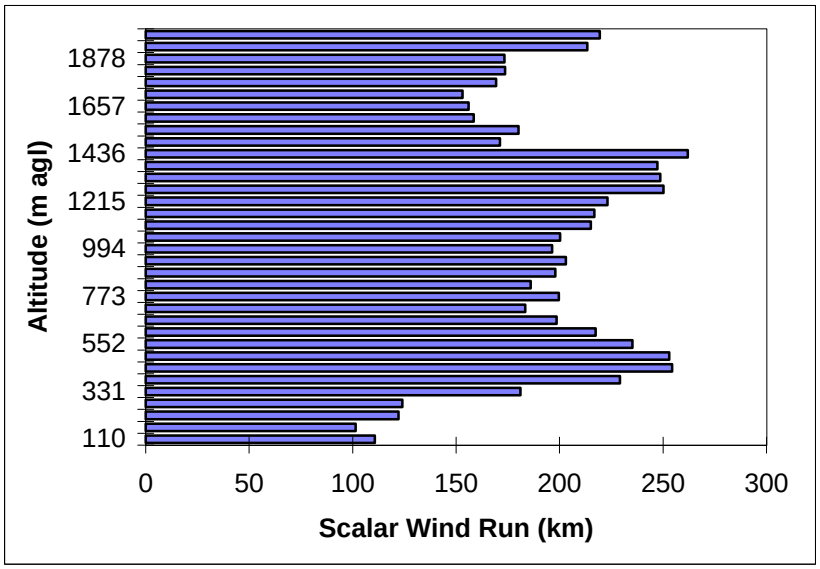

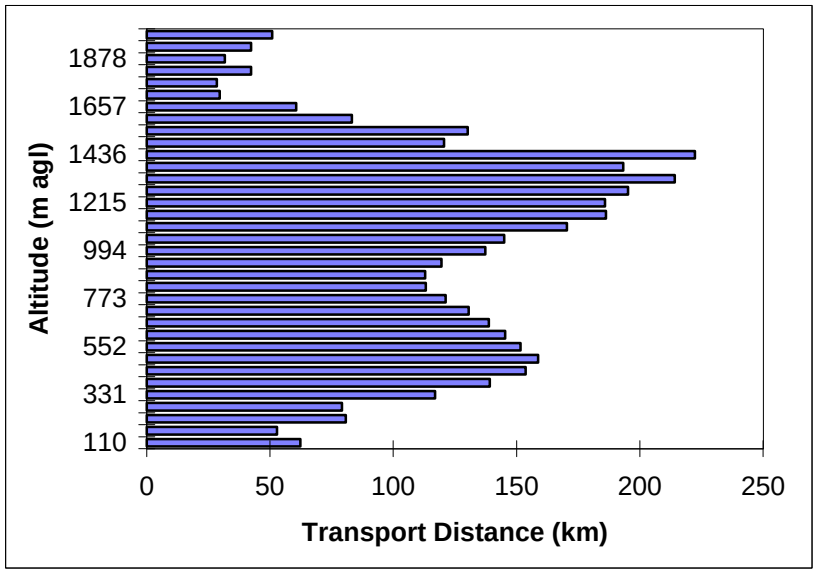

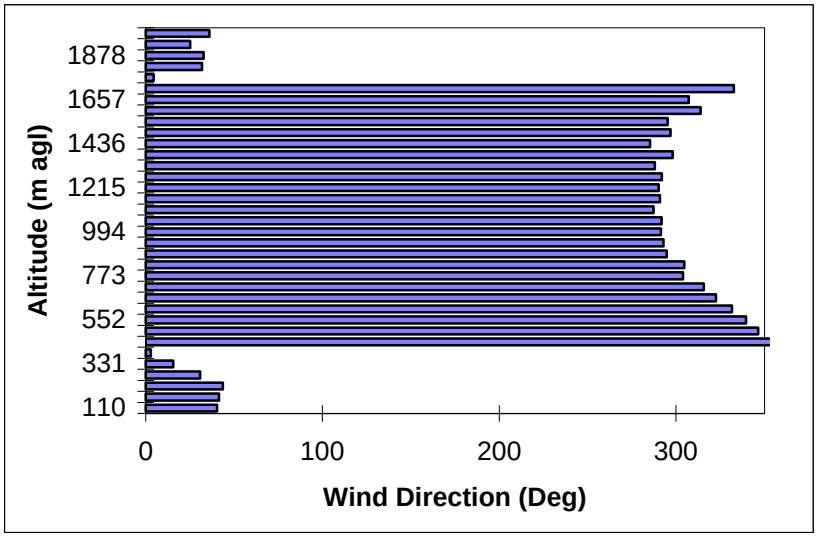

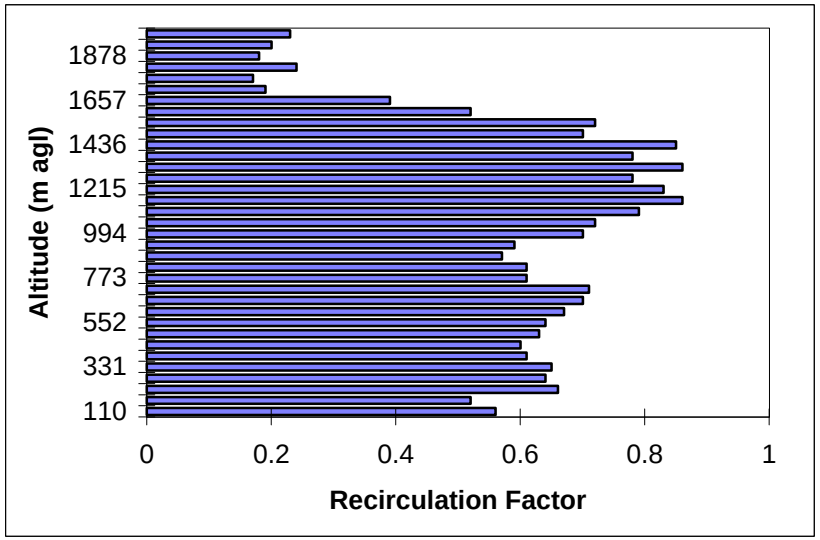

Ventura 08-06-97 0400 to 1600.xls

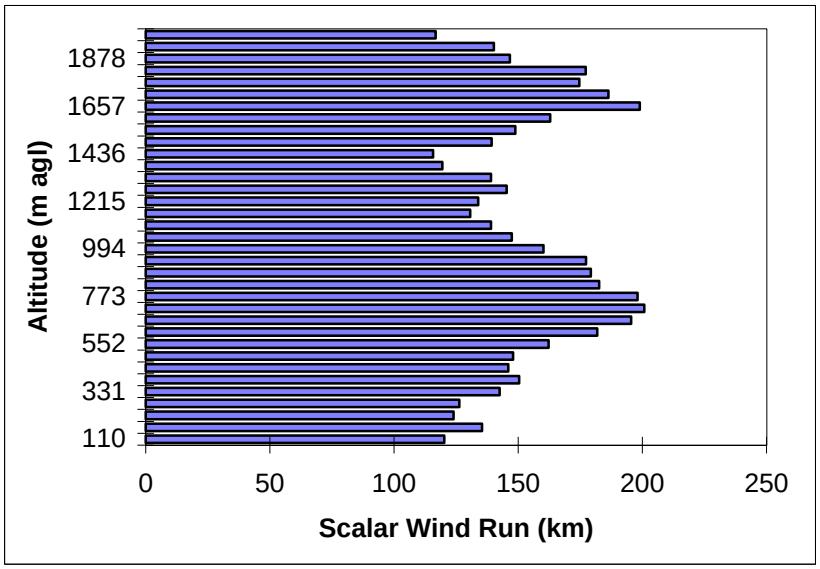

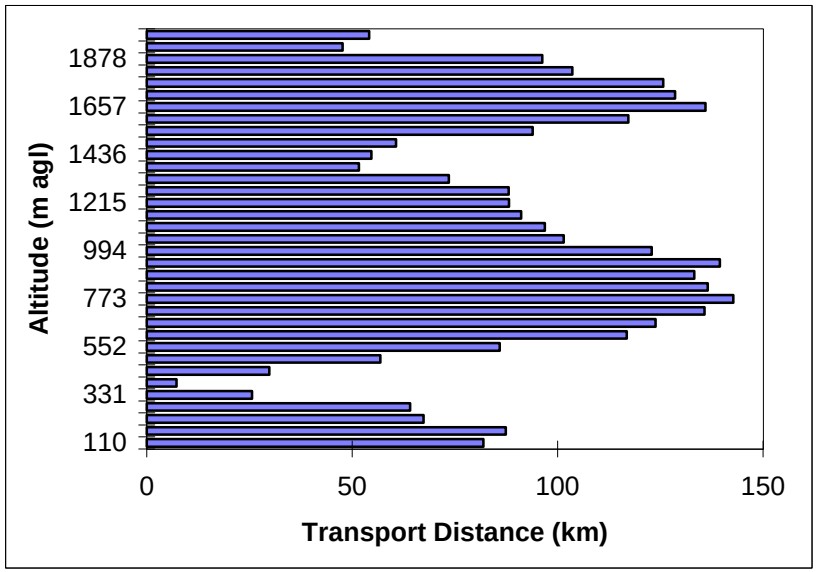

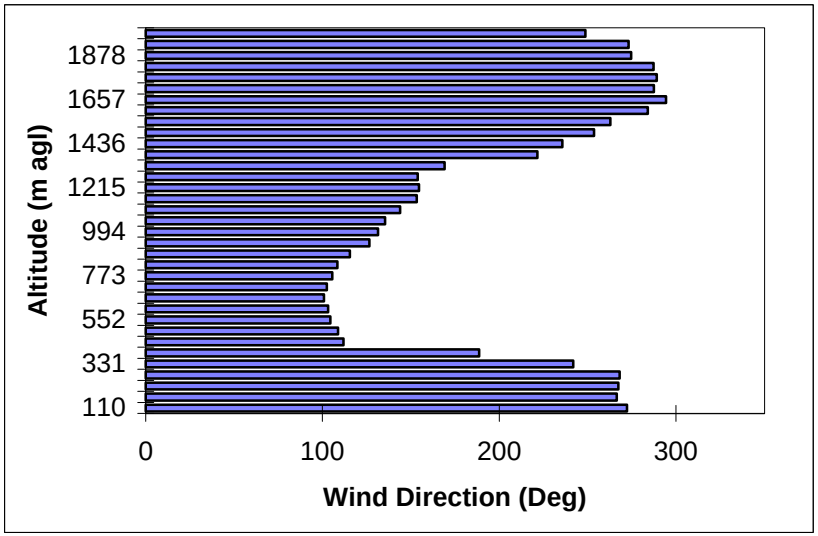

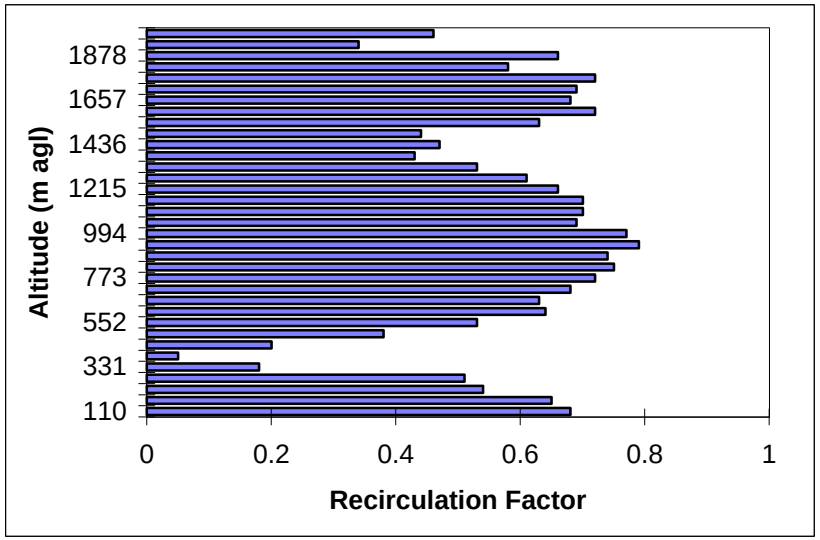

Ventura 08-06-97 1600 to 0400.xls

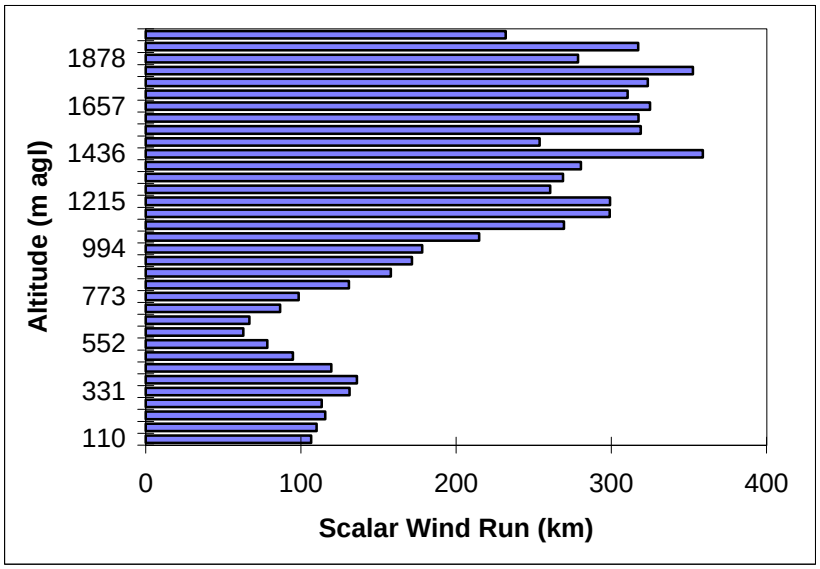

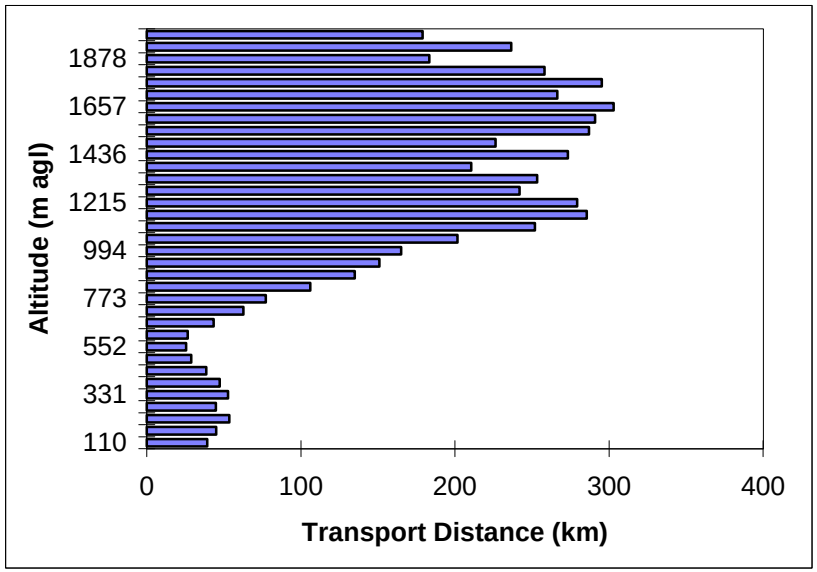

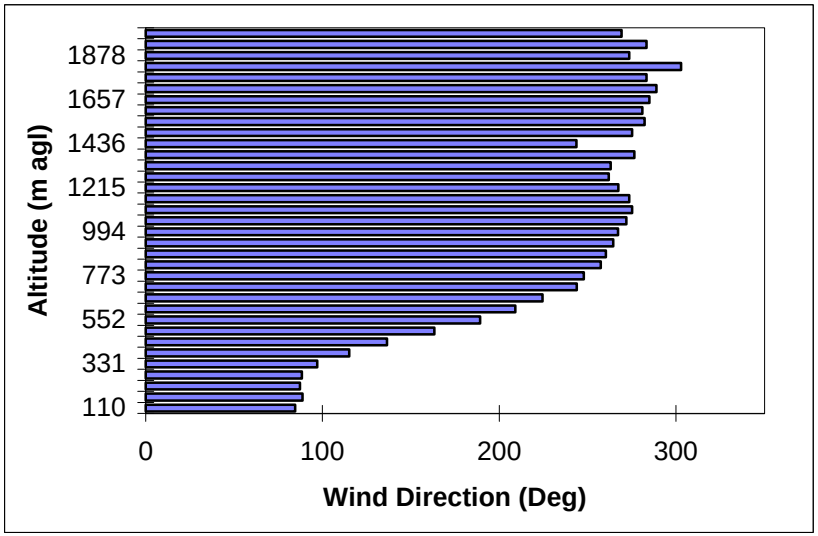

Ventura 08-07-97 0400 to 1600.xls

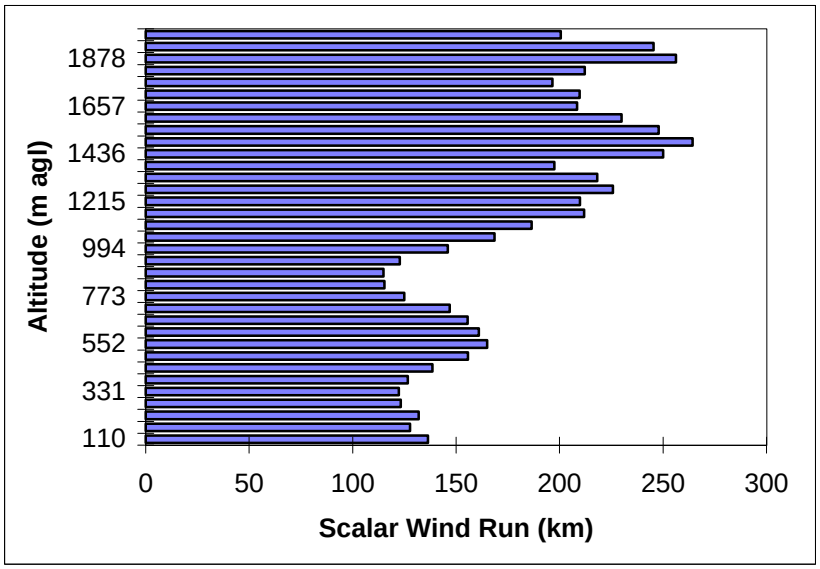

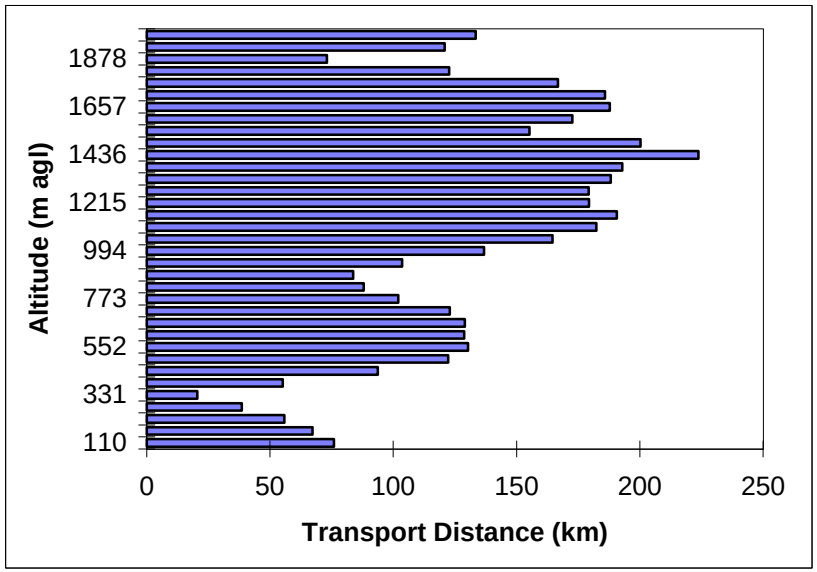

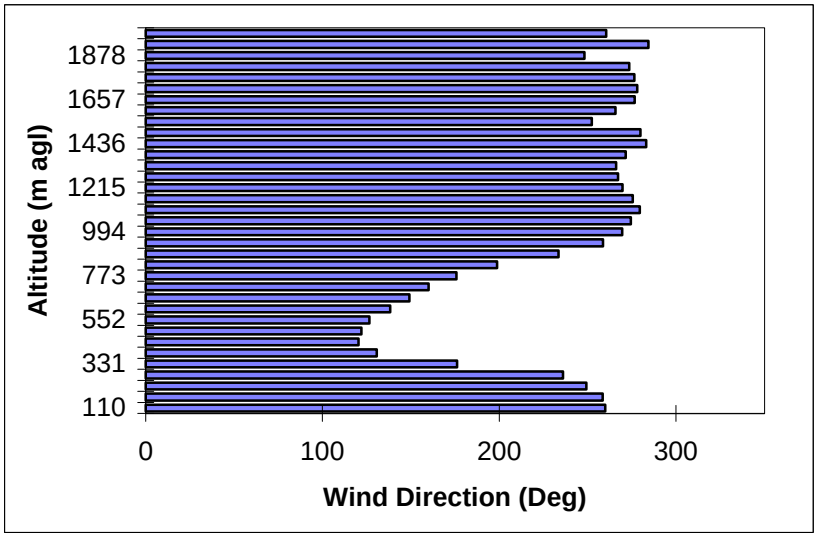

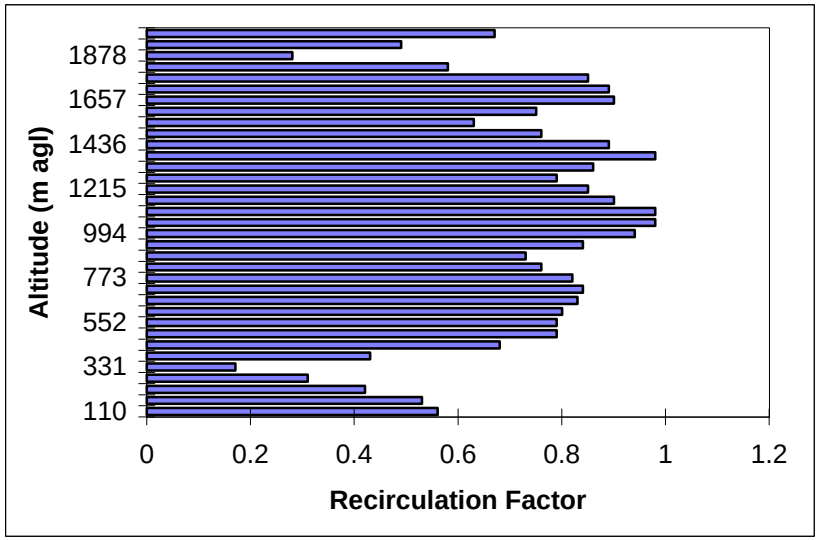

Ventura 08-07-97 1600 to 0400.xls

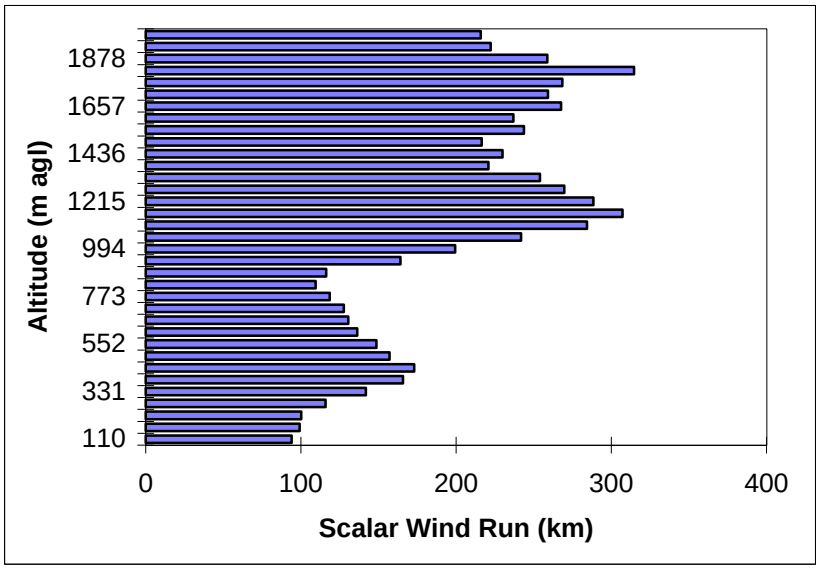

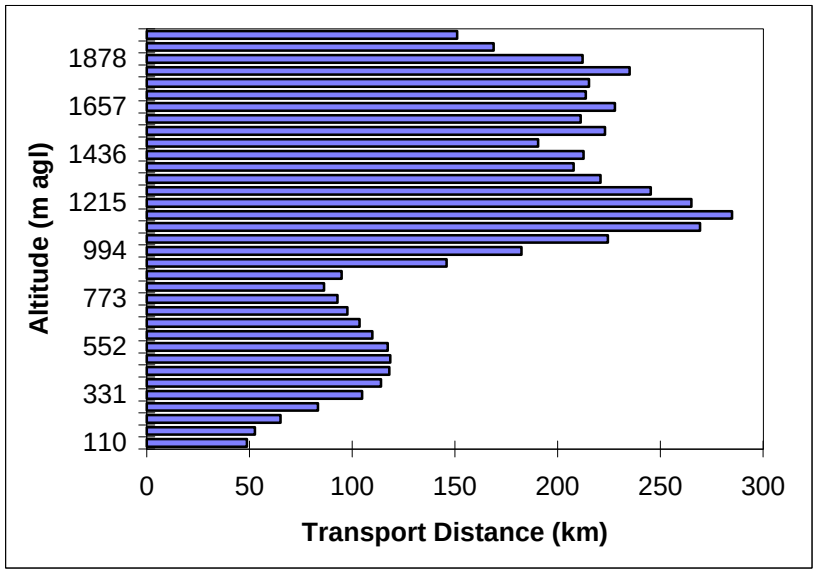

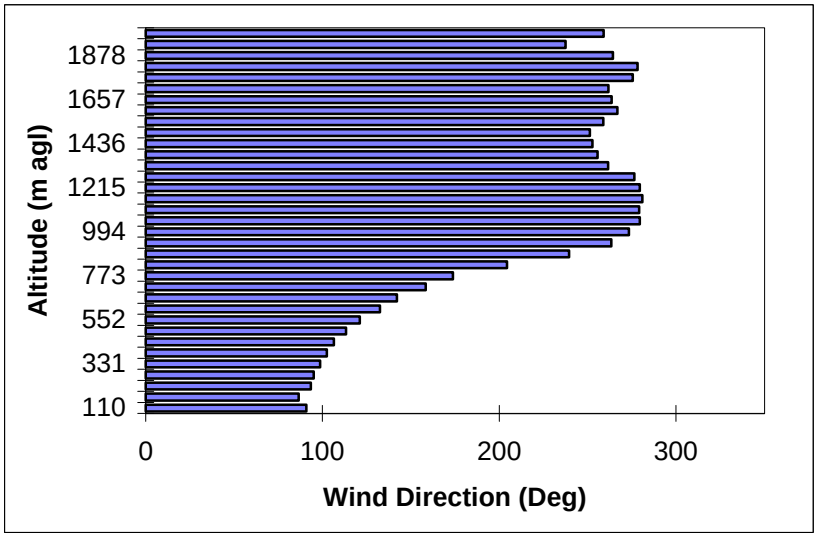

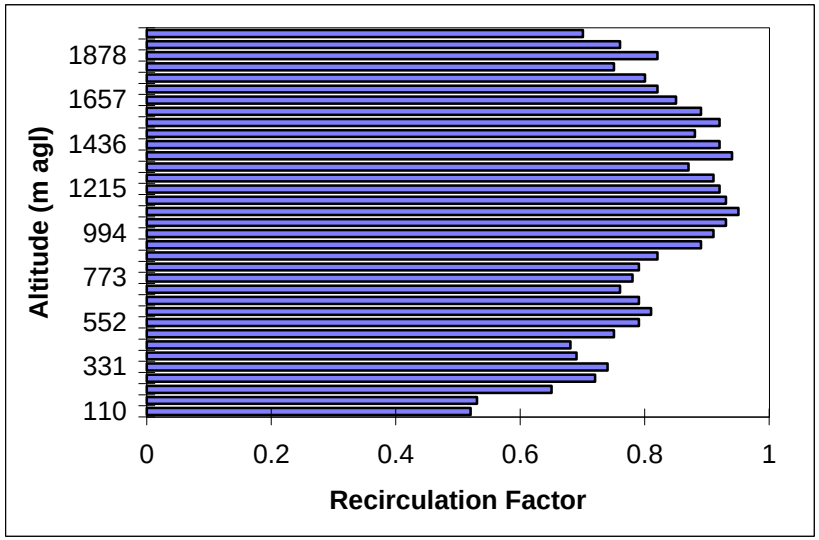

Ventura 08-08-97 0400 to 1600.xls

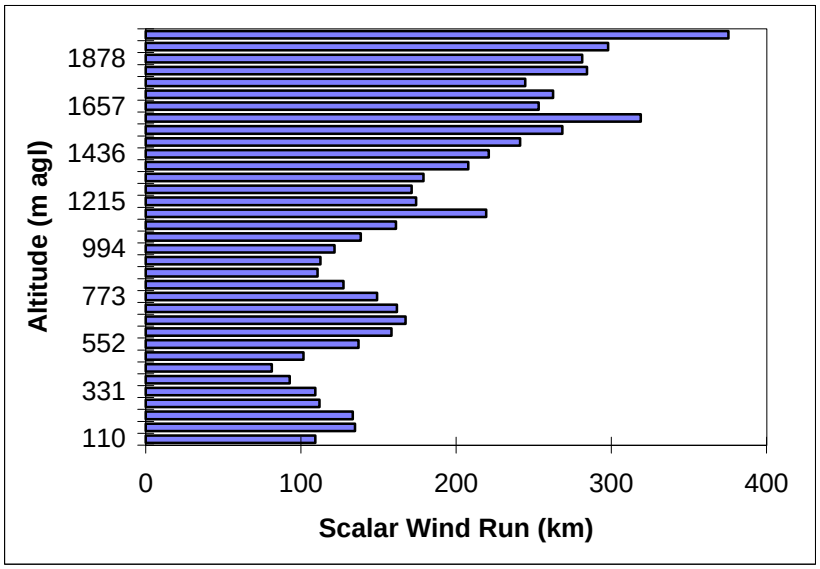

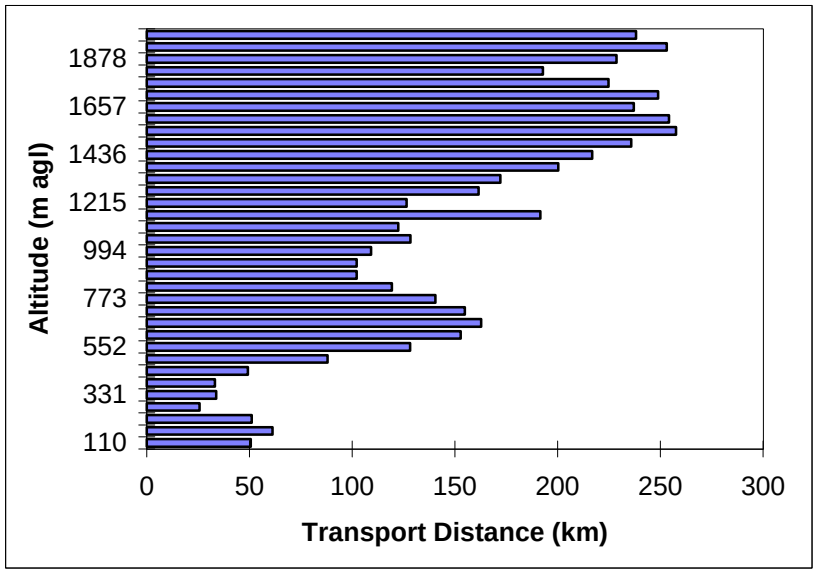

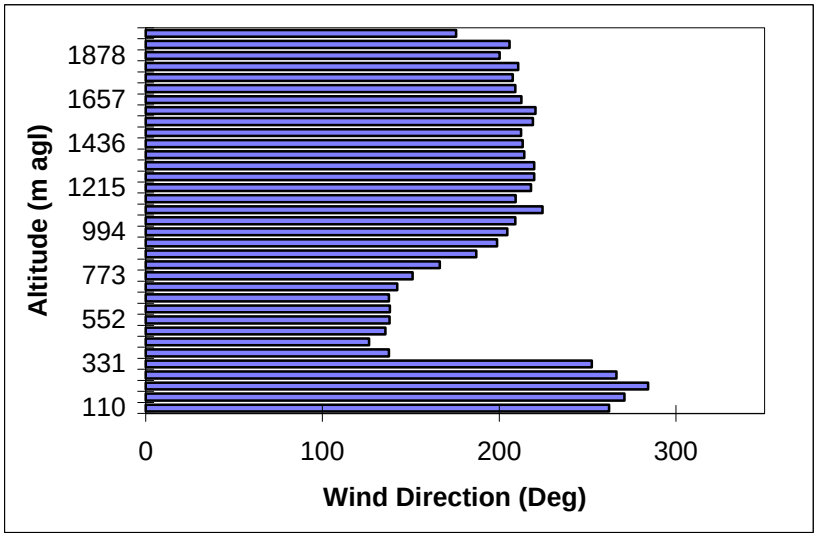

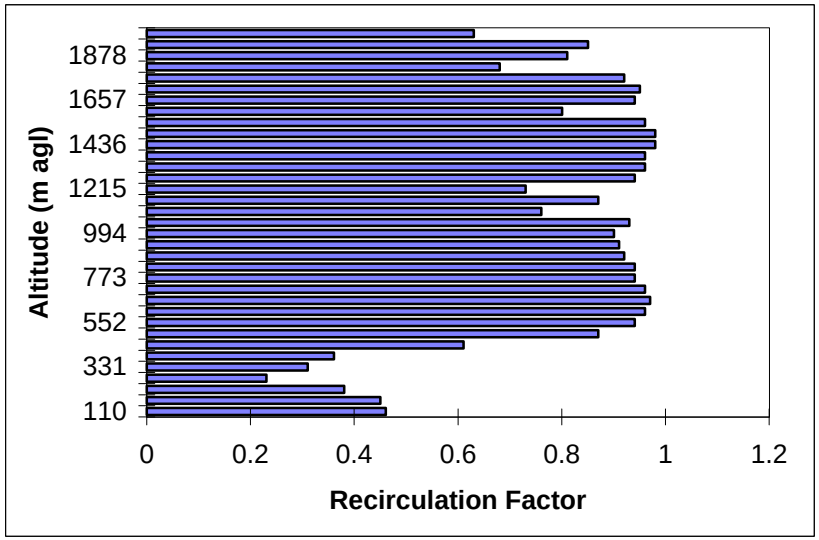

Ventura 07-15-98 0400 to 1600.xls

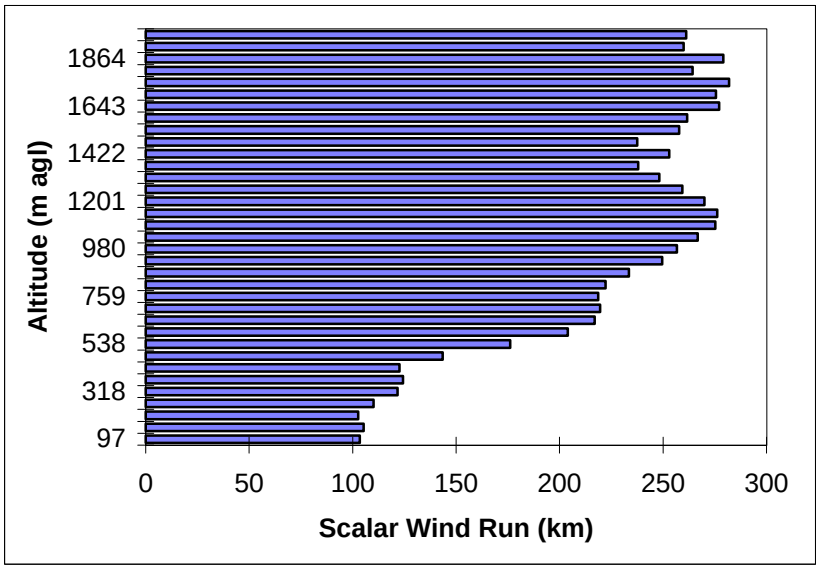

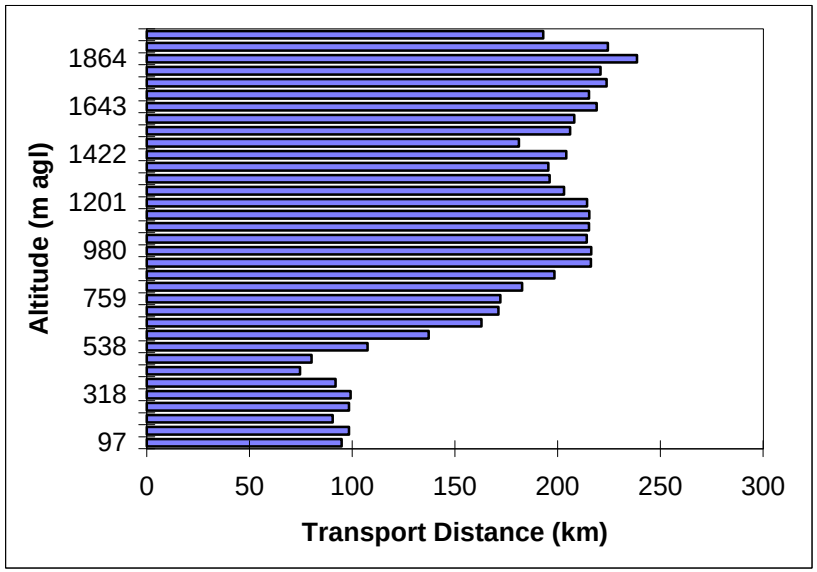

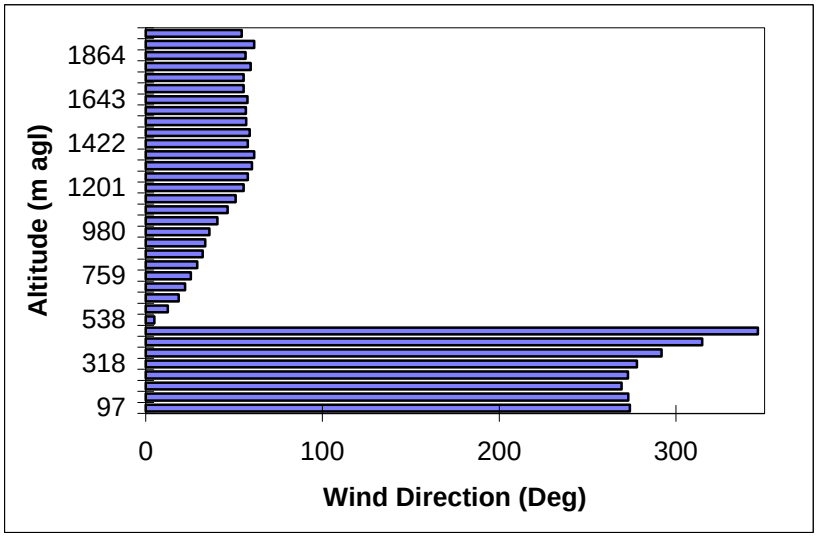

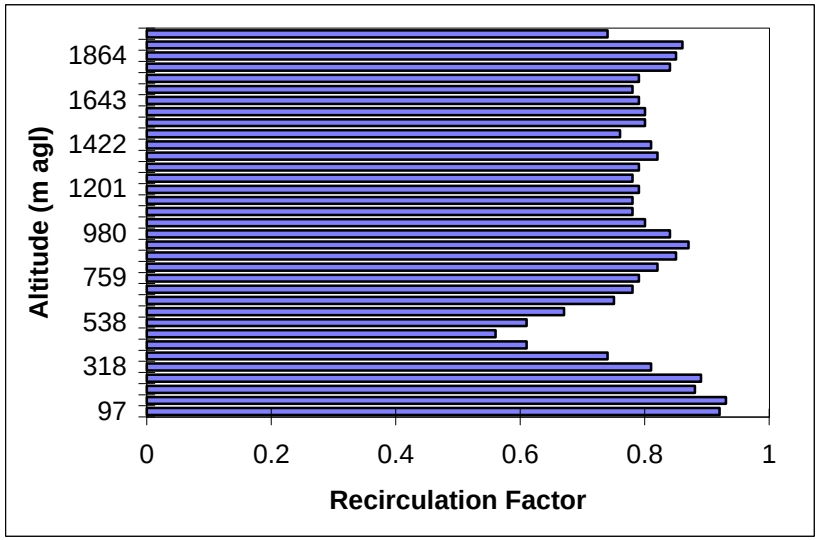

Ventura 07-15-98 1600 to 0400.xls

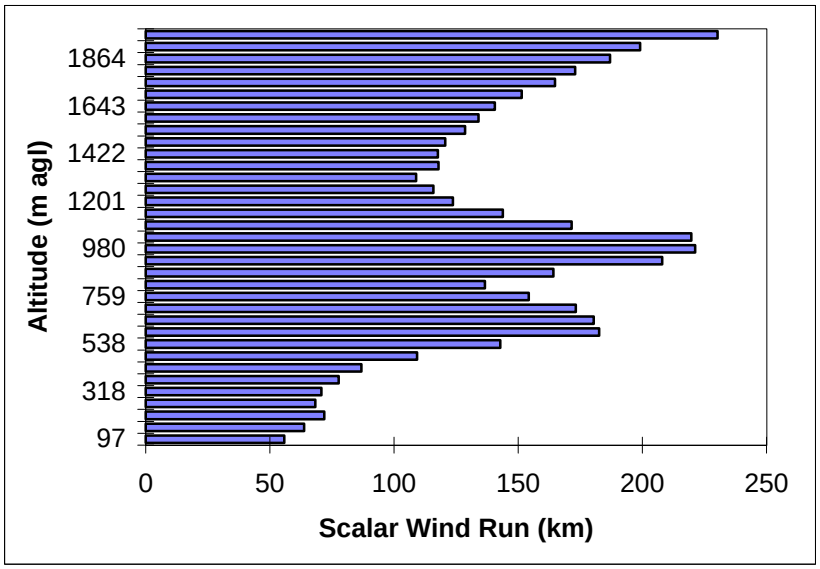

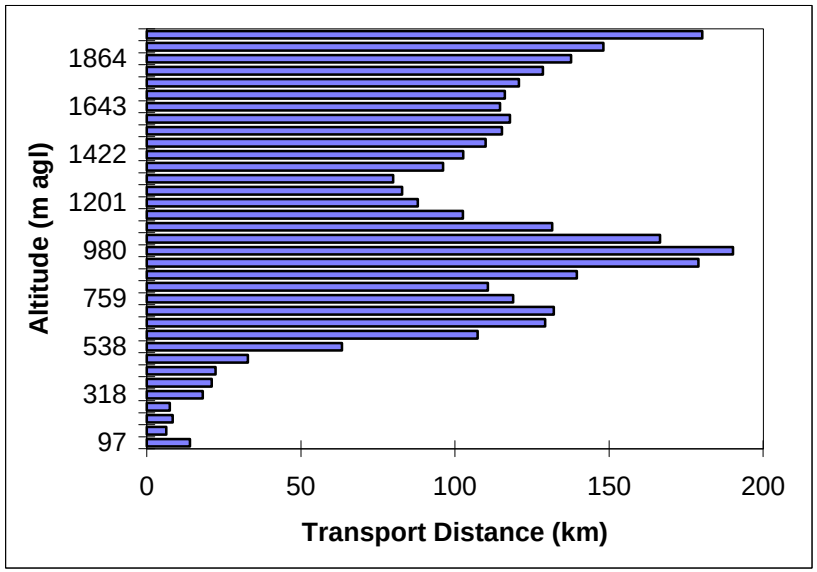

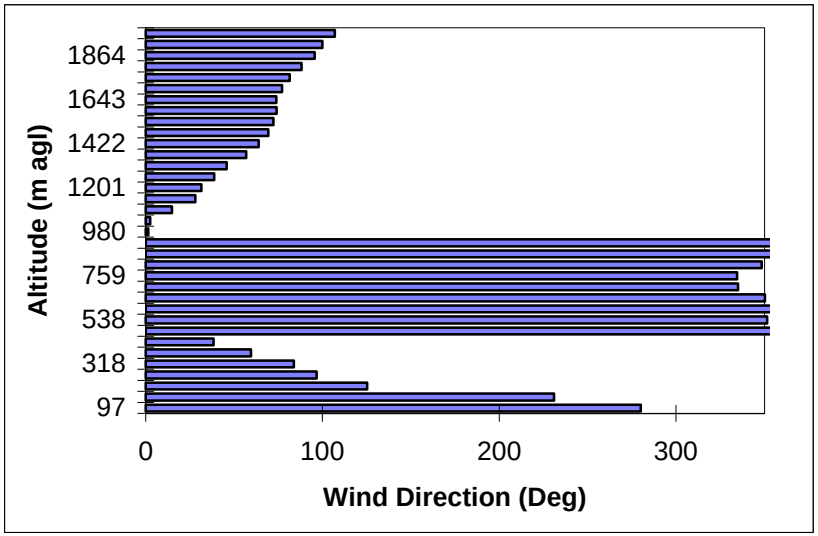

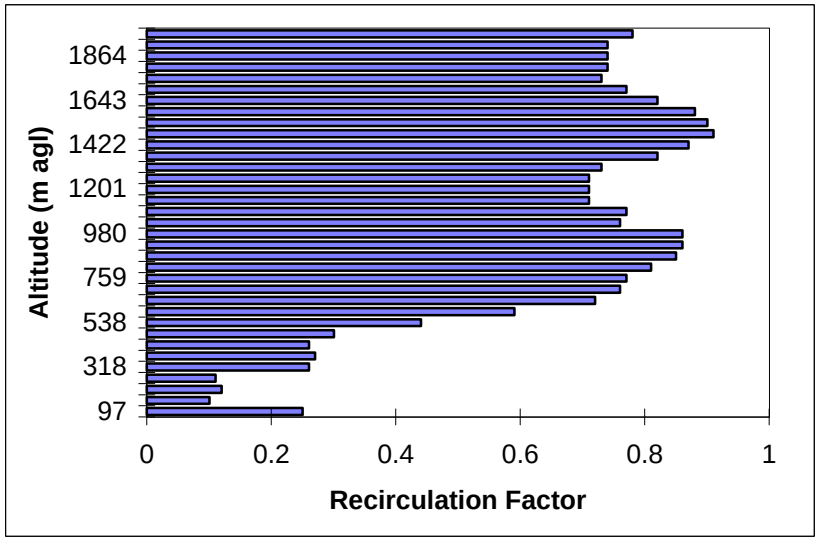

Ventura 07-16-98 0400 to 1600.xls

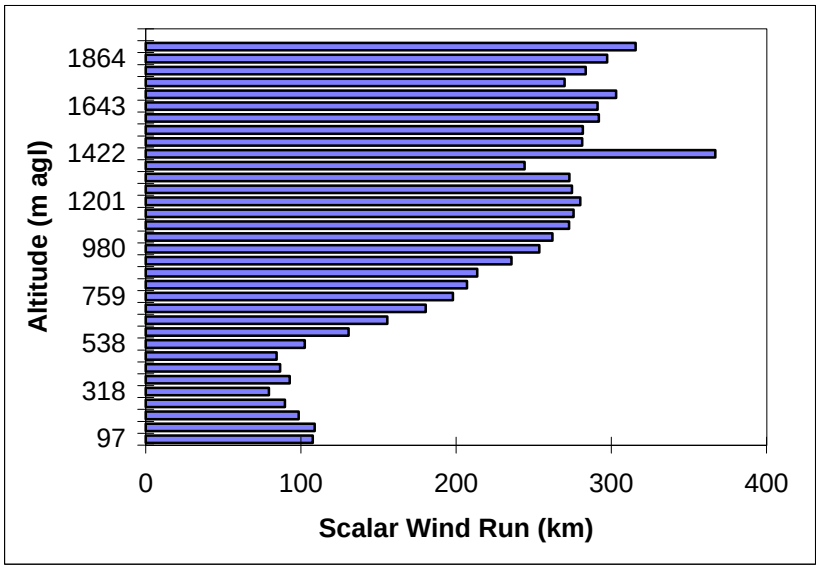

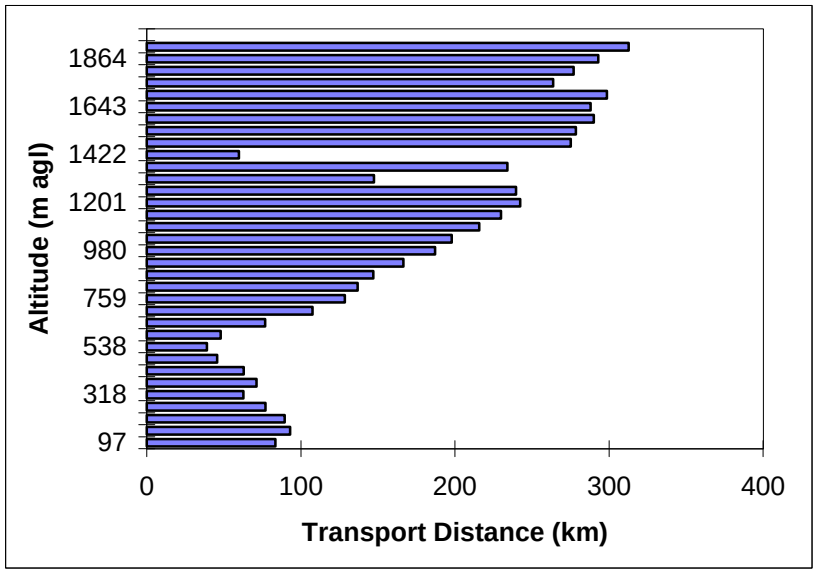

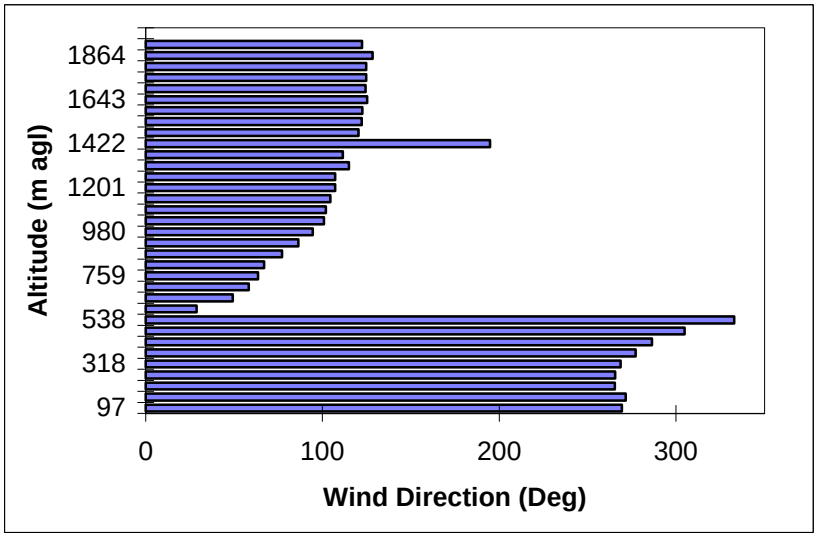

Ventura 07-16-98 1600 to 0400.xls

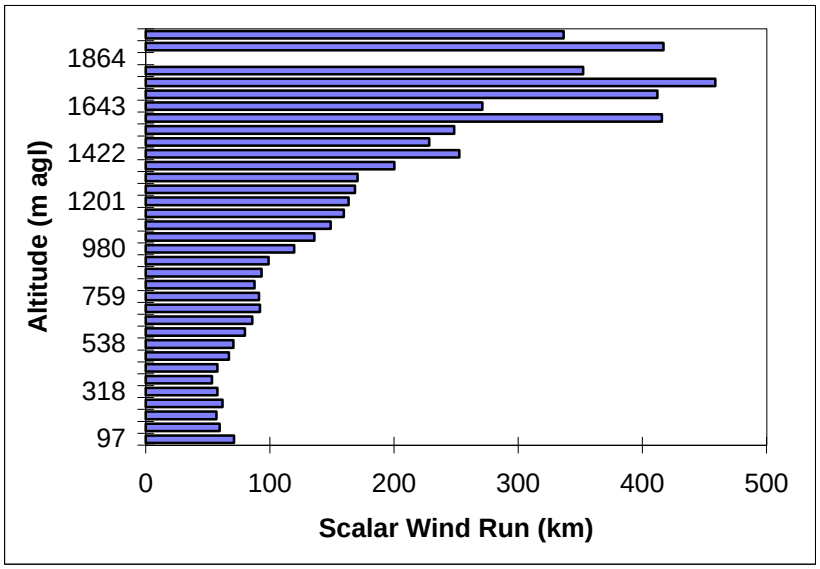

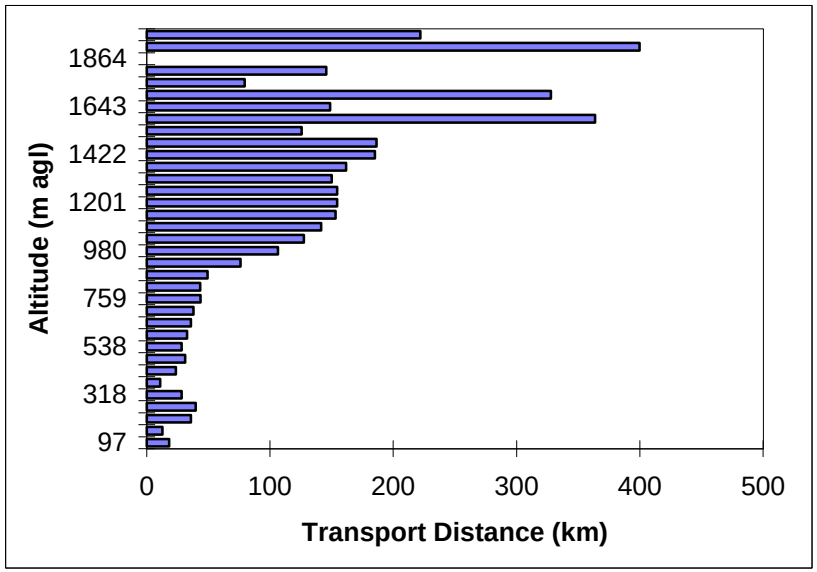

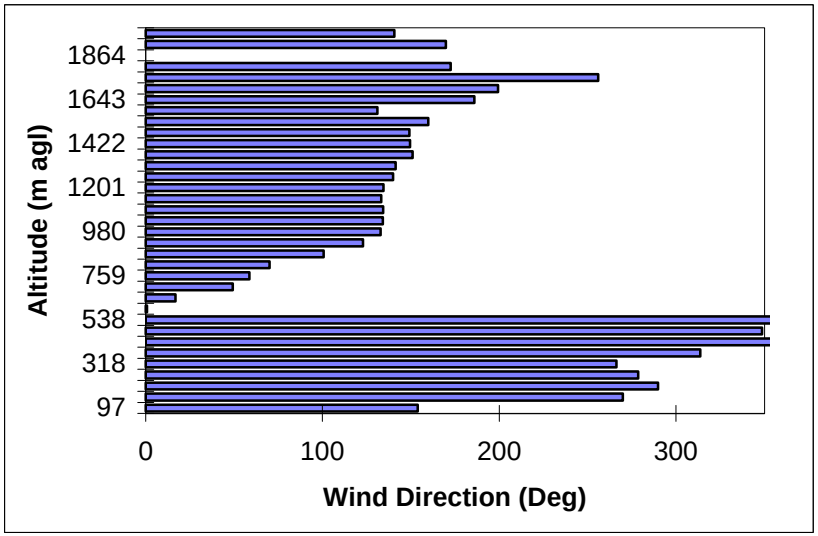

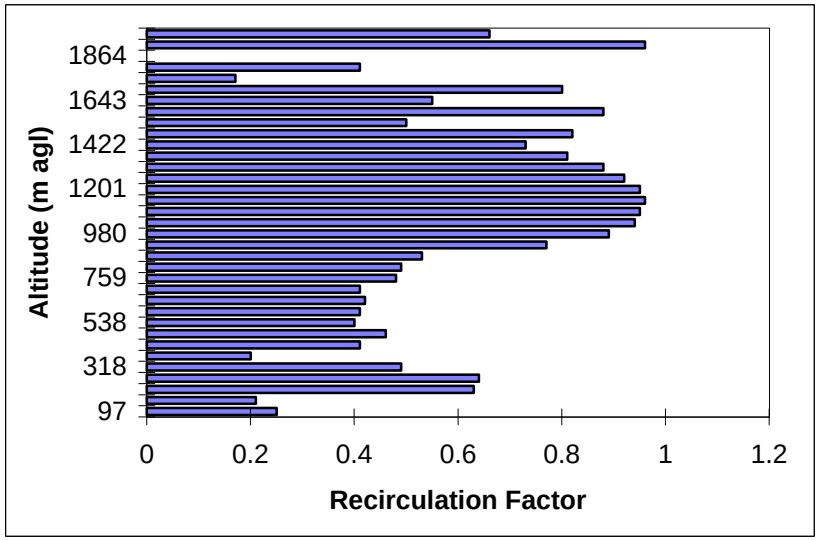

Ventura 07-17-98 0400 to 1600.xls

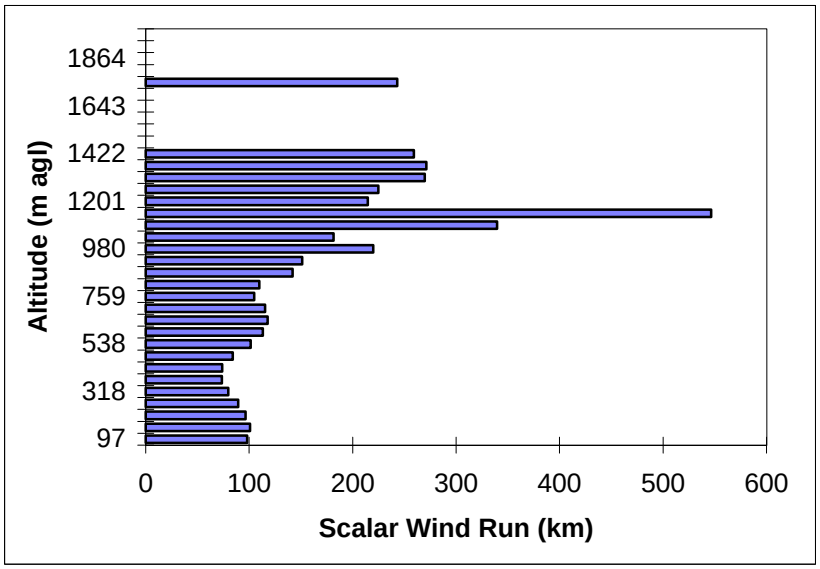

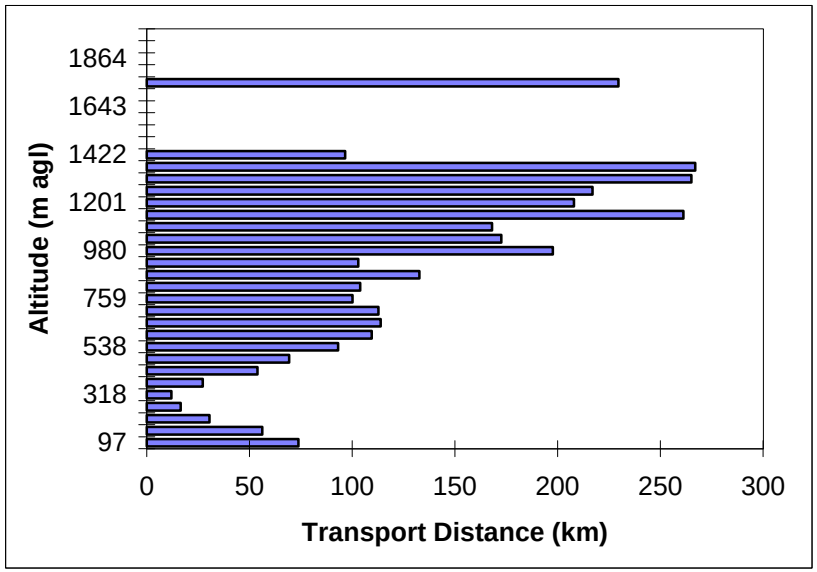

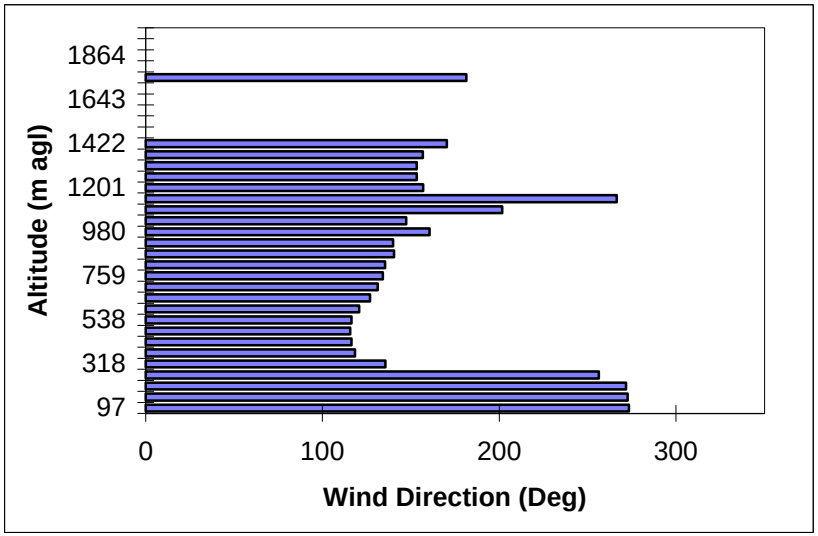

Ventura 07-17-98 1600 to 0400.xls

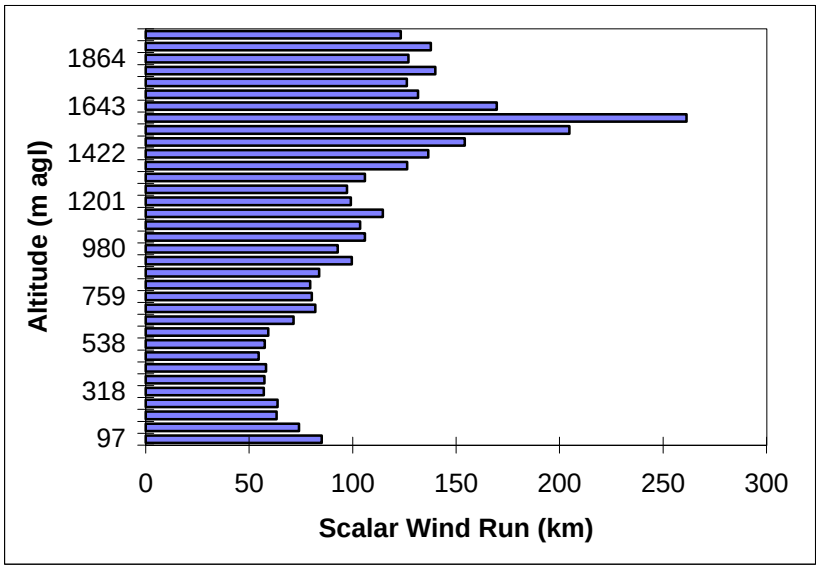

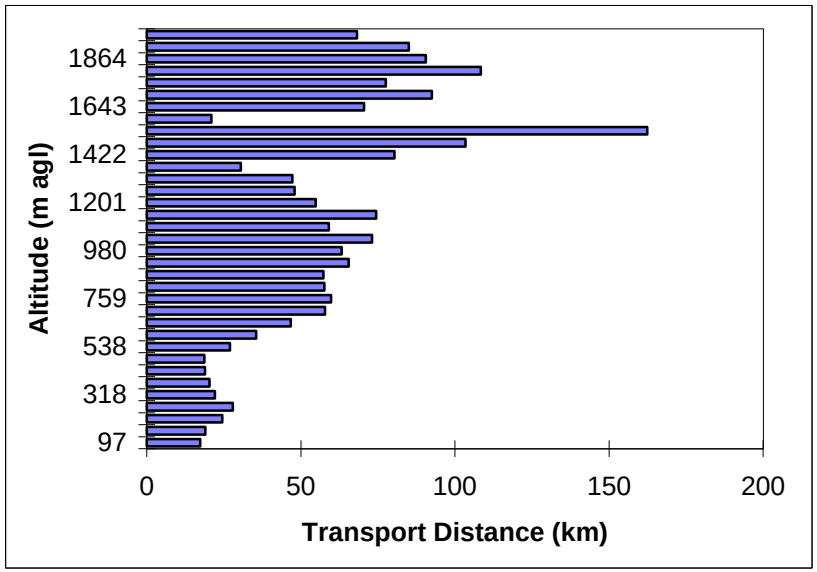

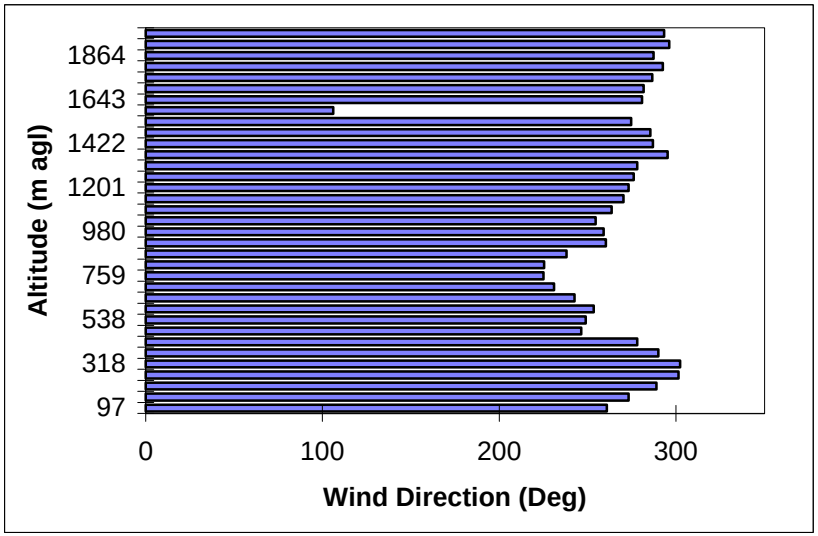

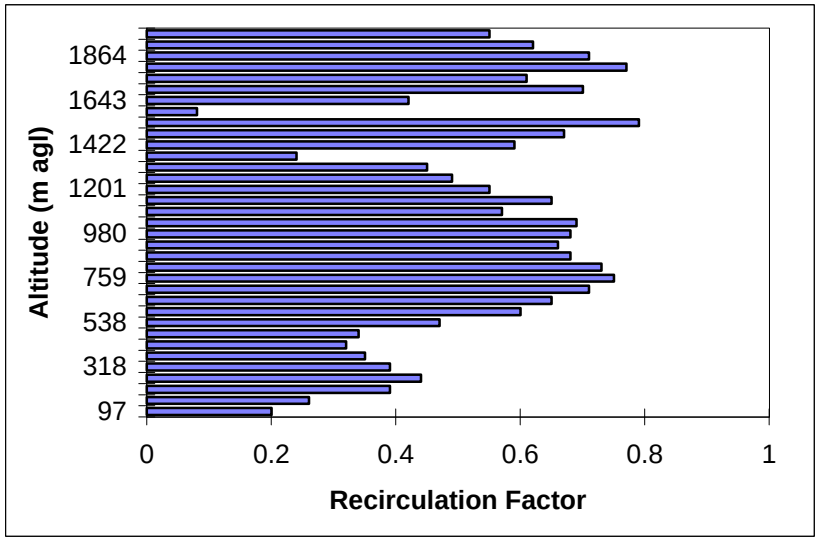

Ventura 07-18-98 0400 to 1600.xls

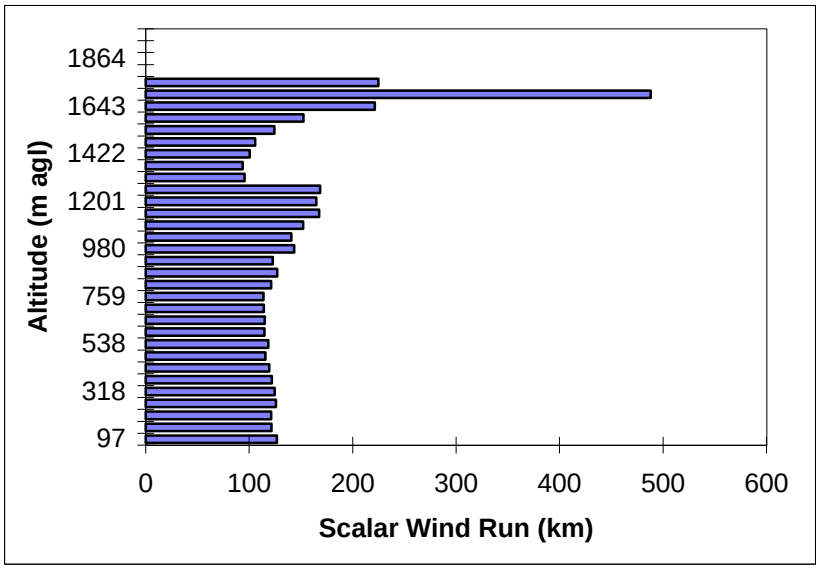

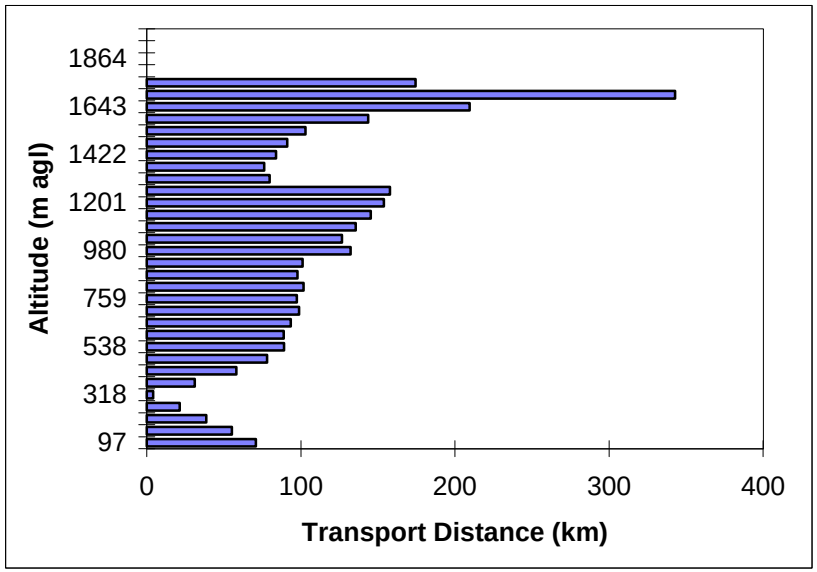

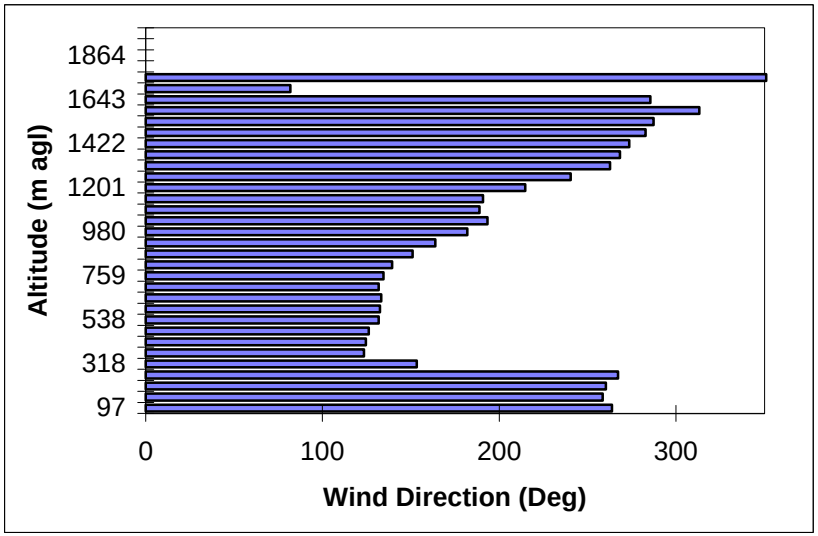

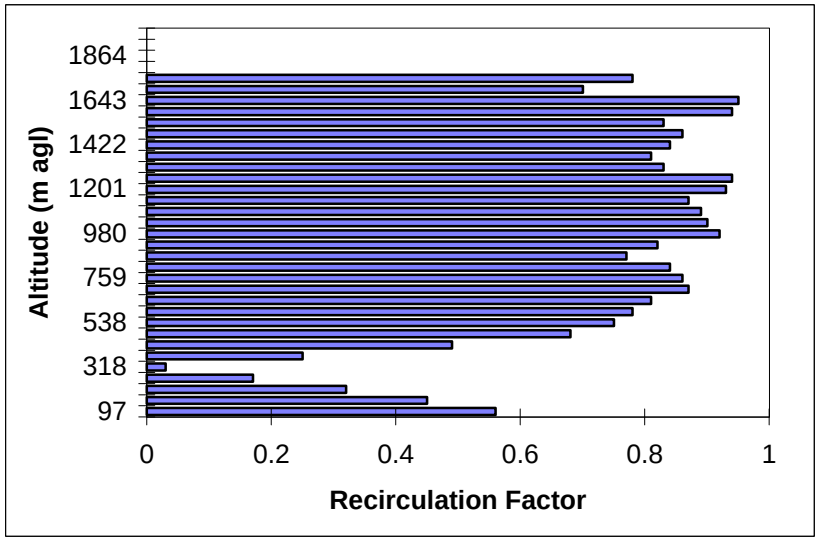

Ventura 07-18-98 1600 to 0400.xls

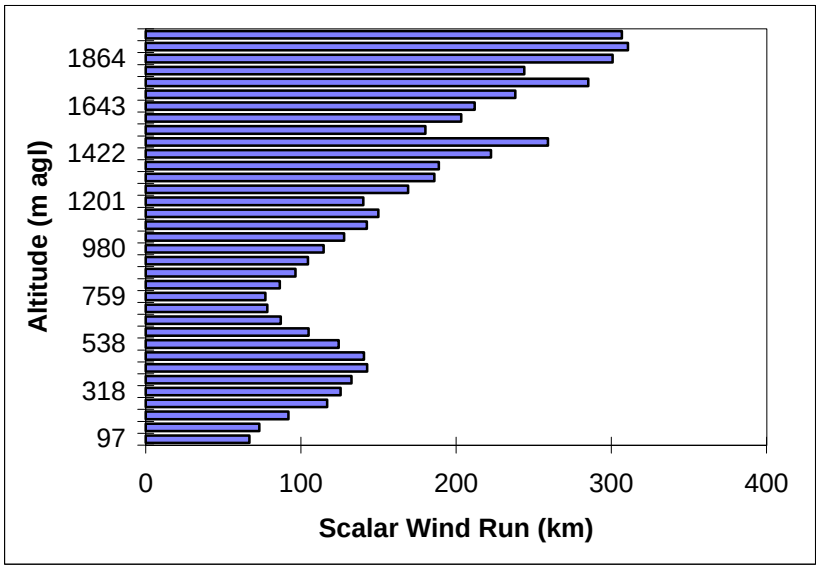

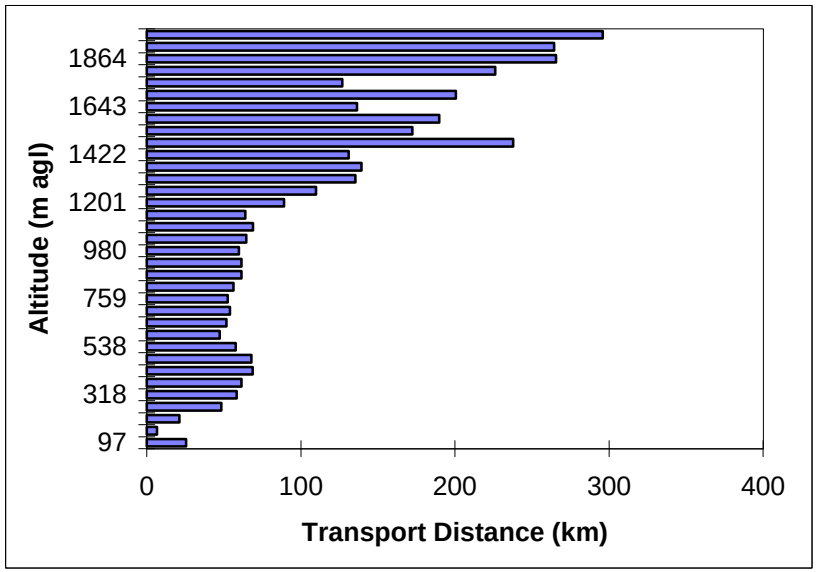

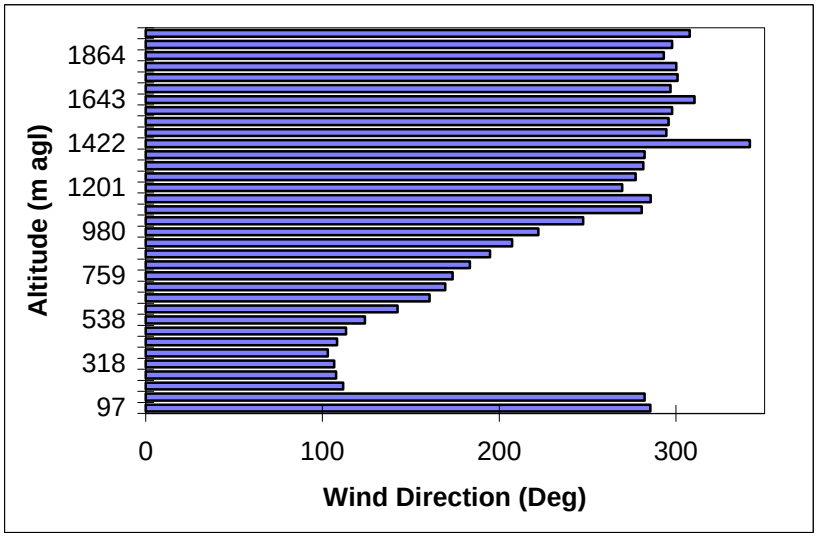

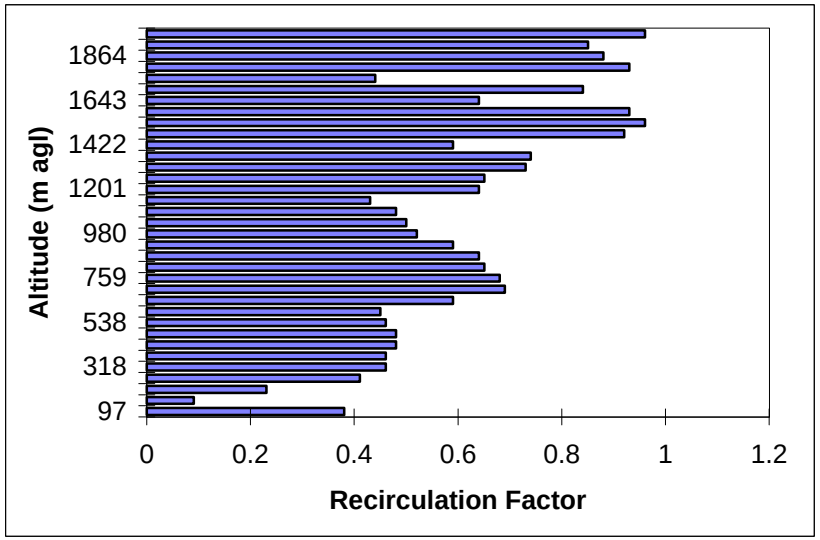

Ventura 07-19-98 0400 to 1600.xls

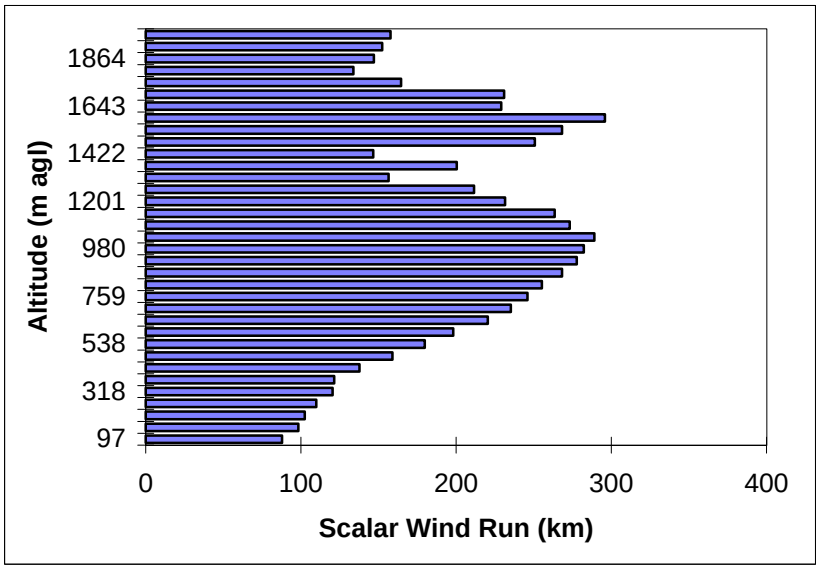

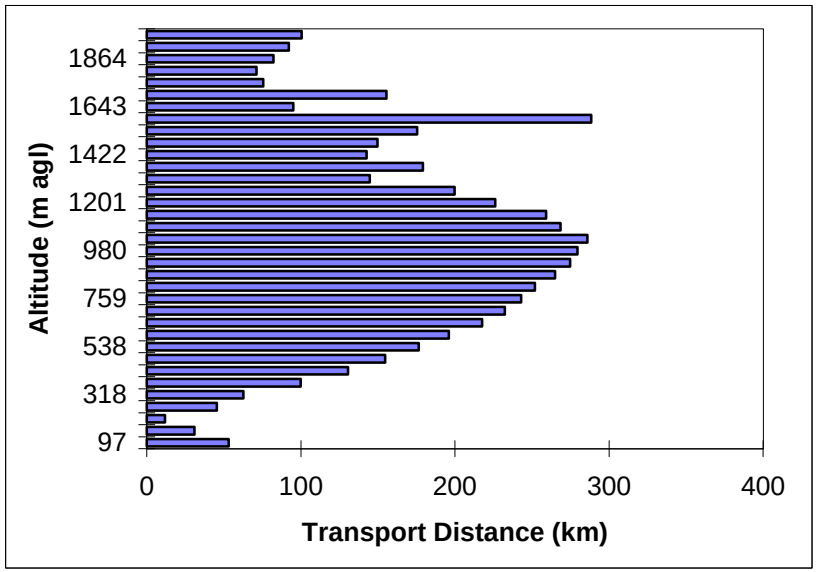

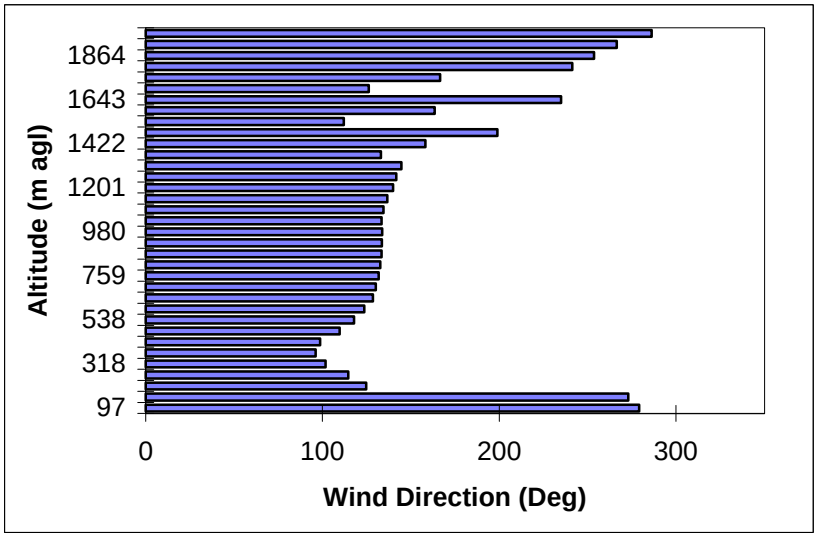

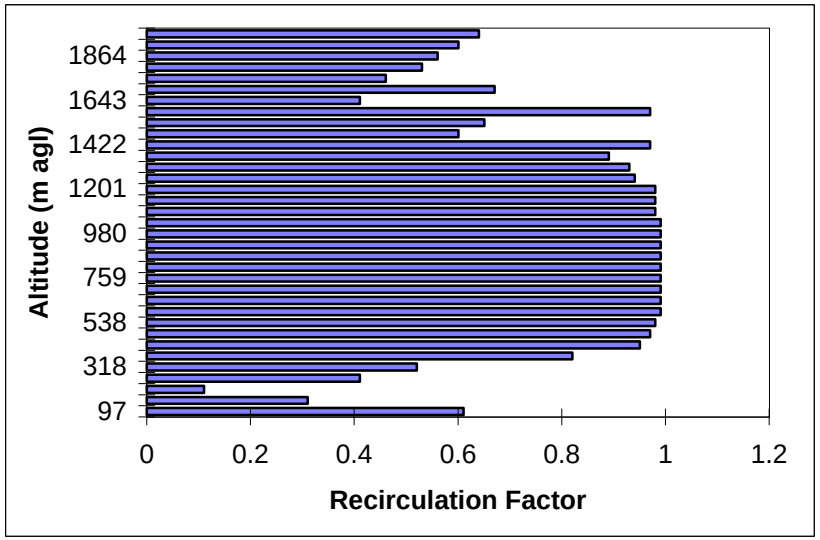

Ventura 07-19-98 1600 to 0400.xls

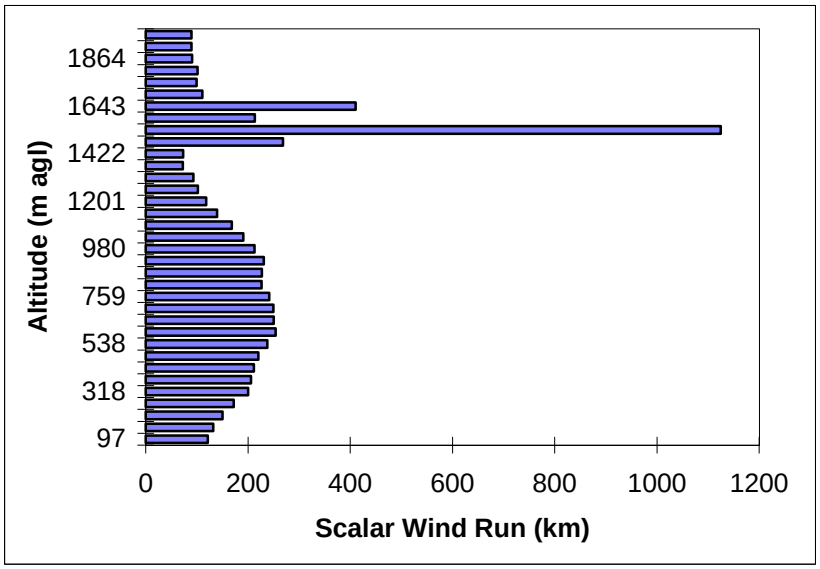

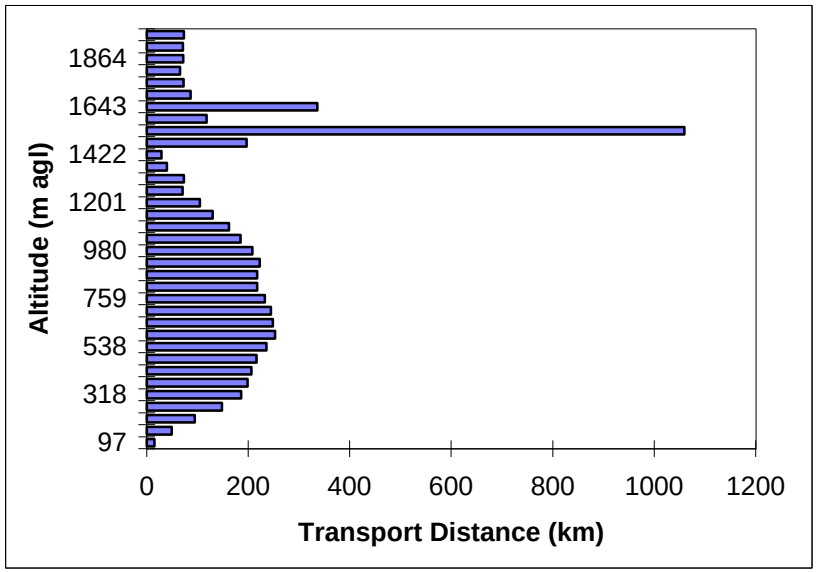

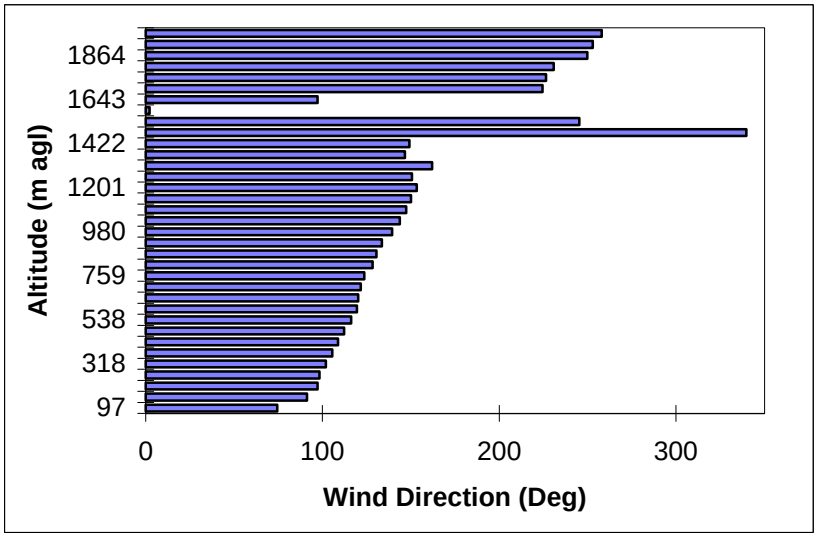

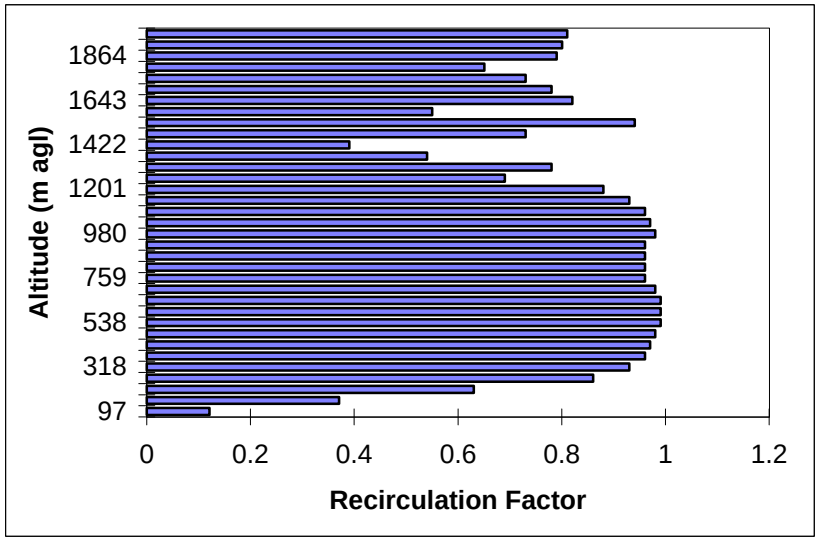
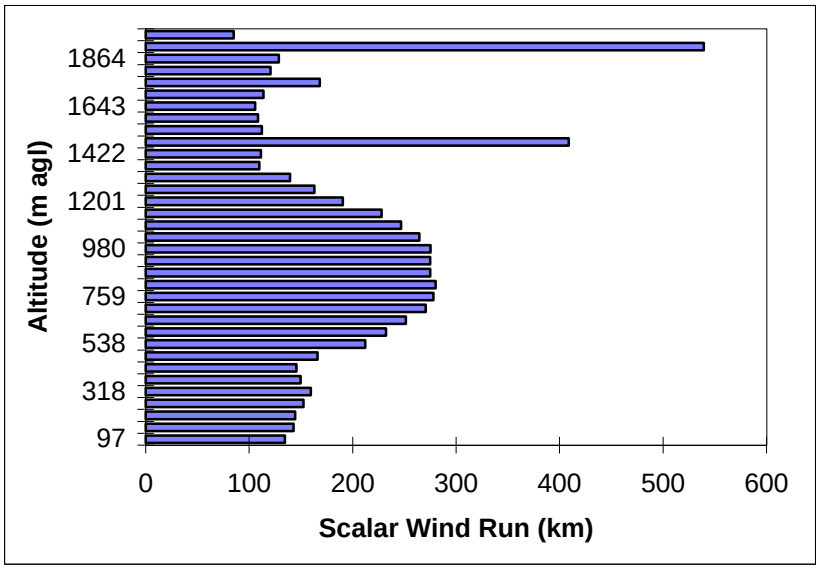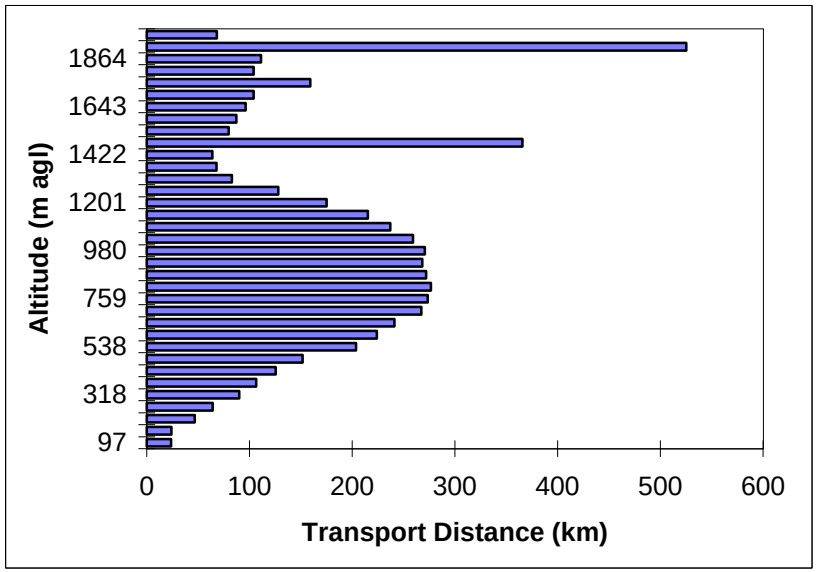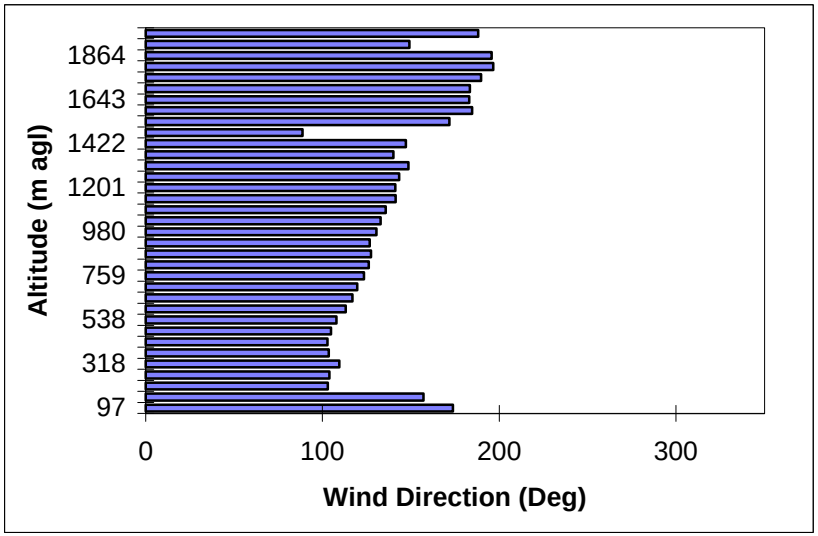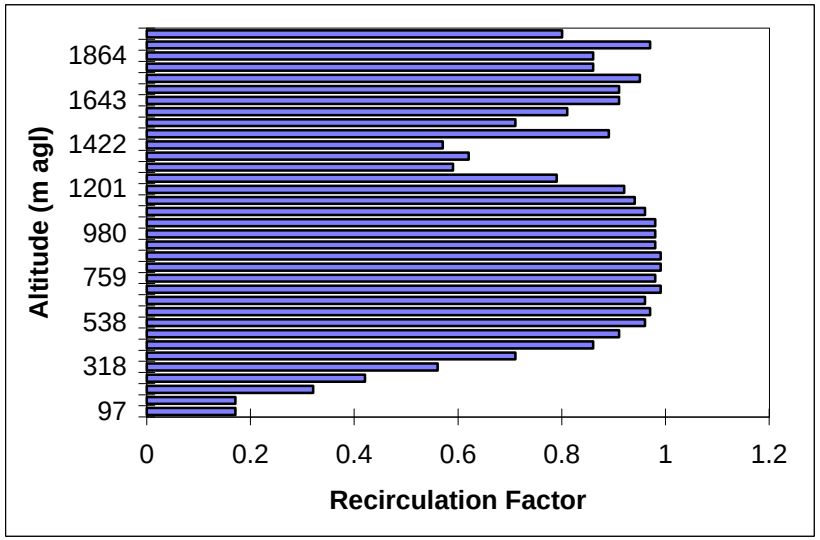
Ventura 07-20-98 0400 to 1600.xls